WATER PURIFICATION BY ION EXCHANGE MIXED BEDS

by

RICHARD RONAYNE HARRIES

A Doctoral Thesis

Submitted in partial fulfilment of the requirements

for the award of

Doctor of Philosophy

of the

Loughborough University of Technology

January 1986

AUTHOR'S RESPONSIBILITY

The work presented in this thesis was planned, executed and interpretted by the author except as indicated in the acknowledgements.

ACKNOWLEDGEMENTS

ABSTRACT

Ion exchange is used extensively for the removal of ionised impurities found in natural waters. The final stage in the production of ultra pure water is normally a bed of mixed anion and cation exchange resins. Three areas within the operating cycle of a regenerable mixed bed - resin separation, resin mixing and anion exchange kinetics - have been investigated.

Complete separation of the two resins by backwashing, prior to chemical regeneration, is necessary to prevent the subsequent release of trace impurities into the purified water. Various published models of particle segregation by backwashing were examined but none accurately described the separation of two ion exchange resins with similar bead size distributions and densities. A new model has been proposed based on variations in fluidised bed porosity combined with overlapping bulk circulation cells of particles. A graphical technique has been developed to predict resin separability and the predictions compared with practical data. The effects of variations in bead size, bead density, backwash flow rate and temperature have been calculated. The variations in bead density with ionic form and polymer/matrix type of the exchanger have been measured.

Following regeneration the resins are remixed by air agitation of a resin/water slurry. A mechanism to describe the progressive stages of air mixing has been proposed, based on bubble transport and bulk circulation of resin beads. The subsequent sedimentation of the resins was also considered. Laboratory and full scale studies confirmed the predicted effects of mixing fault conditions, particularly re-separation of the mixed resins.

A mass transfer equation has been developed to describe the leakage of influent ions through a column of exchange resins. In conjunction with laboratory column tests the equation has been used to investigate the influence on anion exchange of polymer/matrix type, influent anion and the presence of foulants on the resin beads. Sulphate and phosphate ions exchange more slowly than monovalent chloride and nitrate ions. On a fouled exchanger the rate of sulphate exchange deteriorates more rapidly and seriously than for chloride exchange. This has been attributed to steric hindrance of the divalent sulphate ion.
A laboratory method has been developed for the routine assessment of mixed bed anion exchangers and the prediction of their performance potential in service, with particular application to condensate purification for boiler feedwater.

CONTENTS

1   I N T R O D U C T I O N

1.1   PURE WATER

To ensure process continuity and product quality, many modern
industries require a continuously available supply of high purity
water. The term pure is often specific to the requirements of a
particular industry (1); this thesis deals with the removal of ionic
species from water.

There are a number of commercially available techniques for reducing
the concentration of ionic species in water eg evaporation, reverse
osmosis, electrodialysis, and ion exchange. Each method has
advantages in certain situations but, during the last thirty years,
ion exchange has found the most widespread application. Ion exchange
remains the most commercially viable procedure for continuously
producing large volumes of high purity water.

In the context of this thesis high purity is defined as having an
electrolytic conductivity of less than 0.25 micro Seimens per
centimeter* (μS cm^{-1}) while ultra pure water has a conductivity of
less than 0.1 μS cm^{-1}, both measured at 25 $^\circ$C. By comparison
absolutely pure water has a theoretical conductivity of
0.054 μS cm^{-1} (25 $^\circ$C) while an aqueous solution containing one
milligram of sodium chloride per kilogram solution (1.0 mg kg^{-1} NaCl)
would have a conductivity of 2.16 μS cm^{-1} at 25 $^\circ$C. On this basis
ultra pure water would contain less than the equivalent of 20 μg
dissolved sodium chloride per kg solution.

1.2   STEAM GENERATION

One of the largest users of high and ultra pure water are the operators
of modern steam raising boilers. Advances in materials technology
have brought a progressive increase in the pressures and temperatures
at which steam is raised and the advances in steam conditions have

---

*μS cm^{-1} is the practical unit of conductivity measurement. In SI units
1 μS cm^{-1} = 100 μS m^{-1}. All conductivities are quoted at 25 $^\circ$C
unless stated.

been accompanied by a demand for boiler feed water of increasing
purity in order to minimise boiler corrosion (2). In particular the
production of high pressure steam to drive turbines coupled to
electricity generators requires a continuous supply of very large
quantities of high purity water to feed the boilers. (2a)

Most steam driven turbines work on a condensing cycle, the exhaust
steam from the turbine passing over the outside of a large tube nest
through which cooling water flows. The condensate is normally of
sufficiently high purity to be returned directly as boiler feed water,
but in operating any large boiler there are inevitably losses from
the circuit, either by design or through leakage. Such losses are
made up by introducing freshly purified water into the water circuit
and the level of impurities in the 'make up' water must be sufficiently
low so as not to cause corrosion problems when they concentrate in the
boiler during the evaporation of the water. Typical operating losses
are between 1 and 3% of the evaporation rate and in a modern
2000 megawatt (MW) coal fired power station this leads to a daily
requirement of about 1000 m^3 of high purity water.

Almost all modern power stations use ion exchange as a major water
purification process, generally using the ion exchange resins in
fixed beds. By passing a raw water, drawn from a resevoir, well or
river, through successive beds of cation and anion exchangers it is
possible to produce ultra pure water, although the nature of the
processes preclude complete deionisation of water. However, the
economics of ion exchange operations dictate that only partial
deionisation occurs in a two bed system. To achieve water of high
or ultra pure quality it is generally necessary to pass the partially
purified water through an additional bed of intimately mixed anion
and cation exchangers, called a mixed bed.

1.3   WATER PURITY AND BOILER CORROSION

The reason for using such high purity boiler feed and make up water
is to minimise solids deposition and the generation of corrosive
solutions on the waterside of the boiler tubes.

Steam generation in a water tube boiler is a complicated process (3).
Any dissolved impurities in the boiler water will either pass into the

steam phase or concentrate at the tube surface and, under suitable conditions, can result in rapid corrosion of the boiler tubes.

The design of boiler can also affect the feed water purity necessary to minimise corrosive conditions. Drum boilers incorporate a recirculation loop through the heat source, generating a steam-water mixture that is separated in the drum. Once-through boilers are essentially a series of parallel tubes passing through the heat source and all the water entering a tube is converted to steam (3). Any feedwater impurities will progressively concentrate in the evaporating boiler water and, depending on their volatility and the steam temperature and pressure, will either pass into the steam phase, deposit on the tube surface or generate a corrosive solution. All substances exhibit a partition between the steam and water phase that is dependent on temperature and pressure (4).

The current CEGB specification for the make up water for a fossil fueled drum boiler operating at 165 bar pressure is a conductivity not greater than $0.15 \mu S$ cm^{-1} at 25 °C. The purity specification for the feed water to an AGR once-through boiler has been determined with the aid of much corrosion research (3,5,6,7,8) and is currently:-

Conductivity	– not greater than	$0.08 \mu S$ cm^{-1} at 25 °C
Sodium	" " "	$2 \mu g$ kg^{-1} Na ✱
Chloride	" " "	$2 \mu g$ kg^{-1} Cl
Sulphate	" " "	$2 \mu g$ kg^{-1} SO$_4$
Silica	" " "	$20 \mu g$ kg^{-1} SiO$_2$

with the added proviso that the anion to cation balance should be as near stoichiometric as is possible (9). Following tube plate corrosion in many pressurised water reactor (PWR) steam generators the revised feed water purities are equally or more stringent than those demanded for AGR boiler operation (10,11,12) with less than $0.5 \mu g$ kg^{-1} of each of sodium and chloride impurity levels in certain instances. The allowable dissolved silica is higher than other ions because it has a much higher steam solubility and the major problem with silica is its deposition on the blades of the steam turbine.

✱The term microgramme of solute per kilogramme of solution (μg kg^{-1}) is used in the CEGB for expressing low solute concentrations in water or condensed steam.

1.4 CONDENSATE PURIFICATION

A once-through boiler is far less tolerant of feedwater impurities than a drum boiler and, even on a condensing cycle, it is difficult to guarantee ultra pure feedwater. A particular source of impurities is the cooling water used to condense the spent steam from the turbine. Although the condensate is separated from the cooling water by a thin tube there are approximately 800 km of such tubing in a modern condenser with about 40,000 expanded joints at the tube plates. It is almost impossible to prevent some cooling water ingress into the condensate, especially as the steam side of the condenser operates under vacuum.

In the current AGR 660 MW turbines the condensate flow is $1.5 \times 10^3 m^3 h^{-1}$ $(0.4 m^3 s^{-1})$ and the cooling water is highly saline sea water. A cooling water ingress of just one litre per hour, will give a condensate impurity concentration of 25 $\mu g kg^{-1}$ dissolved salts, yet it is very difficult to locate the source of such a small leak and it imposes a great economic penalty if the boiler has to be shut down every time a small condenser leak occurs. Therefore, nearly all modern power stations with once-through boilers, and many with drum boilers that use sea water for cooling, employ a system for the continuous purification of some or all of the condensate before it is returned to the boilers. All condensate purification plants (CPP) use ion exchange for the removal of ionic impurities and in almost all cases it is an ion exchange mixed bed that is the final, and often only, purification stage. The performance of these CPP mixed beds are the major factor controlling feed water purity.

Because the condensate flow rate is so large, CPP mixed beds operate at much higher throughput rates than normal make up water treatment plant units. Typical values for CPP are 100 $m^3 m^{-2} h^{-1}$ and 100 $m^3 m^{-3} h^{-1}$ through a bed 0.9 m deep in a 3 m diameter vessel. At these flow rates the kinetics of new ion exchange resins are sufficient to give satisfactory operation but as the resins age their performance deteriorates, in particular that of the anion exchanger. This deterioration is marked by several effects: an inability to effectively remove chloride ions during condenser leaks; an increase in the background leakage of ions from the mixed bed, notably

sulphate ions; and a prolonged rinse out of sulphate after a freshly regenerated bed has been returned to service (13, 14, 15, 16). These effects have been attributed to the presence of organic foulants on the surface or within the anion exchanger beads which interfere with the anion exchange processes (17, 18, 19). The main organic foulants are considered to be naturally occurring plant decay products, termed fulvic and humic acids, that are present in many raw water supplies and tend to irreversibly accumulate on anion exchange resins, although the magnitude of their effect has never been established.

Additionally it has been shown that poor separation of the mixed bed resins prior to regeneration and poor remixing after regeneration can give rise to ionic leakages during the subsequent mixed bed service cycle (18). From comparisons of the operation of CPP at different sites and with different versions of ion exchange resins it was also thought that the type of polymer/matrix on which an ion exchanger was based may influence the mixed bed performance.

1.5 MIXED BED STUDIES

Having identified a number of factors that appeared to influence mixed bed performance at high flow rates a series of investigations were undertaken into a number of distinct aspects of mixed bed operation and ion exchanger performance. The work was conducted in laboratory pilot columns to simulate operating conditions without the inter-ference of operational variables that inevitably occur when monitoring full scale plant.

Studies associated with mixed bed regeneration have investigated those factors that influence resin separation on backwashing and the re-mixing of resins by air agitation. A theoretical model has been developed to predict resin separability, related to resin bead diameter and density, and has been used to propose revised bead size gradings for mixed ion exchangers. The mixing process has been described, faults that can occur have been identified and optimum mixing conditions have been defined.

In order to predict resin separability it was necessary to determine

how resin bead density varies with ionic form of the resin and its polymer/matrix type. From this data and moisture content determinations it has been possible to identify differences between different manufacturers resins and different batches of one manufacturers products.

To determine if polymer/matrix type played an important role in mixed bed performance, particularly for anion exchangers, the performance of six different new anion exchangers were compared by measuring ionic leakage through the bed under preset flow rate and influent dosing conditions. Both chloride and sulphate exchange was investigated. The influence of organic foulants on anion exchanger performance was studied by deliberately fouling the same six anion exchange resins under controlled conditions and then comparing their chloride and sulphate leakage characteristics with those from the new resins. Additionally used anion exchange resins from operational CPP were compared under similar test conditions.

The results of these investigations have led to a greater understanding of mixed bed operation and the factors that can influence the leakage of potentially corrosive impurities from high flow rate mixed beds.

2 BACKGROUND AND GENERAL LITERATURE SURVEY

A number of authoritative books have been written on the subject of
ion exchange and deal variously with the theoretical approach (20, 21),
the development and general application of ion exchange (22,23)
and the particular application of ion exchange to water purification
(24, 25). Numerous papers have also been published on all aspects
of ion exchange. Over 10 years ago Kunin (23) listed over 1100
references in his book.

2.1 BASIC ION EXCHANGE

Ion exchangers can be either solids or liquids but the process
described in this thesis is a two phase reaction between solid, bead
form, ion exchange resins and ionic solutes in an aqueous solvent.

The solid ion exchanger consists of an insoluble polymeric matrix
onto which ionic groups are chemically grafted. Associated with each
fixed group is a counter ion of opposite charge, and both the fixed
and counter ions have accompanying water of hydration. The counter •
ions are mobile within the exchanger, and their numbers exactly
balance those of the fixed groups to maintain electroneutrality.
Normally all the fixed ions are of the same charge so that an
exchanger is either a cation or an anion exchanger, although mixed
function amphoteric exchangers have been reported (20).

Therefore, cation exchangers are large insoluble polyanions with
associated mobile cations while anion exchangers are insoluble
polycations with associated mobile anions. Modern synthetic ion
exchangers are largely based on either polystyrene-divinylbenzene
or polyacrylate-divinylbenzene copolymers, but naturally occurring
or synthetic zeolites are inorganic silicate polymers that can have
ion exchange properties.

When a solid exchanger is placed in an aqueous solution containing
dissolved salts the ions of appropriate charge in solution may
quantitatively exchange with the mobile counter ions in the exchanger

A Sulphonic acid cation exchanger on styrene/divinylbenzene copolymer

B Quaternary ammonium anion exchanger on styrene/divinylbenzene copolymer

C Quaternary ammonium anion exchanger on propylacrylamide/divinylbenzene copolymer

D Quaternary ammonium anion exchanger on styrene/methylene bridge copolymer

FIGURE No. 2.01   POLYMER TYPES FOR CATION AND ANION EXCHANGERS

until an equilibrium is established. By choosing exchange materials
with suitable equilibria the dissolved impurities in water may be
exchanged for other ions; and if the latter are hydrogen (H^+ – cation
exchange) and hydroxyl (OH^- – anion exchange), the impurities are
effectively removed from solution and replaced by the constituents of
pure water.

2.2 DEVELOPMENT OF SYNTHETIC ION EXCHANGERS

The phenomenon of ion exchange was first described by Thompson (26)
and Way (27) in 1850, but the first commercial application of ion
exchanger, water softening, took place in the early part of the
20th century using natural zeolites. The first synthetic exchangers
were sulphonated coals (20) and at the same time (1934) Adams and
Holmes (28) prepared the first cation and anion exchangers based on
synthetic organic polymers. These exchangers contained functional
groups that were weak acids (cation exchangers) or weak bases (anion
exchangers) and therefore had limited application in water purification
as they were only ionised over certain pH ranges.

2.2.1 POLYMER TYPES

Modern ion exchangers for water purification are based on two types
of copolymer polystyrene crosslinked with divinylbenzene (PS/DVB) or
an acrylic acid derivative crosslinked with DVB (PA/DVB). A
sulphonated styrene /DVB copolymer was first utilised by D'Alelio (29)
to produce a strongly acidic cation exchange with a basic structure
given in Figure 2.01 A. Subsequently strong base anion exchangers
were prepared by chlormethylating then aminating the PS/DVB copolymer
(30,31). The basicity of the anion exchanger could be varied by
aminating with different amines (32). A typical structure is given
in Figure 2.01 B. The chlormethylation stage also introduced
methylene bridge crosslinks into the resin structure.

The second copolymer type, based on acrylic acid is in two different
forms. A weakly ionised cation exchanger can be prepared from
acrylic or methacrylic acid crosslinked with DVB (20, 23). The acrylic
anion exchanger is prepared from an acrylamide, also crosslinked with

DVB (33,34); a strongly basic example is depicted in Figure 2.01 C.

Figure 2.01 D shows a less commonly used styrene copolymer used for anion exchangers which utilises only methylene bridge crosslinking (35).

Early resins were granular products but PS/DVB copolymers were accompanied by the development of suspension polymerisation which produced spherical bead form resins. Beads can be prepared in diameters ranging from several um to several mm but commercial resins for water treatment normally have a size range between 0.3 and 1.2 mm diameter.

For the purposes of the studies described in this thesis the only resins considered are strongly acidic sulphonated PS/DVB cation exchangers and strongly basic anion exchangers with benzyl trimethyl quaternary ammonium functional groups (called type I groups).

2.2.2 MATRIX TYPES

Early workers with synthetic ion exchangers considered the polymer structure to be a regular uniformly crosslinked matrix in three dimensions and likened it to a water permeable gel; hence the term 'gelular' resin used to describe the type of resin structure that exhibits no distinct porosity yet allows the migration of counter ions. It was later shown that the structure was not regular but had areas of greater and lesser crosslinking and also involved chain entanglement (36, 37). The term 'microporous' has also been used for gelular resin matrices.

The amount of crosslinking incorporated into a resin will influence its moisture content, its swelling when converted from one form to another, its preference for one ion relative to another and its physical strength.

In the early 1960's a new type of matrix was introduced, known as 'macroporous' or 'macroreticular' (38). This type of resin had a distinct physical porosity that could be observed under the electron

microscope (39) and could be measured by mercury porosimetry or gas adsorption (40, 41). This matrix type is produced by copolymerising styrene and DVB in the presence of a solvent in which the monomer is soluble but the polymer is not. This caused the production of numerous gelular microspheres that agglomerated and fused together into bead form leaving a distinct porosity in the channels between the agglomerates (42). By adjusting the polymerisation conditions the pore size of the matrix could be varied. Macroporous versions of thePA/DVB polymer are also available. Typical pore diameters for PS/DVB macroporous resins commonly used in water purification are between 5 and 50 nm (40, 43, 44). More recently macroporous resins with a different type of macroporosity have been described and manufactured (45).

The presence of moderate degrees of macroporosity gave macroporous resins much greater physical strength than their gelular counterparts, and this has led to their extensive use in condensate purification plants where the operating conditions are physically more demanding. However highly macroporous resins can be extremely weak (46). The presence of macroporosity also means a loss of exchange capacity compared to a similar volume of gelular resin: the macropores replace active exchange polymer.

Polymers with methylene bridge crosslinking (Figure 2.01 D) are claimed to have a more regular gelular matrix that is termed iso- or homo- porous.

2.3 ION EXCHANGE IN WATER PURIFICATION

To simplify the presentation in this and subsequent sections consideration is   given to strongly acidic and strongly basic (type I) exchangers only, as these types are used in most water purification plants, particularly mixed beds. Many of the concepts also apply to weakly ionised exchangers but their exact mode of operation and application are adequately described elsewhere (23, 25).

The discussion is also confined to the operation of fixed bed ion exchange installations where the bead form exchange resins are held

in a closed vessel, normally cylindrical steel with rubber lining.
The vessel has a suitable pipework for the introduction and distri-
bution of raw water and regenerants and for collecting the treated
water (25). Normal water flows are downward through the resin bed.
Other modes of ion exchanger utilisation such as continuous counter
current operation, fluidised bed or suspended bed operation are
generally used for more specialised applications such as metal
recovery (47, 48, 49, 50).

2.3.1 <u>SELECTIVITY</u>

The major reason for the successful application of ion exchange to
water purification is that the exchangers show a preference for one
ion relative to another. Strong acid cation exchangers will
preferentially exchange hydrogen ($\overline{H}^+$) ions for most other cations
while strong base anion exchangers show a preference for most anions
relative to hydroxyl ($\overline{OH}^-$) ions. Therefore, if an aqueous salt
solution (eg sodium chloride) is passed through successive beds of
hydrogen form strong acid cation exchanger and hydroxyl form strong
base anion exchanger the following reactions occur.

$$\overline{H}^+ + NaCl(aq) \rightleftharpoons \overline{Na}^+ + HCl\ aq \quad \dots\dots\dots(2.1)$$

$$\overline{OH}^- + HCl(aq) \rightleftharpoons \overline{Cl}^- + HOH \quad \dots\dots\dots(2.2)$$

$$\overline{H}^+ + \overline{OH}^- \rightleftharpoons H_2O \quad \dots\dots\dots(2.3)$$
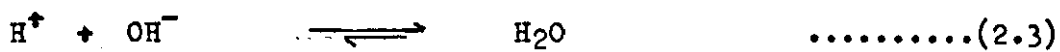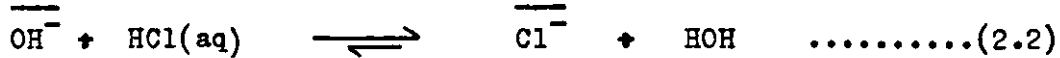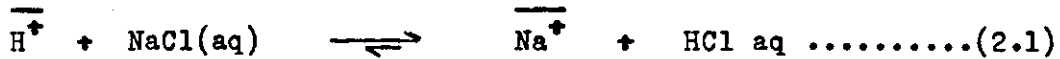
(The notation $\overline{H}^+$, $\overline{Na}^+$ etc indicates an ion within the exchanger phase,
non barred ions are in the aqueous phase).

The nett result is the removal of the salt from solution and its
replacement by an equivalent amount of water.

As reactions 2.1 and 2.2 are both equilibria the law of mass action
can be applied and an equilbrium selectivity coefficient, K, can be
defined. For the general uni-uni valent exchange reaction

$$\overline{A} + B \rightleftharpoons \overline{B} + A \quad \dots\dots\dots(2.4)$$

$$K_A^B = \frac{[\overline{B}][A]}{[\overline{A}][B]} \quad \dots\dots\dots(2.5)$$

The values of $[\overline{A}]$ $[\overline{B}]$ etc can be expressed as either equivalent ion

TABLE 2.01 $K_{H^+}^{M^+}$ - SELECTIVITY OF SULPHONATED STYRENE/DVB CATION EXCHANGER FOR MONOVALENT CATIONS

CATION	8% DVB	12% DVB
H^+	1.0	1.0
Li^+	0.85	0.81
Na^+	1.5	1.7
NH_4^+	1.95	2.3
K^+	2.5	3.05
Rb^+	2.6	3.1
Cs^+	2.7	3.2

TABLE 2.02 $K_{OH^-}^{A^-}$ -SELECTIVITY OF GELULAR STYRENE/DVB STRONG BASE ANION EXCHANGERS (TYPE I) FOR MONOVALENT ANIONS

ANION	K_{OH}^A
OH^-	1.0
F^-	1.6
$CH_3CO_2^-$	3.2
HCO_3^-	6.0
Cl^-	22.0
Br^-	50.0
NO_3^-	65.0
HSO_4^-	85.0

Data for Tables 2.01 and 2.02 taken from Ion Exchange Manual (1969) published by Diamond - Shamrock Corp. Redwood City, California, USA.

concentrations, equivalent ion fraction, mole fractions (20), and for uni - uni valent exchange all give almost identical values of K_A^B. Ion activities are the more correct thermodynamic parameter to use but the activity of an ion within an exchanger must be estimated from other properties of the resin/water system. No variations of K_A^B occur with changes in the aqueous phase concentration but small differences do occur with the relative proportions of A and B in the exchanger phase (51). Hence K_A^B is a coefficient and not a constant. If $K_A^B > 1$ then B is preferred to A and the magnitude of preference is proportional to the magnitude of K_A^B. If the values of K_A^B for different ions are expressed relative to one particular ion eg H^+ or OH^- a selectivity sequence can be defined. Table 2.01 gives such a sequence for univalent cations ($K_{H^+}^{M^+}$) and Table 2.02 for univalent anions ($K_{OH^-}^{A^-}$). Anion exchanger selectivities may also be expressed relative to a chloride ion standard state.

The definition of K for uni - di valent exchange is on a similar basis. For the reaction

$$2\overline{C} \quad + \quad D^{2+} \quad \rightleftharpoons \quad \overline{D}^{2+} \quad + \quad 2C \qquad \ldots\ldots(2.6)$$

$$K_C^D \quad = \quad \frac{\left[\overline{D}\right]\left[C\right]^2}{\left[\overline{C}\right]^2\left[D\right]} \qquad \ldots\ldots(2.7)$$

However, the presence of squared terms introduces a dependance on the relative concentrations of the ions in both solution and the resin phase. For reaction 2.6, going left to right, K_C^D will become smaller as the fraction of C in the resin phase $\left[\overline{C}\right]$ increases and larger as the concentration of C in the aqueous phase $\left[C\right]$ increases. Any definition of K_C^D for uni - divalent exchange must be accompanied by the concentration conditions under which it was determined. It should also be noted that expression of concentration in equivalent or molar terms no longer give the same values of K_C^D.

2.3.2 FACTORS INFLUENCING ION SELECTIVITY

Ion selectivity is concerned with the interaction of three charged, hydrated species: the fixed ion of the exchanger, the counter ion associated with the fixed group and the ion in solution that will be exchanged.

2.3.2.1 Ion Hydration

Early workers noted that for monovalent alkali metal cations their
selectivity on sulphonated PS/DVB exchangers were inversely proport-
ional to their hydrated ion radius (52,53) and that small volume
changes occurred on conversion from one ionic form to another. This
led to the concept of matrix swelling as a governing factor in
determining relative selectivity (20,54,55). Large hydrated ions,
such as H^+ or Li^+ , required more energy to stretch the crosslinked
matrix than a smaller ion such as Cs^+. Hence the exchanger exhibited
a lower selectivity towards large hydrated ions. As the crosslinking
increased the matrix became less able to expand and the relative
selectivity for small ions increased. Application of the hydrated
ion radius theory to anion exchangers worked for the halide ions
but not for other anions (56).

Reichenberg (56) proposed that selectivity is governed by the free
energy changes that occur during exchange, which involve both ion-
ion interactions and the free energies of hydration of the exchanging
counter ions. Reichenberg infers that the counter ions remain fully
hydrated but that hydration water has to be moved aside to permit a
close approach of the fixed and counter ions. For strong acid and
strong base exchangers, where the fixed groups are large, it was
proposed that the exchanger is more selective for the counter ion
with the lower free energy of hydration. Determination of hydration
numbers of ions in exchangers show them to be lower than in aqueous
solution (53), therefore hydration water is probably stripped from
the counter ion going from the aqueous to the resin phase. However,
this still indicates selectivity will be governed by free energies
of hydration.

Diamond and Whitney (57) considered that ion - water interactions in
both the resin and aqueous phase should be considered, particularly
the effect of the exchangingions on the structure of water (58).
They proposed that in the exchange of two ions the aqueous phase
showed a preference for the ion with the greatest hydration require-
ment while the ion with lower hydration requirement was selectively
'rejected' into the resin phase. This was called a hydrophobic effect.

It is probable that all these factors contribute to ion selectivity; ion hydration governing the basic order of ion selectivity and matrix swelling influencing the changes in relative selectivity with crosslinking.

2.3.2.2 Electroselectivity

An observed feature of ion exchangers is their preference for ions of higher valence compared to monovalent ions of similar size. Helfferich (20) attributes this to the Donnan potential set up at the surface of any ionised exchanger. The Donnan potential arises as counter ions try to leave the exchanger surface. This upsets the electroneutrality and a potential difference is set up between the exchanger surface and the adjacent aqueous layer which prevents further counterions leaving. The exchanger surface has a charge opposite to the counter ion and exhibits a larger attraction for ions of higher valence.

It is probable that charge density of the ion also plays a part and the free energy state of the exchanger with two fixed groups associated with a single ion must also be considered.

2.3.3 REGENERATION AND EQUILIBRIUM LEAKAGE

From the selectivity sequences in Tables 2.1 and 2.2 it can be seen that passing a raw water successively through a bed of H^+ form cation exchanger form and OH^- form anion exchanger form would produce a pure water free of all ionic impurities. In theory this is true but in practice the treatment of raw water in a two bed system leaves a residual of ionic impurities in the treated water.

As noted earlier ion exchanger reactions are equilibria that are favourable for the purification of water. However, when sufficient raw water has passed through the bed of ion exchange resin so that its exchange capacity is exhausted it is not discarded but is regenerated back to the H^+ or OH^- form by forcing the equilibrium in an unfavourable direction. Common regenerants are a strong mineral acid, hydrochloric or sulphuric, for the cation exchanger and a strong base,

normally sodium hydroxide, for the anion exchanger. Typical regenerant concentrations are between 0.3 and 1.0 equivalents per litre.

Because the equilibrium is being forced against the preferred direction the regeneration processes are not very efficient in the use of regenerant chemicals and for economic reasons it is common practice to operate a bed of ion exchange resins by regenerating only 30 -50% of the available exchange capacity. Therefore, a significant percentage of the exchange sites on a working exchanger are associated with impurity ions. In the most common operating mode with both exhaustion and regeneration flows passing downward through the bed (co-flow regeneration) the exchanger at the top of the bed becomes most highly regenerated while that at the bottom of the bed contains the highest percentage of unregenerated sites.

2.3.3.1 Equilibrium Leakage

If a solution of a salt of a strong acid and strong base, eg sodium chloride, is passed onto a partially regenerated sodium form cation exchanger the influent sodium is completely exchanged at the top of the bed (15) producing a dilute hydrochloric acid solution. The acid then contacts the partially exhausted resin lower in the bed and reverses the exchange equilibrium (2.1) so that sodium ions are released into the decationised water. This is called equilibrium leakage and for any given influent ion concentration, resin selectivity and degree of regeneration the equilibrium leakage concentration can be calculated.

The water leaving the cation exchange unit contains a strong acid (HCl) plus some sodium ions. On passage through a partially regenerated chloride form anion exchanger the influent chloride is exchanged for hydroxyl and the residual sodium forms sodium hydroxide. Once again this is a dilute regenerant solution that will reverse equilibrium 2.2, giving rise to equilibrium leakage of chloride. Thus a normal two bed cation - anion exchange system will produce water with $1 - 5$ mg kg^{-1} impurities with typical co-flow regeneration conditions.

2.3.3.2 Counter Current Regeneration

The simple expedient of passing the regenerant through the resin
bed in the opposite direction to the service flow of water, counter
current regeneration, ensures that the resins at the bed outlet are
maintained in a highly regenerated state. This has the effect of
reducing the equilibrium leakage by one to two orders of magnitude
compared with co-current regeneration. However, it is necessary to
ensure that the highly regenerated resins remain at the bed outlet
during regeneration which requires a greater degree of engineering
sophistication (49, 50, 59, 60, 61, 62).

2.3.3.3 Mixed Beds

Two bed exchange of a typical British raw water results in
$0.1 - 10$ mg kg^{-1} Na and $0.05 - 0.5$ mg kg^{-1} SiO_2 as the main impurities.
(Silicate is the anion with the lowest selectivity and is, therefore,
the most likely to arise as a result of equilibrium leakage. Silicates
are normally quoted as SiO_2). The treated water has conductivities
between 1 and 100 μS cm^{-1} whereas for boiler make up a conductivity
of $< 0.15 \mu S$ cm^{-1} and silica $< 0.02 \mu g$ kg^{-1} are required.

The further purification may be effected by a second pair of cation
and anion exchange beds (63) or simply a further cation exchange
unit (62) but in the majority of cases, certainly in British and
American practice, the final purification stage is a bed containing
an intimate mixture of H^+ form strong acid cation and OH^- form strong
base anion exchange resins, known as a mixed bed.

Both cation and anion ion exchange reactions occur simultaneously
in adjacent exchange resin beads. Therefore there is no opportunity
for the generation of significant concentrations of acid or alkali that
could give rise to equilibrium leakage. Both exchange equilibria are
pushed to virtual completion by the continued production of essentially
un-ionised water. With a mixed bed it is possible to produce water
of almost absolute purity, approaching the theoretical minimum
conductivity of 0.054 μS cm^{-1} at 25 $^{\circ}C$.
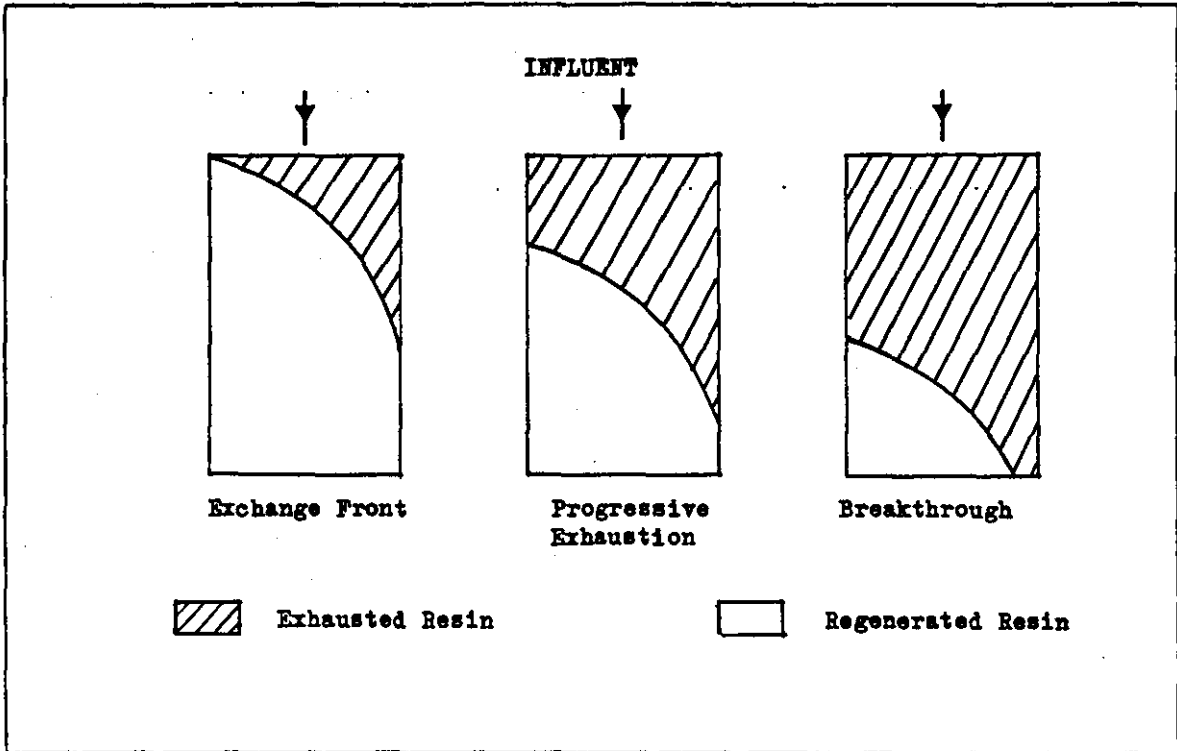
PROGRESSION OF EXCHANGE FRONT DURING EXHAUSTION
SHORT EXCHANGE ZONE
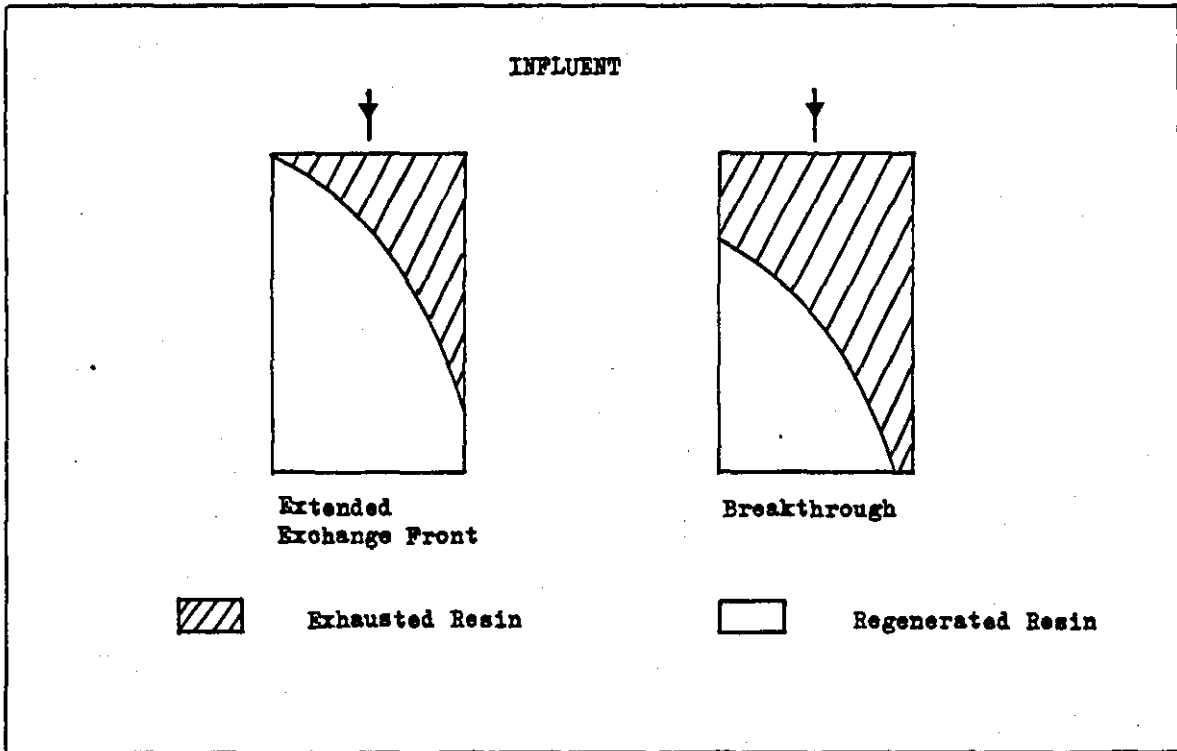
PROGRESSION OF EXCHANGE FRONT
EXTENDED EXCHANGE ZONE

2.3.4 EXCHANGE KINETICS AND KINETIC LEAKAGE

The discussion of equilibrium leakage assumed that the water passed
through a bed of exchanger sufficiently slowly for the equilibrium
to be established, such that influent impurity ions are completely
removed and ions constituting equilibrium leakage were those remaining
on the exchanger after regeneration. However, if the nominal resid-
ence time for water passing through the bed is insufficient for the
equilibrium to be fully established some of the influent impurities
will pass through the bed without exchange and will appear as
effluent impurities. As the residence time is flow rate dependant
leakage of this nature is termed 'kinetic' leakage.

2.3.4.1 Zone of Exchange

As the establishment of an ion exchange equilibrium is not instan-
taneous, the exchange of impurities from an influent passing through
a bed of exchanger takes place over a finite depth of ion exchange
resin, known as an exchange zone. The zone is defined by stipulating
either the impurity concentrations at its upper and lower limits,
or a preset degree of exchange eg 99% removal of influent ions.

The zone of exchange is illustrated in Figure 2.02 where the hatched
portion represents exhausted resin. As the exchanger becomes
exhausted the exchange zone moves down the bed, until the front of the
exchange profile breaks through and impurities appear in the treated
water. If the equilibrium is slow to be established, or if high flow
rates reduce the residence time within the bed, the exchange zone
will become extended (Figure 2.03) such that when breakthrough occurs
there is a relatively high proportion of regenerated resin left
unused. At very high flow rates or with very slowly established
equilibria, the exchange zone may exceed the available depth of
resin and breakthrough will occur immediately the exchanger is put
into service.

The term kinetic leakage is generally reserved for those situations
where a long exchange zone causes premature or continuously unaccept-
able ionic leakage and where only a small proportion of the available

exchange capacity has been utilised. Kinetic leakage is sensitive to operating flow rate and is, therefore concerned with those factors that influence and control the overall rate of ion exchange.

2.3.4.2 Factors Influencing Overall Rate of Exchange

The ion exchange process is generally considered to consist of three distinct phases each of which may be rate controlling on its own or in combination with another. The three phases are:-

i)   the diffusion of ionic species between the bulk solution and the surface of the exchanger bead

ii)   the actual exchange reaction between a pair of counter ions at any particular exchange site

iii)   the diffusion or transport of counter ions between the exchanger bead surface and the interior of the bead.

Control by (i) is generally termed liquid boundary layer or liquid film diffusion control from the concept of a static Nernstian film of liquid surrounding each resin bead as water passes over them. Control by (ii) is known as reaction rate control while the term particle diffusion control is used where (iii) is the overall controlling factor.

Helfferich has dealt comprehensively with the conditions that determine which of the three phases is rate controlling and he proposed a simple criterion for estimating whether film or particle diffusion was the operating factor (20). Reaction rate control is only considered to be significant where complex ion formation is involved or where exchange occurs on weakly ionised groups (20, 23).

For the exchange of fully ionised species by strongly ionised anion or cation exchangers Helfferich's criterion predicts that film diffusion will be controlling in the dilute solutions normally encountered in water purification where the exchange equilibria are favourable, while particle diffusion will be controlling during regeneration involving much higher solution concentrations and unfavourable equilibria.

2.3.4.3 Film Diffusion Control

Diffusion across the Nernstian film is controlling when the rate
of transport of ions to the bead surface is slower than their
subsequent exchange and diffusion into the exchange resin. Therefore
a concentration gradient is set up across the film and diffusion
of ionic species will obey Ficks Laws (64). For example,

  an exchanging species (A) has a concentration C_A in the bulk
solution and C_A' at the bead surface. Then

$$J_A = \frac{D_A \, \Delta C_A}{\mathcal{T}} \qquad\qquad \dots\dots\dots 2.10$$

where J_A is the ionic flux, D_A the diffusion coefficient for ion A,
$\Delta C_A = C_A - C_A'$, and $\mathcal{T}$ is the film thickness. The ionic diffusion
coefficient can be calculated from conductivity data using the
Nernst–Hartley equation (64)

$$D_A = \frac{RT}{F^2} \, \frac{\lambda_A}{|Z_A|}$$

where R is the gas constant, T temperature $^\circ K$, F the Faraday constant
λ_A the equivalent conductance and Z_A the charge of ion A. Empirical
equations for calculating the film thickness have been given by
Gilliland (66) and Glueckauf (67).

As a single ion cannot diffuse through a liquid without an accompanying
co-ion, electrolyte diffusion coefficients must also be considered (65)
and, if the electrolytes associated with the exchanging counter ions
have differing diffusivities, the net diffusion rate is a value
intermediate between the two individual rates (20).

The liquid film diffusion coefficient of an ion is about an order
of magnitude greater than exchanger particle diffusion coefficients
for the same ion (68). This explains why film diffusion control
only occurs in dilute solutions where the shallow concentration
gradient across the film produces a small ionic flux at the bead
surface.

2.3.4.4 Particle Diffusion Control

Particle diffusion control occurs when the rate of arrival of counter
ions at the bead surface is faster than they can diffuse to the
interior of the bead. There is no concentration gradient across
the liquid film but there is one within the exchanger itself.

Diffusion coefficients within ion exchangers cannot be measured
directly but can only be inferred from radio tracer self diffusion
measurements (69) or from the rate of exchange of concentrated
solutions such as regenerants (70). The diffusivity of ions within
the exchanger phase will be influenced by matrix crosslinking, the
regularity of the matrix, the physical porosity and the total exchange
capacity, ie dispersion, of exchange groups. The exact mechanism of
ion transport is not known either. It may be hydrated ion mobility
within the aqueous phase in the exchanger or it may be a 'shuttle'
from one exchange group to the next as suggested by Liberti et al (71).

2.3.4.5 Kinetic Mechanisms and Performance Predictions

To be able to predict column performance it is necessary to know
which of the rate determining factors is controlling. One experi-
mental approach is the stirred batch technique in which a small
sample of exchanger is stirred vigorously in a reaction vessel to
eliminate concentration gradients in the bulk solution (72). The
rate of exchange can be followed by monitoring the appearance or
disappearance of the exchanging species in the bulk solution. The
'stop reaction' technique has been used to identify whether film or
particle diffusion is taking place (20). Stirred batch experiments
have also been used to determine the self diffusion coefficients
of anions or cations within their respective exchanger polymers (69,73).

The stirred batch technique does not take account of the hydrodynamic
influences operating in resin beds, therefore, column tests have been
used to provide kinetic information on packed bed operations. The
most common approach has been to continuously add a solute to the
influent water and then monitor its leakage and breakthrough over
a period of time, although Boyd et al (74) used radioactive tracers
operating at very high flow rates through shallow beds to achieve

short contact times. Most of the work has been carried out for single
component exchange for monovalent cations under favourable equilibrium
conditions (ie $K_A^B > 1$) and with influent solute concentrations in
the range 0.01 M - 1.0 M.

A general data analysis technique first proposed by Michaels (75),
has been to assume an asymptotic exchange front with an exchange
zone of constant depth that progresses down the bed with exhaustion
of the exchanger (Figure 2.02). Several groups of workers have
shown this assumption to be reasonable (66, 76,77,78) and their
results indicate that below 0.01 M solute concentrations film
diffusion is the predominant rate controlling factor while above
0.1 M particle diffusion plays an increasing role. Theoretical
treatments to describe film diffusion have been prepared for an
asymptotic exchange front (77, 78, 79) and from thermodynamic
considerations (80). Gilliland and Badour (66) derived an empirical
expression for the notional film thickness in a packed bed, and
both Gilliland et al and Moisson et al (76) noted that the length of
the exchange zone increased with increasing flow rate.

Multi component exchange, giving rise to several independant but
interelated exchange fronts in one bed has been described theoret-
ically (79, 81, 82) and Gregory (83) investigated the equilibria
and kinetics of a ternary chloride / sulphate / phosphate system.

Kinetics controlled by particle diffusion have also been examined.
Schmuckler et al (84) described a shell progressive exchange
mechanism while the examination of unfavourable equilibria involved
in ion exchanger regeneration has given data on particle diffusion
coefficients of common anions (70). Liberti et al (71, 85) have
reported that in $Cl - \overline{SO}_4$ exchange the rate of the exchange reaction
itself may be an additional rate controlling factor.

Application of these methods and rate equations has enabled predict-
ions to be made of column leakage, capacity and breakthrough
characteristics (67, 68). It is also reported that for a given
influent mass flow rate and exchanger volume the height - diameter
relationship of a packed bed will not affect its performance for
pre set breakthrough criteria (86).
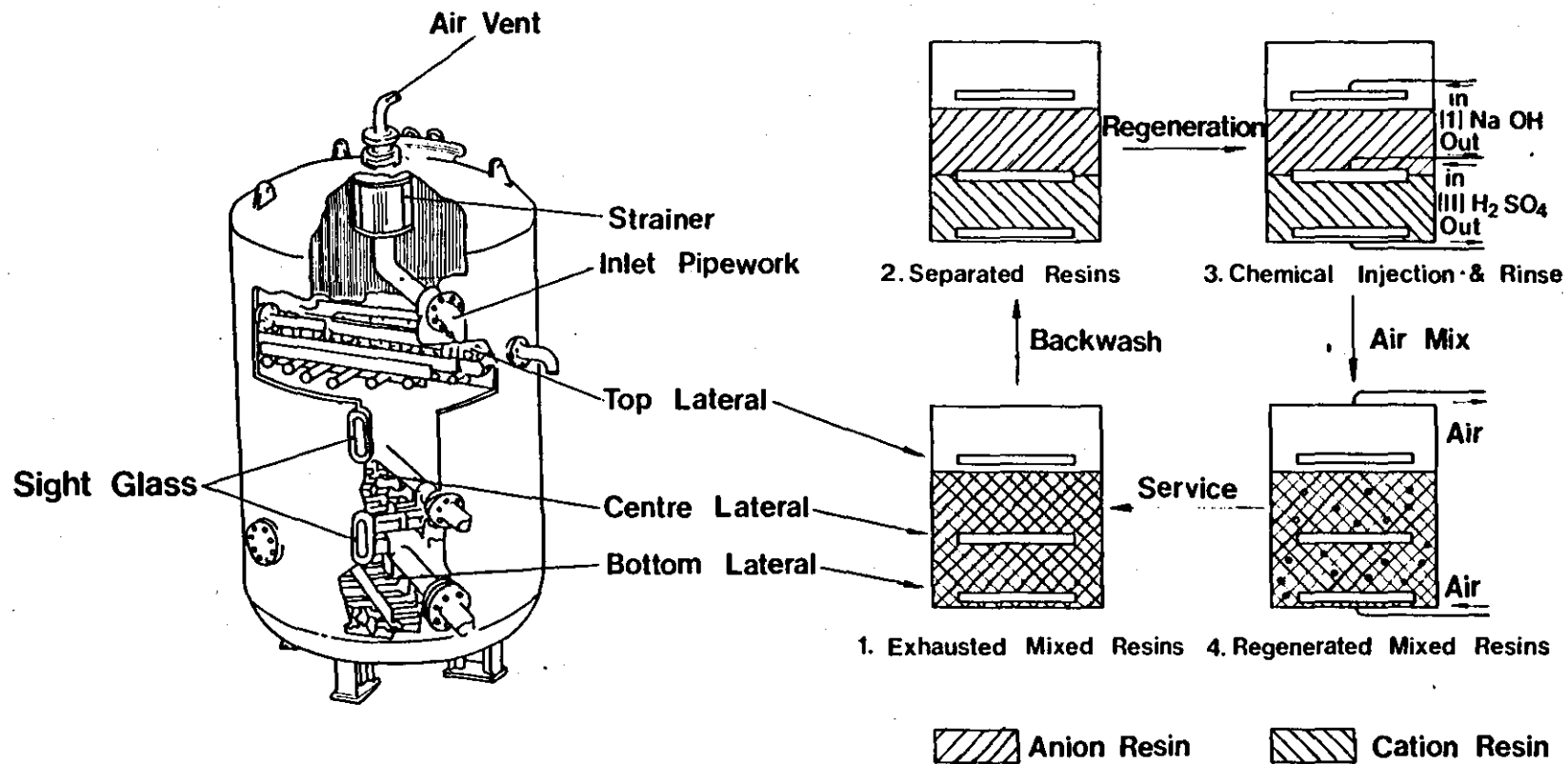
Typical Mixed Bed Sectioned View.

Labels: Air Vent, Strainer, Inlet Pipework, Top Lateral, Sight Glass, Centre Lateral, Bottom Lateral

Mixed Bed Regeneration Sequence-Schematic

2. Separated Resins
3. Chemical Injection & Rinse

[I] Na OH
In / Out

[II] $H_2 SO_4$
In / Out

Regeneration

Backwash

Air Mix

1. Exhausted Mixed Resins

Service

4. Regenerated Mixed Resins

Air
Air

////// Anion Resin   \\\\\\ Cation Resin

FIGURE 2.04   TYPICAL MIXED BED AND REGENERATION SEQUENCE.

2.4 MIXED BED DEVELOPMENT AND DESIGN

It was noted earlier (2.3.3.3) that a simple two stage deionisation process could not economically produce high or ultra pure water and that the most common approach was to use an ion exchange mixed bed to remove the traces of ionic leakage from the two stage process. Whilst the initial deionisation processes can vary in efficiency the performance of the final mixed bed governs the purity of water produced by ion exchange plants. Scott (87) has produced a general history of ion exchange mixed beds. This section will deal briefly with relevent aspects of mixed bed history and their application to water purification for power generation.

2.4.1 EARLY DEVELOPMENT

The first recorded use of mixed anion and cation exchangers used weakly acidic and basic resins and was non regenerable (88, 89). The first use of strongly acidic and basic exchangers was reported by Kunin and McGarvey (90) and was called a mono-bed as the initial aim was to replace two bed deionisation with a single vessel system. Water quality was not a major consideration at this time (1951). The anion exchanger was separated from the more dense cation exchanger by backwashing and was hydraulically transferred to a separate vessel for regeneration. The cation exchanger was regenerated in the service vessel. After regeneration the anion exchanger was returned to the service vessel and the two resins mixed by passing air upwards through a resin water slurry. A second patent by Kunin and McGarvey (91) described a mixed bed where regeneration of both exchangers took place within the service vessel, ie in situ. Two resins, separated by backwashing, formed two layers and a regenerant collector/distributor was located at the interface of the separated resins. Figure 2.04 shows a cut away drawing of a typical mixed bed unit with in situ regeneration. Alongside is a diagram of the regeneration sequence.

It was soon found that the original concept of a single mixed bed replacing a two bed system required more frequent regeneration and higher operating costs. There were also problems with the precipitation of insoluble metal hydroxides during regeneration. These operating difficulties led to the approach of using a two bed

cation-anion exchange system followed by a mixed bed. The duty of
the mixed bed was to remove the trace impurities leaking from the
two bed system. The mixed bed received a relatively small ionic
load and regeneration was more infrequent. The majority of modern
water purification plants adopt the cation-anion exchange plus mixed
bed principle, although some installations with high quality raw
water or low output requirements still adopt a mixed bed only approach.

2.4.2 MIXED BEDS FOR BOILER FEEDWATER PURIFICATION

In the power generation industry ion exchange is used for both
purification of the water used to make up steam/water circuit losses
and in certain instances purification of all or part of the condensate
flow that is returned as boiler feedwater. All these applications
utilise mixed beds but the water purity and operating criteria vary
between the different plant requirements.

2.4.2.1 Make-up Plant

The water purity required from boiler feedwater make-up purification
plants is a conductivity of <0.15 or $0.20\ \mu S\ cm^{-1}$ and a silica
concentration $< 0.020\ mg\ kg^{-1}\ SiO_2$. Most of these plants utilise
in situ regenerated mixed beds, although in a minority of plants
all of the mixed bed resin is transferred hydraulically to a separate
external regeneration plant. In such plants a single regeneration
system will serve a number of mixed bed service units.

Most make-up water treatment plants are designed to meet the average
daily requirements of a power station eg $4.5 \times 10^3\ m^3$ per day for a
2000 MW fossil fueled station. Any peaks in demand are met from
large storage tanks that are continuously topped up with purified
water. These reserve feedwater tanks also serve as level control
tanks for the condenser and may receive contaminated water. There-
fore, in modern power stations the reserve feedwater is passed through
the mixed beds before it is admitted to the boiler feed system. Such
mixed beds are designed to meet peak demand in water requirements,
operating at flow rates up to $55\ m^3\ m^{-2}\ h^{-1}$ whereas mixed beds
designed for treating the two bed leakage impurities alone operate

at flow rates in the range 15 - 30 m^3 m^{-2} h^{-1} . The volume ratio of the mixed exchangers also varies, depending on the expected leakage from the preceding two bed system. Anion : cation exchanger ratios between 3.5 : 1 and 1 : 1 have been used in make-up mixed beds. The excess of anion exchanger is to ensure adequate silica removal.

2.4.2.2 Condensate Recovery Systems

When a boiler is started from cold the feedwater rapidly exceeds the target impurity concentrations, necessitating dumping of large volumes of relatively pure water that are replaced by high purity make-up water. To reduce operating costs it has been recent practice to divert the dumped water to the make-up water treatment plant ahead of the mixed beds. Thus the mixed beds purify this water and return it as boiler feed. However, the mixed beds have to run at higher flow rates at such times, up to 80 or 90 m^3 m^{-2} h^{-1}, and treat a water containing about 0.5 mg kg^{-1} NH_3, added as a conditioning agent to the feedwater, in addition to the other impurities. The recovered condensates may also contain particulate impurities, metal oxides as well as traces of lubricating oils. In some plants separate mixed beds treat recovered condensates to avoid contaminating the make-up mixed beds with particulate or oil impurities, in other plants the make-up mixed beds are protected by in line filters.

2.4.2.3 Full Flow Condensate Purification

As noted in 1.3 certain designs of boiler, notably the once through type, require ultra pure feedwater to ensure their continued operation. If the boiler-turbine-condenser circuit were a totally closed loop there would be little problem in maintaining the desired low levels of ionic impurities, although particulate oxide species may be present. However, it is very difficult to prevent small leakages of cooling water into the condensate so that the feedwater is contaminated. The only way to guarantee ultrapure boiler feed-water has been to continuously purify all the condensate before it returns to the boiler.

The only available technique for purifying the vast quantities of

3 x 50% cation exchange - mixed bed streams per turbine. Two in service, one spare available on either turbine.

2 x 50% mixed beds per turbine 1 x 50% mixed bed available to either unit. Spare charge of regenerated resins. Post filtration.

2 x 50% mixed beds per turbine. Single spare charge of regenerated resins held in reserve.

3 x 33% mixed beds per turbine. 2 x 50% while third bed regenerated. Prefiltration.

C	Cation exchange unit	S	Spare charge of resin
M	Mixed bed	pcf	Pre-coat filter.

FIGURE No. 2.05   TYPICAL ARRANGEMENTS OF CONDENSATE PURIFICATION PLANTS.

water involved ($0.4 \text{ m}^3 \text{ s}^{-1}$ from a 660 MW AGR turbine) is ion exchange, and almost all condensate purification plant (CPP) use mixed beds as the major and often only purification stage. The mixed beds are sometimes preceded by a cation exchange unit and/or filter but many CPP mixed beds operate unprotected ie they also act as filters for particulate debris.

Recently, it has been common practice to use two mixed beds associated with each 500 or 660 MW unit, together with a single spare mixed bed or spare charge of resins to cover for regenerations. Typical modern plant arrangements are given in Figure 2.05. To purify the large volumes of water the mixed beds are operated at very high flow rates, $100 - 120 \text{ m}^3 \text{ m}^{-2} \text{ h}^{-1}$, in beds as shallow as 0.9 m deep but in vessels up to 4 m diameter.

Not only once through boilers employ CPP. The incidence of condenser leaks at sea water cooled power stations with conventional drum boilers has led to the installation of full flow CPP at a number of them to ensure their continued availability. Currently there are 11 power stations in England and Wales with full flow CPP. Of these 10 are at sea water or esturine cooled stations and 3 are drum boiler plant. They involve a total installation of 78 CPP mixed beds the majority of which are expected to continuously provide water with a conductivity $< 0.08 \text{ }\mu\text{S cm}^{-1}$ and less than 2 $\mu\text{g kg}^{-1}$ each of sodium, sulphate and chloride ions. (242)

Pressurised water reactors (PWR) have had boiler corrosion due to poor quality feedwater and mixed bed CPP are now being fitted to many of them. Boiling water reactors also use CPP mixed beds to control both radioactive and dissolved impurities.

2.5 CONDENSATE PURIFICATION

2.5.1 DEVELOPMENT

The first CPP mixed beds were installed in the early 1950's (92) mainly to overcome high boiler water impurity levels resulting in silica deposits on the turbine blades, and to minimise blow down

hence make up water requirements (93). The early plants operated at
the low flow rates of conventional make-up plant and provision was
made for filtration of the condensate prior to the mixed bed treatment.
The advent of super-critical pressure boilers gave serious problems
with copper deposition in the high pressure stages of the turbine (94,
95) due to copper pick-up from the copper alloy tubes in the boiler
feed system. The copper concentrations in the feed water were reduced
by installing partial and later full flow CPP until, in later plant
designs, steel tube replaced the copper alloys. The only two super-
critical boiler/turbine units in Britain employed full flow CPP with
deep sand filters preceding 1.8 m deep mixed beds in 2.4 m diameter
vessels operating, at $75 \ m^3 \ m^{-2} \ h^{-1}$ (96).

The development from partial flow to full flow condensate purification
was due to two main factors. The progressive lowering of the feed
water impurity levels meant that even a very small condenser leak
at a sea water cooled station could give sufficient impurities for a
50% CPP to be unable to meet the feed water impurity targets. Also
the incidence of condenser leaks at certain stations was such that
continuous operation could only be achieved economically if a full
flow CPP was present to treat all the condensate.

2.5.2 FILTRATION

The use of filters preceding mixed beds was primarily to protect the
anion exchangers from metal hydroxide precipitation on their surface
during regeneration, which might affect their subsequent performance.
However, in the early 1960's Frazer et al (97, 98) showed that deep
mixed beds could operate successfully without pre-filtration and
could act as an effective filter in their own right. Unprotected
mixed beds were quickly adopted in the USA and special procedures
were developed for removing the particulate matter, mostly metal
oxides, (99, 100, 101). The first British operation of an unprotected
CPP mixed bed was monitored in 1969 (102) and the mixed bed was shown
to be a highly effective filter for particulate iron oxides. Other
workers made similar observations although the efficiency of filtration
varied with the nature of the oxide species to be filtered (101, 103).
A review of the operation of unprotected mixed beds in 1976 showed

that both filtration and ion exchange performance was generally satisfactory (104). More recently, evidence suggests that mixed bed protection by some form of filtration is desirable if not completely necessary.

2.5.3 AMMONIA REMOVAL

Most high pressure boilers are dosed with a volatile alkali to raise the feed water pH to 9.0 - 9.6 in order to minimise corrosion. The most commonly used reagent is ammonia although some operators use morpholine or other higher amines. Hydrazine is also added to the feed water to scavenge oxygen although a minority of boiler operators use neutral or slightly alkaline feed water with added oxygen. (105, 106, 107). In the boiler the hydrazine degrades to ammonia which, together with the dosed ammonia, passes into the steam phase and then condenses with the condensate. The CPP will remove this ammonia and, in the absence of condenser leaks, ammonia is the major ionic loading onto the CPP. Therefore, most CPP have an excess of cation exchanger over anion exchanger, either as a separate cation exchange unit preceding the mixed bed or by means of an unprotected mixed bed with a volumetric cation : anion exchanger ratio of between 1.5 and 3 to 1. Some plant operators have claimed that the highest purity water is obtained from mixed beds with an excess of anion over cation exchanger (108, 109, 110). However, for economic reasons the unprotected mixed bed with 2 :1 cation : anion exchanger ratio has been the most common CPP design.

2.5.4 AMMONIA CYCLE OPERATION OF MIXED BEDS

Using a CPP to remove ammonia is unproductive as the ammonia is immediately re-dosed to the purified feed water. Also at the higher pH levels, 9.4 - 9.6, (1.0 - 2.0 mg kg^{-1}NH$_3$) regeneration becomes more frequent as the beds exhaust rapidly. To overcome this some operators convert the mixed bed cation exchanger to the ammonium form and work in the NH$_4$/OH cycle as opposed to the conventional H/OH cycle.

NH$_4$/OH operation poses additional problems with equilibrium leakage

of both cations and anions. The selectivity coefficient $K_{Na}^{NH_4}$ is 0.75 ie the cation exchanger is more selective for ammonia than sodium. Therefore, any sodium left on the resin after regeneration will be slowly displaced into the purified condensate. To avoid residual sodium leakage very high acid regeneration levels are applied to the cation exchanger. Calculations show that for pH 9.6 operation less than 0.1% exchange sites must contain sodium ions to achieve below 1 μg kg^{-1} sodium leakage (111, 112).

In NH_4/OH cycle operation the whole mixed bed operates under alkaline conditions and the hydroxyl ions will induce equilibrium leakage of anions. Although $K_{OH}^{Cl} \sim 20$ it is still necessary to achieve a residual chloride ion on the anion exchanger of less than 4% sites to ensure leakage below 1 μg kg^{-1} chloride (111).

Despite the unfavourable ammonium - sodium exchange equilibrium a NH_4/OH bed does have a capacity for sodium exchange, but this is very dependant on the inlet concentration as ultimately all sodium taken up is displaced into the treated condensate again. Therefore, the operating phenomenon of sodium leakage humps or blips is a common feature of NH_4/OH cycle mixed bed operation (113, 114, 115, 116, 117, 118).

2.5.5 POWDERED RESIN MIXED BEDS

This discussion so far has been concerned solely with deep beds of bead form exchangers. Alternatively powdered resins may be used. When mixed together in a water slurry powdered anion and cation exchangers form a floc which can be coated onto a filter support medium (119, 120). The powdered resins are applied as a thin layer (2.5 mm) onto the support medium and are not regenerated when exhausted but are discarded and a new coating applied. The advantages of such a system are low capital cost combining both filtration and ion exchange in one unit and in CPP for BWR's powdered resins provide an easier method for disposal of radioactive species than the further processing of a regeneration liquor. The disadvantages of powdered resins for CPP is the low exchange capacity. They are not suitable for use at sea water cooled stations where quite a small condenser

leak can lead to rapid exhaustion (121, 122). Powdered resin mixed
beds can operate in the H/OH or NH$_4$/OH cycle. They have been installed
in two British CPP but operate either as a pre filter to deep mixed
beds or a post filter beyond deep mixed beds.

2.6 CPP DESIGN, OPERATION AND REGENERATION

In this section deep mixed beds only are considered. In a plant
incorporating deep cation exchange units the principles of design,
operation and regeneration are similar except for the need to
separate the two exchangers.

2.6.1 SERVICE VESSEL DESIGN

Early CPP mixed beds were similar to make up plant mixed beds
ie cylindrical vessels incorporating the necessary laterals and
headers for in-situ regeneration. As condensate flow rates increased
with generating unit size the vessel size became larger in diameter
and the bed depth shallower to minimise the pressure drop at the
higher operating flow rates. In-situ regeneration in a bed 3 m
diameter but only 0.9 m deep was not practical due to difficulties with
uneven resin separation and regenerant distribution. There were also
problems with regenerants leaking into the feedwater at certain
in-situ regenerated CPP (123). Therefore, the common practice is to
transfer the mixed resins from the service vessels to a central
regeneration facility where the vessel design is more appropriate
to regeneration (2.6.2).

Most service vessels are cylindrical with a minimum of internal
obstructions and have either a flat or slightly dished bottom.
Spherical and annular vessels have also been used (124, 125). The
bottom of the vessel has a system for collecting the treated water.
This can be a header and lateral system, a perforated plate, a
supported fine mesh or a drilled plate with nozzles in the holes.
Apart from the header and lateral system the other collectors form
a false bottom to the vessel, the water being extracted from a chamber
under the collector. Each bed outlet will have a resin trap to
prevent resin passing forward to the boiler where it may degrade to

Anion Exchanger

Cation Exchanger

Service Vessel

Separator
and
Regenerator
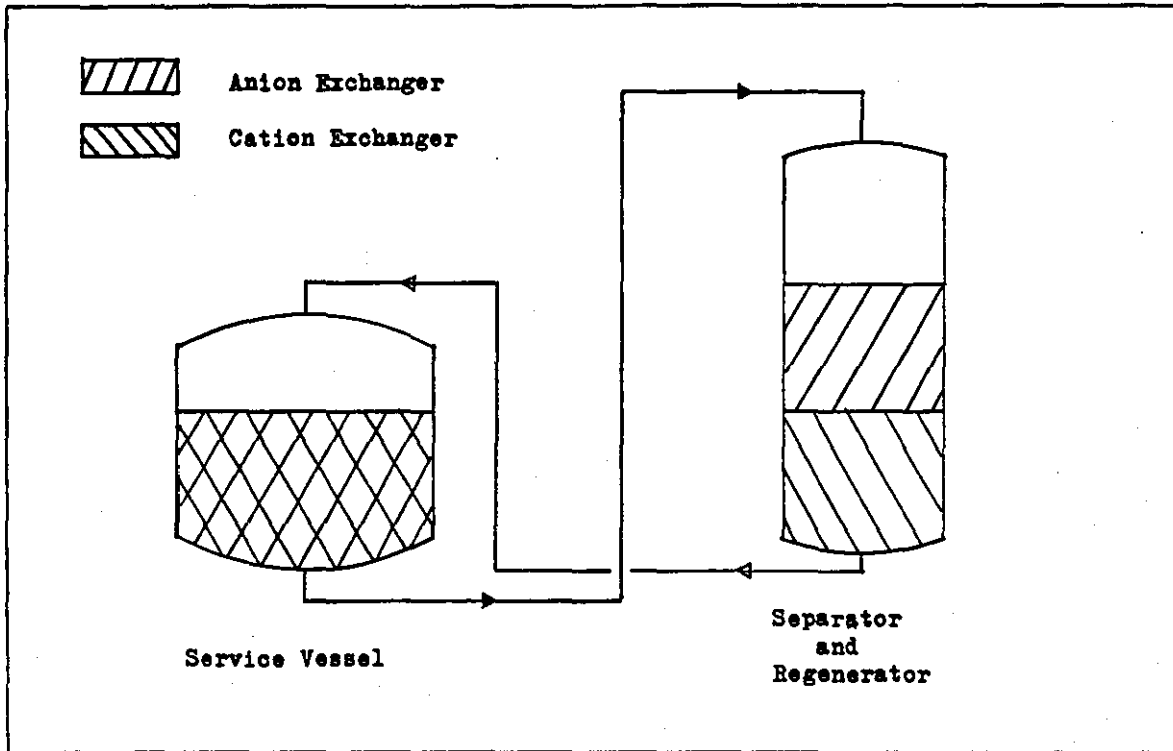
FIGURE
No. 2.06   EXTERNAL REGENERATION - SINGLE VESSEL

Anion Exchanger

Cation Exchanger

Service Vessel

Separator
and
Cation
Regenerator

Anion
Regenerator
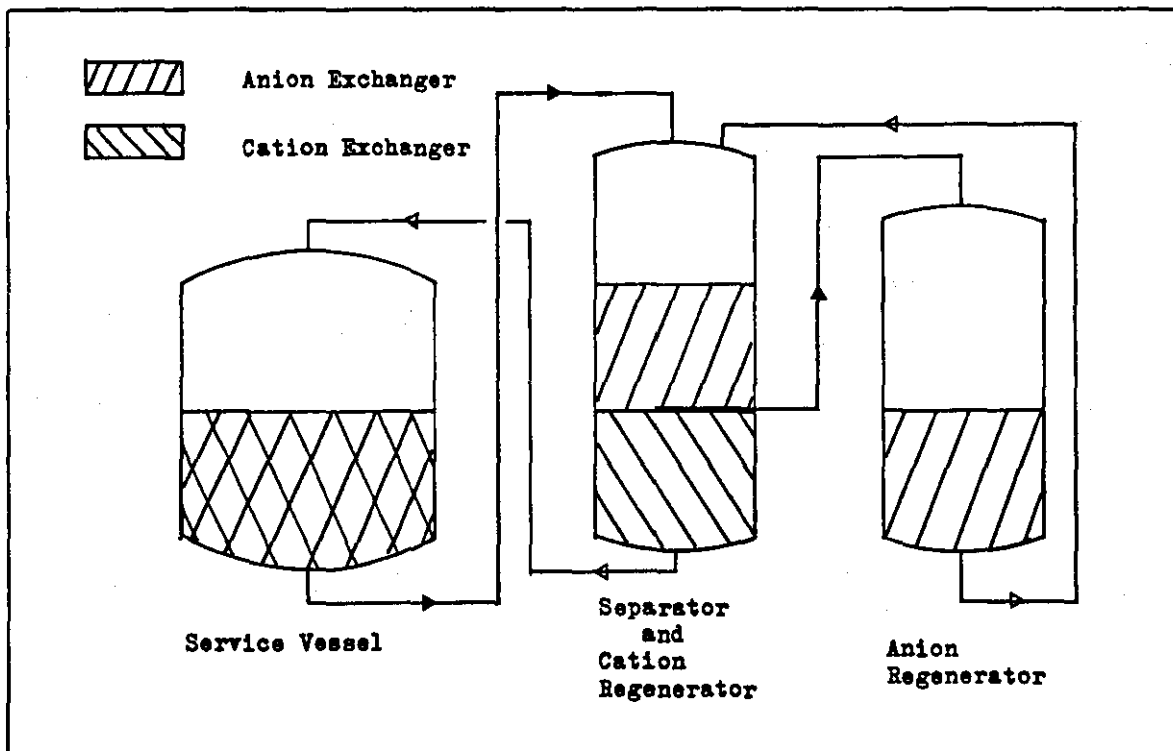
FIGURE
No. 2.07   EXTERNAL REGENERATION - TWO VESSELS

give corrosive contaminants (126). Above the bed is a system for distributing the inlet water. This can vary from a split header and splash plates to a radial lateral system. To reduce the capital cost of vessels split flow mixed beds have been designed. Water enters at the top and bottom of the bed and is extracted via a central lateral system (127, 128).

In externally regenerated beds the resins are removed from the bed at or very close to the bottom of the unit. A dished bottom design ensures more efficient resin removal than a flat bottom design as the resins can be washed towards a central point. Resin extraction may be via a central hole through the base of the vessel or, in older designs through a downward facing pipe terminating a few centimetres above the base of the vessel. This last method is more likely to leave resin in the vessel. In many CPP repeated transfer of resins to and from vessels results in bed volumes becoming unequal and periodic adjustments have to be made.

2.6.2 EXTERNAL REGENERATION

As noted earlier the majority of CPP mixed beds and some make up plant mixed beds are regenerated externally. Resins are transported to and from the various vessels in a resin/water slurry that is propelled either hydraulically or pneumatically. External regeneration systems can be either one vessel (Figure 2.06) or two vessel (Figure 2.07) systems and there may be an additional resin storage vessel for a regenerated charge of resin. The single vessel regenerator is very similar to the in-situ regenerated mixed bed (Figure 2.04) while the two vessel regenerator is essentially the same as the original regeneration scheme devised by Kunin and McGarvey (90). External regeneration vessels are taller and narrower than the service vessel which gives deeper beds of separated resins and better backwash water and regenerant distribution. The units can be designed purely for regeneration and not as a compromise between operation and regeneration.

2.6.3 BACKWASHING

In CPP mixed bed regeneration backwashing has a dual role of separating and cleaning the resins. Cleaning is necessary to remove particulate oxides that may have accumulated on the resin and is often accompanied by air scouring of the resin/water mixture (100, 101). The use of ultrasonic waves to remove debris from resins has also been applied (129).

2.6.4 CROSS CONTAMINATION

One of the major problems in mixed bed regeneration is contamination of the exchangers by the wrong regenerant. One or both resins may become contaminated leading to long rinses down after regeneration, ionic leakage in service and loss of operating capacity.

There are a number of causes of cross contamination. Poor resin separation will lead to a zone of mixed resin around the nominal separated resin interface. The volumes of resins in the vessels may not be correct so that the separated resin interface does not correspond with laterals or resin extraction points. Poor efficiency of resin transfer in two vessel regeneration system may leave anion exchanger on top of the cation exchanger (130). The injection pattern of the regenerant distributors may pass a regenerant onto the wrong resin.

The effects of cross contamination depend on the mode of operation of the mixed bed. In neutral operation, with H/OH form exchangers, the major problem has been acid leakage from acid contaminated anion exchange resin. Either hydrochloric or sulphuric acid contaminated resins exhibit a prolonged rinse out of acidic ions, attributed in part to hydrolysis of chloride or sulphate form weakly basic groups on the anion exchanger (18). Such sulphate released near the base of mixed bed may not be completely exchanged and thus released into the treated water. The presence of organically fouled resins serves to exacerbate this leakage giving extended rinse periods before or during service (14,51). Sodium hydroxide contamination of the cation exchanger may cause loss of cation exchange capacity but does not

give rise to significant leakage in H/OH operation. However in
NH_4/OH form operation a small amount of sodium form cation exchanger
can give rise to unacceptable sodium leakages in service (see 2.5.5)
therefore considerable efforts have been made to overcome sodium
hydroxide contamination of the cation exchanger.

A number of solutions to cross contamination in NH_4/OH form beds have
been proposed. Most have concentrated on mitigating the effects of
contamination and only recently have several developments attacked
the fundamental problems of resin separation and resin transfer.
Engineering solutions to isolate the mixed resin interfacial layer
have included double centre laterals (131) or interfacial layer
isolation and removal (132). Chemical engineering solutions seeking
to convert the contaminated resin to a more acceptable ionic form or
to isolate it from the bulk resins have been widely used (120, 133,
134). A combined regeneration, service, repeat regeneration process
has also been described (118).

More recently the problem of poor separation of the exchangers has
been addressed by the resin manufacturers who have produced triple
resin systems consisting of specially size graded resins that
separate completely and an inert resin, also specially size graded
and of intermediate density, which forms an intermediate barrier
layer between the separated anion and cation exchangers. The concept
was proposed by McMullen in 1953 (135) but was first adopted in 1976
at Doel in Belgium (136, 137, 138). To complement resins which
separate completely a new design of resin separation vessel with
bottom transfer of the cation exchanger has been developed (51). A
different approach to avoiding cross contamination is the use of
separate beds for cation and anion exchangers (139).

2.6.5 RE-MIXING OF RESINS

After the resins have been regenerated and rinsed free of excess
regenerant they are remixed. In a single vessel regenerator mixing
takes place in the same vessel. In two vessel regenerators the
resins are recombined in one of the vessels or, alternatively, both
transferred to a third vessel which is the spare charge storage vessel.

Resin mixing is achieved by lowering the water level to a few centimetres above the top of the bed and passing low pressure air through the bottom distributor system. This agitates and mixes the resin water slurry. Arden (25) noted that air distribution must be uniform to achieve good mixing and the amount of free water above the resin has a great influence on the final resin mixture (140). The latter is hard to control in CPP where resin levels vary and mixing may take place in a vessel remote from the operator. Failure to achieve proper mixing may result in ionic leakage as trace regenerants are leached from the resins but are not exchanged within the bed.

2.7 MIXED BED PERFORMANCE

As mixed beds are the final purification stage in make up or condensate purification plant greater emphasis is placed upon the purity of water produced rather than ion exchange capacity. Numerous papers have been published on the quality of water obtained from high flow rate mixed beds under various operating conditions but some are written from a commercial as well as technical basis and give no insight into the factors influencing mixed bed performance. The remaining papers can be divided into two groups: investigations into full scale operating mixed beds and investigations involving laboratory or pilot scale columns. In the second group the experimental conditions can be controlled more closely without the influence of plant operating factors.

Mixed bed performance is normally assessed in terms of impurity content and hypotheses as to the controlling factors have changed as more accurate analytical information has become available. Electrolytic conductivity or resistivity has been determined for many years, but is now normally referred to a 25 $^{\circ}$C standard. Analytical determinations at the μg kg^{-1} level have become standard practice in recent years. The sodium responsive glass electrode (141) or flameless atomic adsorption spectrophotometry can determine sub μg kg^{-1} concentrations of sodium but it is only relatively recently that methods for μg kg^{-1} levels of chloride and sulphate have become available (142, 143) and in particular the very versatile ion chromatographic technique, based on ion exchange (144, 145).

In this section only H/OH form mixed beds are considered with the emphasis on high flow rate operation.

2.7.1 OPERATIONAL MIXED BEDS AND ASSOCIATED STUDIES

An early study by Thompson et al (146) compared two bed and mixedbed performance for make up water production. They showed mixed beds were capable of producing water of 16 MΩ resistivity ($0.0625 \mu S \ cm^{-1}$) but the flow rates were very modest - about 10 $m^3 \ m^{-2} \ h^{-1}$. Their major concern was not the conductivity but the silica concentration which was maintained at $< 0.02 \ mg \ kg^{-1}$ with an influent of 9 $mg \ kg^{-1} \ SiO_2$.

As noted earlier CPP mixed beds found their first major application in once through supercritical pressure boilers. Various studies monitoring the performance of these mixed beds showed them to be capable of maintaining feedwater copper concentrations below the limit of 3 - 5 $\mu g \ kg^{-1}$ Cu (93, 94, 96). Other parameters of concern were sodium and silica.

2.7.1.1 Sodium Leakage

Of the three major ions of current interest - sodium, chloride and sulphate - sodium was the first that could be measured accurately at $\mu g \ kg^{-1}$ concentrations, using a sodium responsive glass electrode (141). Sodium as sodium hydroxide can rapidly corrode mild steel and stress corrode austenitic steels if concentrated to a sufficient degree. Therefore, early once through boilers had a feedwater specification of $< 5 \mu g \ kg^{-1}$ Na.

A long term survey of a CPP associated with a once through supercritical unit showed the sodium leakage to increase from 0.8 to 2.2 $\mu g \ kg^{-1}$ over a nine month period, (96, 104), a significant rise for AGR boilers which are limited to a maximum of 2 $\mu g \ kg^{-1}$ Na. The increased sodium leakage was attributed to the physical breakdown of the gelular cation exchanger, giving resin fines that did not separate from the anion exchanger on backwashing. These fines became contaminated with sodium hydroxide that was subsequently eluted into the treated water. Whilst sodium hydroxide does elute

slowly from a cation exchanger more recent laboratory investigations
(18) indicate another contributory cause (see 2.7.2).

The use of radio active tracers on salts simulating a sea water
condenser leak into an operating CPP mixed bed demonstrated that
the traces of sodium at the bed outlet did not arise from kinetic
leakage of influent ions, (15) but must have presumably been
equilibrium leakage. It was also shown that in the absence of
condenser leaks the sodium at the bed outlet was slightly greater
than that at the bed inlet, again attributable to equilibrium
leakage (137).

In general, CPP mixed beds will operate with sodium leakages well
below the $2 \mu g$ kg^{-1} target figure until breakthrough at exhaustion
occurs (14, 15, 137).

2.7.1.2   Chloride Leakage

Particularly high kinetic leakages of chloride, up to 80% of the
influent concentration during sea water condenser leaks, (13), led
to the development of an on line chloride monitor for μg kg^{-1} Cl
determinations (142). The leakage was attributed to fouling of the
CPP mixed bed anion exchanger by naturally occurring organic species
in the raw water (see 2.8) that passed through the make up plant
and accumulated on the anion exchanger. These organic foulants
were considered to have reduced the chloride exchange kinetics,
thereby increasing the kinetic leakage of chloride which was
particularly apparent in this particular design of CPP.

Radio tracer tests at another CPP mixed bed (using Br^{82} as the halide
ion) showed significant kinetic leakage (up to 40% of influent) of
halide ions through a mixed bed containing an old and organically
fouled anion exchanger, while a parallel bed with new anion exchanger
gave very little leakage. Cleaning the fouled resins by soaking
in brine improved the old anion exchangers performance when tested
in a pilot column (15).

White and Crits (101) monitored the performance of two CPP for

chloride leakage and noted an increase in leakage during condenser leaks from the mixed bed operating at 125 m h^{-1} , but only from 0.3 to 1.0 μg kg^{-1} Cl. No information on the state of the anion exchanger was given.

Tittle et al (148) used a multi-point probe to sample at various depths and diameter positions in a 3.05 m dished bottom mixed bed operating at 98 m h^{-1}, with a 2:1 cation:anion exchanger ratio and an influent ammoniated to pH 9.3. It was found that during sodium chloride injection, to simulate condenser leakage, the chloride exchange front rapidly moved ahead of the sodium exchange front, by a greater factor than might be indicated by the 2:1 mixed resin ratio. The inferrence drawn was that anion exchange for chloride was significantly slower than cation exchange for sodium.

2.7.1.3 Sulphate Leakage

During the radio tracer studies for halide leakage (15) it was noted that the measured ionic leakages (Na and Cl) were insufficient to account for the observed conductivity at the CPP outlet. The extra conductivity was found to be due to ionic sulphate and having identified sulphate at one plant other workers have subsequently found sulphate as a major ionic leakage from many sulphuric acid regenerated mixed beds (14, 136, 137, 149).

Further plant associated investigations have shown that as the mixed bed anion exchanger aged the rinse down after regeneration and remixing took longer to reach the working conductivity. Once again sulphate leakage or elution was identified as the major contaminant and in certain cases a long sulphate rinse tail could last for many hours (150). This either prevented a regenerated bed from returning to service or released sulphate, a potential corrodant, into the boiler feed water. The extension of sulphate rinse out was generally accompanied by an increase in the background leakage of sulphate ion during the whole service cycle, up to or exceeding the 2 μg kg^{-1} SO$_4$ limit for AGR feed water.

2.7.2 LABORATORY AND PILOT SCALE STUDIES

In the 1950's several groups of workers investigated the performance of mixed beds at flow rates up to 250 m h^{-1} in columns varying from 9 to 500 mm diameter (92, 151, 152, 153). The main control parameter was conductivity and conductivities of 0.06 - 0.08 μS cm^{-1} could be achieved even at the very high flow rates. Thompson and Reents (92) noted that at 125 m h^{-1} a freshly regenerated mixed bed could treat the equivalent of 100 mg kg^{-1} salts (CaCO$_3$) in the influent without affecting the outlet water quality (0.06 μS cm^{-1}), until the bed was 50% exhausted. After this point the leakage into the treated water slowly increased until at 90% exhaustion the outlet conductivity was 0.2 μS cm^{-1}. Through into the 1960's the greater emphasis on high flow rate mixed bed investigations was on filtration of particulate oxides as the outlet conductivities then specified, often ≯ 0.2 μS cm^{-1}, could be relatively easily achieved under normal operating circumstances.

Blight and Jackson (102) operated a 150 mm diameter pilot column mixed bed alongside an operating CPP, primarily for filtration tests but they also monitored sodium leakages during simulated sea water condenser leaks.

Kunin (154) used radio active tracer techniques to examine the differences in kinetics between ion exchangers based on gelular or macroporous matrices and concluded that macroporous resins gave similar ionic leakages as gelular resins but offered advantages in operational capacity. This view is opposed by Wirth who claims that gelular resins offer superior performance in condensate purification (109, 110, 155).

Harries and Ray (18) investigated the effects of regenerant cross contamination of both anion and cation exchangers on the treated water quality. The worst effect was due to acid contacting some of the anion exchanger, resulting in a prolonged acidic anion bleed from the bed which became worse when aged and organically fouled anion exchangers were used in the pilot column mixed beds. The prolonged acid leakage was attributed to hydrolysis of the acidified exchange sites, particularly the 5 -10% of weak base sites that are

always present on strong base anion exchangers. Sodium hydroxide
contaminated cation exchangers gave few problems, most of the eluted
sodium being removed within the bed. The only time sodium leakage
increased was when the acidic anion leakage reduced the pH within
the bed and caused an increase in equilibrium leakage from sodium
form sites on the cation exchanger.

Emmett (51) examined the rinse characteristics of single beds of
sulphuric acid contaminated anion exchangers and showed a large
increase on acid release with the age of the resin. Note that as
anion exchangers age there is a gradual conversion of strong base
groups to weak base functionality (156, 157).

Several groups of workers have recently attempted to compare the
chloride removal performance of anion exchangers by measuring the
dynamic leakage from a small mixed bed operating at the correct
specific flow rate ($m^3 m^{-3} h^{-1}$), giving a within bed residence time
similar to full scale plant but a superficial linear velocity much
lower than normal practice. The interpretation of the results has
been conflicting. Ray et al (158) considered that the polymer/matrix
combination is the controlling factor while Emmett (159), Harries (19) and
McNulty (160) considered that bead size is the major influence in
determining the degree of kinetic leakage.

2.7.3   MIXED BED THEORY

There have been a number of equations produced to describe the
operation of columns of a single resin (see 2.3.4.5) but very few
attempts have been made to mathematically describe the operation of
mixed beds. Frisch and Kunin (161) used the results from mixed bed
columns only 13 mm diameter operating at superficial flow rates up
to 250 m h^{-1} and treating influents containing up to 0.01 equivalents
NaCl per litre. The model was developed on the basis of both
exchangers operating at the same overall reaction rate and acting as
if there was only one, amphoteric, exchanger in the system. Conduct-
ivity was the main analytical parameter as suitable methods for low
concentration leakages were not available.

Frisch and Kunin concluded that the overall exchange rate was film diffusion controlled at the relatively low influent concentrations used. They developed an assymptotic equation to describe the depth of the exchange zone for a given leakage, which was dependent on both flow rate and bead size, and equations for predicting the working exchange capacity of a bed to a fixed break through concentration, which requires a knowledge of the regenerated capacity of the exchangers.

2.8 ORGANIC FOULING OF ANION EXCHANGERS

Within a few years of the commercial introduction of strong base anion exchangers the literature contained references to the irreversible fouling of these resins by large organic molecules (162, 163). The effect of the fouling was to reduce both water quality and output between regenerations from beds containing strong base anion exchangers. Since those early reports there have been many papers on both the causes and effects of organic fouling and methods for overcoming fouling; yet organic fouling remains a major problem in producing high and ultra pure feed water from ion exchange water treatment plants (19, 164, 165, 166).

2.8.1 NATURE OF ORGANIC FOULANTS

The main source of organic foulants is considered to be the natural decay products of vegetation that occur in natural water supplies, especially those from peat covered moorland areas. However, other sources may be the large variety of organic compounds that may be discharged to a river flowing through industrial areas or the wastes from manufacturing process, lignin sulphonates from paper making having received attention (167).

The decay products of vegetation are a group of compounds loosely termed fulvic and humic acids generally thought to be polymeric - aromatic - hydroxy - carboxylic acids (168) with molecular weights varying from several hundred to several hundred thousand (169, 170). Fulvic acids are differentiated from humic acids by the latters' insolubility in both mineral acid and alcohol (171, 172). Fulvic acids are the more common species and are generally of lower

molecular weight than humic acids (168). The molecular weights and ratios of fulvic to humic acids will vary both with the water source and the time of year (173). Tilsley (166) presented two potential structures for fulvic/humic acids, one of which incorporated complexed metal ions such as iron.

The degradation products from cation exchangers, short chain polymer fragments that had been released by oxidative attack on the polymer, were reported to have fouled down stream anion exchangers (174, 175). The problem was overcome by using a more highly crosslinked polymer, more resistant to degradation.

2.8.2 SELECTIVITY OF ANION EXCHANGERS FOR ORGANIC MOLECULES

Because fulvic/humic acids are very complicated and undetermined structures most of the work on selectivity has been carried out with simpler species. A review by Semmen (176) showed that strongly basic anion exchangers can have very high equilibrium selectivity coefficients for organic compounds compared to inorganic species eg $K_{OH}^{Cl} \simeq 20$, $K_{Cl}^{aromatic\ sulphonate} \simeq 10,000$. Also the nature of both the exchanger polymer and the organic anion can have a significant influence.

The selectivity of strongly basic exchangers for simple organic anions such as formate or acetate is similar to that for inorganic anions such as bisilicate or bicarbonate (177). However, as the aliphatic chain length of the acid anion increases its selectivity for the exchanger increases and the introduction of aromatic character further increases selectivity. The nature of substituents on the aromatic nucleus can also affect selectivity coefficients (33, 176, 178, 178a).

The high selectivities for large organic anions are attributed, in part, to hydrophobic bonding (33) but the interaction is not wholly ionic as the basic styrene/DVB polymers used for preparing ion exchange resins act as adsorptive agents for removing organic species from aqueous solutions (179). There is probably a pi-bond interaction between the aromatic nuclei in the organic species and those in the styrene/DVB polymer. Gregory et al (178) showed that anion exchangers based on an acrylamide polymer had selectivities for carboxylate ions an order of magnitude less than anion exchangers based on styrene.

The lower selectivity of the acrylamide based resins has found
commercial application in treating waters that cause serious organic
fouling problems with styrene based resins (180) as the acrylamide
resins release the organics more easily on regeneration (164).

2.8.3   MECHANISM OF ORGANIC FOULING

Most published work on organic fouling relates to the primary anion
exchange bed in water treatment plant, whereas mixed beds are
secondary or tertiary anion exchange stages. Therefore, the organics
passing to the mixed bed are those that have not been sorbed or
exchanged by the primary anion exchanger. The polymer/matrix
combination of the primary anion exchanger can influence the size
(molecular weight) of organic species that are removed or pass
through the bed (170).

Herz (181) considers that the larger organic molecules are only sorbed
onto the bead surface and can block access of inorganic ions to the
bead surface whereas Martinola (182) believes the large organics
do not impede access of small anions. Other workers (25,35) have
proposed that fulvic/humic acids are selectively held in areas of
high crosslinking within the polymer by physical entanglement and
therefore resist elution. This argument is used to explain the
claimed resistance to organic fouling of isoporous resins (35). The
greater internal area and shorter pathways from polymer to solution
is claimed to allow better elution of organics and thereby minimise
organic fouling (183). Ungar (184) believes that on regeneration
with sodium hydroxide the organic anions become more ionised and more
hydrated inhibiting their release from the resin. Wall et al (185),
studying dye sorption onto anion exchangers, proposed an initial
saturation of the bead surface followed by a slower diffusion into
the bead. Arden (186) has proposed that acid insoluble humic acids
would precipitate on an anion exchanger contaminated by mineral acids
and then in the subsequent cycle the humic acids would redissolve and
re-exchange onto the exchanger polymer.

Several workers (181, 186) have proposed that the ratio of inorganic
to organic anions is important. Low concentrations of inorganic ions
means long service cycles allowing the organics time to penetrate

the resin matrix while the relatively short regeneration time only allows removal of organics near the bead surface. This may be particularly important for CPP mixed beds that can operate for several weeks or months without regeneration.

2.8.4 RATE OF ORGANIC FOULING

Whilst there are many reports on organic foulants accumulation for one particular resin at one particular site there are very few comparative studies of the rate of organics uptake by different types of resin on one water supply. In one such investigation, covering a number of operating cycles, Wolff (187) showed that the net rate of organic foulant accumulation did not depend greatly on the polymer/matrix type but more on the basicity of the exchange groups.

3 THE SEPARATION OF MIXED RESINS BY BACKWASHING

The success of the regenerable mixed bed in producing ultra pure water lies in the utilisation of an intimate mixture of anion and cation exchangers during the purification stage and then separating the resins again prior to regeneration. Incomplete separation will lead to cross contamination by the wrong regenerant, which can subsequently cause leakage of impurities into the treated water. Therefore, if the purity of water from mixed beds is to be maintained at very low contaminant concentrations it is important to ensure that the ion exchange resins supplied for mixed beds will separate completely.

Resin separation is achieved by backwashing the mixed resins with water to give controlled fluidisation. The less dense anion exchanger separates as a layer above the more dense cation exchanger and within each layer of resins there is some classification of the beads by size, smaller beads in the upper regions of each layer.

Preliminary trial separations of mixed resins in 25 mm diameter clear laboratory columns indicated that the standard size grades of ion exchange resins (0.3 - 1.2 mm) normally supplied for mixed beds would not always separate completely. Separation appeared to depend on the polymer/matrix types of the two resins and their respective ionic forms. Poorly separating resins produced a middle layer of intermixing small cation exchanger and large anion exchanger beads.

3.1 ASSOCIATED WORK

When this study of resin separation commenced there was no published information on the separability of ion exchange resins or the factors that might influence or control separation. The advent of triple resin systems has led to the publication of resin bead terminal velocity versus bead diameter diagrams by several resin manufacturers (188, 189) to demonstrate that their systems will work. They give little information on bead density, ionic form of the resins or the separation conditions or whether the data is calculated or practically measured. This information is admitted to being deliberately vague in some instances to protect commercial interests. In the published

data Wolff (190) has used Allens approximation (191) to calculate resin bead terminal velocities and Emmett (159) has measured terminal velocities of individual beads.

Ion exchange resin separation is essentially a problem concerned with the fluidisation of two particulate species with densities close to each other and to the fluidising medium, water. Furthermore both species have relatively wide size distributions that are similar to each other. In the general field of fluidisation studies this is an area that has not received any attention. Most investigations have been carried out with monosize monodensity particles, a few workers have investigated the interaction of two monosized monodensity particles with various size ratios of the particles and there have also been investigations of fluidisation of particles of narrow size distribution and widely differing densities. Many workers have used glass ballotini as the solid phase and either water or an organic liquid as the fluidising medium.

Richardson and Zaki (193) investigated sedimentation and fluidisation of single size monodensity particles and derived an empirical equation to describe the porosity (voidage) of the fluidised bed (see 3.3.3). Many workers have noted that in a fluidised bed of closely graded particles axial bulk circulation patterns are set up. The particle motion is generally upwards in the centre of the bed and downward at the walls (194, 195). Happel (196) attributed this bulk circulation to lower liquid velocities near the vessel walls due to viscous drag between the fluid and the wall. Other workers have developed the concept of axial diffusion to describe bulk circulation (194, 197).

A number of studies have been undertaken employing mixtures of two or more discrete size fractions with beads of uniform density. The term size ratio is commonly used to describe the ratio of maximum to minimum bead diameter. Richardson and Zaki (193) used mixed glass beads with a size ratio of 2.02 and recorded separation of the two components. They also noted that the properties of the two component fluidised bed could be predicted from calculations on the separate components. Wen and Yu (198) fluidised two and three component mixtures of discrete size fractions with a number of different size

ratios. They reported that with size ratios less than 1.3 intermixing
of the two components took place. Wen and Yu also claimed that the
expansion of the mixture could be predicted from the expansion of a
single equivalent particle diameter given by the Sauter mean
(see 3.6.1.1). Hoffman, Lapidus and Elgin (199) fluidised mixtures
with two discrete particle sizes and found that with a size ratio
of 1.24 intermixing occurred, while with size ratios of 1.58 or
greater the two components seggregated. No intermediate ratios
were studied. Finklestein, Letan and Elgin (200) investigated
mixtures with size ratios of 1.62 to 6.0. They did not establish
equilibrium conditions but considered that the properties of a
uniform mixture could be characterised by a mean diameter which
equates to the Sauter mean for monodensity mixtures (201).

Scarlett, Blogg and Freshwater (202) examined the fluidisation of
glass ballotini with a Gaussian size distribution, using a parallel
plate apparatus. Scarlett and Blogg (203) also described similar
fluidisation tests in a cylindrical column. In both apparati
samples of the fluidised bed could be extracted at various heights
for subsequent bead size analysis. Overall size ratios between
1.35 and 3.0 were examined and at 1.35 there was virtually no
seggregation, ie intermixing occurred. At size ratios greater than
2.0 seggregation was observed. Al Dibouni and Garside (201) mixed
particles from adjacent sieve fractions to give continuous distrib-
utions with size ratios of 2.0 to 6.7. Al Dibouni et al claim that
at size ratios of 2.0 or less mixing was the dominant feature while
for size ratios greater than 2.2 classification becomes the signifi-
cant feature. They also noted that mixing tended to become more
intense at fluidised bed porosities around 0.70.

Several groups of workers (194, 202, 203) have noted that the design
of the fluid inlet distributor could influence the mode of particle/
fluid interaction. In particular a poor distributor could induce
turbulence and particle circulation in the lower parts of a fluidised
bed.

All the work reviewed so far has dealt with the fluidisation of
monodensity particles, whereas ion exchange mixed beds contain two or
three components of different density. The nearest approach to mixed

bed separation is the backwashing of multimedia filters, which contain two or more filter media that are closely size graded but of differing densities. The difference in the approach is that the aim is to prevent the individual media from intermixing on backwashing. A number of workers have investigated the problem and have proposed a variety of equations to describe and predict the separability and/or mixing of any two media (204, 205, 206, 207, 208). These equations generally deal with media of widely differing densities and closely graded particle size and may not be sufficiently refined to be applicable to ion exchange resins with bead densities similar to each other and very close to the fluidising medium while also having a relatively wide size distribution.

Cleasby and Woods (205) compared two published models for predicting intermixing in multi media filters. The difference in the bulk densities of two adjacent media was proposed by Pruden (207, 208) and Le Clair (201) as the driving force for separation. The bulk density concept treats the fluidised particle/liquid mixture as a single component of composite density. If two particulate species separate on backwashing the upper component, with lower bulk density effectively floats on the lower component with a greater bulk density. The bulk density (B) is defined as

$$B = E\rho + (1 - E)\delta$$

where ρ is the density of the backwash fluid

δ is the density of the particles

E is the porosity of the fluidised bed

$$E = \frac{\text{Interstitial volume}}{\text{Total fluidised component volume}}$$

The separation model of Camp et al (204) considered that two particulate media would separate if the particulate density of the upper medium was less than the bulk density of the lower medium. As this did not represent the observed state of fluidised multi media filters Camp et al subtracted a drag term from the density of the upper component. Cleasby gave Camp's equation as

$$B_{lower} = \delta_{upper} - C_D \frac{3\rho}{4dg} \left(\frac{V_f}{E}\right)^2$$

where C_D is the drag coefficient of the particle

V_f is the superficial backwash velocity

d is the particle diameter

g is the gravitational acceleration.

Bulk density calculations take account of the particle diameter through the fluidised bed porosity term (E) but in Camp's model the particle size of the upper layer only occurs in the drag term indicating particle size has a very minor effect. Cleasby's comparison of these two models concluded that the bulk density model predicts the general behaviour of any two media while the model of Camp et al depends on a number of empirical relationships that are not easily measured. The bulk density approach to particle separation was considered further below (3.3.2)

3.2 CRITERIA FOR RESIN SEPARATION

Fluidisation studies on single density particles with a range of sizes, reviewed in 3.1, have shown that if the ratio of maximum to minimum particle diameter is above 1.5 to 2.0 then the particles will classify by size on backwashing to give the smallest at the top and largest at the bottom of the bed. However, with size ratios below 1.5 the particles start to circulate and intermix within the bulk of the fluidised bed.

In an ideal mixed bed the resins should separate into two distinct layers on backwashing, the upper being the less dense anion exchanger and the lower the more dense cation exchanger. The resin particles in each of the layers will be classified by size, with the largest at the bottom and the smallest at the top. A sharp interface will divide the smallest cation exchanger beads from the largest anion exchanger beads. A typical standard grade ion exchanger has a particle diameter ratio of 4 (0.3 - 1.2 mm). Therefore, in a fluidised bed of single density, exchanger beads classification will be dominant and ideally any small increment of bed height may be considered to contain particles of only one diameter. The beads within that increment may

be characterised by a calculable separability parameter, P, which
will be a function of both the resin bead properties and the fluid-
ising conditions.

If the cation and anion exchangers have separated perfectly the beads
in the increments either side of the separated resin interface can be
characterised by P_{A-max} and P_{C-min}, where A-max and C-min are the
largest anion exchanger and the smallest cation exchanger beads
respectively. A condition for separation can now be defined such
that

$$P_{A-max} \quad < \quad P_{C-min}$$

and the limiting criterion of separation is defined as

$$P_{A-max} \quad = \quad P_{C-min} \cdot$$

If the two resins do not separate completely they will overlap to
some extent to form a mixed resin zone which has an interface with
the completely separated portion of each resin. Then

$$P_{A-max} \quad > \quad P_{C-min}$$

and it is assumed that within any height increment in the mixed
resin zone the relationship

$$P_A \quad = \quad P_C$$

holds. This will also be the limiting condition at the two mixed
resin/separated resin interfaces.

3.3   POTENTIAL SEPARABILITY PARAMETERS

Three parameters have been investigated for their potential to act
as indicators of resin separability. These are the bead terminal
velocity approach used by the resin manufacturers, the bulk density
approach as described by Pruden and Epstein and a third, new,
approach involving the variation in porosity (voidage) in a fluidised
bed of multisize, mixed density resins.

3.3.1 <u>RESIN BEAD TERMINAL VELOCITY</u>

At its terminal velocity, V_o, the gravitational acceleration acting
on a particle falling through a liquid is balanced by the viscous
drag on the particle and its buoyancy in the fluid. This balance
of forces is the same if a particle is suspended at a point in an
upward flowing liquid. The latter condition approximates to the
suspension of particles in a fluidised bed. Accordingly, resin
bead terminal velocities are a potential comparative parameter for
resin separability. Terminal velocities are strictly applicable
only to single particles in an infinite fluid (ie no effects due to
vessel walls or other particles). However, they are a basic
hydrodynamic parameter and may be a suitable separability parameter, P .

Another hydrodynamic parameter is the Reynolds number at the
terminal velocity, Re_o. Reynolds number is defined by

$$Re_o = \frac{V_o\, d\, \rho}{\eta}$$

where d is the bead diameter, ρ is fluid density and η is the fluid
dynamic viscosity. The value of the Reynolds number determines
whether, at its terminal velocity, a particle is falling under
laminar or turbulent flow conditions. At values of $Re_o < 0.2$
laminar flow prevails while for $Re_o > 500$ turbulent flow conditions
exist (209). For values of $0.2 < Re_o < 500$, the flow conditions
are intermediate between laminar and turbulent flow.

Due to the combination of size and bead density most ion exchange
resin beads, in water, have values of Re_o that place them in the
intermediate zone between laminar and turbulent flow regimes
(Appendix 3, Table A 3.01). Therefore, the standard Stokes equation,
which is applicable only to laminar flow, cannot be used to calculate
terminal velocities. There is no simple equation to derive V_o in
the intermediate flow regime and in this work terminal velocities
have been calculated using the widely accepted relationships derived
by Heywood (210).

An alternative method for calculating Re_o, used by Wolff (190), is
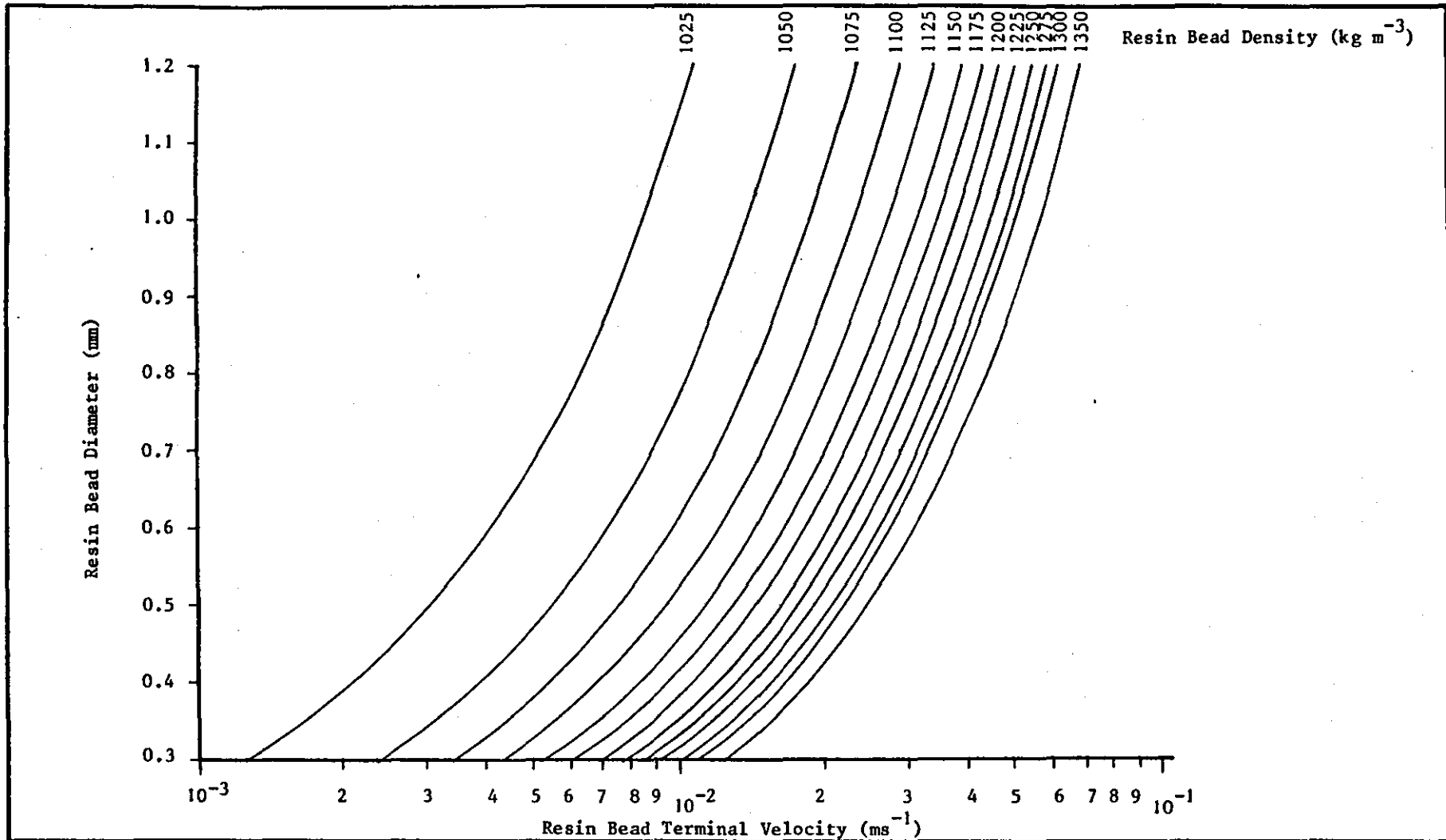
FIGURE No. 3.01 — TERMINAL VELOCITY MODEL SEPARATION CHART
Calculated for water at 20°C

the Allen approximation (191). This assumes that the relationship between V_o and Re_o at the mid point of the intermediate flow regime holds for all other points. This gives a straight line relationship between bead diameter and terminal velocity whereas the Heywood derived relationship is a curve. The latter effect would be expected in the intermediate flow regime where the drag coefficient versus Reynolds number relationship is also curved (209).

Terminal velocities were calculated for resin beads of 0.3, 0.5, 0.7, 1.0, 1.2 and 1.4 mm diameter at densities from 1025 to 1350 kg m^{-3} in water at 5, 20 and 40 ^oC (Table A 3.02). The values for 20 ^oC were plotted on a separation chart (Figure 3.01) in terms of the variation of terminal velocity with resin bead diameter at 25 kg m^{-3} increments in bead density. According to the criteria set out in 3.2 an anion exchanger resin bead will separate above a cation exchange resin bead if $V_{oA} < V_{oC}$ while if $V_{oA} > V_{oC}$ there would be a reversal and the cation exchanger bead would separate above the anion exchanger. Therefore, knowing the size gradings and densities of any pair of anion and cation exchangers the terminal velocities for the largest anion and smallest cation exchange particles can be determined from a diagram similar to Figure 1. If the condition

$$V_{o\ A-max} \quad < \quad V_{o\ C-min}$$

is satisfied, clean separation of the two exchangers will occur, otherwise there will be some overlap and interfacial mixing.

An alternative approach is to determine the terminal velocity of the largest anion exchange bead $(V_{o\ A-max})$ and, knowing the density (δ_C) of the cation exchanger, to ascertain from the separation chart the cation exchanger bead diameter, d_C, that has the same terminal velocity. Comparing d_C with the actual cation exchanger size grading will show whether separation will occur. If $d_{C-min} < d_C$ then the two resins will overlap and the percentage of cation exchanger that separates above the largest anion exchanger will be equal to that part of the bead size distribution lying between d_{C-min} and d_C. Similarly by repeating the procedure for $V_{o\ C-min}$ and determining d_A for a known δ_A, the amount of anion exchanger remaining below the smallest cation exchanger bead can be determined.

Therefore, if resin bead terminal velocity is a characteristic parameter of resin separability, a simple graphical method can be used to predict both the degree of separation and the depth of the mixed resin zone and requires knowledge only of the bead size distributions and bead densities of the two resins.

3.3.2 FLUIDISED BED BULK DENSITY

As noted above Pruden and Epstein used the bulk density (B) of the fluidised bed as an index of separability. Using bulk density as the resin separability parameter, P, the proposition can be made that two resins will separate if

$$B_{A-max} \quad < \quad B_{C-min}.$$

where $B = \delta - E(\delta - \rho.)$

Values of E, the fluidised bed porosity, for various resin bead size and density combinations were determined using the equation of Richardson and Zaki (193). This is an empirically derived equation to describe the rate of sedimentation of a multiparticle system but was found by Richardson et al to apply equally well to fluidisation.

The basic form of the equation for describing the fluidised bed porosity (E) is:

$$\frac{V_f}{V_i} \quad = \quad E^n \qquad \ldots\ldots\ldots\ldots(1)$$

or

$$\log V_f \quad = \quad n \log E + \log V_i \qquad \ldots\ldots(2)$$

where V_f is the empty column backwash/fluidisation velocity and V_i is the corresponding fluidisation velocity at infinite dilution of particles. Single particle terminal velocity, V_o, is given by:

$$\log V_i \quad = \quad \log V_o - \frac{d}{D_v} \qquad \ldots\ldots\ldots(3)$$

where d is the resin bead diameter and D_v the column diameter, and, for the range of terminal velocity Reynolds numbers (Re_o) covering most ion exchange resin beads, ie $1 < Re_o < 200$,
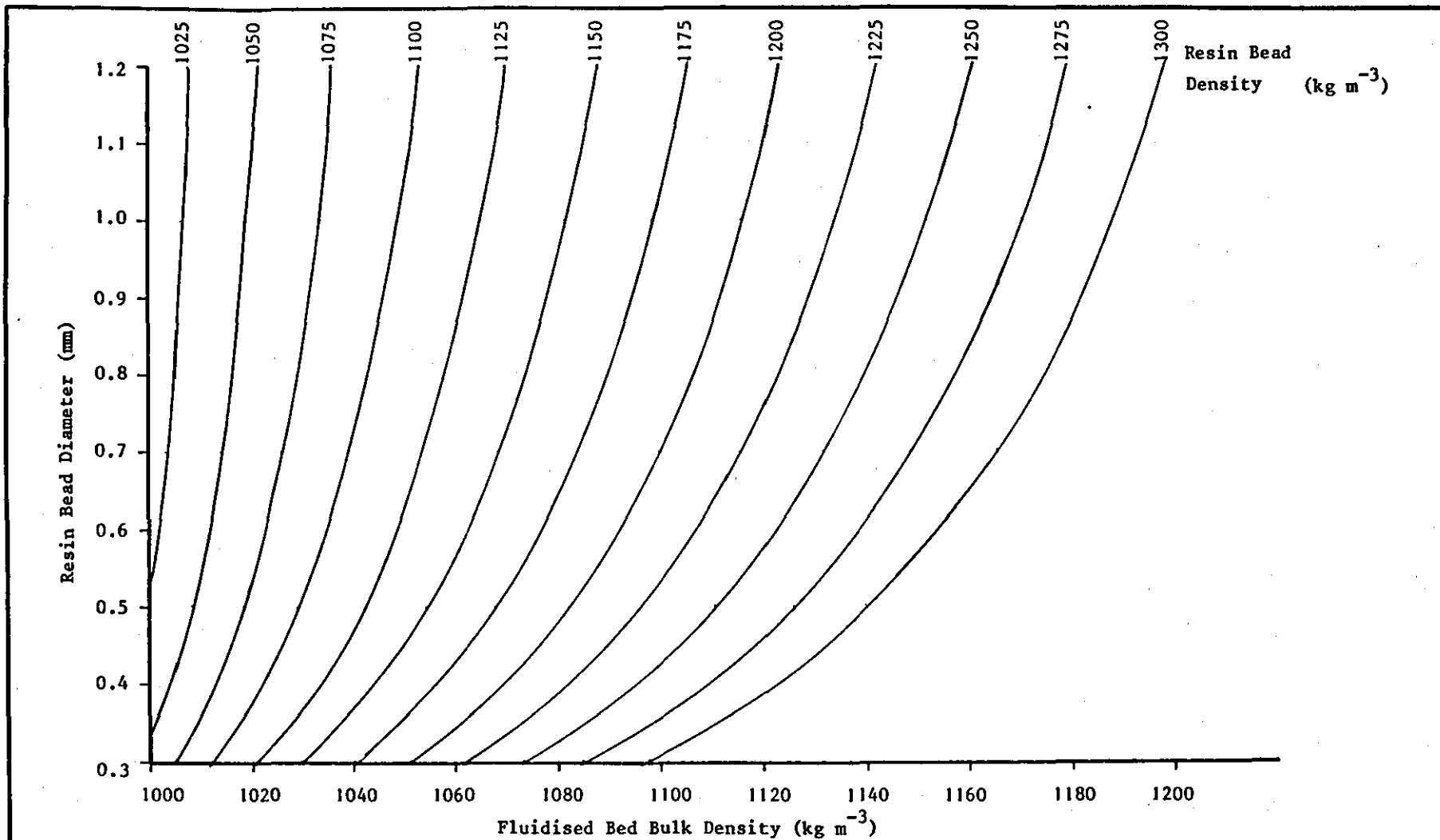
FIGURE No. 3.02   SEPARATION CHART FOR FLUIDISED BED BULK DENSITY MODEL

Calculated for water at 20^0C and backwash flow rate $8mh^{-1}$ in a 100mm diameter column

Increasing
Fluidised Bed
Porosity (E)

Decreasing
Interstitial
Velocity (V_{int})

$$V_{int} = \frac{V_f}{E}$$

Backwash/Fluidisation
Superficial Velocity (V_f)

FIGURE
No. 3.03   INTERSTITIAL VELOCITY AND FLUIDISED BED POROSITY
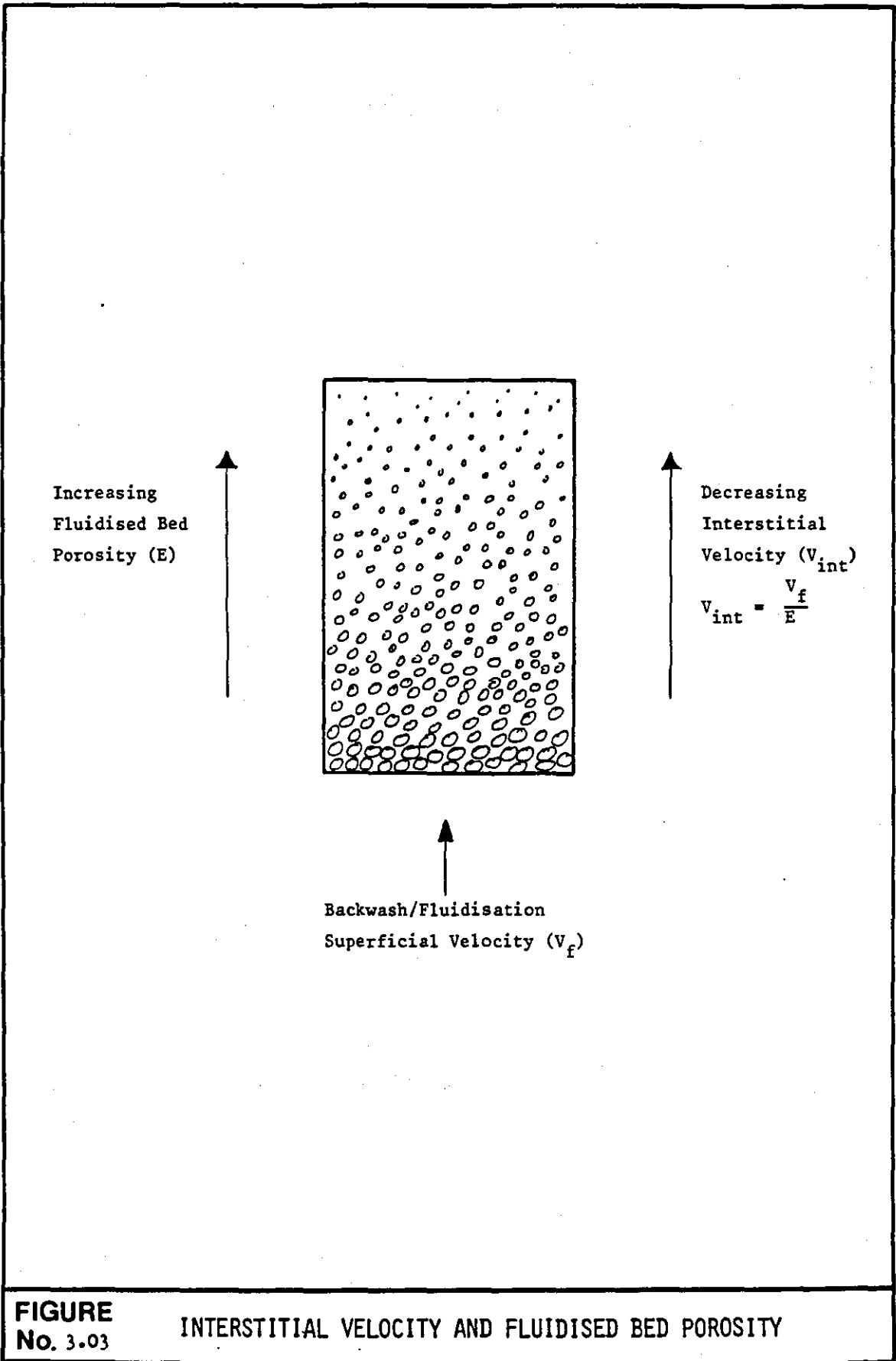
$$n = (4.4 + 18 \frac{d}{D_v}) Re_o^{-0.1} \qquad \ldots\ldots\ldots\ldots (4)$$

Rearranging

$$\log E = \frac{\log V_f - (\log V_o - \frac{d}{D_v})}{n} \qquad \ldots\ldots\ldots (5)$$

Therefore, knowing both the diameter and density of any resin bead, hence the value of V_o and Re_o, the fluidised bed porosity (E) for a bed of such particles can be calculated for any given backwash flow rate (V_f) and water temperature (Tables A3.03, A3.04). Values of V_o and Re_o are determined from the Heywood relationships (210) as in 3.3.1.

A separation chart drawn for calculated values of B at 20 $^\circ$C and a typical backwash flow rate of 8 m^3 m^{-2} h^{-1} in a 100 mm diameter column is presented in Figure 3.02. A bulk density separation chart is used in a similar manner to the terminal velocity chart (Figure 3.01) and the overall trends indicated by both models are similar. However, for two exchangers of fixed densities the bulk density predicts complete separation of resins with much wider bead size distributions than the terminal velocity model.

3.3.3 INTERSTITIAL VELOCITY AND FLUIDISED BED POROSITY

From the author's observations of separating mixed beds in clear laboratory columns it was noted that in a perfect separation the resin interface remained sharply defined and no resin beads crossed the interface despite mild turbulence and circulation within each of the bulk resins. Any resin beads reaching the interface were rejected back into their own resin layer.

A third, and new, resin separability index is now proposed, based on the interstitial velocity of the fluidising liquid, which is inversely proportional to the fluidised bed porosity.

In any fluidised bed that is classified by size the fluidised bed porosity (E) increases up through the bed and the interstitial fluid velocity shows a comparable decrease (Figure 3.03). If the resins
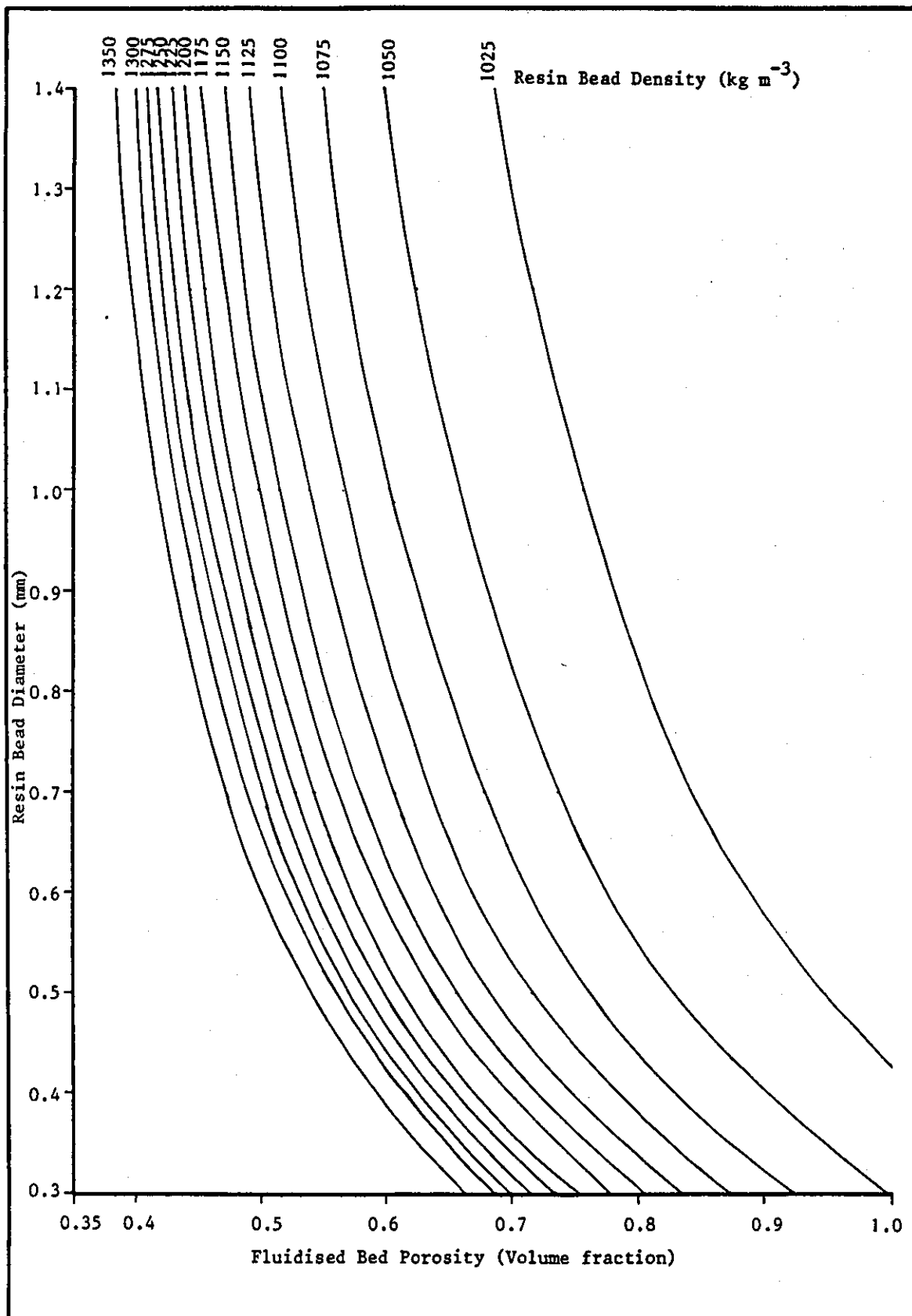
FIGURE No. 3.04 PRACTICAL SEPARATION CHART - FLUIDISED BED POROSITY MODEL Calculated for water at 20°C, backwash flow 8m h⁻¹ in 20mm diameter column

TABLE 3.01   <u>COMPARISON OF RESIN SEPARABILITY PREDICTIONS FROM</u>
             <u>DIFFERENT MODELS</u>

Separation Model	d_A = 1.0 mm δ_A = 1075 kg m^{-3} δ_C = 1250 kg m^{-3}	d_C = 0.5 mm δ_C = 1250 kg m^{-3} δ_A = 1075 kg m^{-3}
Terminal Velocity	d_C = 0.50	d_A = 1.00
Bulk Density	d_C = < 0.30 mm	d_A => 1.2 mm
Fluidised Bed Porosity	d_C ⌐ 0.52	d_A = 0.96

Backwash Conditions: Temperature 20 ^{o}C
                       Flow rate 8 m h^{-1}
                       Column Diameter 100 mm

separated completely then $E_{A-max} < E_{C-min}$ and there would be a
sharp decrease of interstitial velocity at the interface, which
would act to maintain the interface. Any cation exchanger particle
crossing the interface would suddenly encounter a zone of lower
interstitial velocity that would not support it in a fluidised state
and it would fall back into the bulk cation exchanger. Similarly,
a large anion exchanger bead trying to cross the interface would
encounter a higher interstitial velocity and be ejected back into
the bulk anion exchanger.

It is proposed that any fluidised bed of mixed resins will react to
maintain the progressive reduction of interstitial velocity and if
resin overlap occurs the anion and cation exchangers in any bed
height increment will be characterised by an equal fluidised bed
porosity giving an equal interstitial velocity. Therefore, the
limiting criterion of separation is

$$E_A = E_C$$

As noted in 3.3.2, E is dependant on water temperature, backwash
flow rate, vessel size and Re_o. Figure 3.04 is a separation chart
based on calculated fluidised bed porosities for a typical plant
backwash flow rate of 8 m^3 m^{-2} h^{-1} at 20 °C in a 100 mm diameter
column. Again the method of using the chart is similar to that
described for the terminal velocity model (3.3.1).

3.4 COMPARISON OF SEPARATION MODELS

Table 3.01 gives examples of the predicted separability for two
resins, calculated from the separation charts for each of the three
models (Figures 3.01, 3.02, 3.04). The method fixes three of the
four parameters, bead size and density of one resin and bead density
of the second resin leaving the fourth parameter, bead diameter of
the second resin, to be determined. Examination of the calculated
values (Table 3.01) shows that the terminal velocity (TV) and fluid-
ised bed porosity (FBP) models give very similar predictions while
the bulk density (BD) model indicates that the separation margin of
resins is much greater. The TV and FBP models also show similarities

in that all the iso-density lines are parallel but the separation between them becomes greater with decreasing density. The BD model exhibits a different trend: the iso density lines are not parallel and they become further apart with increasing bead size. The BD model suggests that almost all standard grade (0.3 - 1.2 mm) anion exchangers would separate quite easily from most standard grade cation exchangers. This is not the practically observed case and not the indications from the TV and FBP models.

The FBP model is based upon the assumption of a continuous increase, in the fluidised bed porosity and, therefore, continuous decrease in interstitial velocity upwards through a bed of resins during backwashing. However, if the limiting criteria of separation is applied to the BD model $(B_A = B_C)$ the reverse situation is predicted ie a decrease in fluidised bed porosity across the separated resin interface and an increase in interstitial velocity on passing from the lower cation exchanger to upper anion exchanger layers. This increase in interstial velocity can be demonstrated by considering two resins A and C that just separate where $\rho < \delta_A < \delta_C$.

$$B_A = \delta_A - E_A(\delta_A - \rho) = (1 - E_A)(\delta_A - \rho) + \rho$$
and
$$B_C = \delta_C - E_C(\delta_C - \rho) = (1 - E_C)(\delta_C - \rho) + \rho$$

At limiting separation $B_A = B_C$
therefore
$$(1 - E_A)(\delta_A - \rho) = (1 - E_C)(\delta_C - \rho)$$
hence
$$\frac{\delta_C - \rho}{\delta_A - \rho} = \frac{1 - E_A}{1 - E_C}$$

since $\delta_C > \delta_A > \rho$, $\delta_C - \rho > \delta_A - \rho$

then $1 - E_A > 1 - E_C$

ie at the limiting separation conditions the BD approach predicts $E_C > E_A$ whereas it was a condition of the FBP model that $E_C < E_A$. This inversion of the fluidised bed porosities, which would promote interfacial mixing, may explain why the Pruden and Epstein (207) bulk density model was not wholly successful in predicting the

TABLE 3.02   VARIATION OF PREDICTED RESIN SEPARABILITY WITH BACKWASH WATER TEMPERATURE IN A 100mm COLUMN — TERMINAL VELOCITY (TV) AND FLUIDISED BED POROSITY (FBP) MODELS

Fixed Resin Parameter / Backwash Water Temperature	Sep'n Model	d_A 1.0; δ_A 1075 δ_C 1250	d_C 0.5; δ_C 1250 δ_A 1075	d_I 0.6; δ_I 1175 δ_A 1075	d_I 0.7; δ_I 1175 δ_C 1250
5°C	TV	d_C 0.49	d_A 1.01	d_A 0.98	d_C 0.57
	FBP	d_C 0.52	d_A 0.97	d_A 0.950	d_C 0.58
20°	TV	d_C 0.50	d_A 1.00	d_A 0.98	d_C 0.57
	FBP	d_C 0.52	d_A 0.96	d_A 0.95	d_C 0.58
40°C	TV	d_C 0.50	d_A 1.00	d_A 0.98	d_C 0.57
	FBP	d_C 0.53	d_A 0.96	d_A 0.95	d_C 0.58

A – anion exchanger;   C – cation exchanger;   I – inert resin;

δ – bead density (kg m^{-3}).   d – bead diameter (mm)

Backwash flow rate 8m^{3}m^{-2}h^{-1}.

behaviour of multimedia filters on backwashing and led to Pruden
(208) proposing a 'reduced bulk density factor' to account for
discrepencies between the model and practically observed case. In
view of the basic anomoly in the bulk density approach the BD model
is not given any further consideration here.

3.4.1 EFFECT OF OPERATING VARIABLES

In resin separation there are a number of plant design and operating
variables that may affect the degree of separation achieved. The
three major factors are backwash water temperature, backwash flow
rate and the diameter of the vessel in which separation is carried
out.

Both the FBP and TV models can accommodate variations in backwash
water temperature through the water density and viscosity terms,
but the FBP model, through the Richardson and Zaki equation, can
also reflect variations in backwash flow rate and vessel diameter.
The effect of these variables on the predictions from both models
has been assessed by taking three fixed parameters for any pair of
resins, eg d_A, δ_A, δ_C, and determining the effect of the variable
on the fourth parameter (d_C) using the method described in section
3.3 above.

3.4.1.1 Temperature

The temperature of the backwash water can vary, from less than 5 ^{o}C
for a surface water in winter to 35 - 40 ^{o}C for reserve feed water.
Increasing the water temperature reduces the buoyancy and drag
induced lift on the particles, thus increasing the terminal velocity
and Reynolds number but decreasing the bed expansion on fluidisation.
Table 3.02 compares separation predictions from the FBP model for
temperatures of 5 ^{o}C, 20 ^{o}C and 40 ^{o}C at a typical backwash flow
rate of 8 m h^{-1}. There is no significant variation in the resin
separability predictions over the range 5 - 40 ^{o}C with the FBP model,
ie the changes in the variables effectively cancel out each other.

Similar calculations with the TV model (Table 3.02) produce a

TABLE 3.03 VARIATION OF PREDICTED RESIN SEPARABILITY WITH BACKWASH SUPERFICIAL FLOW RATE AT 20°C IN 100mm COLUMN FLUIDISED BED POROSITY MODEL

Fixed Parameter / Backwash Flow Rate $m^3m^{-2}h^{-1}$	d_A 1.0; δ_A 1075 δ_C 1250	d_C 0.5; δ_C 1250 δ_A 1075	d_I 0.6; δ_I 1175 δ_A 1075	d_I 0.7; δ_I 1175 δ_C 1250
8	d_C 0.53	d_A 0.96	d_A 0.95	d_C 0.58
12	d_C 0.52	d_A 0.97	d_A 0.95	d_C 0.58

A - anion exchanger; C - cation exchanger; I - inert resin;
δ - resin bead density (kg m^{-3}); d - resin bead diameter (mm).

TABLE 3.04 VARIATION OF RESIN SEPARABILITY WITH COLUMN DIAMETER AT 20°C - FLUIDISED BED POROSITY MODEL

Fixed Parameter / Column Diameter (mm)	d_A 1.0; δ_A 1075 δ_C 1250	d_C 0.5; δ_C 1250 δ_A 1075	d_I 0.6; δ_I 1175 δ_A 1075	d_I 0.7; δ_I 1175 δ_C 1250
25	d_C 0.48	d_A 1.06	d_A 1.20	d_C 0.55
100	d_C 0.53	d_A 0.96	d_A 0.95	d_C 0.58
2000	d_C 0.54	d_A 0.94	d_A 0.94	d_C 0.58

A - anion exchanger; C - cation exchanger; I - inert resin;
δ - resin bead density (kg m^{-3}); d - resin bead diameter (mm).
Backwash flow rate 8$m^3m^{-2}h^{-1}$.

similar conclusion with this model, the degree of resin separability is not affected by backwash water temperature. Data on variations of TV and FBP with temperature are given in Appendix 3, Tables A 3.02 and A 3.05 respectively.

3.4.1.2 Backwash Flow Rate

Several factors govern the choice of backwash flow rate. It must be sufficient to fluidise the whole bed but not so high that small beads of anion exchanger are elutriated. For condensate purification plant, ideally, it should induce the removal of particulate oxides from the resin surface. In practice the backwash flow rate for separation generally lies between 8 and 12 $m^3 \, m^{-2} \, h^{-1}$ (211). Table 3.03 compares separation predictions at these two flow rates for the FBP model at 20 $^{\circ}$C in a 100 mm diameter column. As with temperature there is no significant effect on resin separability due to backwash flow rate variations between 8 and 12 $m^3 \, m^{-2} \, h^{-1}$. Hence the FBP and TV models remain comparable despite the latters insensitivity to backwash flow rate. Data on the variation of FBP with backwash flow rate is presented in Appendix 3, Tables A 3.03 and A 3.04.

3.4.1.3 Column Diameter

The Richardson and Zaki equation for fluidised bed porosity includes the term $18(d/D_v)$ in calculating the exponent, n, (see 3.3.2) where d is the bead diameter and D_v the diameter of the column in which separation occurs. In practice the separation vessel diameter may vary between 0.9 m and 2.4 m (211). Therefore, the term d/D_v is very small - between 1.2×10^{-4} and 1.3×10^{-3} for the normal range of bead diameters.

Table 3.04 compares calculated separation predictions for columns of 25 mm, 100 mm and 2 m diameter based on the FBP model (Data from Table A 3.03). There is little difference between the predictions for a 100 mm and a 2 m diameter column, demonstrating the small effect of d/D_v in commonly used separation vessels. However, calculations for a 25 mm diameter column indicated a significant improvement in the predicted separability. The FBP model predicts that in a 25 mm diameter column complete separation will be achieved by a cation

exchanger with bead size 10% smaller or an anion exchanger with bead size 10% larger than in a 100 mm or larger diameter column. Narrower columns (<25 mm) will produce even better separation.

It follows from these calculations that the use of small diameter laboratory columns to test resin separability will indicate a better separation than will be achieved in full scale practice with the same resins. Therefore, if a 25 mm laboratory column test indicated that two resins separated there is no guarantee that they will do so in practice. If two resins do not separate in a small laboratory column then separation is likely to be even worse in practice. Whilst it is possible to apply corrections to narrow column results, derived from FBP model calculations, the concept of the separation chart approach was to avoid such column tests. The calculations described above indicate that a single separation chart will cover all of the full scale vessel diameters.

3.5 PRACTICAL SEPARATION DATA

To test the validity of the predictions of the FBP and TV models samples of resin have been taken from full scale and pilot column separated mixed beds and the core samples analysed for anion and cation exchanger and inert resin content and bead size distribution of each component.

3.5.1 FULL SCALE MIXED BED TRIALS

These trials took place at Walsall Power Station which had a conventional cation plus anion exchange water treatment plant followed by a single, 0.91 m diameter, mixed bed. The mixed bed contained 0.36 m^3 each of anion (Amberlite IRA 402) and cation (Amberlite IR 120) exchangers to give a total bed depth of 1.40 m. The bed was in situ regenerated with upflow acid injection and the unit contained unwrapped perforated pvc bottom, centre and top laterals.

This particular mixed bed was exhibiting extremely long post regeneration rinses down, in excess of 24 hours to reach a conductivity of <0.2 μS cm^{-1}. This was not an operational problem at this plant as

the boiler pressure did not require feed water $< 1.0 \mu S \ cm^{-1}$.
However, it was thought that cross contamination of the anion
exchanger by sulphuric acid due to poor separation of the resins
was a possible cause of the long rinses and to mitigate the effects
of this it was decided to add $0.07 \ m^3$ of inert resin (Ambersep 359)
to the bed. It was appreciated that this would not improve the
exchanger separation but the intention was to dilute the mixed
exchangers in the interfacial zone and raise the bulk of the anion
exchanger, due to the presence of the inert resin, so that acid contact
with the anion exchanger was minimised.

To assess the effect of adding the inert resin a vertical sample
core was taken after the bed had been backwashed at $8.8 \ m \ h^{-1}$ for
20 minutes. A core sampler had been made from 225 mm long sections
of 24 mm internal, and 33 mm external, diameter pipe made from
acrylonitrile butadiene styrene copolymer (ABS). Each section was
threaded internally at one end and externally at the other and could
be assembled into a core sampler up to 2 m long. Limited head room
within the mixed bed meant the sampler had to be assembled as it was
inserted vertically downwards into the bed. The core sampler could
only be pushed into the bed if there was a sufficient backwash flow
to just fluidise the whole bed. Even so the bottom of the core
sampler became bridged with resin about 150 mm from the base of the
bed so that the sample core was 150 mm less than the bed height.
After the sampler had been inserted the backwash flow was stopped
and the bed drained completely. A tight fitting rubber bung was
inserted into the top of the sample tube and the whole sample tube
plus resin core then withdrawn from the bed. It was necessary to
carefully unscrew the sampler after about 1 m was withdrawn, and to
seal both exposed ends of the core with polythene sheet and tape,
before the remainder of the sampler was extracted.

3.5.1.1 Resin Core Analysis

It was anticipated that the resin core contained just cation exchanger
at the bottom changing to cation exchanger plus inert resin, cation
plus anion exchanger plus inert resin, anion exchanger plus inert
resin and finally anion exchanger at the top of the core. Each 150 mm

TABLE 3.05 <u>SUMMARY OF CORE SAMPLE ANALYSIS. TRIAL SEPARATION IN 0.91 m DIAMETER MIXED BED, THREE RESIN SYSTEM</u>

SAMPLE (Height above bottom of core)	SIZE PARAMETER	ANION EXCH $\delta_A = 1080$	INERT RESIN $\delta_I = 1180$	CATION EXCH $\delta_C = 1220$
890 - 915 mm	Mean (mm) Range (mm) Ratio (max-min) Volume fraction %	0.76 0.48 - 1.17 2.44 97	. 0	3
675 - 700 mm	Mean (mm) Range (mm) Ratio (max-min) Volume fraction %	0.89 0.45 - 1.25 2.78 96	4 (Inert + Cation)	
590 - 620 mm	Mean (mm) Range (mm) Ratio (max-min) Volume fraction	0.92 0.59 - 1.4 2.37 50	0.48 0.40 - 0.59 1.48 32	0.36 0.28 - 0.52 1.86 18
450 - 480 mm	Mean (mm) Range (mm) Ratio (max-min) Volume fraction %	2	0.56 0.47 - 0.68 1.45 33	0.49 0.35 - 0.73 2.08 65
370 - 395 mm	Mean (mm) Range (mm) Ratio (max-min) Volume fraction %	0	0.60 0.50 - 0.71 1.42 4	0.60 0.43 - 0.89 2.07 96
190 - 215 mm	Mean (mm) Range (mm) Ratio (max-min) Volume fraction %	0	1	0.65 0.45 - 0.95 2.1 99

The range excludes the smallest 5% and largest 5% (volume fraction) of beads.
Backwash flow rate:- 8.8 m h^{-1} at 10 $^\circ$C.
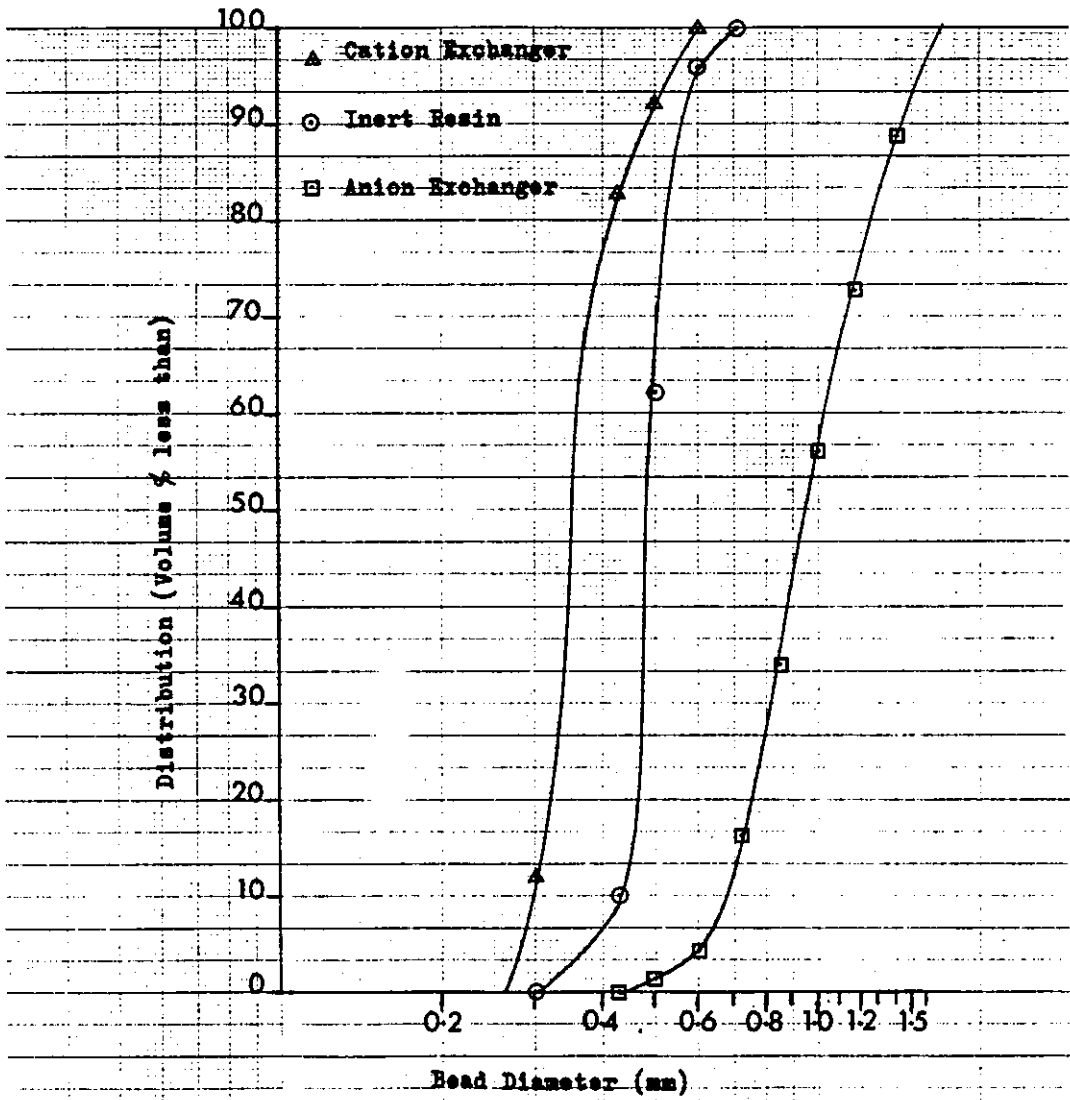
WALSALL MIXED BED RESIN CORE. SIZE DISTRIBUTION OF RESINS IN SAMPLE
SEGMENT AT HEIGHT 590 - 620 mm.

vertical segment of the core was separated and a sample representing
a 25 - 30 mm depth of separated resin bed removed from one end of
each segment. This gave six samples at approximately 150 mm intervals.
Additional samples from the uppermost and lowest segments, representing
wholly anion and cation exchanger respectively were also removed for
bead density measurement. A sample of inert resin was retained for
bead size analysis and bead density measurement.

Each resin sample was wet sieved through a stack of sieves with mesh
sizes 1.4, 1.19, 1.0, 0.85, 0.71, 0.60, 0.50, 0.425, 0.30, 0.125 mm.
If a size fraction contained mixed resins the cation exchanger was
separated from the anion and inert resins by differential flotation
in saturated brine. The settled volume of each resin type in each
size fraction was recorded.

Detailed procedures for wet sieving, resin separation and volume
measurement are given in Appendix 3 (A 3.1 and A 3.2). Only one
sample contained significant quantities of both anion exchanger and
inert resin and because the anion exchanger was mostly larger than
the inert resin there was little problem in separating the two bead
size distributions. Where a sieve fraction did contain both resins
a visual estimate of the percentage of each resin was made. This
did not significantly affect the accuracy of the measurements.
Details of the resin size analysis of each sample core is given in
Appendix 3 (Table A 3.07) and a summary of the results is given in
Table 3.05. This gives the Sauter mean diameter of each resin type
(A 3.1) found in each sample, the range of bead diameters excluding
the smallest and largest 5% of beads by volume, the ratio of the
maximum to minimum diameters within the 5 - 95% band and the volume
fraction of each resin type in the sample. The upper and lower 5%
of the bead size distribution were eliminated from the range because
the distributions tended to tail out considerably at the extremities.
In many batches of resin there are a small minority of high or low
density beads and in small sample volumes a few large beads may
distort the distribution. Figure 3.05 gives a size distribution
graph for the core segment containing anion and cation exchangers and
inert resin. The results from the Walsall mixed separation trial
will be discussed in section 3.5.3 along with the results from pilot
column trials presented in 3.5.2.

BACKWASH OUTLET

COLUMN
95 mm I.D.
1300 mm LONG

470 mm

270 mm

SAMPLE
PORTS

70 mm

PERFORATED RESIN SUPPORT

BACKWASH INLET

AIR INLET
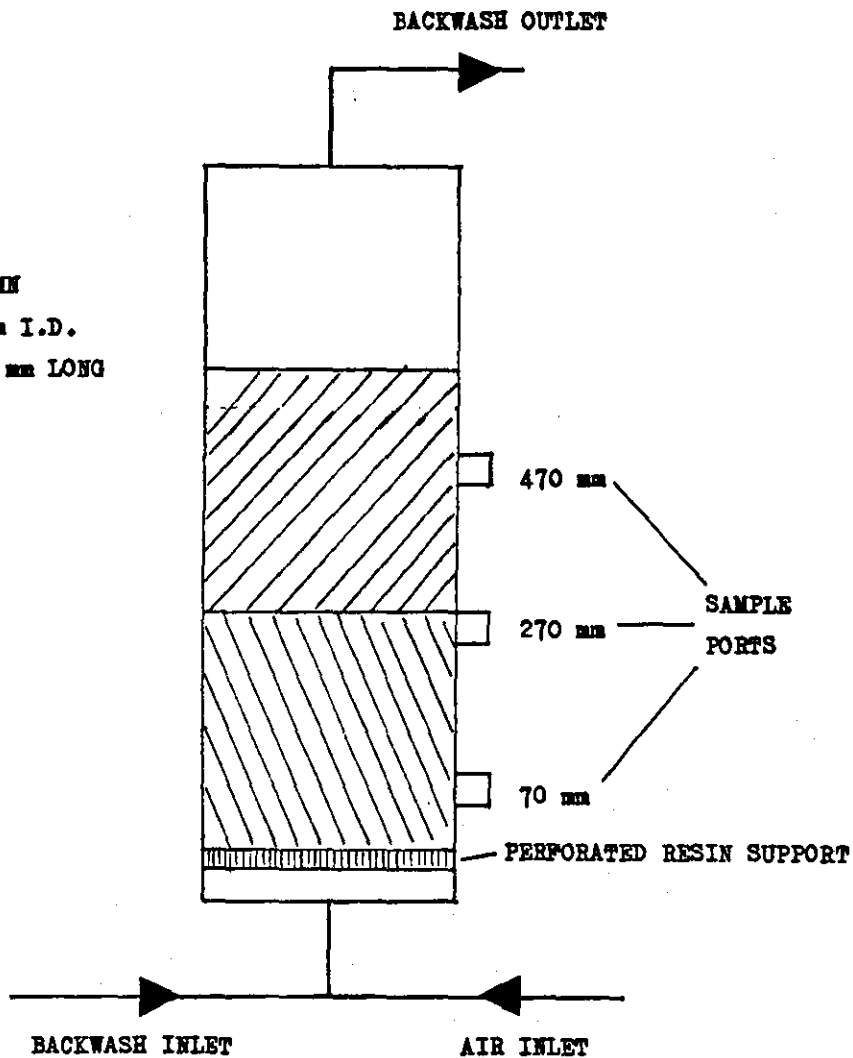
FIGURE
No. 3.06

TEST COLUMN FOR BACKWASHING AND SEPARATION OF RESINS

3.5.2 LABORATORY PILOT COLUMN INVESTIGATIONS

The sample core taken from Walsall mixed bed is a practical
separation and most core segments contain a mixture of resins. A
laboratory scale investigation into separation could proceed in
two ways. It would be possible to take resins of known density
grade them by sieving and determine the bead size distributions,
particularly d_{A-max} and d_{C-min} where separation just occurred.
Whilst this would be a true test of resin separability it would be
very time consuming in the preparation of the sieved and graded
samples and there is the difficulty of deciding exactly when separ-
ation has changed to marginal interfacial mixing. The alternative
is to mix two resins of known density backwash to separate and sample
them at various points through their depth to establish the size
distribution of each resin and the degree of intermixing. From the
criteria set up in 3.2 they should satisfy the condition $P_A = P_C$.
This second approach was adopted and a 100 mm diameter clear acrylic
column was set up with a suitable perforated resin support plate
and backwash water inlet and outlet. Plugged sample ports were
located at 70 mm, 270 mm and 470 mm above the resin support plate
so that 20 mm diameter resin cores could be extracted horizontally
from a drained bed. Figure 3.06 is an outline of the test column
and full constructional details are given in A 3.3. The 270 mm
sample port corresponded to the upper surface of 2 litres of
settled resin and a trial bed normally contained 2 litres each of
anion and cation exchanger.

3.5.2.1 Separation Trials

A number of trial separations were undertaken with several different
resin and ionic form combinations. For each resin combination
sample cores were taken for analysis by differential flotation
and sieving as described in Appendix 3 (A 3.1 and A 3.2). Bead
densities of the resins were determined on representative samples
before loading or from samples extracted from the bulk separated
exchanger. These separation trials were included in part of a wider
investigation of mixed bed performance not reported here and it is
not intended to present comprehensive details of the changes in
ionic form involved. For the purposes of this discussion it is

TABLE 3.06   100 mm PILOT COLUMN SEPARATION TRIALS
            ANALYSIS OF SAMPLE CORES
            TWO AND THREE RESIN SYSTEMS.

		ANION EXCH	INERT RESIN	CATION EXCH
Test 1a	Bead density(kg m^{-3})	1065		1240
	Mean (mm)	1.15		0.39
	Range (mm)	0.89–1.3		0.33–0.50
Centre	Ratio	1.46		1.52
Port				
	Volume Fraction (%)	43	–	57
Test 1b	Bead density(kg m^{-3})		1180	1240
	Mean (mm)		0.57	0.43
	Range (mm)		0.46–0.66	0.35–0.61
Centre	Ratio		1.43	1.74
Port				
	Volume Fraction (%)	2	64	34
Test 2a	Bead density(kg m^{-3})	1090	1180	1260
	Mean (mm)	1.10	0.49	0.39
	Range (mm)	0.77–1.43	0.44–0.58	0.35–0.52
Centre	Ratio	1.86	1.32	1.49
Port				
	Volume Fraction (%)	58	17	25
Test 2b	Bead density(kg m^{-3})	1090	1180	1260
	Mean (mm)	1.04	0.53	0.45
	Range (mm)	0.78–1.3	0.46–0.62	0.37–0.59
Centre	Ratio	1.67	1.35	1.6
Port				
	Volume Fraction (%)	7	47	46
Test 2c	Bead density(kg m^{-3})			1260
	Mean (mm)			0.59
	Range (mm)			0.47–0.75
Centre	Ratio			1.6
Port	Volume Fraction (%)	3	1	96

Backwash flow rate: 1.05 litres per minute ($\equiv$ 8.8 m h^{-1}).

TABLE 3.07   100 mm PILOT COLUMN RESIN SEPARATION TRIALS
ANALYSIS OF SAMPLE CORES
TWO RESIN SYSTEMS Duolite C26/Zerolit FF(1p).

SAMPLE	MEASURED PARAMETER	ANION EXCH Zerolit FFip	CATION EXCH Duolite C26
Test 3a	Bead density (kg m^{-3})	1105	1200
	Mean (mm)	1.13	0.56
	Range (mm)	0.70-1.45	0.48-0.68
Centre Port	Ratio	2.07	1.42
	Volume Fraction (%)	23	77
Test 3b	Bead density (kg m^{-3})	1095	1190
	Mean (mm)	1.20	0.52
	Range (mm)	0.81-1.47	0.45-0.58
Centre Port	Ratio	1.81	1.29
	Volume fraction (%)	67	33
Test 3b	Bead density (kg m^{-3})		1190
	Mean (mm)		0.94
	Range (mm)		0.77-1.21
Bottom Port	Ratio		1.57
	Volume Fraction (%)	0	100
Test 3c	Bead density (kg m^{-3})	1115	1185
	Mean (mm)	0.70	0.38
	Range (mm)	0.59-0.87	0.34-0.45
Top Port	Ratio	1.47	1.32
	Volume Fraction (%)	96	4
Test 3c	Bead density (kg m^{-3})	1115	1185
	Mean (mm)	1.09	0.54
	Range (mm)	0.9-1.3	0.46-0.62
Centre Port	Ratio	1.44	1.35
	Volume Fraction (%)	69	31
Test 3c	Bead density (kg m^{-3})		1185
	Mean (mm)		0.92
	Range (mm)		0.75-1.22
Bottom Port	Ratio		1.63
	Volume Fraction (%)	0	100

Backwash flow rate 1.3 litres per minute ($\approx$ 11 m h^{-1}).

sufficient to know the bead density and size distribution of the sampled resins.

Tests 1 and 2 were part of the Walsall mixed bed investigation. Test 1a was a separation of the original Walsall exchangers and test 1b was a trial separation of the same resins after addition of inert resin. Test 2 involved the Walsall anion exchanger plus inert resin with a different (10% DVB crosslinked) cation exchanger. All samples were taken at the centre port with successive additions of cation exchanger which effectively raised the interfacial and inter-mixed zones of the bed. A summary of the separation core analyses for tests 1 and 2 are given in Table 3.06 and full sieve analyses of each resin are given in Tables A 3.08 and A3.09.

Tests 3a,b, and c were all carried out with a mixture of Zerolit FF(ip) gel anion exchanger and Duolite C26 macroporous cation exchanger. This combination gave a good visual indication of separation as the C26 was grey and opaque while the FF(ip) was amber and translucent. The different tests were with the resins in different ionic forms and the number and position of the core sample depended on the visual assessment of the degree of separation. A summary of the resin separations achieved in test 3 is given in Table 3.07 and the full results in Table A3.10.

3.5.3 ASSESSMENT OF PRACTICAL SEPARATION DATA

One factor stands out from all the separation trials listed in Tables 3.05, 3.06, and 3.07. This is that the maximum to minimum diameter ratio in the core sample is much larger than would be expected if a standard resin had undergone perfect classification by size. A 20 mm deep core from a laboratory trial mixed bed represented about 7% of the total bed depth of each resin, while in the Walsall core sample a 25 - 30 mm segment represented about 4% of the depth of each resin. In a standard grade resin of typical distribution a 7% depth segment would have a size ratio of around 1.1 near the mid point of the size range. As the distribution tailed off towards the extremes of the size range the size ratio would become larger. At the upper size limit the size ratio might be 1.2 - 1.3 while at the

the lower size limit it might be as large as 1.4 or 1.5. If the
sample core contained mixed, but classified, resins the size ratio
of a particular component would be reduced in line with the propor-
tion of that resin in the mixture.

In the samples from the Walsall mixed bed (Table 3.05) smaller size
ratios than those given above would be expected for perfect class-
ification yet the Walsall core samples show larger sample size ratios
than the laboratory column tests. Another feature of note is that
where samples are taken at several depths in a particular test the
size ratios of a particular resin are generally very similar for all
samples, whether in a mixed resin zone or a predominantly single
resin zone. This is particularly evident in Table 3.05 for the
Walsall core sample.

3.5.3.1 Bulk Circulation

The bead size ratios mostly lie within the 1.5 to 2.0 range that
was quoted by Al-Dibouni and Garside (201) as the change over point
from bulk circulation to classification in fluidised multisize
particulate beds. Therefore, it is considered that the particle
motion in fluidised ion exchange resin beds is a series of over-
lapping bulk circulation cells, each cell containing resin beads
with a diameter ratio between 1.5 and 2.0. There will still be
a nett increase in fluidised bed porosity up through the bed and a
stepwise discontinuity across the interface between two separated
resins.

3.5.3.2 Bead Size Ratio

The larger size ratios in the Walsall core segments could be explained
by poor flow distribution generating turbulence in the bed. In any
in-situ regenerated mixed bed the backwash inlet is also the treated
water collector. It is designed primarily for the latter role and
is not an efficient distributor. Additionally there are two further
sets of laterals plus support steelwork that could interfere with
uniform flow. The laboratory column had better distribution and no
laterals.

An alternative explanation is that all the beads were not of a uniform density. This is quite possible in a partly exhausted bed, but as it was a mixed bed the density differences would be spread throughout the size distribution. A spread of densities might also explain why the size ratio of the anion exchanger was larger than that for the cation exchanger in the Walsall core sample. Figure 3.04 indicates that FBP values vary much more for small changes in anion exchanger density than for small changes in cation exchanger density. Therefore, a spread of densities in the anion exchanger might enlarge the bulk circulation cells as assessed purely by bead size. The more controlled conditions of resin preparation in the laboratory column tests would not give such a great variation in bead densities and would therefore result in narrower bead size ratios in the sample cores. The measured bead densities in all cases were average values for the bulk resin.

The inert resin, used in some of the trials, had a narrower size distribution (0.35 - 0.8 mm) than standard grade exchangers and was probably of more uniform density. The inert resin still showed a size ratio of 1.4 to 1.5, indicating that this would be the ratio for beads of uniform density.

An assessment of the results of Scarlett et al (202, 203) showed that the size ratio of 1.4 - 1.6 was a common feature of a small bed depth sample taken from a fluidised bed of multisize particles of uniform density. In some instances Scarlett et al (203) took up to nine different height samples from a fluidised bed. All samples had a sigmoid distribution and the size ratio of 1.4 - 1.6 appeared to hold for several different backwash flow rates. Therefore, it would appear that bulk circulation cells with a bead size ratio of 1.4 - 1.6 are a fundamental feature of the fluidisation of mono-density particles with a distribution of bead sizes.

3.5.3.3 Cell Average Fluidised Bed Porosity

Each bulk circulation cell will contain a specified range of bead diameters and, if the cell were to exist on its own, would have, effectively, an average fluidised bed porosity. This could be

defined by some average parameter of the bead size distribution within the cell eg the Sauter mean diameter (209). Therefore, if two resins are separated on backwashing the FBP's on either side of the interface are those related to the mean diameters of the bulk circulation cells adjacent to the interface rather than those equivalent to the limits of the respective bead size distributions (d_{A-max}, d_{C-min}). It follows that if a FBP model (Figure 3.04) is used for resin separability predictions it should be based on the mean diameters of resins in the bulk circulation cells rather than the upper and lower size limits of the anion and cation exchangers, respectively. Predicted resin separability based on cell mean diameters will be enhanced compared with that based on the limits of the distributions.

For example, assume that each bulk circulation cell has a max:min size ratio of 1.4 and that the FBP model predicts that two resins will separate when $d_A = 1.00$ mm, $d_C = 0.6$ mm. With the perfect classification model originally proposed d_A and d_C represent the limits of the anion and cation exchanger size distributions d_{A-max} and d_{C-min}. In the revised model d_A and d_C represent the means of the bulk circulation cells adjacent to the interface. Assuming that the Sauter mean is equivalent to the median value of the size ratios then for the bulk circulation model

$$d_{A-max} = d_A \times 1.2 = 1.2 \text{ mm}$$
$$d_{C-min} = d_C \div 1.2 = 0.50 \text{ mm.}$$

Thus the bulk circulation model shows an improvement in resin separability compared to the classification model.

The bulk circulation cell model has been used to describe resin separation with a sharply defined interface. Unfortunately the data summarised in Tables 3.05, 3.06 and 3.07 cannot test this directly as all samples taken around the interfacial zone deliberately contained mixed resins. The original criteria of separation, set out in 3.2, envisaged that in mixed resin zones the separability parameter would be equal for both resins. This can be tested by comparing the tabulated data with predictions from the FBP separation chart (Figure 3.04). Since the mean diameter of each resin in Tables 3.05, 3.06 and 3.07   . . . .

TABLE 3.08   COMPARISON OF OBSERVED AND PREDICTED MEAN DIAMETERS OF
INTERMIXED RESINS

| TEST SAMPLE | FIXED PARAMETERS | | | DIAMETER (2) (mm) | | ERROR ($\%$) |
	DENSITY(1) ($kg\ m^{-3}$)	DIAMETER(1) (mm)	DENSITY(2) ($kg\ m^{-3}$)	OBSERVED	PREDICTED	
Walsall	1080	0.92	1180	0.48	0.59	−23
Walsall	1220	0.36	1180	0.48	0.41	−14
Walsall	1180	0.56	1220	0.49	0.51	−4
Walsall	1220	0.60	1180	0.60	0.66	+10
1a	1065	1.15	1240	0.39	0.54	−38
1b	1240	0.43	1180	0.57	0.51	−10
2a	1090	1.10	1260	0.39	0.62	−59
2a	1180	0.49	1260	0.39	0.41	−5
2b	1180	0.53	1260	0.45	0.44	+2
2b	1260	0.45	1090	1.04	0.80	−23
3	1115	1.09	1185	0.54	0.81	−50
3	1185	0.54	1115	1.09	0.67	−38
4	1095	1.20	1190	0.52	0.79	−52
4	1190	0.52	1095	1.20	0.77	−39
4	1105	1.13	1200	0.56	0.79	−41

For any pair of intermixed resins (1) and (2) three parameters were
fixed ie Density (1), Diameter (1) and Density (2). The fourth
parameter Diameter (2) was compared between observed and predicted
data.

represents the mean of a bulk circulation cell the measured and
predicted bead diameters should be comparable. Table 3.08 presents
the observed and predicted bead diameters for a number of examples
taken randomly from Tables 3.05, 3.06 and 3.07. An error factor has
been included representing the percentage difference between the
two diameters relative to the observed value. The error is negative
if the prediction was pessimistic, positive if optimistic.

In a majority of the examples the predictions were pessimistic. Of
the two positive predictions that for Walsall is due to an anomoly
in the measured data, ie both resins have the same mean size for
different densities, while that for test 2b is virtually a correct
prediction. The size of the percentage error varies considerably,
although the largest errors do not represent very large differences
in bead diameter terms. It is notable that those resin pairs that
have errors of 10% or less have very similar size distributions,
while the larger errors apply to resin pairs with widely spaced size
distributions.

The bulk circulation of monodensity multisize bead distributions is
a dynamic equilibrium requiring complex description, although certain
average characteristics can be defined by a mean bead diameter. The
interaction of two, or even three, differently sized distributions
will almost certainly establish a new set of dynamic equilibria that
are depemdent both on the individual distributions and the relative
amounts of each in the whole. It is unrealistic to expect two resins
of differing size distribution but similar FBP when fluidised singly
to have the same FBP value when they intermix. The mixing of two resins
with similar size distribution is more likely to have an FBP close to
the predicted value.

3.5.4 MODIFIED SEPARATION MODEL

Despite the fact that the FBP's of individual components in a resin
mixture do not always correlate with predictions from FBP calcula-
tions it is considered that a model for separated resins based on
the FBP's of the bulk circulation cells either side of the interface
is realistic. Remembering that one aim of this work was to produce
a simple method for predicting resin separability from routinely
available laboratory measurements, ie bead size and bead density,

it is also considered that the use of Sauter mean bead diameter is an
acceptable parameter for calculating the FBP of a bulk circulation
cell. The data obtained from trial separations indicates
that a monodensity distribution of beads will have a minimum size
ratio of 1.4. The smaller the size ratio the more pessimistic the
separation predictions become and for the purposes of specifying
practical resin size gradings and bead densities a pessimistic
model provides a safety margin.

Since the FBP (classification) and terminal velocity (TV) models
gave very similar separability predictions a TV separation chart
combined with the mean diameter of the bulk circulation cell could
also be used.

3.6 APPLICATION TO MIXED BED OPERATION

Ion exchange resins produced for water treatment combine a number of
physico-chemical characteristics eg porosity, capacity, selectivity,
kinetics, bead density and physical strength. To vary one inevitably
causes changes in several other of these characteristics and not
always in a beneficial direction. Therefore, it is not possible to
optimise bead densities for resin separation whilst maintaining other
desirable characteristics of an exchanger. Fortunately the other
major influence on resin separation, bead size, is easily varied in
resin production, although there is generally an added cost premium
to take account of resin wastage in producing narrower bead size
distributions.

Before making predictions and specifications for resin bead sizes
it is necessary to consider the state of the resins prior to separ-
ation, ie their ionic forms and likely bead densities. It would be
possible to consider every likely combination of mixed bed resins,
even combinations of different manufacturers products, and produce
individual bead size specifications. Clearly this would produce a
multitude of bead size gradings that no manufacturer would be pre-
pared to produce or stock. Instead, the approach used here has been
to examine three common mixed bed applications in water purification
for boiler feed and to establish the worst likely conditions for

resin separation that would occur in normal operation.

It was first necessary to investigate the variation of bead density
with both polymer/matrix type and ionic form. The data obtained is
summarised in 3.6.1. Using the bead density data, predictions were
made of the necessary bead size gradings to ensure separation for
various types and combinations of resins. This resulted in a general
specification for two resin mixed beds, with certain noted exceptions.
Triple resin beds require a more detailed analysis as manufacturers
offers a slightly different combination of bead sizes and inert resin
densities (3.6.5.3).

3.6.1. RESIN BEAD DENSITIES

Some resin manufacturers give nominal values for resin bead densities,
generally in the chloride form for anion exchangers and sodium or
hydrogen form for cation exchangers. Resin bead densities for
specific purposes are reported in the literature (212, 213, 214) but
no general study has been published. Therefore, an investigation
was undertaken into the variation of bead density with counter ionic
form, with polymer/matrix type and between different batches of the
same product.

Resin bead density (δ) is defined as the mass per unit volume of
polymer plus fixed ionic groups plus counter ions plus moisture within
an envelope formed by the outer surface of the moist resin bead.
The sum of the masses of polymer, fixed ions and counter ions is
referred to here as the skeletal mass and the skeletal mass per unit
swollen volume is termed the skeletal density (ψ). When one counter
ion is exchanged for another the skeletal mass varies with the
equivalent weight of the counter ion. At the same time the moisture
content varies and the volume of the bead may also change. All
three factors contribute to a change in density of the resin particle.

The bead density, moisture content and skeletal density of any
particular resin type in a particular ionic form is given by

$$\delta \quad = \quad \psi \quad + \quad 1000 \, M_v \qquad \ldots\ldots\ldots(3.2)$$

where δ =   bead density (kg m^{-3})

             ψ =   skeletal density (kg m^{-3})

            M_v =   moisture content as a volume fraction of the moist (swollen) bead volume.

Because M_v is a dimensionless volume fraction it is necessary to multiply by 1000 kg m^{-3},   the density of water.

The more commonly determined moisture content is M_w - moisture content as a weight fraction of the moist bead, determined by drying the moist resin at 105 $^{\circ}$C. M_w and M_v are related by

$$M_v = M_w \, x \, \frac{\delta}{1000} \qquad \ldots\ldots\ldots(3.3)$$

The procedures used for bead density measurement are outlined below together with a general survey of resin bead density variations with ionic form and polymer/matrix type.

3.6.1.1   Bead Density Determination

Because ion exchange resins contain moisture that is easily lost on exposure to air at ambient temperatures it is necessary to use a method of density measurement that keeps the beads moist without leaving residual water on the external surface of the bead. Density measurements on single beads would be extremely difficult and may not be representative. Therefore, an average density of a number of beads in a single sample has been determined.

Two methods for achieving a sample of moist resin beads free of residual water have been reported and centrifuging a sample in a porous base centrifuge tube (215, 216) was chosen in preference to 'blotting' resin on an adsorbent paper (217).

Resin mass is easily measured to an accuracy of 0.1 mg using a standard laboratory analytical balance, but accurate measurement of resin bead volume is not so easily achieved and two methods were used. Initially an existing device for measuring resin volumes by

TABLE 3.09 SULPHONATED STYRENE/DVB CATION EXCHANGERS.
VARIATIONS OF BEAD DENSITY (kg m^{-3}) WITH
COUNTER ION AND POLYMER/MATRIX TYPE.

MATRIX	GELULAR						MACROPOROUS			
DVB CROSSLINKING	8%			10%			12%			20%
MANUFACTURER DESIGNATION	R&H IR120	D-I C20	D-I C225	R&H IR132	D TG-650C	D-I C255	D-I Z625	D-I C26	R&H IR252	R&H IR200
H$^+$	1180					1215	1207		1181	1206
NH$_4^+$	1184			1250	1232	1227	1200	1184	1184	1213
Na$^+$	1245	1286	1282	1318		1277	1251	1257	1241	1254
Mg^{2+}						1303				1262
Ca^{2+}						1336				1284
K$^+$						1356				1296

D
Dow
(Dowex)

D - I
Duolite International
(Duolite)

R & H
Rohm & Haas
(Amberlite)

displacement was used and the resin sample recovered but latterly
a specific gravity bottle has been used to determine the resin bead
volume by weighing using the standard specific gravity measurement
technique (see A 3.4). The displaced volume method gave a standard
deviation of less than $\pm 1\%$ while the specific gravity method gave
a standard deviation of $< 1 \times 10^{-3}\%$ (Table A 3.11)

3.6.1.2 Cation Exchanger Bead Density Variations

Two resins, one 10% gelular (Duolite C255) and one 20% DVB macro-
porous (Amberlite IR200) were converted to six different ionic forms
likely to be encountered in water treatment, H^+, Na^+, K^+, NH_4^+, Ca^{2+}
and Mg^{2+}. The bead densities in each form were measured for both
resins and densities in the more common H^+, Na^+ or NH_4^+ forms
measured for a wider variety of sulphonated polystyrene resins, both
gelular and macroporous (Table 3.09). A general trend in density
variation with counter cation was found, with increasing density in
the order

$$H^+ < NH_4^+ < Na^+ < Mg^{2+} < Ca^{2+} < K^+ .$$
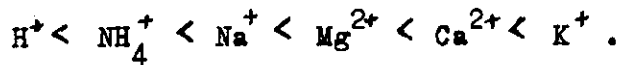
There is no direct correlation between bead density and counter cation
equivalent weight, because the differences in hydration of the various
cations lead to swelling or shrinking of the matrix on conversion
from one form to another as well as changes in skeletal mass.

From Table 3.09 it can be seen that there is a spread of densities
amongst polymer/matrix types. The 10% DVB gelular resin has the
highest density while the 8% DVB gelular resin has densities similar
to the macroporous types. The latter will be influenced by porosity.
There are also variations between polymer/matrices of the same type
and there are variations between different production batches of the
same product. All manufacturers quote a range of moisture values
for a particular resin and this can result in bead density variations
of up to 30 kg m^{-3}. All these variations in bead density can affect
resin separability; it is not sufficient to rely on a manufacturers
average value for bead density.

TABLE 3.10 ANION EXCHANGE RESINS

VARIATION OF BEAD DENSITY $(kg\ m^{-3})$ WITH IONIC FORM AND

POLYMER/MATRIX TYPE.

POLYMER	PS/DVB	PS/MB	PS/DVB	PS/DVB	PA/DVB
MATRIX	Gelular	Isoporous	Macroporous	Macroporous	Gelular
MANUFACTURER	R&H	D-I	R&H	D-I	R&H
TYPE	IRA400	FF(ip)	IRA900	MPF	IRA458
OH^-	1100	1075	1062	1054	1086
Cl^-	1106	1094	1085	1071	1091
CO_3^{2-}	1112	1102	1077	1070	-
$HSiO_3^-$	1120	1107	1089	1075	-
HCO_3^-	1141	1109	1094	1079	1104
SO_4^{2-}	1144	1118	1100	1087	1116

PS - Polystyrene.   DVB - Divinylbenzene

PA - Polyacrylamide.   MB - Methylene bridge.

R & H;Rohm & Haas (Amberlite)

D - I;Duolite International (Duolite formerly Zerolit)

Zerolit FF(ip) and MPF are no longer manufactured.

TABLE 3.11   <u>ANION EXCHANGER BEAD DENSITIES</u> $(kg\ m^{-3})$

<u>VARIATIONS BETWEEN POLMER MATRIX TYPES FROM</u>

<u>DIFFERENT MANUFACTURERS.</u>

POLYMER	PS/DVB					PA/DVB
MATRIX	GELULAR					
CROSSLINKING	HIGH	LOW	MEDIUM	HIGH	LOW	LOW
MANUFACTURER	R&H	R&H	R&H	D	D-I	R&H
DESIGNATION	IRA400	IRA402	IRA420	SBR-C	A113	IRA458
Cl^- form	1106	1072	1060	1097	1081	1091
SO_4^{2-} form	1144	1119	-	-	1124	1116

POLYMER	PS/MB		PS/DVB			PA/DVB
MATRIX	ISOPOROUS		MACROPOROUS			GEL
CROSSLINKING	MEDIUM	LOW	MEDIUM	HIGH	MED/HIGH	MEDIUM
MANUFACTURER	D-I	D-I	R&H	D-I	D-I	D-I
DESIGNATION	A101D	FFip	IRA900	A161	MPF	A132
Cl^- form	1085	1094	1085	1081	1071	1089
SO_4^{2-} form	1116	1118	1100	1110	1087	1118

PS - Polystyrene   DVB - Divinylbenzene
PA - Polyacrylamide   MB - Methylene bridge

D - Dow (Dowex)
D-I - Duolite International (Duolite formerly Zerolit)
R&H - Rohm & Haas (Amberlite)

Zerolit FF (ip) and MPF are no longer manufactured.

3.6.1.3 Anion Exchanger Bead Density Variations

In a similar way anion exchangers showed bead density variations
with both counter anion and polymer/matrix type. Anion exchangers
are not so easily characterised by % DVB and this leads to certain
minor variations. Anion exchangers based on five different polymer/
matrix types were each converted to six different ionic forms
representing anions commonly found in water treatment. Bead density
measurements were made on each form and are given in Table 3.10.
Counter anions can be placed in order of increasing bead density:

$$OH^- < Cl^- < CO_3^{2-} < HSiO_3^- < HCO_3^- < SO_4^{2-}$$
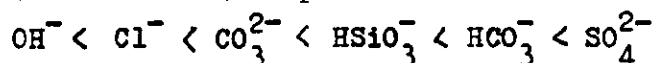
although the order was not as clearly defined as with the cation
exchangers. This is because a much smaller spread of densities
$35 - 45$ kg m^{-3} covers the range of counter anions from OH^- to SO_4^{2-}
and any minor variations due to the effects of crosslinking become
more apparent.

Variations of bead density with polymer matrix type are not so easy
to characterise for anion exchangers because of the differences in cross-
linking due to the presence of methylene bridges. Table 3.11
compares the bead densities for chloride and sulphate forms of a
number of polymer/matrix types and manufacturers versions. Cross-
linking has been loosely grouped into high, medium and low. The
high crosslinked gelular styrene/DVB anion exchanger has a higher
density than other types and the macroporous styrene/DVB resins
generally have lower bead densities. As with the cation exchangers
there are also production batch differences, which can result in
variations of up to 20 kg m^{-3} and manufacturers sometimes alter the
polymer/matrix slightly or increase the capacity marginally, both of
which can increase the bead density.

3.6.2 MAKE-UP MIXED BEDS

Most mixed beds in make-up water treatment plant are used only to
'polish' the low concentrations of impurities leaking from the
preceding two stage cation-anion exchange beds. In the power
industry there are very few mixed beds that operate directly on the
raw water, although they may be more common in smaller installations

in other industries. The ionic load onto make up mixed beds is low
and is derived from two sources. From the preceding anion exchange
unit the major inorganic ions are Na^+ , $HSiO_3^-$ and HCO_3^-. There may
also be some naturally occuring organic anions eg fulvic acids.
From within the mixed bed itself Na^+ and SO_4^{2-} ions arise from
unrinsed regenerants ($NaOH$ and H_2SO_4) and from cross contamination by
the wrong regenerant. Those resin beads that undergo cross contam-
ination will be converted fully to the Na^+ or SO_4^{2-} forms whereas
other resin beads in the bed may contain a mixture of ions.

At the end of an operating cycle the most dense anion exchanger is
likely to be fully sulphated beads from cross contamination and these
are also likely to be large beads from near the interface. The
least dense cation exchanger is likely to be some hydrogen form, ie
regenerated, cation exchanger that has not been utilised during the
operating cycle. This is quite common in mixed bed operation as
many beds are run to a fixed through put rather than a breakthrough of
influent ions. Therefore, in make up mixed beds the worst likely
combination of bead densities is SO_4^{2-} form anion exchanger, H^+ form
cation exchanger.

3.6.3 COMBINED MAKE-UP AND CONDENSATE RECOVERY BEDS

In some modern power stations mixed beds in the make up water treat-
ment plant have a dual role of polishing water from the preceding
two stage deionisation plant and purifying recovered condensate
and stored reserve feed water. The latter waters introduce a wider
range of ions to the mixed beds. The main additional cation is NH_4^+,
from the ammonia used to condition the feed water to the steam/water
circuit. Additional anions may be Cl^-, HCO_3^-, SO_4^{2-} and possibly NO_3^-
derived from ingresses of impurities into the steam/water circuit or
the reserve feed water tank. The possibilities of cross contamination
by Na^+ and SO_4^{2-} during regeneration are also present.

As with the straight make up mixed bed the anion exchanger with the poor-
est separation is the high density sulphate form. The low density
forms of cation exchanger likely to be present are H^+ or NH_4^+, both
of very similar density.

3.6.4 CONDENSATE PURIFICATION MIXED BEDS

In condensate purification mixed beds that are not protected by
cation exchange units the major ionic load is NH_4^+, although the
utilisation of the available capacity is poor at the high flow rates
employed so that significant amounts of hydrogen form resin may
remain prior to regeneration. The anion exchanger load is normally
small, largely HCO_3^- /CO_3^{2-} due to CO_2 from air ingress into the
condensate and the breakdown of organic species in the boiler.
There may also be small quantities of ions from the make up mixed
beds and the usual possibilities for trace regenerant uptake and
cross contamination during regeneration. During condenser in
leakage of cooling water additional ions reaching the condensate
purification mixed beds. At sea water cooled plants the major
additional ions are Na^+ and Cl^- with less SO_4^{2-} and minor amounts of
other anions and cations. At inland power stations the additional
ions will reflect the analysis of the cooling water ie river water
rather than sea water.

If there are cation exchange units protecting the mixed beds, the
latter see a very small cation load and will remain largely in the
H^+ form. If the mixed beds operate on the ammonium cycle the cation
exchanger will be virtually 100% ammonium form. In both these
cases the anion exchanger will be very similar to the unprotected bed.

The nett result of these considerations is similar for all types of
CPP mixed beds. The densest anion exchanger is, once again, the
SO_4^{2-} form while the least dense cation exchangers are either the
NH_4^+ or H^+ forms, both of similar density.

In all the instances described above sulphuric acid has been the
cation exchanger regenerant, giving the SO_4^{2-} form resin on cross
contamination. If hydrochloric acid were used instead this would
result in the lower density Cl^- form resin as a result of cross
contamination. Although sulphate ions are still present in the
influent to mixed beds in certain circumstances they would be
distributed over a range of bead sizes and would be in equilibrium
with other anions, so as not to form 100% SO_4^{2-} form beads. However,

in Britain, the USA and a number of European countries sulphuric acid is the commonly used regenerant.

3.6.5 BEAD SIZE SPECIFICATION

From the discussion on mixed bed exhaustion conditions it is clear that the ionic forms on which separation predictions must be based are:

Anion exchanger – sulphate form

Cation exchanger – hydrogen or ammonium form.

Inspection of the bead density data in 3.6.1.2 and 3.6.1.3 indicates that the minimum cation exchanger density for 8% DVB gelular resins and most macroporous resins is around 1185-1200 kg m^{-3}. Only the 10% DVB gel cation exchanger appears to have greater density but some batches of this type of resin have had H$^+$ form densities as low as 1205 kg m^{-3}. Similarly the data in Tables 3.10 and 3.11 indicates that for many types of anion exchanger gelular and macroporous the sulphate form density lies in the range 1100-1120 kg m^{-3}. The major exception to this is the high cross linked gelular anion exchanger, eg IRA400, which has SO$_4^{2-}$ form densities up to 1150 kg m^{-3}. Therefore, as common limits for specification purposes, the following densities have been used:-

Anion Exchanger   1120 kg m^{-3}

Cation Exchanger   1185 kg m^{-3}.

The case for the higher density anion exchanger is considered separately.

3.6.5.1 Method of Prediction

In separation predictions the largest anion exchanger diameter (d_{A-max}) and the smallest cation exchanger (d_{C-min}) must be specified as well as the overall size range of each resin bead distribution. If the overall size range is less than 1.4 then the resin will act as a single bulk circulation cell on backwashing characterised by its Sauter mean diameter. If the overall size ratio is greater than 1.4, classification by means of overlapping bulk circulation cells will occur. The method of prediction is similar to that described in 3.5.3.3 and used for the comparisons in Table 3.08. Three parameters, the two resin densities and one

TABLE 3.12   SEPARATED RESINS -BEAD SIZE PREDICTIONS FOR CATION EXCHANGER 1185 kg m^{-3} AND ANION EXCHANGER 1120 kg m^{-3}.

1.

Fixed Cation Exchanger		Calculated Anion Exchanger	
d_{C-min} (mm)	d_{C-mean} (bulk circ)	d_{A-mean} (bulk circ)	d_{A-max} (mm)
0.3	0.36	0.48	0.58
0.4	0.48	0.60	0.72
0.5	0.60	0.79	0.95
0.6	0.72	0.91	1.09
0.7	0.84	1.07	1.28

2.

Fixed Anion Exchanger		Calculated Cation Exchanger	
d_{A-max} (mm)	d_{A-mean} (bulk circ)	d_{C-mean} (bulk circ)	d_{C-min} (mm)
1.2	1.0	0.76	0.63
1.1	0.91	0.71	0.59
1.0	0.83	0.65	0.54
0.9	0.75	0.58	0.48
0.8	0.67	0.53	0.44

Calculations based on Fluidised Bed Porosity Separation Chart Calculated for Backwash at 8 mh^{-1}, 20 ^{o}C in a 100 mm Diameter Tube. (Figure 3.04)

bead diameter are fixed and the FBP separation chart is used to calculate the fourth parameter ie the second resin bead diameter that will just separate. The bead diameters are the means of the bulk circulation cells adjacent to the separated resin interface and are calculated from

$$d_{A-mean} = d_{A-max} \div 1.2$$
$$d_{C-mean} = d_{C-min} \times 1.2$$

For example $\delta_A = 1120$ kg m^{-3}, $\delta_C = 1185$ kg m^{-3} and $d_{C-min} = 0.5$ mm are the three fixed parameters leaving d_{A-max} to be calculated.

$$d_{C-mean} = 0.5 \times 1.2 = 0.6 \text{ mm}$$

From the FBP separation chart (Figure 3.04) a bead of 0.6 mm diameter and density 1185 kg m^{-3} has an equivalent FBP to a bead 0.79 mm diameter with a density of 1120 kg m^{-3}.

$$d_{A-mean} = 0.79 \text{ mm}$$
$$d_{A-max} = 0.79 \times 1.2 = 0.95 \text{ mm.}$$

Therefore a cation exchanger of density 1185 kg m^{-3} and minimum bead diameter 0.6 mm will just separate from an anion exchanger maximum bead diameter 0.95 mm and a density of 1120 kg m^{-3}.

Similar calculations have been made for the specified densities of $\delta_A = 1120$ kg m^{-3}, $\delta_C = 1185$ kg m^{-3} for cation exchangers of 0.3, 0.4, 0.5, 0.6 and 0.7 mm diameter and anion exchangers of 0.8, 0.9, 1.0, 1.1 and 1.2 mm diameter. The results of these calculations are given in Table 3.12.

3.6.5.2 Two Resin Mixed Beds

The first conclusion from Table 3.12 is confirmation that standard grades of resins (0.3-1.2 mm) will not separate completely. The results for standard resins ' also demonstrate another facet of intermixing resins. If the separation bead sizes are written vertically as if classified,

Anion	Cation	(mm)
0.30		
0.58	0.30	
1.20	0.63	
	1.20	

it will be seen that whilst only a small size range of cation exchanger, 0.30 - 0.63 mm, does not separate from the anion exchanger, the smallest cation exchanger bead has penetrated a long way into the anion exchanger zone. However, the large anion exchanger beads do not descend very far into the bulk cation exchanger. This has been confirmed by practical observations and from the data in Tables 3.05 and 3.07 where small amounts of small diameter cation exchanger are found distributed well into the anion exchange resin.

From Table 3.12 a number of cation and anion bead size ranges can be defined to ensure separation. Rounded to the next higher or lower 0.1 mm for anion and cation exchangers respectively the two main possible size ranges are

   i) - Anion, 0.3 - 0.9 mm; Cation, 0.5 - 1.2 mm

or ii) - Anion, 0.3 - 1.0 mm; Cation, 0.6 - 1.2 mm.

As anion exchangers are more than twice the cost of cation exchangers it is more cost effective to narrow the size range of the cation exchanger by a larger amount. Increasing the minimum cation exchanger size will also reduce the risk of any below size limit resin beads separating well into the anion exchanger. Therefore, the preferred size ranges are those given in (ii).

It was noted earlier that whilst these bead sizes will apply to the majority of combinations of polymer/matrix types there may be problems with the higher density high crosslinked gelular anion exchangers. These resins have SO_4^{2-} form densities up to 1150 kg m^{-3} and calculations, similar to those described, indicate that a maximum anion exchanger diameter of 0.80 mm is necessary to separate from all types of cation exchanger, with a minimum diameter of 0.6 mm. However, if a 10% gelular cation exchanger, (H^+ form density $\geqslant$ 1205 kg m^{-3}) is used with the high crosslinked gelular anion exchanger the size specifications in (ii) will achieve complete separation.

Therefore, the recommended bead size ranges for mixed bed resins are:

  Anion exchanger 0.3 - 1.0 mm

  Cation exchanger 0.6 - 1.2 mm

with the restriction that a highly crosslinked higher density

TABLE 3.13 **MANUFACTURERS SPECIFICATIONS FOR TRIPLE RESIN SYSTEMS.**

ANION EXCHANGERS

Manufacturer		D-I	D-I	R&H	R&H	R&H	B	S	S
Resin		A113	A161	IRA400	IRA420	IRA900	MP500	3AS	3A
Polymer/matrix		G	M	G	G	M	M	M	G
Size Range	min	0.4	0.4	0.35	0.35	0.35	0.4	0.3	0.3
(mm)	max	0.8	0.8	0.85	0.85	0.85	1.0	1.0	1.0
Bead Density(kg m^{-3})		1120	1120	-	-	-		1070	1070
Ionic form		SO$_4$	SO$_4$					Cl	Cl

INERT RESINS

Manufacturer		D-I	D-I	R&H	B	S
Resin		S3TR	S5TR	359	1039TR	275BZ
Size Range	min	0.7	0.7	0.4	0.4	0.4
(mm)	max	0.9	0.9	0.7	1.0	0.85
Bead Density (kg m^{-3})		1150	1170	1160-1180	1160	1140-1150

CATION EXCHANGERS

Manufacturer		D-I	D-I	D-I	R&H	R&H	R&H	R&H	B	S	S
Resin		C26	C225	C255	IR120	IR132	IR200	IR252	SP112	C-250	CFZ
Polymer/matrix		M-12%	G-8%	G-10%	G-8%	G-10%	M-20%	M-12%	M	G-10%	M
Size Range	min	0.7	0.7	0.6	0.5	0.6	0.6	0.6	0.63	0.6	0.6
(mm)	max	1.2	1.2	1.2	1.2	1.2	1.2	1.2	1.2	1.2	1.2
Bead Density(kg m^{-3})		1220	1220	1240	-	-	-	-		1320	1300
Ionic form		NH$_4^+$	H$^+$	H$^+$						Na$^+$	Na$^+$

KEY   B - Bayer Trennschicht   D-I - Duolite International - Triobed

R&H Rohm & Haas - Ambersep

S Sybron/Resindion Blue Zone   G - Gelular x% DVB M - Macroporous

gelular anion exchanger should only be used with a 10% DVB cross-
linked gelular cation exchanger.

Examining the various triple resin size grades for exchangers (Table 3.13)
indicates that almost all the cation exchangers, except Ambersep 120,
and all the anion exchangers meet or improve upon the required
specification. As the Ambersep anion exchangers have an upper size
limit of 0.85 mm, Ambersep 120 (d_{C-min} = 0.5 mm) will separate from
all of them except Ambersep 400, the high crosslinked gelular anion
exchanger.

As a result of this work it is now recommended to all mixed bed
users . that they purchase triple resin grade exchangers, without
the inert resin, for use in mixed beds; the restrictions applying
to high density anion exchangers also being noted. It is also
recommended that triple resin systems are only used where there is
a clear need to overcome identified problems of regenerant cross
contamination.

3.6.5.3 Triple Resin Beds

The concept of a layer of inert resin to separate between the
two exchangers and thus avoid cross contamination was proposed by
McMullen in 1954 (135) but was only put into practice in 1976 (137).
Since then most major resin manufacturers have produced an inert
resin plus graded exchangers to form triple resin beds.

Examination of Table 3.13 indicates that different manufacturers
have set different standards for their size gradings of exchangers
and inert resins. Maximum anion exchanger diameters vary between
0.8 and 1.0 mm while minimum cation exchanger diameters vary between
0.5 and 0.7 mm. The inert resins have densities within the range
1140 - 1180 kg m^{-3} and their size ranges vary from 0.7 - 0.9 mm to
0.4 - 1.0 mm. As all manufacturers offer similar types of resin
with comparable densities there is either some gross overestimation
of the narrowness of the bead size ranges needed to achieve separ-
ation or some equally optimistic estimation of the ability of
resins to separate.

BAYER
Trennschicht

SYBRON
Blue Zone

DUOLITE
Triobed

A   Anion Exchanger   I   Inert Resin
C   Cation Exchanger

ROHM & HAAS
Ambersep
(except Ambersep400)

ROHM & HAAS
Ambersep 120/359/400
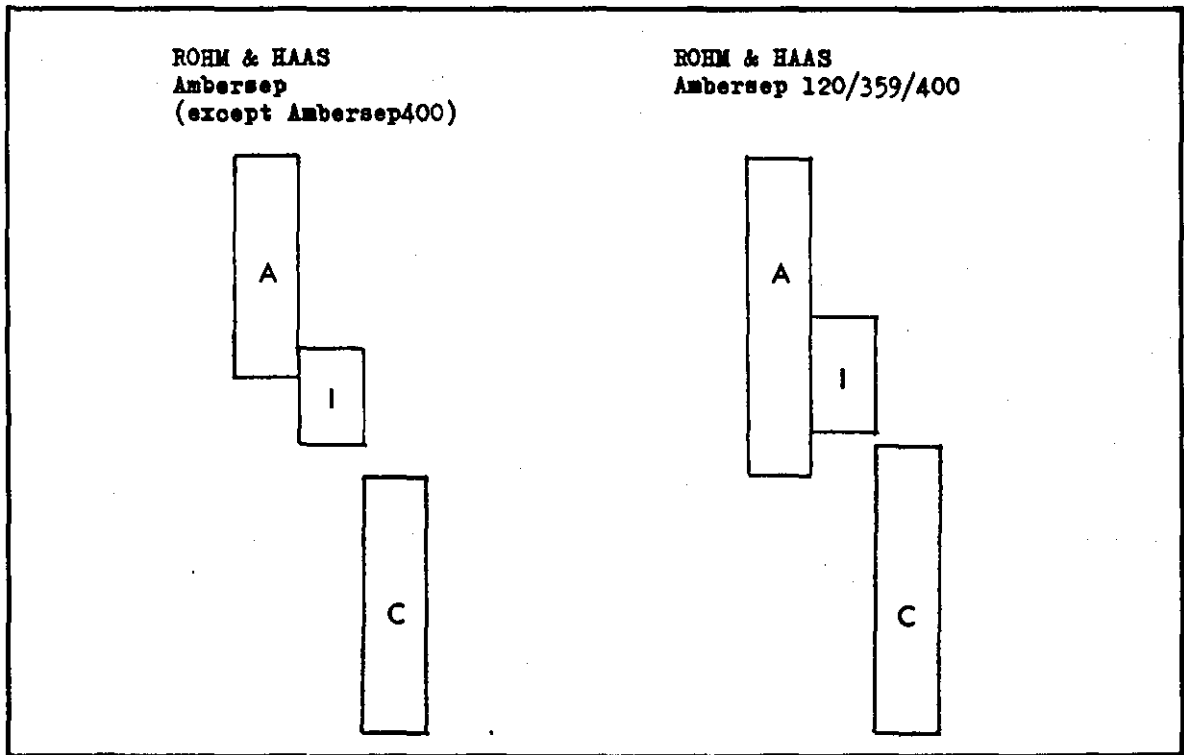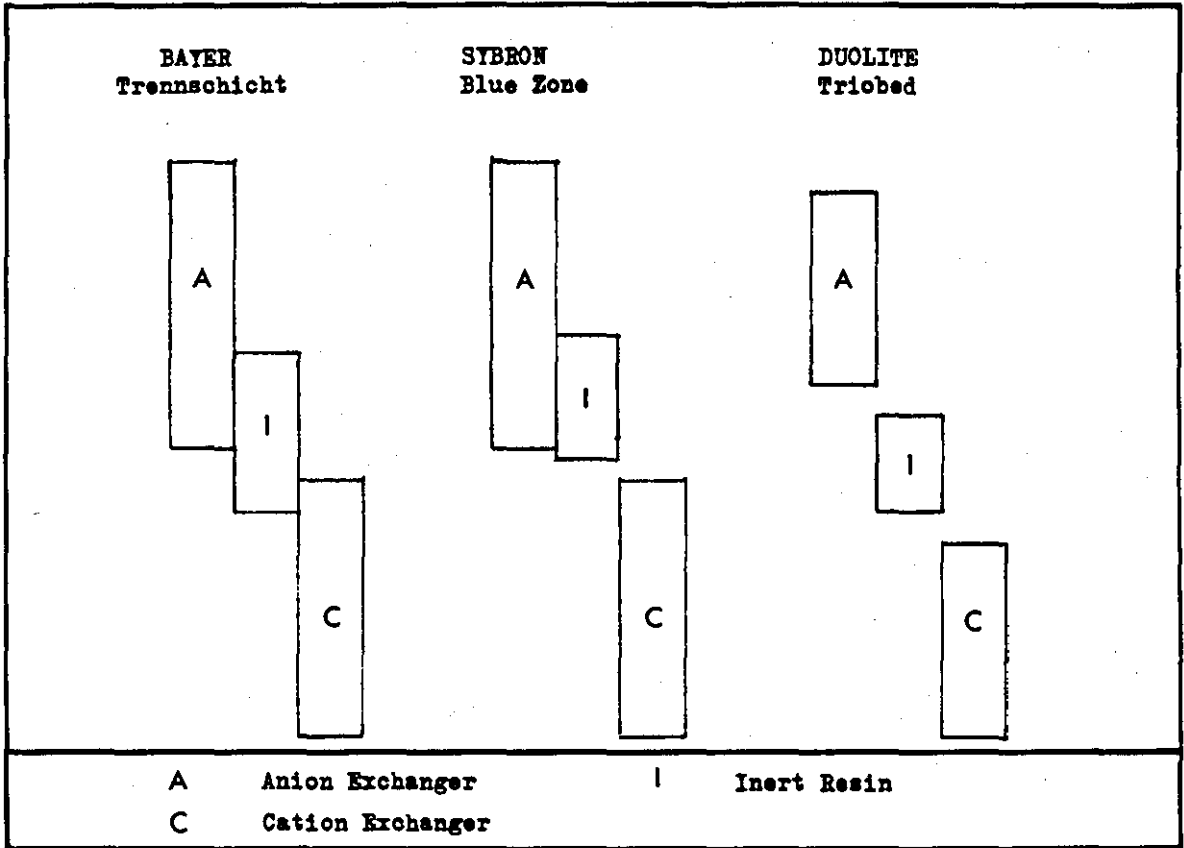
FIGURE
No. 3.07   SEPARABILITY OF VARIOUS TRIPLE RESIN SYSTEMS

It is not practicable to propose a set of standard size gradings
for all triple resin systems as different manufacturers have
approached the problem in slightly different ways. Therefore, the
triple resin systems offered by four manufacturers have been assessed
for potential separability into three distinct layers using the same
bead density criteria as in 3.6.5.

The first requirement of any three resin system is that the two
exchangers should separate completely. If the separation is
marginal the addition of an inert resin of intermediate density will
only give interfacial dilution, but not triple layer separation.
Figure 3.07 is a representation of the predicted   separability
of a number of triple resin systems under the worst likely conditions.
The Bayer and the Sybron systems have exchangers that just meet
the bead size specifications for exchanger separation and both have
inert resins with a wide size range. In the Bayer Trennschicht
system both exchangers will penetrate into the inert layer, a
feature observed in laboratory column tests. In the Sybron Blue
Zone system the inert is of lower density and will not form an
effective barrier but will remain largely mixed with the anion
exchanger, although it will separate from the cation exchanger.

The Rohm & Haas Ambersep system has exchangers that will separate,
apart from the high density anion exchanger noted in 3.6.5.2. The
inert resin density, up to 1180 kg m^{-3}, is very close to the lower
density H^+ form cation exchangers of 1185 kg m^{-3}. However, the bulk
circulation ensures that all Ambersep cation exchangers will separate
from the inert resin, although when $d_{C-min} = 0.5$ mm the separation is
marginal. The Ambersep anion exchangers are unlikely to separate
completely from the inert resin, but a clear zone of wholly inert
resin should be maintained. The system Ambersep 120/359/400 with low
density cation exchanger and high density anion exchanger will not
separate completely as currently specified. There will be a broad
centre zone of intermixed anion and cation exchanger and inert resin.
This was observed in a laboratory column (25 mm diameter) trial.

The Duolite Triobed system has the narrowest bead size ranges and
two inert resins are specified; S3TR for macroporous exchangers and

TABLE 3.14   BEAD SIZE AND DENSITY DATA FOR
             DOW MONOSPHERE RESINS

ANION EXCHANGER

Batch N$^{o.}$	Bead Diameter (mm)		Bead Density (kg m^{-3})	
	Range	Mean	Cl^-	SO_4^{2-}
XFS 43379	0.52 − 0.68	0.60	1075	1113
841125	0.50 − 0.62	0.58	1082	1120
850102	0.48 − 0.62	0.57	1084	1124

CATION EXCHANGER

Batch N$^{o.}$	Bead Diameter (mm)		Bead Density (kg m^{-3})	
	Range	Mean	H^+	Na^+
XFS 43285	0.61 − 0.77	0.70	1229	1309
841014	0.60 − 0.80	0.72	1227	1312
841228	0.60 − 0.78	0.71	1227	1314

INERT RESIN

Batch N$^{o.}$	Bead Diameter (mm)		Bead Density (kg m^{-3})
	Range	Mean	
XFS 43323	0.52 − 0.68	0.60	1146

S5TR for gelular exchangers. S3TR has a slightly lower density than S5TR (Table 3.13). Both inert resins have size ratios of 1.29 which means they will form a single bulk circulation cell on back-washing and their separation properties can be characterised by the Sauter mean of the distribution. All ion exchanger/inert combinations in the Triobed system should separate completely into three distinct layers.

3.6.6 <u>VERY CLOSELY GRADED RESINS</u>

The Dow Chemical Co. have recently introduced a new method for resin bead production (218) that produces uniformly sized beads with a very narrow bead size distribution. Table 3.14 gives the manufact-urers data and size measurements made on early samples together with bead density data. All the resins have size ratios less than 1.4 and should each form a single bulk circulation cell on backwashing. Bulk circulation predicts separation should be achieved by two resins with the same narrow size distribution and only a difference in density.

A trial separation of H^+ form cation exchanger, inert resin and SO_4^{2-} form anion exchanger in a 50 mm diameter column showed virtually complete separation of the three components. There was no cation exchanger in the anion exchanger and $< 0.2\%$ of the cation exchanger was dispersed within the inert resin. There were pronounced bulk circulation currents in all three components, the whole of each layer acting as a single bulk circulation cell. This is in accord-ance with the bulk circulation model of resin separability outlined earlier, and confirms that density differences can effect separation of very closely graded resins.

Wet sieving is not practicable for sizing closely graded resins. A HIAC particle size analyser has been used for this and other resin size measurements (A3.5).

4 M I X I N G   O F   R E S I N S   B Y   A I R   I N J E C T I O N

In order to obtain the highest quality water from a mixed bed the two
exchangers must be thoroughly mixed. This ensures that the exchange
equilibria are driven to virtual completion, with pure H_2O as the
product, and that residual regenerants which may elute from the resins
are exchanged within the bed. Harries and Ray (18) have shown that
poorly mixed beds rinse down more slowly after regeneration and
mixing, generally due to the elution of regenerants from unmixed
resin near the bed outlet.

4.1 MIXING PROCEDURE ON PLANT

After regeneration and rinsing the two exchangers are recombined in
a single vessel, if they were not regenerated in the same vessel.
Normally the cation exchanger lies below the anion exchanger, but
in systems where resins are transferred from one vessel to another
the anion exchanger may lie below the cation exchanger. The more
common case – cation below anion – is dealt with here with reference
to any differences in the text.

The method of mixing is essentially the same as that first described
by Kunin and McGarvey (91). The vessel containing the separated
resins is drained until there is a small head of 'free' water above
the resins. Low pressure air is then injected into the bottom
collector system and passes up through the bed as discrete bubbles
before venting to the outside of the vessel. The passage of the
bubbles agitates and mixes the resins until, after a suitable time
(10 - 20 minutes), the air flow is stopped and the mixed resin bed is
settled. The vessel is then filled with water and a final rinse to
achieve the operating conductivity is commenced.

4.2 CONTROL OF MIXING ON PLANT

There are practical problems in the control of resin mixing that
can be difficult to overcome. The air flow rate may fluctuate,
especially if the supply is drawn from a common compressed air main,
but the major problem is in the control of the free water level above
the unmixed resins.

Manual control of the water level is by observation through a sight
glass (Figure 2.4) located at the design level of the settled resins.
The free water level achieved in practice is individual to the
operator and if the surface of the resins is above or below the limits
of the sight glass all control is lost. Under automatic control
the water level is drained to a pre-set height on the vessel above
the nominal resin level, without the opportunity of visual correction.
Particular problems can occur in externally regenerated systems where
resin transfer takes place. Resin transfer is rarely 100% efficient
and if the regenerator serves several mixed beds of resins the
individual charges exhibit inequalities of volume over a period of
time; some greater and some smaller than the design values. There-
fore, the settled resin level and free water level vary from one
regeneration to another.

In certain externally regenerated mixed beds the resins are mixed a
second time after return to the operator vessel, but this will be
under remote control with no visual checks possible.

Settling the bed after mixing is assisted by draining water from the
bottom of the bed whilst filling the vessel from the top. However,
because the air enters through the same lateral system as the drain
water exits there is inevitably some delay while valves are closed
and opened. On automatic plants a deliberate delay may occur to
ensure the closing valves are fully seated. Any delay may result in
some reseparation of the resins.

4.3 PREVIOUSLY PUBLISHED WORK

There is very little published data on resin mixing. Arden (25) notes
that a small misalignment of the bottom lateral system relative to
the horizontal will result in poor air distribution and poor mixing.
Mishenin (219) studied mixing in a 3.8 m diameter vessel with 1.6 m
depth of resins. He noted a minimum air flow rate ($0.85 \ m^3 \ m^{-2} minute^{-1}$)
and a minimum free water depth of between 50 and 100 mm to ensure
good mixing throughout the bed. A two stage mixing procedure was
proposed with reduced free water in the second stage. Harries and
Ray (140) using a 0.6 m deep bed in a 0.1 m diameter pilot column
with 25 mm free water reported a minimum air flow rate of
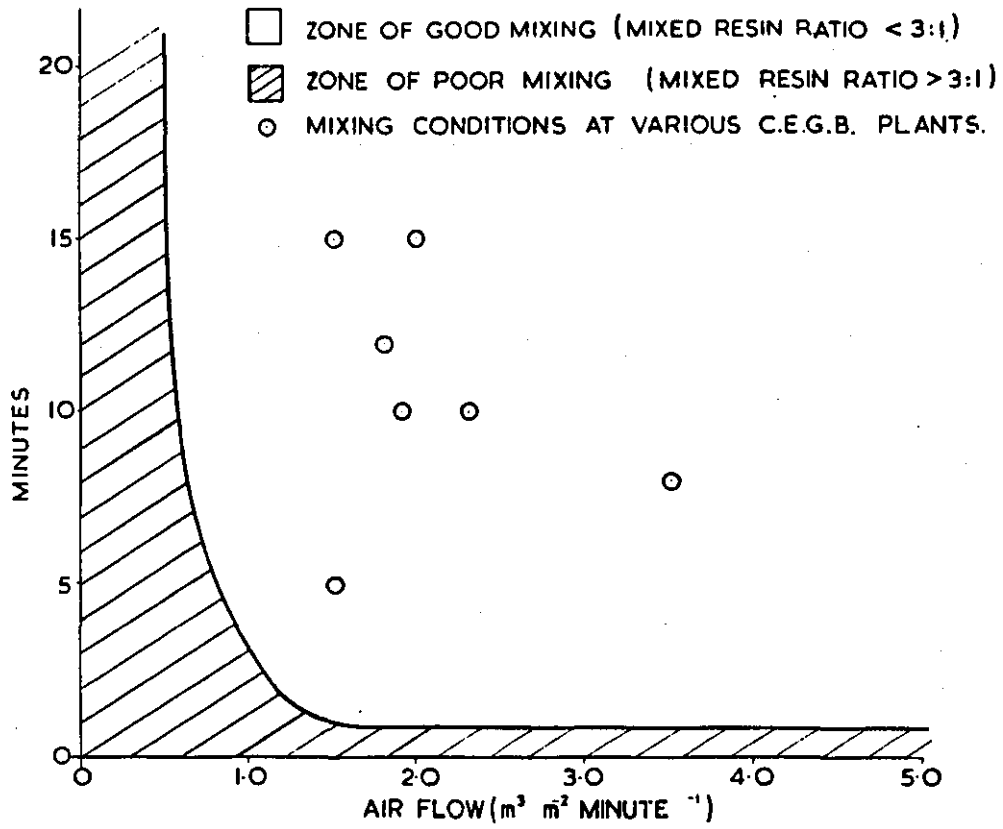
FIGURE No. 4.01 COMBINATIONS OF AIR FLOW RATE AND TIME TO PRODUCE WELL MIXED RESINS

o/o ANION EXCHANGER

SETTLED BED DEPTH (mm)

o/o CATION EXCHANGER

FREE WATER
DEPTH.

1. – 10 mm

2. – 15 mm

3. – 30 mm

4. – 45 mm

5. – 65 mm

6. – 110 mm

7. – 190 mm
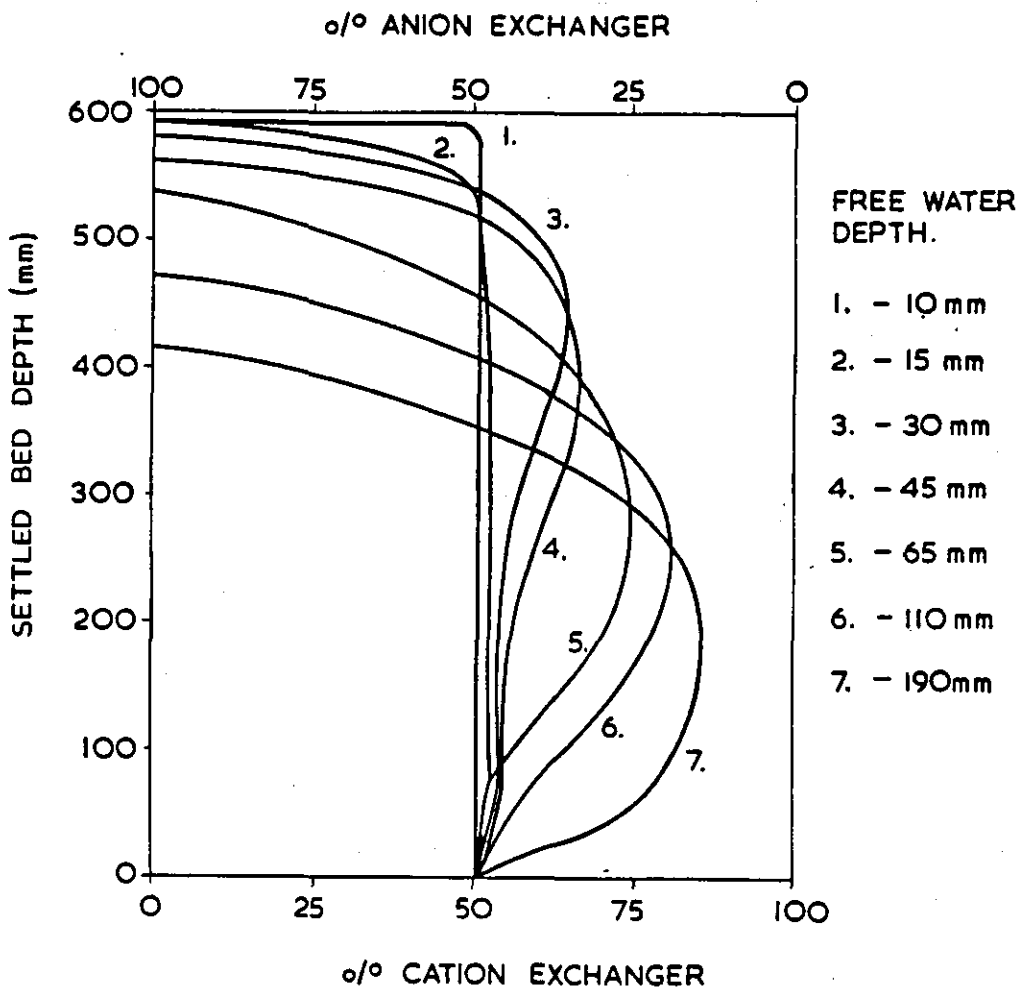
**FIGURE
No. 4.02**   VARIATION IN MIXED RESIN RATIO PROFILE WITH DEPTH OF FREE
WATER ABOVE SETTLED RESINS

$1.0 \ m^3 \ m^{-2}$ minute^{-1} and a minimum mixing time of three minutes
(Figure 4.01). A survey of installed mixed bed plant revealed
that all mixed beds met these mixing criteria but there
were variations by a factor of 2 or 3 in both air flow rates and
mixing times. Brost and Martinola (63) have recommended a free
water depth of 300 - 500 mm is necessary for good mixing.

4.4 LABORATORY INVESTIGATIONS

Having identified variations in free water level as a major variable
in resin mixing a series of mixing tests were undertaken using a clear
acrylic column to observe the mixing process. The column (95 mm internal
diameter) contained sample ports from which horizontal resin cores
could be extracted at three different heights, 70, 270 and 470 mm
above the resin support plate. An equal volume mixture of anion and
cation exchangers was used with a settled bed depth of 0.6 m. A series
of eight mixing tests were run, each with a different head of free
water varying from 0 - 190 mm. Mixing was achieved by passing low
pressure nitrogen gas through the perforated bed support plate at
$1.25 \ m^3 \ m^{-2}$ minute for ten minutes, after which time the bed was
allowed to settle freely. Sample cores were then extracted from a
drained bed, the component resins separated and the mixed resin ratio
determined for the three sample port heights. Full details of the
column arrangement and experimental procedure are given in the
appendix to chapter 4 (A4.1).

4.5 VARIATION IN FREE WATER LEVEL

All the beds with an initial free water depth of 10 mm or more
achieved thorough and free mixing during injection of the mixing gas.
With less than 10 mm of free water the mixing was sluggish and not
uniform throughout the bed. This is discussed in 4.6.

Figure 4.02 illustrates the vertical mixed resin ratio profiles
obtained with differing depths of free water (10 mm - 190 mm) after
mixing and natural settlement. (Tabulated results are given in
Appendix 4). As the bed settles four zones of mixed resins can form.
The lowest zone is thoroughly mixed resins, above this a zone rich
in cation exchanger, then a zone rich in anion exchanger and an

uppermost layer of pure anion exchanger. The relative position and
proportions of each zone vary with the depth of free water.

4.5.1 DIFFERENTIAL SEDIMENTATION

When the mixing gas flow is stopped the mixture of resin beads is
left in suspension in the combined interstitial and free water and
immediately starts to settle by sedimentation. Because the two
exchangers are of differing densities (cation exchanger greater than
the anion exchanger) sedimentation of each resin will occur at
different rates, giving rise to the imbalanced mixed resin ratio
profiles depicted in Figure 4.02.

The description of the differential sedimentation of anion and cation
exchange resins is complex due to their having differing densities
and wide size ranges. For multisize, single density dispersions of
particles it has been noted that the smaller particles can have
negative sedimentation velocities due to size segregation during
settling (220) but the tendency towards segregation reduces as the
dispersion of particles becomes more concentrated. Richardson and
Meikle (221) investigated the sedimentation of mixtures of particles
of differing densities but with monosized components. They produced
an equation to describe the sedimentation rate of each component
which can, in principle, be applied to ion exchange resins

$$V_{sed(A)} = V_{0(A)} \cdot \frac{\delta_A - \rho_D}{\delta_A - \rho} \cdot f(E) \qquad \ldots\ldots\ldots(4.1)$$

and
$$V_{sed(C)} = V_{0(C)} \cdot \frac{\delta_C - \rho_D}{\delta_C - \rho} \cdot f(E) \qquad \ldots\ldots\ldots(4.2)$$

where $V_{sed(A)}$, $V_{sed(C)}$ are the anion and cation exchanger bead
sedimentation velocities; $V_{0(A)}$, $V_{0(C)}$ are the terminal velocities for
free settling particles; δ_A, δ_C are the exchanger bead densities;
ρ is the liquid density; ρ_D is the density of the mixed resin/water
dispersion on cessation of mixing and f(E) is factor to represent the
effects of particle concentration.

For a mixture containing equal volumes of anion and cation exchanger

$$\rho_D = \rho \cdot E_D + \left(\frac{1 - E_D}{2}\right) (\delta_A + \delta_C) \qquad \ldots\ldots\ldots(4.3)$$

where E_D is the voidage factor of the dispersion.

Despite $f(E)$ being unknown it is presumably an equal value, for a given set of conditions, in both equations (4.1) and (4.2). Therefore application of these equations will give information on the relative rates of sedimentation, if not the actual values. Two examples will serve to illustrate this.

Example 1   Laboratory mixing tests.

$\delta_A = 1080$ kg m^{-3}; $\delta_C = 1275$ kg m^{-3}; ρ (20 $^{\circ}$C) $= 998$ kg m^{-3};
Settled bed depth $= 600$ mm;   Free water $= 20$ mm;
Settled bed voidage $E_S = 0.35$.
Mixed resin dispersion voidage $E_D =$

$$\frac{E_S \text{ (settled bed height)} + \text{free water height}}{\text{settled bed height} + \text{free water height}} \qquad \ldots\ldots(4.4)$$

substituting values into equations (4.3) and (4.4)
$E_D = 0.371$ and $\rho_D = 1111$ kg m^{-3}
Incorporating these values into equations (4.1) and (4.2)

$$V_{sed(A)} = -0.378 \ V_{0(C)} \ f(E)$$

$$V_{sed(C)} = 0.592 \ V_{0(A)} \ f(E)$$

Therefore, irrespective of the bead size of the resins that would influence $V_{0(A)}$ and $V_{0(C)}$, the value of $V_{sed(A)}$ is negative ie the movement of the anion exchanger is upward. This is because the cation exchanger displaces water upwards as it settles and the interstitial velocity of this water is sufficient to overcome the natural tendency of the anion exchanger to sediment ie it is fluidised. As the voidage of the dispersion increases with greater depths of free water the interstitial velocity of the water displaced by the cation exchanger will decrease until there is no longer any tendency for the anion exchanger to move upwards. This point is reached when $V_{sed(A)} = 0$ and $\rho_D = \delta_A$. In example 1 this occurs when $E_D = 0.543$, equivalent to a free water depth of 255 mm over a 600 mm resin bed. At values of $E_D > 0.543$ both resins will sediment.

The conclusions drawn from the application of equations 4.1 and 4.2 apply only to the moment the mixing gas supply is terminated. As soon as some of the resin has settled the voidage of the remaining suspension increases. Nevertheless resin segregation due to differential rates of sedimentation will continue. $V_{sed(C)}$ will always be greater than $V_{sed(A)}$ if the two resins have been chosen for their separation characteristics on backwashing ie $V_{0(C)} > V_{0(A)}$ (see chapter 3).

Curve 2 in Figure 4.02 corresponds to example 1. The majority of the bed has remained mixed in equal proportions with a sharp transition to a thin layer of pure anion exchanger at the upper surface of the bed. Mixing with small depths of free water results in a resin dispersion with small voidage which settles rapidly as a complete mixture but the negative sedimentation velocity of the anion exchanger is sufficient to give a thin layer of anion exchanger at the top of the bed. Curve 1 in Figure 4.02 - 10 mm free water - shows a very sharp transition from mixed resin to pure anion exchanger.

As the depth of free water increases the dispersed bed takes longer to settle and there is a progressive reduction in the amount of fully mixed bed that has settled before significant segregation occurs (curves 3-7, Figure 4.02). This gives rise to the four zones within the mixed resin profile noted in 4.5: a lower zone of fully mixed resins; a zone of faster sedimenting anion exchanger; an upper zone of pure anion exchanger separated out by a nett upward displacement. For curves 6 and 7 in Figure 4.02 the lowest, fully mixed, zone is very shallow and is envisaged as a rapid settlement only of those resins at the base of the column.

Example 2   Condensate Purification Plant

The macroporous resins used in condensate purification plant have different densities to those described in example 1. Example 2 is to determine if the density differences have any appreciable effect on differential sedimentation.

δ_A = 1060 kg m^{-3}; δ_C = 1200 kg m^{-3}; ρ(20 °C) = 998 kg m^{-3}

Settled bed depth = 600 mm;   Free water = 20 mm

Settled bed voidage E_S = 0.35
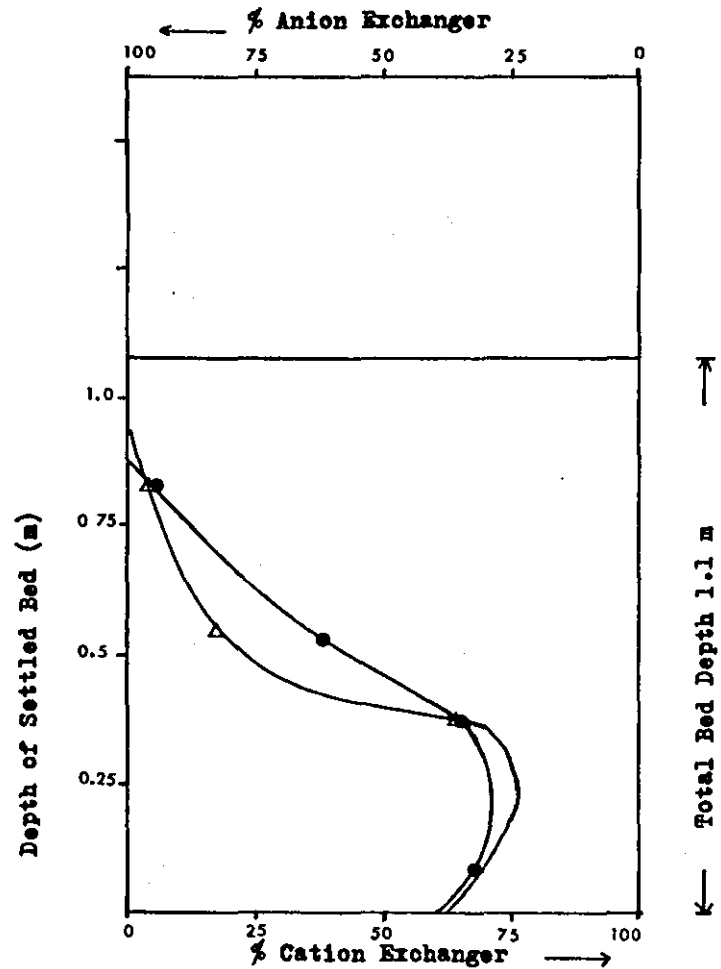
FIGURE No. 4.03 — MIXED RESIN PROFILES. IDENTICAL BEDS IN SITU REGENERATED. 1:1 CATION:ANION RESIN RATIO.
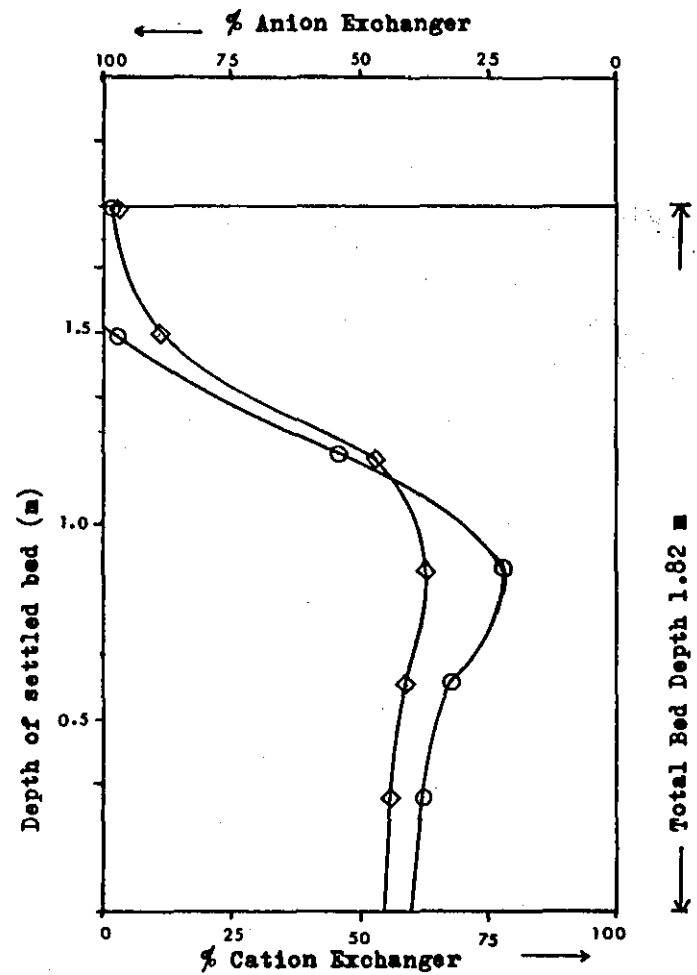
FIGURE No. 4.04 — MIXED RESIN PROFILES. CPP MIXED BED 1 : 1 CATION : ANION RESIN RATIO

From equations (4.3) and (4.4)

$E_D = 0.371; \quad \rho_D = 1081 \text{ kg m}^{-3}$

Substituting into equations (4.1) and (4.2)

$V_{sed(A)} = -0.323 \; V_{0(A)} f(E)$

$V_{sed(C)} = 0.589 \; V_{D(C)} f(E).$

Exactly the same behaviour is found in example 2 as was found for example 1, ie the anion exchanger exhibits separation by a net upward movement on cessation of mixing. The dispersed bed voidage at which both resins start to sediment $E_D = 0.530$ is also very similar to example 1. Therefore, resin bead density, within the limitations found in normal water treatment practice, does not affect the mechanism of resin segregation during free settling after mixing. Differences in bead density will cause variations in the value of V_0 and hence the absolute value of V_{sed}, but this will only serve to alter the proportions of resin in each of the four settled resin zones not the basic pattern of separation.

4.5.2 MIXED RESIN PROFILES FROM OPERATING MIXED BEDS

When samples of resin are taken from operational mixed beds this is best done by sampling the resin during mixing to obtain a representative sample. However, this is often not convenient and, instead, samples are taken from mixed resin in the operator vessel by extracting vertical core sample from a drained bed, using an auger. Depending on the bed depth three or four samples, each from a separate depth, are normally supplied by the operators. In four instances these samples have been analysed for the mixed resin ratio and the mixed resin profiles are plotted in Figures 4.03 and 4.04. Full data is given in Appendix 4.

The profiles in Figure 4.03 represent two identical in-situ regenerated mixed beds each containing a 1:1 mixture of anion and cation exchangers. The profiles in Figure 4.04 represent cored samples from a single condensate purification mixed bed after two separate remotely controlled mixings in the operator vessel. The precise mixing conditions are not known for either pair of mixed beds but the general form of the mixed resin profiles is the same as that found in the laboratory columns ie excess cation exchanger in the lower bed and

excess anion exchanger in the upper bed leading to pure anion
exchanger at the top of the bed.

The two mixed beds in Figure 4.03 show very similar patterns
indicating a fault of common magnitude on both beds. The mixed resin
profiles for the beds in Figure 4.04 show different shapes. This
is probably due to two factors influencing the depth of free water;
variable resin volumes in externally regenerated beds and a lack of
visual confirmation of the free water level in a remotely controlled
mixing procedure.

4.6 RESIN MIXING MECHANISM

The visual observations of the mixing process have been linked to
the concepts of bubble transport of particles and bulk circulation
in fluidised beds. The mixing of resins has been likened to the
fluidisation by air of a resin/water slurry.

4.6.1 BUBBLE TRANSPORT OF SOLID PARTICLES

In a bed of solids fluidised by a gas rapid mixing will occur under
aggregative (bubble flow) conditions. Rowe and Partridge (222) and
Murray (223) have shown that the mixing gas bubbles carry with them
tails of particles which are continually shed and reformed. The
nett effect is the transport of particles from the lower to upper
regions of the fluidised bed and mixing ensues. Reuter (224)
injected gas bubbles into the base of a liquid fluidised bed of
solid particles and found a similar bubble transport mechanism to
that in a gas fluidised bed. However, he noted that solid particles
could rise right through the bed in association with one bubble or if
the bubble became unstable and collapsed the particle load would be
deposited at the point of collapse within the bed. The nett effect
is still transport of solids upwards through the bed.

The air mixing of a resin/water slurry contains elements of both the
aggregatively fluidised gas/solids system and the bubble in liquid/
solids fluidised bed. As the bubble transport mechanism is essentially
the same in both cases the concept can be applied to resin mixing.
Østergaard (225) has reported the rapid mixing of 1 mm diameter

FIGURE No. 4.05 PROGRESSIVE MIXING OF TWO ION EXCHANGE RESINS BY AIR INJECTION INTO A RESIN/WATER MIXTURE
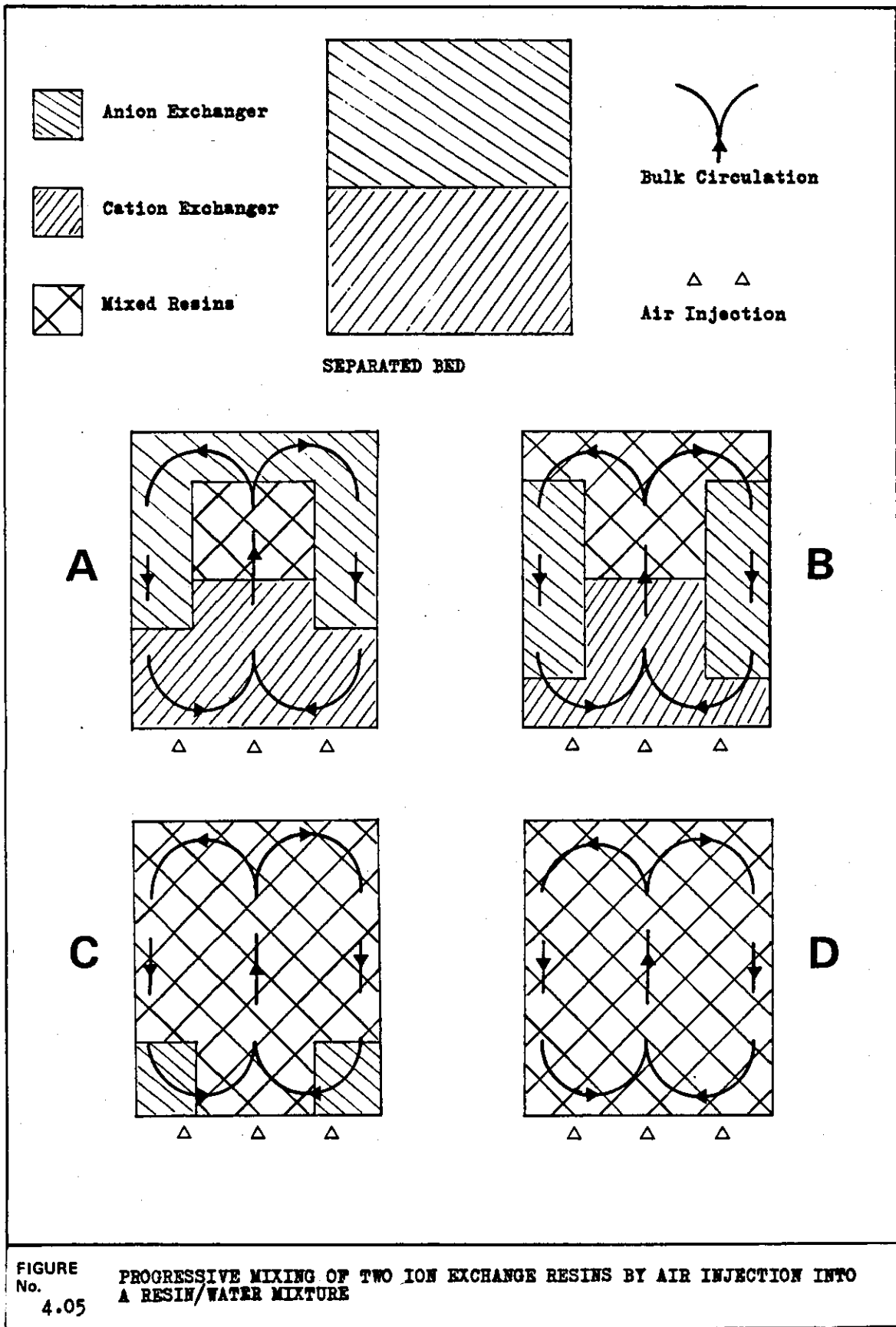
particles in a bed fluidised by gas and liquid and noted that the
size and stability of the bubbles played an important part in the
rate of mixing.

4.6.2 BULK CIRCULATION

When bubble transport of resin beads and water upwards through the
bed commences more resin must move downwards to fill in the voids
left at the bottom of the bed. This resin comes from higher in the
bed and soon a bulk circulation of resin/water slurry is set up
upwards through the centre of the bed and downwards at the walls.
This is a typical bulk circulation pattern observed in fluidised
beds (196, 226).

Figure 4.05 is a schematic representation of the progress of mixing
of two resins. In stage A cation exchanger is being transported
into the anion exchanger and more cation exchanger replaces it at
the base of the bed; anion exchanger is being drawn down at the walls
with the descending annulus of cation exchange resin. In stage B
cation exchanger has been transported to the top of the bed and a
layer of mixed resin is present at the top of the bed. Cation
exchanger is still being drawn into the bottom of the bed and the
annulus of anion exchanger is slowly moving down the walls. At
stage C the annular anion exchanger has reached the bottom of the
bed and anion exchanger is now being drawn into the bubble stream and
transported upwards. The whole central core of the mixing bed now
consists of mixed resins. Finally in stage D all the anion exchanger
has been drawn into the mixing bubble flow and the whole bed consists
of mixed resins. Mixing was then continued to ensure an even
distribution of the component resins.

4.6.3 FREE WATER LEVEL

The amount of free water above the bed influenced the fluidity of
the mixing resins which, in turn, governed the freedom of bulk
circulation. When the mixing air was first introduced to the base
of the column it pushed the interstial water out of the lowest
layers of resin and tried to force the bed upwards as a plug. The
low air flow and pressure was insufficient to support the bed, so

the plug collapsed and several large slugs of air passed up through the bed. This started the bubble transport mechanism and if there was sufficient free water available a resin /water mixture would flow down the sides of the column to fill the momentary void at the base of the column. Once water reached the base of the bed discrete bubble generation would start and the bulk circulation pattern described above would be set up.

When the free water level dropped below 15 mm above the 600 mm separated bed there was insufficient water to establish total fluidity and bulk circulation. Interstitial water at the bottom of the bed tended to be pushed into the upper layers to maintain fluid mixing there while the air slugged through the lower bed. With zero free water slugging was very pronounced and bulk circulation was almost none existant. Complete mixing could be achieved given sufficient time but on stopping the air flow the lower bed contained many voids that would lead to liquid chanelling and poor exchange performance in service. A general feature of a low free water level was the presence of unmixed cation exchanger at the bottom of the bed. Mishenin (219) noted this after a three minute air mix with zero free water level.

4.6.4 OBSERVATION OF MIXING ON PLANT

It is difficult to observe the true resin mixing process in full scale mixed beds as the only observation points are two small windows and occasionally an open manhole cover in the top of the unit. There are often complicating factors in the presence of a centre lateral and support steelwork that will interrupt the free passage of the mixing resins. Nevertheless, the author's experience is that where sufficient free water is present mixing starts with the bed heaving, corresponding to the initial plug rise and collapse, followed by the gradually increasing downward movement of resin past the observation window at centre lateral level. Observation through a top manhole showed the centre of the bed to be 'boiling' indicating the majority of the air and resin/water movement was upwards in the centre of the bed. Therefore, it is considered that the basic mechanism described in 4.6.1 and 4.6.2 is an accurate description of the air mixing of ion exchange resins.

4.7 PROPOSED MIXING CONDITIONS

The investigations above showed that for the common case of cation
exchanger below anion exchanger either too much or too little free
water above a separated bed prior to mixing leads to essentially
the same fault, an excess of cation exchanger at the bottom of the
bed. If the anion exchanger is below the cation exchanger prior to
mixing too little free water would give an anion exchanger rich
layer at the bottom of the mixed bed while too much free water would
result in a cation exchanger rich lower layer. Whichever resin is in
excess near the base of the bed means that any residual regenerant
eluting from that resin will not be effectively removed due to the
absence of the opposite exchanger. For the most common case of excess
cation exchanger any residual acid regenerant, normally sulphuric
acid, is likely to bleed into the treated water. This could cause
an extended rinse down period to reach an acceptable operating
conductivity and a subsequent prolonged trace leakage of acid into
the purified water. A lower anion exchanger rich layer would give an
alkaline bleed of residual sodium hydroxide regenerant.

Therefore, for the production of high and ultra pure water it is
necessary to choose mixing conditions that ensure a good mixture of
resins in the lower part of the bed. Reference to Figure 4.02
shows that mixing conditions 1,2 and 3 produce an almost perfect
mixed resin ratio in the bottom half of the bed. As condition 2 is
the borderline between good bubble mixing and air slugging with too
little free water it is proposed that a free water level equivalent to
condition 3 is adopted as a standard mixing condition. Because it is
the voidage of the dispersed bed on cessation of mixing that governs
the degree of reseparation that occurs, the chosen mixing conditions
can be extrapolated from Figure 4.02 to a standard level of free
water per unit separated bed depth.

The recommended level of free water prior to air mixing is 50 mm
water per metre of settled bed of separated resins. This will ensure
free bulk circulation during mixing whilst preventing undue resepara-
tion of the exchangers due to free settling of the bed when mixing
ceases. Unless the level of resin in the regenerator can be guaran-
teed for successive regenerations the only successful and simple
method of control of the free water level is by visual observation.

5   ANION EXCHANGE KINETICS IN MIXED BEDS

5.1   INTRODUCTION

As noted in section 2 many power stations employ high flow rate
condensate purification plants to ensure boiler feed water quality
is maintained with very low impurity levels. The current CEGB
standards for AGR boilers are conductivity $<0.08 \mu S$ cm^{-1} with
concentrations of Na^+, Cl^- and SO_4^{2-} each $< 2\mu g$ kg^{-1}, while in the
USA the feed water quality for some PWR boilers has been set as low
as conductivity $<0.06 \mu S$ cm^{-1} and concentrations of Na^+, Cl^- and SO_4^{2-}
less than $0.2 \mu g$ kg^{-1} each anion. (9, 11, 12.)

All condensate purification plants utilise ion exchange for the
removal of ionic impurities, either as deep mixed beds or as
powdered resin mixtures applied to pre coat filters. In the CEGB
all CPP have deep mixed beds as the main anion removal stage and
in the majority of plants, without preceding cation exchange units,
mixed beds are also the cation removal stage. In the CEGB all CPP
currently operate on the hydrogen/hydroxide cycle. (242)

There are very few instances where the cation exchanger has failed
to perform satisfactorily either in removing ammonia used for steam/
water circuit conditioning or sodium arising from condenser leaks
and any shortfalls in capacity have been attributed to poor flow
distribution (148). The major problem area has been the deterior-
ating performance of the mixed bed anion exchange resins after a
relatively short service life, as little as six months. The first
observed instance of this deterioration was the increase in chloride
leakage fron CPPs under condenser leak conditions (13, 15, 148).
This was attributed to fouling of the anion exchange resin by large
naturally occurring organic molecules present in the raw water supply
which are not completely removed by the make-up water treatment plant
and find their way into the boiler feed water. Further investigations
into feed water quality showed that increasing sulphate leakage from
mixed beds was also a problem as the resins aged. The effects were
extended rinse down times following regeneration and a progressively
higher steady background bleed of sulphate in service (14, 51).

Cross contamination of the anion exchanger by sulphuric acid during cation exchanger regeneration has already been identified as one cause of sulphate leakage (16, 18).

Most CPP in the CEGB use macroporous resins (242) for their superior physical strength in withstanding high pressure drops and transfer from the service to regeneration vessels and back. The penalty for high physical strength was a reduction in exchange capacity compared to gelular resins, but in the majority of cases capacity was not a primary concern. In the USA about 40% of all CPP mixed beds use gelular resins. This was not based on any technical merit but was due to the marketing policies of various resin manufacturers. However, there have been a number of conflicting claims as to the relative merits of gelular or macroporous anion exchangers, particularly with respect to their kinetics of exchange.

At the start of this work there were no published comparisions of the performance of exchangers based on different polymer/matrix types carried out under controlled conditions. Neither were there any comparative assessments of the effects of organic foulants on anion exchange kinetics.

The investigations described below have examined the characteristics of the exchange of hydroxide ion with either chloride or sulphate ions in solution for a number of type I anion exchangers based on different polymer/matrix types, both gelular and macroporous. The evaluation technique used was a mixed bed column test where the leakage of chloride or sulphate dosed to the bed inlet was monitored at the bed outlet. The bed operating parameters combined with the test results yielded a mass transfer coefficient which was used for comparative purposes. The influence of operating flow rate on mixed bed performance was also monitored. Additionally the effect of the presence of organic foulants was investigated by deliberately fouling anion exchangers of different polymer/matrix type on the same water supply and then assessing them in the same way as used for new resins. The change in mass transfer coefficient was used as a measure of kinetic deterioration. Samples of used anion exchanger taken from operating CPP were also assessed by the same method.

5.2 EARLIER STUDIES

5.2.1 POLYMER/MATRIX TYPE

Wirth (155) noted that the direct replacement of gelular resins by
macroporous types in CPP mixed beds gave a 30% loss in exchange
capacity. He also noted that as the influent concentration of
sodium increased the leakage from the macroporous resin was higher
than from a gelular type. Kunin (227) employed a radiotracer
technique to follow the uptake of sodium onto test mixed beds with
either gelular or macroporous resins and concluded there was no
marked difference in capacity under CPP operating conditions.
Wirth (109) has also claimed that gelular resins are more resistant
to oxidation than macroporous types.

Ray, Ball and Coates (158) used small laboratory column mixed beds
(100 ml resin in a 25 mm diameter column) operating at specific flow
rates ($m^3 m^{-3} h^{-1}$) equivalent to full scale CPP. They assessed anion
exchanger performance by dosing sodium chloride into the bed influent
and monitoring the chloride ion leakage. Ray et al observed that
gelular anion exchangers gave smaller leakage concentrations of
chloride than macroporous types and concluded that gelular exchangers
had superior exchange kinetics, although no account was taken of
differences in mean bead size of the different resins. Bevan and
McNulty (228) employed a very similar technique to Ray et al and
concluded that gelular and macroporous resins had very similar kinetics
when bead size was taken in account.

5.2.2 EXCHANGE KINETICS IN PACKED BEDS

A large number of workers have investigated the kinetics of the
exchange processes occurring in packed beds. Much of the early work
involved strong acid cation exchangers and the $\bar{H}^+ - Na^+$ exchange
reaction at ionic concentrations around 0.01 to 0.1 M.

Boyd, Adamson and Myers (74) considered three possible rate
controlling steps, liquid boundary layer diffusion, particle (within
bead) diffusion or exchange reaction rate. They used a shallow bed
technique to investigate $\bar{H}$-Na exchange on a phenol-formaldehyde

% Influent Concentration

Total Bed Depth

Exchange Zone

Z

Asymptotic Exchange Front
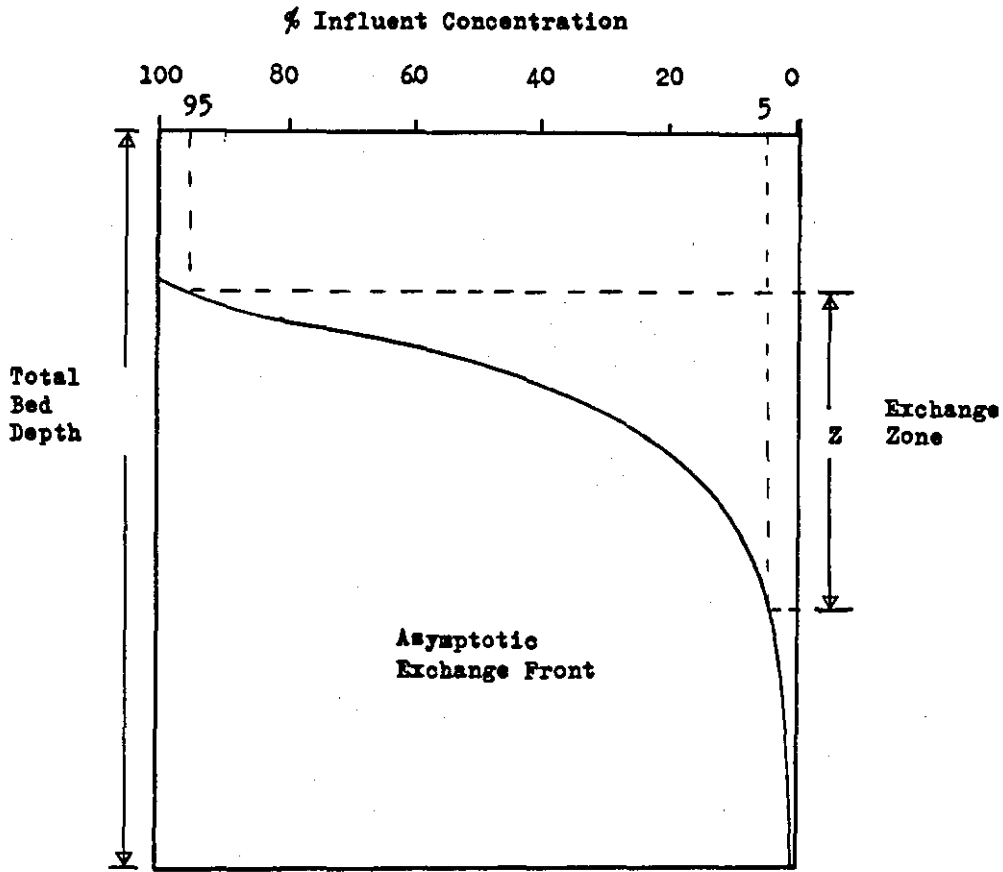
FIGURE No. 5.01   EXCHANGE ZONE AND ASYMPTOTIC EXCHANGE FRONT

based resin and concluded that at influent concentrations ≥ 0.1 M particle diffusion was rate controlling while for concentrations < 0.003 M boundary layer diffusion was the dominant factor. They also noted that ion diffusion within the exchanger was an order of magnitude slower than diffusion of the same ion across the liquid boundary layer.

Michaels (75) set out the basic premises from which many subsequent descriptions of ion exchange column performance have been derived. He monitored the increasing Na^+ concentration at the bed outlet during $\bar{H}^+ - Na^+$ exchange and found an S shaped concentration profile. He assumed this profile had progressed down the bed as the exchanger was exhausted and, knowing the capacity of the resin, he calculated an exchange zone, defined as the region of bed necessary to reduce the influent ion concentration from 95% to 5% of its initial value (Figure 5.01). The limits of the exchange zone could be set at any pair of concentration values, but Michaels chose 95% and 5% for analytical convenience. Michaels noted that the exchange zone should be dependent on temperature, bead size, ionic concentration and superficial fluid velocity but for a fixed superficial velocity it should be independent of bed diameter and bed depth. Michaels plotted the exchange zone height (Z) versus superficial velocities (V_L) between 1.8 and 29 mh^{-1} and derived the relationship $Z = KV_L^{\frac{1}{2}}$ where K is a constant.

Gilliland et al (66), Lapidus et al (77) and Moisson et al (76) followed Michaels approach employing different bed depths, bead diameters, influent concentrations and flow rates. Gilliland examined flow rates up to 83 mh^{-1} and gave an empirically derived equation for the boundary layer thickness, $\mathcal{T}$,

$$\mathcal{T} = d\ 0.049\ Re^{-0.84} \qquad \dots\dots\dots(5.1)$$

relating the mean bead diameter, d, and the Reynolds number, Re. Moisson et al noted that the shape of the concentration profile in the exchange was fixed as time progressed and that boundary layer diffusion was rate controlling below 0.01 M influent ion concentration Lapidus et al proposed that an asymptotic solution could apply to the boundary layer diffusion model of exchange rate control. The asymptotic solution was adopted because ion exchange is generally an equilibrium process and complete exchange of an influent ion is

not possible. However, there is an asymptotic approach to complete exchange with increasing bed depth (Figure 5.01), hence the need to define the limits of the exchange zone.

Glueckauf (67) adopted a different approach to defining the kinetic characteristics of a packed bed. He used an analagous approach to the description of distillation columns and defined an effective height of the theoretical plate for exchange.

Carberry (78) pointed out the difference between the hydrodynamic boundary layer and the effective diffusion boundary layer thicknesses in packed bed ion exchange. A slowly diffusing species may have a boundary layer within the hydrodynamic layer thickness while a fast diffusing species may have a boundary layer of greater thickness than the hydrodynamic layer. The effective diffusion boundary layer varies with fractional power of the Schmidt number (S_c)

$$S_c = \frac{\eta}{\rho D}$$, where η is the viscosity, D is the diffusivity

of the ionic species and ρ the fluid density.

Cooney et al (79) confirmed the applicability of the asymptotic solution in dilute solution boundary layer diffusion controlled exchange provided certain conditions were satisfied. These were uniform bed porosity, uniform initial bed composition (ionic distribution), uniform temperature, constant feed rate, constant feed composition and plug flow. Bunzl (80) adopted an experimental technique based on these criteria with an addition that only a small amount of exchange took place to provide minimum disturbance to the system.

Frisch and Kunin (161) applied the asymptotic solution to mixed bed ion exchange. They used beds up to 960 mm deep but only 12 mm diameter at flow rates up to 200 mh^{-1} and influent concentrations down to 0.0002 M NaCl (4.6 mg l^{-1} Na^+ and 7 mg l^{-1} Cl^-). The resin mixture was treated as a single salt exchanging species releasing an equivalent amount of water. The outlet conductivity was monitored and the excess conductivity above the conductance of pure water was attributed to NaCl leakage, assuming that the anion and cation exchange processes were proceeding at the same rate. Frisch and

Kunin proposed a mass transfer equation to describe the exchange process

$$\ln \frac{C}{C_o} = \frac{-M \ S' \beta' \ L}{V'} \qquad \ldots\ldots(5.3)$$

where
C = column outlet concentration $(eq. \ l^{-1})$

C_o = column influent concentration $(eq. \ l^{-1})$

M = liquid boundary layer mass transfer coefficient (ms^{-1})

S' = specific surface area of resin per mass of moist resin mixture $(\ m^2 \ kg^{-1})$

β' = bulk density of moist mixed bed resin $(kg \ m^{-3})$

L = bulk packed volume of mixed bed resin (m^3)

V' = fluid mass flow rate $(kg \ s^{-1})$.

Whilst this equation contains the elements of a mass transfer equation it does not balance dimensionally. The left hand side has no dimensions, the right hand side has units $kg^{-1} \ m^3$.

Frisch and Kunin used this equation to calculate an exchange zone of Michaels type from knowledge of the mass of mixed resin, hence bed depth, necessary to achieve a certain leakage. From this an operating capacity could be estimated for various total bed depths. Analysis of the variation of the exchange zone depth with flow rate confirmed the relationship $M = KV_L^{\frac{1}{2}}$ held for exchange at 15, 25 and 45 $^{\circ}$C. Frisch and Kunin concluded that liquid boundary layer diffusion was the rate controlling mechanism in mixed bed exchange with dilute influent concentrations below 0.01 M.

Tittle (17) measured the passage, hence concentration profile, of Na^+, NH_4^+ and Cl^- ion exchange fronts as they progressed down an operating H/OH form CPP mixed bed. He applied a general equation of the type $C = C_o \ e^{-qx}$
where q is a constant and x is the bed depth at which ionic concentration C occurs. Tittle calculated a term D/γ, equivalent to a mass transfer coefficient. For cation exchange he found general agreement with previously published results but for chloride exchange the value of D/γ was an order of magnitude lower than anticipated from diffusion coefficient data. This discrepancy was attributed to a layer of foulant on the anion exchanger bead surface which inhibited diffusion of chloride ions between the bulk liquid and the exchanger surface.

Harries and Ray (19) used a modified, dimensionally correct, version of Frisch and Kunin's mass transfer equation to investigate anion exchanger performance in a mixed bed. They studied $\overline{OH}$ exchange for Cl^- and SO_4^{2-}, on a number of different anion exchangers, both new and organically fouled resins. They noted that exchange of divalent ions was inherently slower than for monovalent ions and this effect was enhanced on organically fouled resins. This work is presented in greater detail in the following sections, where the exchange zone concept has been applied to predicting the performance of full scale CPP's.

5.3 EXPERIMENTAL PROGRAMME

5.3.1 EXPERIMENTAL APPROACH

The basic experimental method was to prepare a mixed bed in a test column with a standard cation exchanger and the anion exchanger in question. The mixed bed was operated at a fixed temperature at flow rates typical of operational CPP's. Solutions containing known concentrations of chloride or sulphate ions as the sodium salts were dosed into the column influent and the leakage of chloride or sulphate measured at the column outlet. The performance of different anion exchangers was compared by calculating a mass transfer coefficient for chloride or sulphate exchange.

The flow through a packed bed can be described as the superficial (empty bed) linear flow rate, expressed as fluid volume per unit area cross section of bed per unit time $(m^3 m^{-2} h^{-1})$, or as the specific flow rate, fluid volume per unit volume of packed bed per unit time $(m^3 m^{-3} h^{-1})$. Both flow parameters of a full scale bed can only be simulated in a single test column if the latter is equal to the full bed depth. For comparative testing of exchange kinetics it was considered essential to reproduce the correct hydrodynamic conditions in the test column by operating at linear flow rates typical of CPP operation, rather than at the correct specific flow rate, as used previously (158, 228), which gives low linear flow rates in short laboratory columns.

The settled volume ratio of cation:anion exchanger (C:A) in the

TABLE 5.01 – PHYSICO-CHEMICAL DATA FOR NEW STRONG BASE ANION EXCHANGE RESINS

Resin Designation	Polymer/Matrix	Moisture Content (Volume Fraction)	Skeletal Density Cl form (kgm^{-3})	Total Exchange Capacity $(meq\ ml^{-1})$	Sauter Mean Diameter (mm)
Amberlite IRA 402	Styrene/DVB Gel.	0.588	489	1.2	0.66
Amberlite IRA 458	Acrylic/DVB Gel.	0.655	413	1.1	0.74
Amberlite IRA900	Styrene/DVB Macro.	0.655	417	1.0	0.79
Duolite A101D	Styrene/Isoporous Gel.	0.559	520	1.3	0.67
Duolite A161	Styrene/DVB Macro.	0.591	496	1.2	0.63
Zerolit MPF	Styrene/DVB Macro.	0.654	415	1.0	0.77

mixed bed was set at 2:1. This is a typical figure for CPPs with mixed beds alone and, for a given bed depth there will be greater anion leakage from a 2:1, C:A bed than a 1:1, C:A bed due to the smaller volume of anion exchanger. The test column bed depth was set at 0.55 m (800 ml cation exchanger plus 400 ml anion exchanger) as preliminary trials indicated that this would give measurable leakage with new resins without excessive leakage with fouled resins. The influent concentrations of chloride and sulphate were chemically equivalent, as ion exchange is based on charge equivalents, and were chosen to give measurable leakages while being of the same order as those likely to be found in actual practice.

5.3.2 CHOICE OF NEW ANION EXCHANGE RESINS

Six new strong base (type I) anion exchangers were selected to represent a variety of polymer/matrix types. The resins were sampled from material delivered to CEGB power stations and represented standard production quality. The resin types are listed in Table 5.01. Four of the exchangers were based on styrene/DVB copolymers, one on a styrene/methylene bridge polymer and one on an acrylamide/DVB structure. Three were gelular and three were macroporous.

The choice of resins was made with the aim of including all major polymer/matrix types and those versions that looked as if they would continue to be available for several years. Three macroporous types were included as they represented the most common type of CPP anion exchanger. The acrylamide resin would not normally be considered for CPP use because it has a temperature limit of 40 $^\circ$C in operation and gives higher pressure drops than comparable styrene resins. Its inclusion was purely comparative. Since the work was carried out, mergers and take overs amongst ion exchange resin manufacturers means that Zerolit MPF is no longer manufactured, although it is still in use.

The cation exchanger used in all the column tests was from a single batch of Amberlite IR200 macroporous resin with 20% DVB cross linking. This is the most commonly used cation exchanger in CPP in the UK.

5.3.3 CHARACTERISATION OF THE ANION EXCHANGERS

If there proved to be differences in exchange kinetics attributable
to polymer/matrix type the latter would need to be characterised.
A number of standard physico-chemical measurements were made on each
anion exchanger, including total exchange capacity on a weight and
volume basis, moisture content, skeletal density and scanning electron
micrographs of the surface and interior of the different polymer/matrix
types.

Moisture content and skeletal densities were determined as described
in A3.4. Total, strong base and weak base exchange capacity were
determined by a standard method (229) on a dry weight basis in the
chloride form. Volume based exchange capacity was calculated from
the weight based determination and the skeletal density.

Table 5.01 gives the physico-chemical data for the six anion exchangers.
The scanning electron micrographs are presented in the Appendix to
chapter 5 (A5.1) and clearly illustrate the difference between
macroporous and gelular matrices. At the magnifications used
(x 10,000) no structural features could be observed with the gel
resins but differences between the macroporous types could be seen.

5.3.4 CONDITIONING AND REGENERATION OF NEW RESINS

All new ion exchange resins require conditioning before use, especially
in comparative tests, to minimise the amount of manufacturing residues
that are always present and to ensure all the resins are in a
standard ionic form.

About three litres of each of the six new anion exchangers were
separately conditioned by three cycles of successive conversions to
the hydroxide and chloride forms with sodium hydroxide and sodium
chloride solutions respectively. Each resin was rinsed with
deionised water after each conversion and the resulting chloride
form resin was seived to remove beads above 1.0 mm and below 0.5 mm
diameter in an attempt to minimise bead size variations between the
different resins. Each conditioned and graded chloride form resin
was sampled for bead size distribution measurements by wet seiving
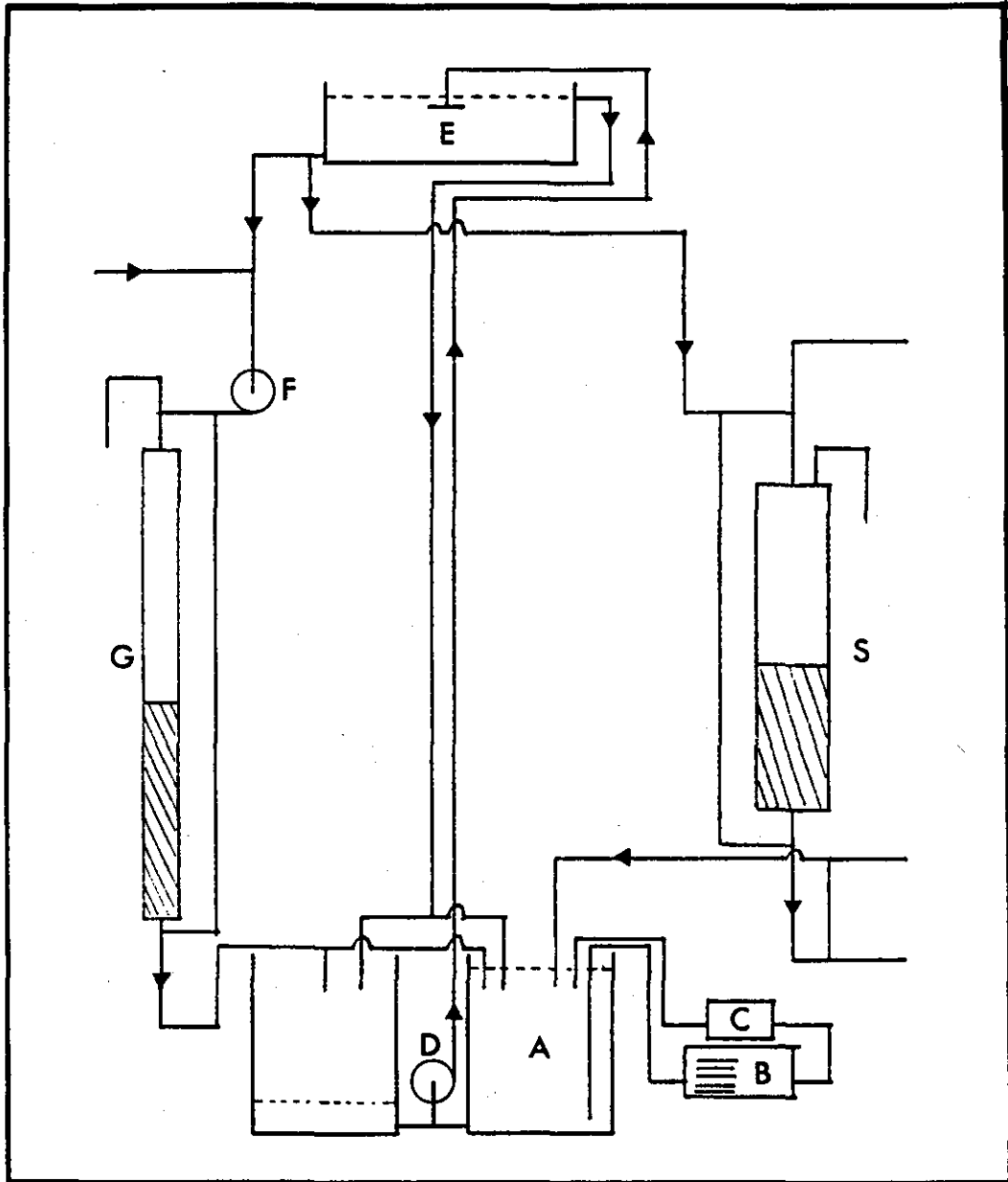
FIGURE No. 5.02 MIXED BED TEST COLUMN – GENERAL ARRANGEMENT

and the remaining bulk resin was stored in a moist condition in a
sealed five litre polyethylene container. Seive analyses are
presented in Table A5.09.

Prior to use in a mixed bed one litre (settled volume) of the
appropriate anion exchanger was regenerated with eighty grams of
sodium hydroxide made up as a one molar solution. The details are
given in A5.2.4. The rinse volume was several times that used in full
scale practice and reduced the residual regenerants/regeneration
products to an acceptably low value. If not used immediately the
regenerated resins were stored under deionised water in a litre
polyethylene bottle with screw cap. It was not policy to store
regenerated anion exchangers for more than a month as they can slowly
absorb carbon dioxide from the atmosphere that has diffused through
the polyethylene container and they also degrade slowly in the
hydroxide form.

A single batch of macroporous Amberlite 200C cation exchanger was
used in all mixed bed tests. It was conditioned by three cycles of
conversion between the hydrogen and sodium forms using hydrochloric
acid and sodium chloride solutions with intermediate rinses. Eight
litres of IR200C were conditioned in two four litre lots and the
sodium form resin was regenerated with seventy gram of hydrochloric
acid per litre of resin as a one molar solution. Each four litres of
resin was rinsed with deionised water until the rinse outlet conduct-
ivity was below 10 μS cm^{-1}. The regenerated resin was stored in
sealed five litre polyethylene containers.

Full details of the conditioning, regeneration and seiving procedures
and the apparatus used are given in A5.2.

5.3.5 COLUMN TEST APPARATUS

Figure 5.02 is a diagramatic outline of the mixed bed test column
and its associated water storage, pumping, dosing, measurement and
sampling arrangements. Further details of the test column construction
and operation are given in A5.3

Deionised water in the 200 litre bulk storage tank 'A' was maintained

FIGURE No. 5.03   MIXED BED TEST COLUMN – DETAIL ARRANGEMENT
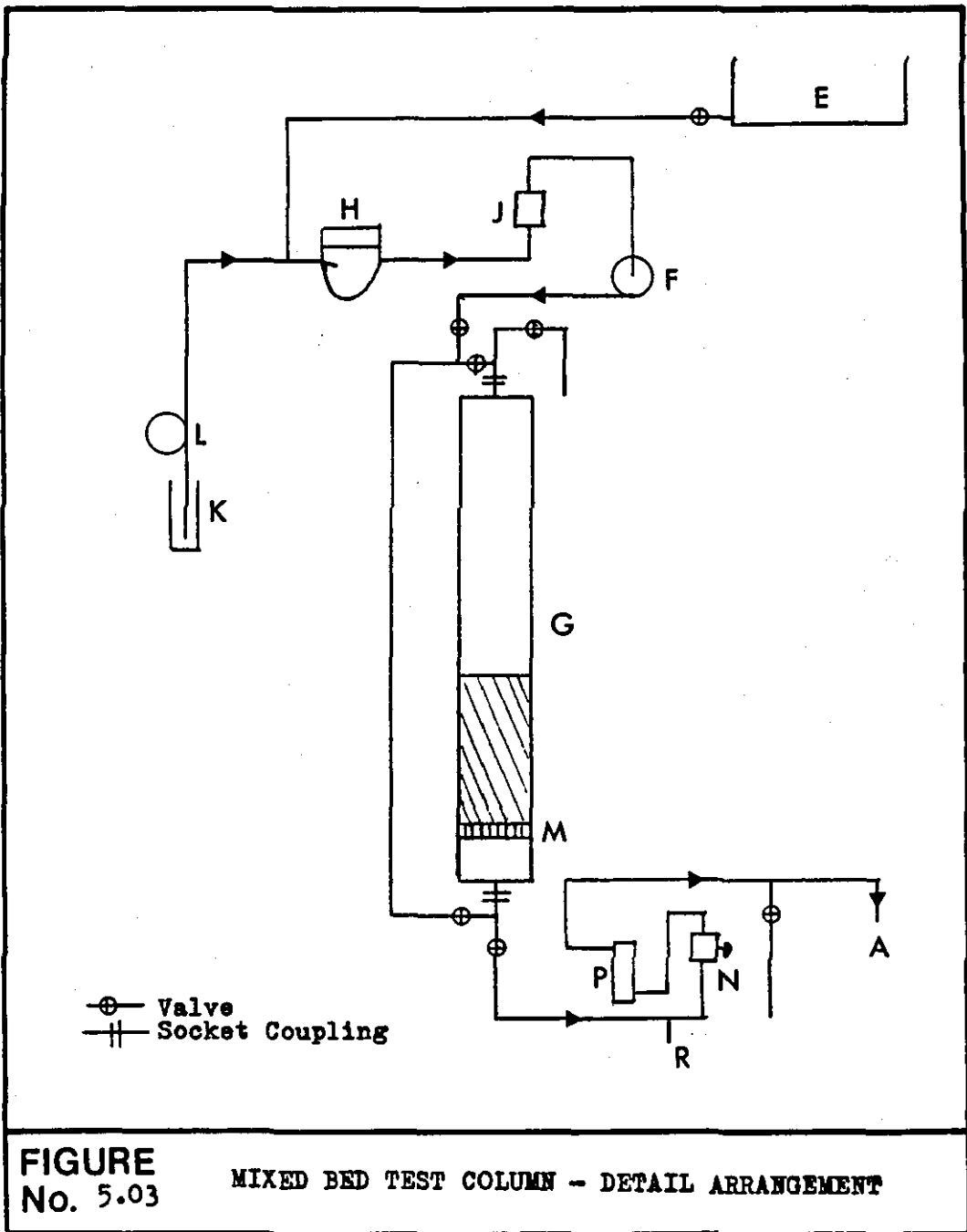
at 20 $^{\circ}$C $\pm$0.5 $^{\circ}$C by circulation through the cooler and heater units
B and C. Water from tank A was pumped (D) to the 60 litre header
tank E and overflowed back to A. From tank E water could be taken
by the booster pump F and passed through the 50 mm diameter test
column 'G', containing the mixed bed under test, and returning to
tank A. At the same time water from tank E passed through column, S
(95 mm diameter), which contained a 2.5 litre H/OH form mixed bed,
and returned to the bulk storage tank, A. The mixed bed in S
continuously polished the bulk supply water and maintained the
impurities in the influent to the test column below 5 μg kg each of
Na^+, Cl^-, and SO_4^{2-}. The outlet from the polishing mixed bed was
monitored continuously for conductivity and was maintained at less
than 0.1 μS cm^{-1}.

Figure 5.03 gives more detail of the test column and associated valves,
pumps and monitoring equipment. Deionised water from tank,E, passed
through the industrial pH cell,H, then through the conductivity cell,
J, and via the booster pump, F, into the top of the test column, G.
The dosing solution, K, was pumped by a variable speed peristaltic
pump L into the deionised water flow before the pH cell, which acted
as a mixing chamber.

The test column, G, was a clear acrylic tube 51 mm internal diameter
and 1200 mm long. The resin support, M, was a perforated acrylic disc
covered with a fine mesh stainless steel screen and was located 30 mm
above the base of the column to ensure uniform flow through the resin
support. After leaving the test column the water passed through a
flow controller, N, an outlet conductivity cell, P, and was returned
to the bulk storage tank, A. A tee off the column outlet line, R,
enabled a sample of outlet water to be taken directly to a sodium ion
analyser. Inlet and outlet conductivities from the test column and
the polishing column outlet conductivity were monitored and recorded
continuously.

5.3.6 MIXED BED PREPARATION

The test column was located in position in the rig, with the bottom
connections made and the top end cap removed. 800 ml (settled volume)
of regenerated IR200 cation exchanger were measured in a 1 litre

measuring cylinder and transferred to the test column. The cation
exchanger was backwashed and drained several times to remove
particulate manufacturing residues that had diffused out of the resin
during storage. The rinse procedure proved necessary as the residues
could contribute both chloride and sulphate ions to the effluent.
(See 5.5.2). 400 ml of the appropriate regenerated anion exchanger
were measured out and added to the cation exchanger in the column.
The water level was adjusted to give 50 mm free water above the
surface of the settled resins.

The resins were mixed by inserting a stainless steel sparge tube,
1.5 mm internal diameter, down to the resin support plate. Nitrogen
gas, from a compressed gas cylinder, was passed through the sparge
tube at 3 litres per minute for 20 minutes. The sparge tube was then
gradually withdrawn whilst slowly draining the column to the upper
surface of the resin, thus obtaining a settled, mixed bed. The column
was then carefully filled with deionised water to cause minimum
disturbance to the resin mixture, the top plate replaced and the column
reconnected into the water circuit. The mixed bed was then rinsed
with deionised water from the header tank until the outlet conductivity
reached a stable value below $0.06 \, \mu S \, cm^{-1}$ at 20 ^{o}C. This rinsing
normally took place without the booster pump in circuit at a linear
flow of around 50 mh^{-1}.

5.3.7 TEST PROCEDURE

Each test mixed bed was operated at three separate flow rates, 1.85,
3 and 4 litres per minute which were equivalent to 55, 88 and 118 mh^{-1}
linear flow rates. This covered the range of linear flow rates found
in most CPP. The tests were run with the booster pump in circuit and
the flow was adjusted by means of the flow regulator (N in figure 5.03).
The flow was measured by the time taken to collect one litre of
water at the rig outlet in a previously calibrated measuring cylinder.
The flows are quoted as 55, 90 and 120 mh^{-1} which represents the
accuracy of setting up a flow rate of 88 or 118 mh^{-1}.

At each flow rate the outlet conductivity was allowed to stabilise
before dosing commenced. Then a 0.2 M solution of sodium chloride
was dosed to the column inlet via the peristaltic pump. The dosing

pump speed was adjusted to give successive influent concentrations of 1480, 2960 and 5920 μg kg^{-1} Cl, the influent chloride concentration being monitored by the influent conductivity. Table A5.05 gives the conductivities at 20 ^{o}C corresponding to the various influent concentrations.

At each influent concentration the column outlet conductivity was monitored. Ionic leakage was indicated by a rise in outlet conductivity and when this had stabilised a sample of the column outlet water was collected in a 500 ml screw capped polyethylene bottle that had been conditioned by soaking in deionised water for several weeks. The column outlet conductivity had normally stabilised within five minutes of dosing being introduced.

When the sample from the first influent concentration had been taken, the dosing pump rate was stepped up to give the second chloride concentration and after this had been sampled the dosing was stepped up to the third concentration. When the three chloride influent concentrations had been completed deionised water replaced the dosing solution to flush the line and the column outlet conductivity allowed to stabilise in the undosed condition. The procedure outlined above was then repeated with an 0.1 M sodium sulphate solution to give influent concentrations of 2000, 4000 and 8000 μg kg^{-1} SO$_4$, which were chemically equivalent to the chloride influent concentrations, and column outlet samples taken.

When the three chloride and three sulphate influent concentrations had been completed at the lowest flow rate, the flow was increased to 90 mh^{-1} and the chloride and sulphate dosing and sampling programme repeated, followed by the same procedure at 120 mh^{-1} flow rate.

5.3.7.1 Analysis of Outlet Samples

Each test run on a particular anion exchanger gave 18 column outlet samples taken during dosing and a further 3 outlet samples taken during the undosed stabilisation of each flow rate. These samples were analysed for chloride and sulphate by means of high pressure ion chromatography (HPIC) using a Dionex 10 analyser. HPIC separates ions of a given charge on an ion exchange column and the eluted ions are

detected by conductivity (144, 145). Full details of HPIC analysis are given in A5.4.3.

During each test run a sample was continuously taken from the column outlet via a tee (R in Figure 5.03) and fed to a continuous sodium ion monitor which utilised a sodium responsive glass electrode. Details of the sodium ion monitor are given in A5.4.2.

5.3.7.2 Leakage Tests for other Anions

A single test was carried out, using Amberlite 900, to examine the leakage of nitrate and phosphate ions in addition to chloride and sulphate. For this test the IRA900 was conditioned to the bicarbonate form with 5 litres of 0.5 M $NaHCO_3$ per litre of resin, to remove residual chloride that might give equilibrium leakage of chloride ions (230). The bicarbonate form resin was regenerated in the standard manner. The column was operated at the 90 and 120 mh^{-1} flow rates and dosing of either NaCl, Na_2SO_4, $NaNO_3$ or $NaHPO_4$ was restricted to the equivalent of 4000 μg kg^{-1} SO_4. Inlet and outlet conductivities were monitored and outlet samples taken as before.

5.3.8 DELIBERATE ORGANIC FOULING OF ANION EXCHANGERS

Organic fouling of mixed bed and CPP anion exchangers usually takes place in the presence of low influent concentrations of both organic and inorganic species with exhaustion cycles lasting between several days and several weeks. To make a realistic comparison of the effects of organic foulants on different polymer/matrix types it is necessary to obtain resins fouled on the same water supply. This is not possible on a full scale plant which usually employs a single type of resin. Therefore, it was necessary to deliberately foul the six types of anion exchanger used in the study of new resin polymer/matrix types on a single water supply. This was most conveniently carried out at an operating water treatment plant where organic fouling was known to be a problem.

Such a plant was at Staythorpe PS which draws its raw water from the River Trent and treats it successively by lime/ferric sulphate flocculation, sand filtration, counter current regenerated cation

Resin Support

Flow
Integrator

Pump

To and From
15 m^3 Holding Tank

Resin

Valve

FIGURE
No. 5.04   RESIN FOULING COLUMN ARRANGEMENT
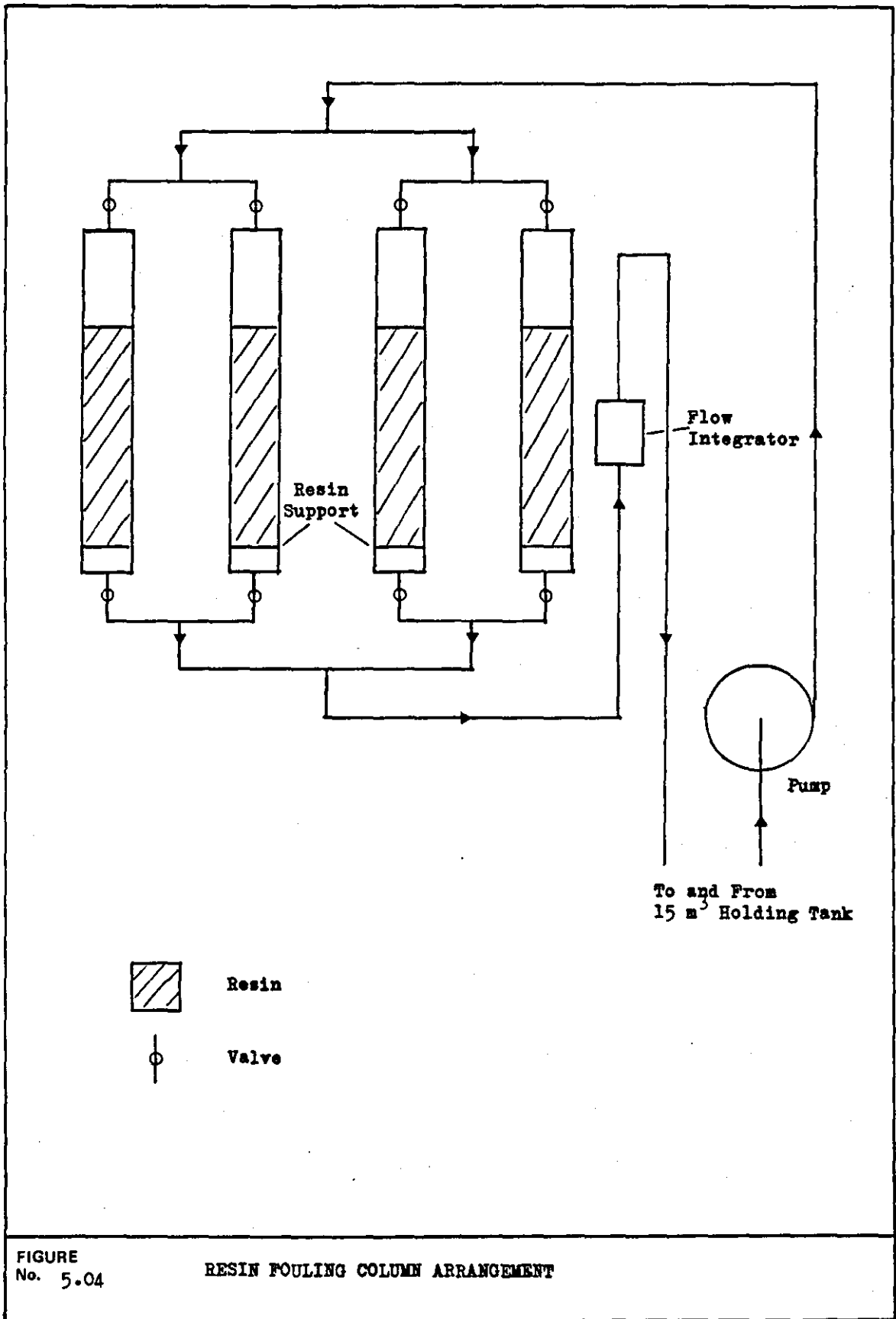
TABLE 5.02   COLUMN OPERATING DATA - DELIBERATE FOULING

Cycle No.	Date	Exposure to Fouling Environment (hrs)	Total Volume Throughput (m^3)	Anion Exchangers Installed		Notes
1	20. 9.79 – 19.10.79	693	302.4	IRA900 IRA402	A161 A101D	Resins in upper part of column coloured dark brown. Fungal growths in resin bed.
2	24.10.79. – 20.11.79	651	282.8	IRA900 IRA402	A161 A101D	Columns protected from light. Air and/or CO_2 building up in free board above resins.
3	23.11.79 – 20.12.79	649	251.1	IRA900 IRA402	A161 A101D	
4	15. 1.80 – 28. 2.80	1052	413.4	IRA900 IRA402	A161 A101D	Run length extended to 1000hours
5	2. 4.80 – 21. 5.80	1173	343.8	Z-MPF IRA402	A161 A101D	Particulate fouling by algae which blocked porous resin support plate and severely reduced flow rate towards end of run.
6	2. 6.80 – 25. 6.80	550	144.5	Z-MPF IRA402	IRA458 A101D	Run terminated due to disintegration of pump impeller. Algal fouling also present.
7	3. 7.80 – 6. 8.80	812	261.5	Z-MPF IRA402	IRA458 A101D	Run terminated because of algal fouling of resin support plate which severely reduced flow rate.
8	19. 8.80 – 30. 9.80	1007	420.6	Z-MPF IRA900(II)	IRA458 A101D	Algal fouling present but not sufficient to significantly affect flow rate.
9	9.10.80 – 19.11.80	982	453.6	IRA900(II) IRA900(II)	IRA458 A101D	

then anion exchange followed by mixed beds (231). Between the anion exchange unit and the mixed bed the water passes into a 15 m^3 holding tank. This tank held an adequate supply of partially demineralised water to feed a four column rig for fouling anion exchangers.

Figure 5.04 outlines the column arrangement for fouling the anion exchangers. The rig was of simple, robust construction as it received attention only once every two weeks. The new anion exchangers placed in the columns were drawn from the conditioned and graded chloride form resin described in 5.3.3. To simulate operational practice the fouling resins were regenerated and cleaned every four to six weeks. Regeneration was similar to that described in 5.3.4.
Physical cleaning of the resins, necessary because of algal and fungal deposits, was achieved by repeated air scouring and backwashing. Occasionally algae partially blocked the porous polythene support discs and reduced the duration and/or throughput of some cycles. The polythene support plates were replaced after each cycle. The algal problem was reduced but not totally overcome by sheathing the columns in black plastic sheet.

Samples of each exchanger were taken at the end of each cycle, both before and after regeneration, for determination of the accumulated organic foulants (See A5.4.4). When a particular exchanger had accumulated a predetermined level of extractable foulants (2 weight percent fulvic acids on a dry resin) it was removed from the test apparatus, cleaned and stored in a sealed container in an exhausted form. Because the test rig had only four columns two of the six anion exchangers were placed in the fouling columns after the first two resins had become fouled. Table 5.02 gives the dates, water through puts and resins installed in the rig for each cycle.

At the fortnightly inspection of the rig, samples of the test column influent and common effluent were taken for total organic carbon (TOC) analysis. The average inlet TOC concentration was 0.7 - 0.8 mg kg^{-1} carbon, but varying between 0.3 and 1.5 mg kg^{-1} carbon.

⊕— Valve
╫—Socket Coupling

FIGURE No. 5.05   MODIFIED MIXED BED TEST COLUMN
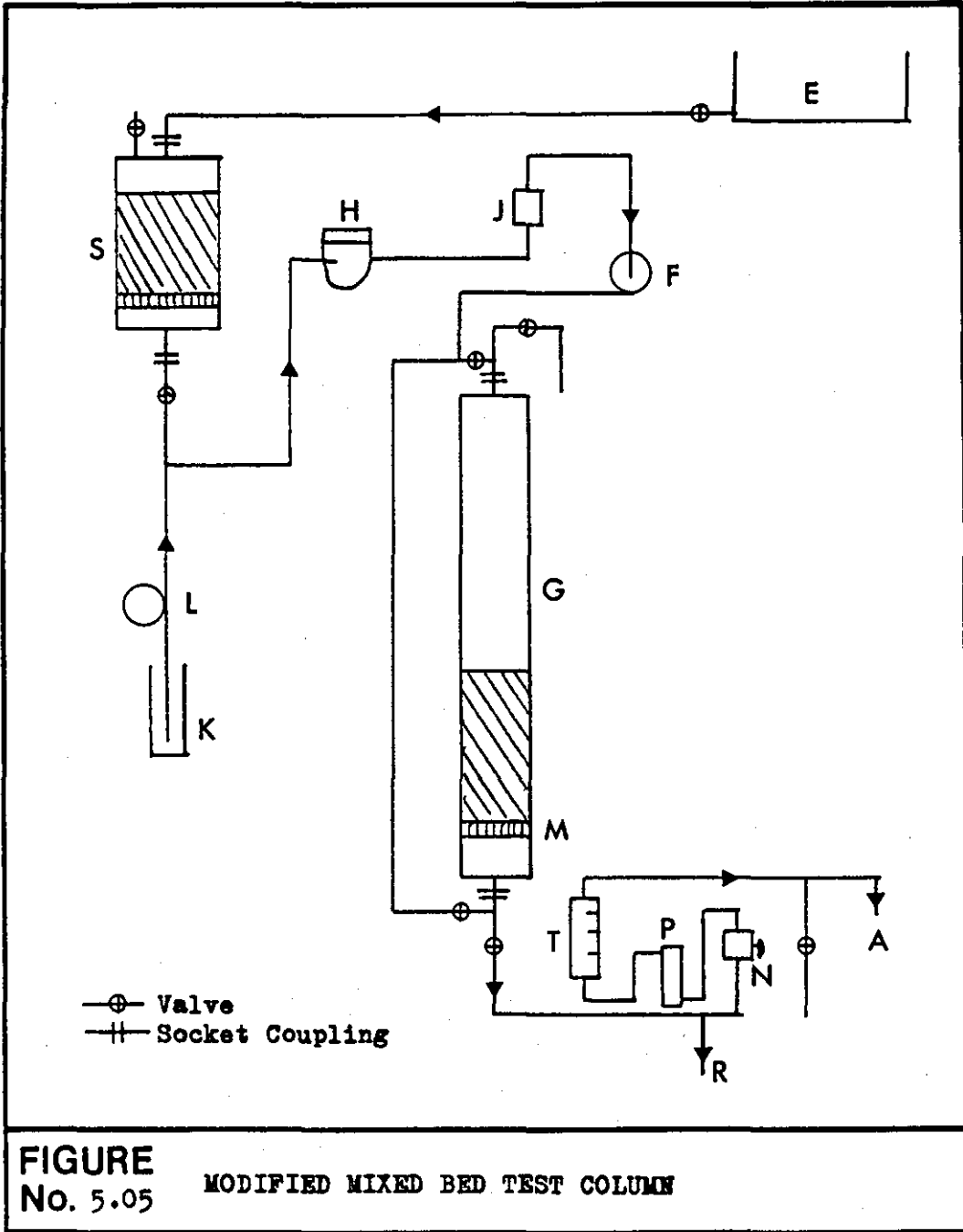
5.3.9 IONIC LEAKAGE TESTS WITH DELIBERATELY FOULED RESINS

Anion leakage tests with the deliberately fouled resins were carried
out in mixed beds with exactly the same experimental parameters as
were used for the new resin tests (see 5.3.7). The fouled resins
taken from the fouling rig columns were not converted to the chloride
form prior to final regeneration as this could have eluted some of
the organic foulants. The deliberately fouled resins were regenerated
according to the procedure outlined in A5.2.4, from the exhausted
state as removed from the fouling rig.

5.3.10 IONIC LEAKAGE TESTS WITH USED RESINS

The test procedures outlined above were quite comprehensive with
three chloride and three sulphate dosing concentrations for each of
three flow rates but proved very time consuming for the semi-routine
assessment of resin samples taken from operating CPP. Therefore a
simplified test procedure was introduced together with some small
modifications to the apparatus (Figure 5.05).

The total volume of the mixed bed was reduced from 1200 to 900 ml
ie 600 ml cation exchanger plus 300 ml anion exchanger. This gave
larger ionic leakages, especially for new resins; with the 1200 ml
bed some new small resins gave leakages approaching the limit of
detection of HPIC. The polishing mixed bed (S), that was originally
on a separate loop, was installed between the header tank (E) and
the dosing point. This ensured the feed to the test column was
fully deionised. The third addition was a flow meter (T) on the
column outlet. Although nominally calibrated for water at 20 $^{\circ}$C it
proved inaccurate and was only used as a flow indicator. Bead size
measurements on used resin samples were carried out with a HIAC
particle size analyser (A3.5).

The mixed bed test column was only operated at one flow rate, 100 mh^{-1},
as this was the typical value for modern CPP. The influent dosing
was retained as sodium chloride or sodium sulphate but the influent
concentration was adjusted to give leakages that were both measurable
but not excessive ie $<20 \mu g$ kg^{-1} Cl or $<50 \mu g$ kg^{-1} SO$_4$. Influent
concentrations used were any consecutive group of three from

100, 250, 500, 1000, 2000 or 5000 $\mu g \ kg^{-1}$ Cl and the equivalent
135, 338, 676, 1352, 2760 or 6760 $\mu g \ kg^{-1}$ SO$_4$. The poorer the resin's
kinetics the lower the influent concentrations that were used.

5.4 MASS TRANSFER EQUATION

From the kinetic work reviewed in 5.2 the mass transfer equation of
Frisch and Kunin (161) offered the greatest potential for use with
the experimental data generated by the column tests. However,
Frisch and Kunin's equation used the specific surface area per
unit mass of moist mixed resin, the bulk density of the mixed resins
expressed as mass of moist resin per unit settled volume and mass
flow rate. If determined accurately these parameters would give
a very precise appreciation of the flow rate and bead surface area
within the mixed bed. However, as noted earlier (3.6.1), measure-
ments on moist resins are not very accurate unless carefully
controlled. Also measurements of settled volume are liable to
variations in the packing of the beds.

The mass of the moist resin in a mixed bed is not an easily determined
parameter and will vary with the skeletal density of the resin which
in turn can vary with ionic form or polymer/matrix type. Thus two
resins with the same settled volume and bead size distribution but
differing skeletal density would have different specific surface
areas in the Frisch and Kunin equation.

Therefore, a modified version of the Frisch and Kunin equation is
proposed, dimensionally balanced, based on resin volume and volume
flow rather than resin mass and mass flow. In addition a term R is
introduced, the volume fraction of either anion or cation exchanger
in the mixed bed so that the equation now becomes specific for a
particular exchanger. The new equation is

$$\ln {}^{C}/_{C_o} \quad = \quad - \frac{M\ S\ Z\ A\ R}{V} \qquad \ldots\ldots(5.4)$$

where :

C$_o$ − column influent concentration

C − column outlet concentration

M − mass transfer coefficient (ms^{-1})

S − specific surface area of resin beads
$(m^2 m^{-3}$ settled volume basis)

Z − depth of exchange zone (m) for $C_o \longrightarrow C$

A − cross sectional area of test column or bed (m^2)

R − volume fraction of particular exchanger in bed

V − volumetric flow rate through column or bed $(m^3 s^{-1})$

For a resin with a distribution of bead sizes the specific surface area (S) is calculated from the Sauter mean bead diameter d_s allowing a porosity factor of 0.35 for a packed bed.

$$d_s \ = \ \frac{1}{\sum \frac{x_i}{d_i}} \qquad \ldots\ldots(5.5)$$

where x_i is the volume fraction of beads of diameter d_i in the overall size distribution.

Then
$$S \ = \ \frac{(1-\varepsilon)\ 4\pi\left(\frac{d_s}{2}\right)^2}{\frac{4}{3}\pi\left(\frac{d_s}{2}\right)^3} \ = \ \frac{6.\ (1-\varepsilon)}{d_s} \qquad \ldots\ldots(5.6)$$

where ε is the porosity factor of the settled bed.

5.4.1. ERRORS

5.4.1.1 Specific Surface Area (S)

It was noted earlier that the Frisch and Kunin mass transfer equation could introduce an error in comparisons of resin types by relating the specific surface area to the mass of moist resin, rather than the volume of resin. As reported in section 3 the determination of the mass of moist resin, without residual moisture, is a difficult process for several ml of resin let alone several hundred ml. However, it is equally difficult to measure the displaced volume of

TABLE 5.03 SETTLED BED POROSITY

ANION EXCHANGE RESIN TYPE	MEAN DIAMETER (mm)	SETTLED BED POROSITY (ε)
Amberlite IRA900	0.75	0.36
Duolite A161C	0.68	0.35
Ambersep 900	0.66	0.35
Monosphere TG550A	0.60	0.33

Average for anion exchangers $\varepsilon = 0.35$

CATION EXCHANGE RESIN TYPE	MEAN DIAMETER (mm)	SETTLED BED POROSITY (ε)
Ambersep 200	0.85	0.34
Amberlite IR120	0.72	0.31

resin on a large scale. In all the column tests the resins were
measured on a settled volume basis and an average voidage factor
applied. Thus, the voidage (ε) used in the equation for the specific
surface area should be that in the measuring cylinder when measuring
out the resins, not the voidage of the mixed bed itself.

The voidages given in the literature for settled resins or mixed
spheres vary between 0.32 and 0.41 (232, 233, 234). The recorded
value will depend on whether the beads were allowed to settle
naturally from a suspension or were tapped down to minimum volume
after settling.

The settled resin voidage under the experimental conditions used for
the column tests was measured for a number of resin samples and an
average value taken. About 300 ml settled volume of resin were added
to water in a 500 ml measuring cylinder, lightly tapped and the
settled volume noted. The resin was washed into a Buchner funnel
and vacuum applied to remove residual water but leave a moist resin.
The displaced volume of this resin was measured by adding it to a
known volume (250 ml) of water in a 500 ml measuring cylinder and
noting the increase in volume. The measured voidages are presented in
Table 5.03 and an average factor of $\varepsilon = 0.35$ was used in subsequent
calculations.

A similar problem arises when the experimentally determined mass
transfer coefficient is used to estimate plant performance. A design
figure for settled volume is generally all that is known, not the
actual volume loaded, hence an average porosity factor must be applied.
Although these errors cannot, simply, be avoided the comparison
between mass transfer coefficients of different ions is valid for a
given resin in a particular column test. Comparisons between
different resins will be subject to a small error, as discussed in
5.5.1.1.

5.4.1.2 Depth of Exchange Zone (Z)

The mass transfer equation is of the first order type $C = C_o e^{-kt}$,
although the time term (t) is incorporated in the flow rate term (V),
and gives rise to an asymptotic exchange front concentration profile
(Figure 5.06). For the purpose of calculating M from the experimental

Concentration

C_o C

Total
Bed
Depth

Exchange
Front
Profile

Exchange
Zone (Z)
$C_o \longrightarrow C$

0   100

% Removal

| FIGURE No. 5.06 | EXCHANGE ZONE FOR TEST COLUMN MIXED BEDS |
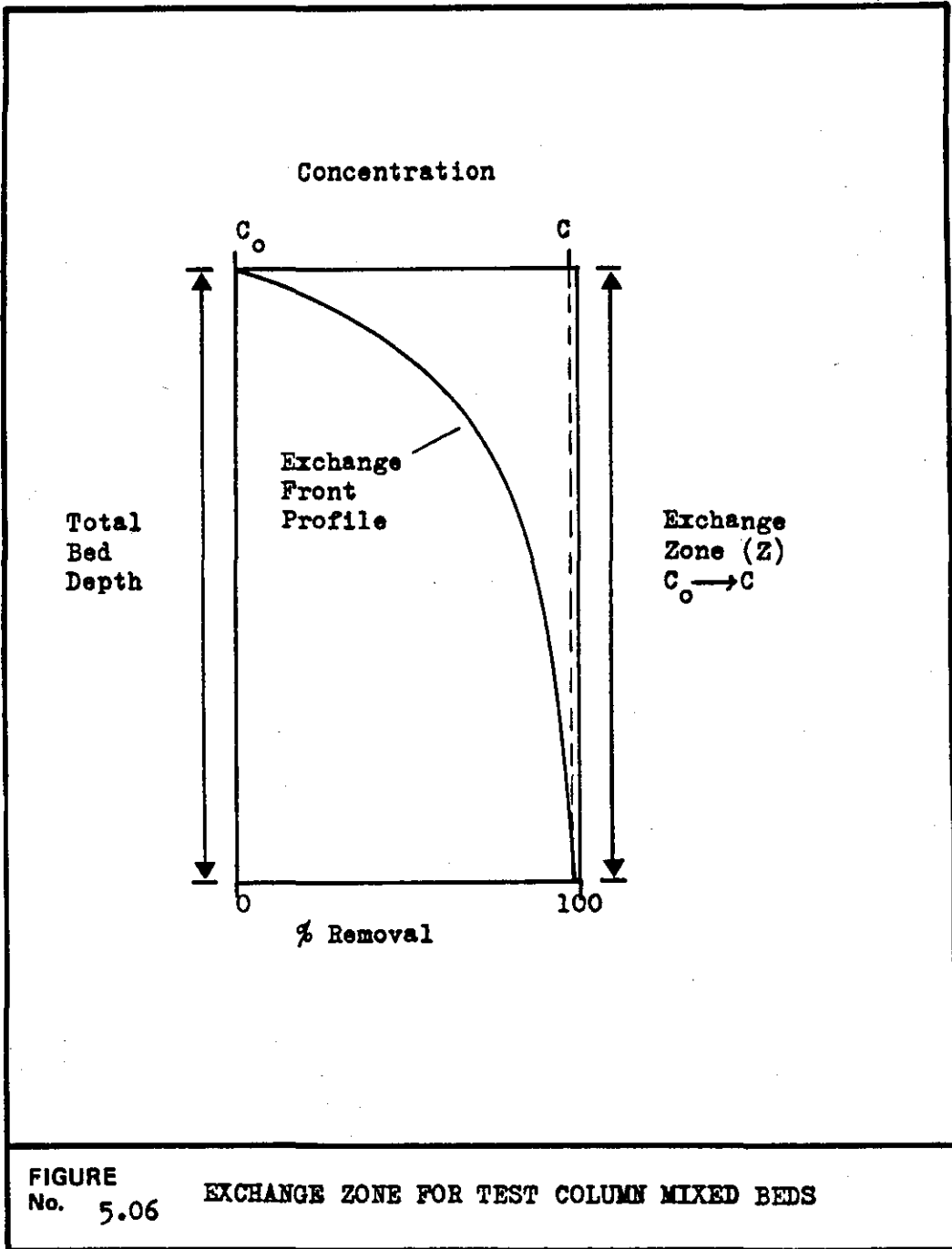
data the depth of the exchange zone is the full depth of the test
column as the only two ionic concentrations known are those at the
inlet to and outlet from the column.

In the column tests each flow rate-dosing combination was run for
only as little time as was necessary to establish the dynamic
equilibrium leakage. In this way only a small fraction of the total
anion exchange capacity was used. If each dosing combination were
continued for five minutes a total of 25.6 milli equivalents (m eq)
of anions $(Cl + SO_4)$ were dosed onto the 400 ml of anion exchanger
in the column. The total anion exchange capacity of the resin was
approximately 450 m eq. Thus the dosing used 5.7% of the total
capacity and it was assumed that the depth of exchange zone (Z) for
$C_o \rightarrow C$ was always equal to the column bed depth.

In the mass transfer equation the group ZA represents the mixed bed
settled volume and the group ZAR is equal to the volume of exchanger
under investigation.

5.4.1.3 Other Parameters

The errors in the inlet and outlet concentrations, C_o and C, are
those of the analytical methods and are fairly well defined (A5.4.3).
The cross sectional area, A, of the column is accurately measurable.
The flow rate through the column, measured by timing the collection
of 1 litre of water was accurate to < 0.1 seconds in 15 seconds at
120 mh^{-1}.

In the case of calculation of leakages from full scale units the
design flow rate for the plant can be substituted into the equation.
In practical examples there are also problems in knowing the exact
resin ratio in a particular bed, the depth of the bed or the bead
size distribution of the resins in the bed. If the resins were not
examined when newly loaded the results gained from a single sample
of resin can be misleading.

TABLE 5.04 <u>MASS TRANSFER COEFFICIENTS FOR CHLORIDE AND SULPHATE</u>

<u>EXCHANGE IN A MIXED BED - NEW RESINS</u>

Resin Designation	Mass Transfer Coefficient (10^{-4}ms^{-1})			
	Chloride Ion Exchange		Sulphate Ion Exchange	
	Flow Rate (mh^{-1})			
	90	120	90	120
Amberlite IRA402	1.88	2.39	1.90	2.33
Amberlite IRA458	1.97	2.51	1.97	2.36
Amberlite IRA900	2.05	2.42	2.01	2.41
Duolite A101D	1.85	2.29	1.92	2.37
Duolite A161	1.76	2.12	1.75	2.23
Zerolit MPF	1.98	2.41	1.92	2.18

5.5 KINETICS OF NEW ANION EXCHANGERS

5.5.1 CHLORIDE AND SULPHATE LEAKAGE

The mixed bed test column leakage results are given in full in Table A5.10 for chloride dosing and Table A5.11 for sulphate dosing. The mass transfer coefficients calculated from this data are given in Tables A5.12 and A5.13 based on a typical porosity factor of 0.35. Table 5.04 summarises the mass transfer coefficients for the $\overline{OH} - Cl$ and $\overline{OH} - SO_4$ exchange reactions by taking the mean value of the three dosing concentrations at the 90 mh^{-1} and 120 mh^{-1} flow rates.

5.5.1.1 Evaluation of Errors

Before proceding further with analysis and discussion of the results it is worth examining the source of errors in greater detail and putting numerical values on the likely errors.

As an example take an anion exchanger with a mean bead diameter 0.8 mm, operating under the 'new resin' test conditions with a column flow rate of 4 litres per minute ($\equiv$ 120 mh^{-1}) and with a chloride ion mass transfer coefficient M = 2.36×10^{-4} ms^{-1}.

The standard value of porosity factor $\mathcal{E}$ was 0.35. This could vary as much as $\pm$ 0.02, but more probably by $\pm$ 0.01, and Table 5.05a demonstrates the variations that can occur. A range of $\pm$ 0.01 on porosity factor gives a variation of $\pm 4 \times 10^{-6} ms^{-1}$ on the mass transfer coefficient.

Variation in flow rate could also affect the value of M. The nominal flow rate was 1 litre in 15 seconds, 6.67×10^{-5} $m^3 s^{-1}$, but this could vary between 14.75 and 15.25 seconds, giving flow rates of 6.78×10^{-5} and 6.55×10^{-5} $m^3 s^{-1}$ respectively. Table 5.05b indicates that this flow rate variation would also result in a $\pm 4 \times 10^{-6} ms^{-1}$ fluctuation in M.

The third parameter likely to cause errors in M is the column outlet analysis. Chloride concentrations were accurate to ± 0.2 μg kg^{-1} Cl. At an influent level of 5920 μg kg^{-1} Cl under standard conditions

TABLE 5.05   ERROR CALCULATIONS

Standard Test Conditions $\varepsilon = 0.35$; $d_s = 0.8mm$

$$V = 6.67 \times 10^{-5} \, m^3 s^{-1}$$

(a)   Variation of ε fixed mean bead diameter

ε	S $m^2 m^{-3}$	M $10^{-4} ms^{-1}$
0.33	5025	2.29
0.34	4950	2.33
0.35	4875	2.36
0.36	4800	2.40
0.37	4725	2.44

(b)   Variation of V at fixed leakage concentration

V $10^{-5} m^3 s^{-1}$	M $10^{-4} ms^{-1}$
6.55	2.32
6.67	2.36
6.78	2.40

(c)   Variation of column leakage at fixed influent concentration

Inlet $\mu g\ kg^{-1} Cl$	Outlet $\mu g\ kg^{-1} Cl$	M $10^{-4} ms^{-1}$
1480	1.3	2.41
	1.5	2.36
	1.7	2.32
5920	5.7	2.375
	5.9	2.36
	6.1	2.35

(ϵ=0.35, V = 6.67 x 10^{-5} $m^3 s^{-1}$) the leakage would be 5.9 μg kg^{-1} Cl.
A $\pm$ 0.2 μg kg^{-1} Cl error in analysis would give a $\pm$ 0.015 ms^{-1}
variation in M. However at an influent level of 1480 μg kg^{-1} Cl
the leakage would be only 1.5 μg kg^{-1} and a $\pm$ 0.2 μg kg^{-1} Cl
variation has a larger effect on M ie $\pm$ 5x10^{-6} ms^{-1} (Table 5.05c).

These calculated errors in the value of M represent the variations
between column tests with different resins. The differences between
the mass transfer coefficients of different ions on the same resin at
the same flow rate would only be subject to the errors in analysis.

5.5.2 POLYMER/MATRIX TYPE

From Table 5.04 it can be seen that the mass transfer coefficient is
nearly constant for all polymer/matrix types at a particular flow
rate for either chloride or sulphate exchange. The value of M is
lower for the lower flow rate because the 'film thickness', τ, and
therefore the diffusion path increases as the flow rate decreases.
The correlation between polymer/matrix types is poorer at 90 mh^{-1}
because the leakages are mostly in the 0.5 - 1.5 μg kg^{-1} range and any
small background leakage from the column or analytical error has a
relatively large effect on M. For this reason no values of M are
given for the 55 mh^{-1} flow rate where the majority of leakages were
$<$ 1 μg kg^{-1} Cl or SO_4.

The data indicate that within the limits of experimental error, the
mass transfer coefficients for chloride and sulphate were independant
of the influent concentration. The similarity in mass transfer
coefficients for all polymer/matrix types and the reduction in mass
transfer coefficient with reduced flow rate are both conditions that
satisfy the condition M = D/τ indicating that liquid film boundary
layer diffusion is the rate controlling mechanism for all new anion
exchangers, irrespective of polymer/matrix type, at the influent
concentrations and flow rate conditions found in CPP operation.

There is an obvious exception to these general conclusions drawn from
the results in Table 5.04. The low mass transfer coefficients for
both chloride and sulphate exchange with Duolite A161 were due to
high background leakages of both chloride and sulphate ion from this

TABLE 5.06   AVERAGE CHLORIDE TO SULPHATE LEAKAGE RATIOS

- NEW AND DELIBERATELY FOULED RESINS

	Anion Exchanger Type Ionic Leakage Ratio	DUOLITE A161	AMBERLITE 900	ZEROLIT MPF	AMBERLITE 458	DUOLITE A101D	AMBERLITE 402
A	Sulphate : Chloride New Exchangers	0.8	1.4	1.6	1.4	1.2	1.3
B	Sulphate : Chloride Organically Fouled Exchangers	2.6	2.9	2.4	2.1	2.7	2.4
C	Chloride Leakage Fouled : New Exchanger	0.8	1.5	1.4	1.8	1.1	1.1
D	Sulphate Leakage Fouled : New Exchanger	2.6	3.2	2.1	3.0	2.4	2.1

The values quoted are average values of the individual leakage ratios for the following conditions. Leakages are expressed in chemically equivalent concentrations.

$$84\mu eqkg^{-1} \text{ at 90 and } 120mhr^{-1}$$
$$167\mu eqkg^{-1} \text{ at 55, 90 and } 120mhr^{-1}$$

particular column. The impurity leakages were traced to the washing
out of manufacturing residues from the macroporous cation exchanger.

All newly manufactured ion exchangers release short chain oligomers
and colloidal species after standing for a period of several weeks.
These are manufacturing residues that diffuse to the bead surface.
Macroporous resins also release slightly larger particulate species.
Cation exchangers are swollen in a chlorinated hydrocarbon before
sulphonation. Therefore both chloride and sulphate ions are
potential residues. A sample of dark brown residues was isolated
from the IR200 cation exchanger used in these tests. Dispersing
125 μg of these residues in 1000 ml of deionised water produced a
solution containing 8 μg kg^{-1}Cl and 20 μg kg^{-1}SO$_4$. Subsequently the
experimental procedure was modified to rinse the cation exchanger
immediately prior to adding the anion exchanger and mixing the resins.

A subsequent column test with a different batch of Duolite A161
confirmed that this resin fitted the pattern of liquid boundary layer
diffusion control. Details of this test are given in Table A5.14.

5.5.3 RELATIVE RATES OF EXCHANGE FOR CHLORIDE OR SULPHATE

Another factor to emerge from this study is that the mass transfer
coefficient for sulphate exchange is slightly, but consistently,
smaller than that for chloride exchange, ie sulphate exchange is
slower. Because of the relative insensitivity of the logarithmic C/C$_o$
term in equation   5.4 .   to small changes in C, the effect is more
marked if the chloride and sulphate leakages are compared in terms
of percentage influent concentration. Table 5.06 lists the ratio of
sulphate to chloride leakage for the six new anion exchangers. As
explained above the results for Duolite A161 are anomolous, but the
other five polymer/matrix types have sulphate:chloride leakage ratios
of   between 1.2 and 1.6 with an average of 1.4. This indicates
that $\overline{OH}$ - SO$_4$ exchange is an inherently slower process than $\overline{OH}$ - Cl
exchange.

If liquid boundary layer diffusion is the rate controlling process
the difference in mass transfer coefficients between chloride and
sulphate exchange should reflect differences in diffusion rates of
the exchanging species. Table 5.07 lists the ionic equivalent

TABLE 5.07   CONDUCTANCE AND DIFFUSION DATA

A.   <u>Limiting Equivalent Conductances</u> λ^o $(cm^2 \, \Omega^{-1} \, equiv^{-1})$

Ion	Temperature		Ion	Temperature	
	20 °C	25 °C		20 °C	25 °C
H^+	324.9	349.8	NO_3^-	64.9	71.5
Na^+	44.9	50.1	$H_2PO_4^-$	(29.7)	33
Cl^-	69	76.4	$\frac{1}{2}HPO_4^{2-}$	(51.3)	57
OH^-	182.5	199.1	$\frac{1}{2}SO_4^{2-}$	71.7	80.0

B.   <u>Ionic Diffusion Coefficient (D_i) at 20 °C</u> $(10^{-9} \, m^2 s^{-1})$

Ion	$D_{i(20 \, °C)}$	Ion	$D_{i(20 \, °C)}$
H^+	8.50	NO_3^-	1.70
Na^+	1.17	$H_2PO_4^-$	0.78
Cl^-	1.80	$\frac{1}{2}HPO_4^{2-}$	1.34
OH^-	4.77	$\frac{1}{2}SO_4^{2-}$	1.88

C.   Molecular Diffusion Coefficient (D_m) at 20 °C $(10^{-9} \, m^2 s^{-1})$

Molecule	$D_{m(20 \, °C)}$	Molecule	$D_{m(20 \, °C)}$
NaCl	1.42	HCl	5.23
$NaNO_3$	1.39	H_2SO_4	2.30
NaOH	1.88	Na_2SO_4	1.08
NaH_2PO_4	0.94	Na_2HPO_4	0.94

Data from Robinson and Stokes (65)

   Lange (235)

conductances and ion and molecular diffusion coefficients for the range of species likely to be involved in the H/OH mixed bed exchange of sodium chloride, sodium sulphate, sodium nitrate and sodium phosphate. Diffusion coefficients were calculated from electrolytic conductance data using the Nernst – Hartley equation (65).

Examination of ionic diffusion coefficients shows that chloride ion diffuses more slowly than sulphate ion. This is the opposite of the observed trend and indicates that simple ionic diffusion is not the rate controlling mechanism. In order to preserve electroneutrality in the boundary layer cations will accompany the diffusing anions but will be deterred from close approach to the exchanger by the electric charge double layer at the bead surface. Molecular diffusion coefficients certainly indicate that sodium sulphate diffuses more slowly than sodium chloride, but the ratio of diffusion coefficients gives a greater difference between chloride and sulphate exchange rates than is observed in practice. Even if the relationship $M \propto D^{2/3}$ (78, 236) is used the ratio of chloride:sulphate diffusion coefficients (1.20) is greater than the observed difference in mass transfer coefficients (1.033).

However, if it is assumed that the practical diffusion coefficient is the mean of the exchanging and exchanged species, ie NaCl or Na_2SO_4 and NaOH respectively, the diffusion coefficient for $\overline{OH}$-Cl exchange becomes $1.65 \times 10^{-9} ms^{-1}$ and the diffusion coefficient for $\overline{OH} - SO_4$ exchange becomes $1.48 \times 10^{-9} ms^{-1}$. Applying the $M \propto D^{2/3}$ relationship gives a factor of 1.11 for the ratio of chloride:sulphate mass transfer coefficients. This is much nearer the observed values calculated from Table 5.04, ranging between 1.01 and 1.11 with an average of 1.033.

However, Robinson and Stokes (65) note that diffusion coefficients derived from conductance data do not always agree with practical observations. This is because in conductance measurements the positive and negative ions move in opposite directions whereas in diffusion both ions move in the same direction along the concentration gradient. The disparity between calculated and observed diffusion coefficients is more noticable for 'unsymmetrical' salts, such as Na_2SO_4, where the observed diffusion coefficient is slightly faster than the calculated value.

TABLE 5.08   CORRELATION BETWEEN MASS TRANSFER COEFFICIENT AND FLOW RATE

NEW RESINS

FLOW RATE (mh^{-1})	RESIN	FLOW RATE CORRELATION FACTOR $K = MV_L^{-\frac{1}{2}} \times 10^5$	
		Chloride Exchange	Sulphate Exchange
90	IRA458	2.08	2.08
90	IRA900	2.16	2.12
90	Z MPF	2.09	2.02
120	IRA458	2.29	2.15
120	IRA900	2.21	2.20
120	Z MPF	2.20	1.99

DELIBERATELY FOULED RESINS

FLOW RATE (mh^{-1})	RESIN TYPE	FLOW RATE CORRELATION FACTOR $K = MV_L^{-\frac{1}{2}} \times 10^5$	
		Chloride Exchange	Sulphate Exchange
90	IRA458	1.97	1.78
90	IRA900	2.03	1.52
90	Z MPF	2.03	1.79
120	IRA458	2.04	1.83
120	IRA900	2.13	1.78
120	Z MPF	2.05	1.80

TABLE 5.09 <u>VARIATION OF MASS TRANSFER COEFFICIENT WITH INFLUENT CONCENTRATION FOR NEW RESINS; 120 mh^{-1} FLOW RATE</u>

	MASS TRANSFER COEFFICIENT (10^{-4} ms^{-1})					
	Chloride Exchange			Sulphate Exchange		
Influent (μg kg^{-1})	1480	2960	5920	2000	4000	8000
Amberlite IRA458	2.49	2.49	2.54	2.39	2.35	2.33
Zerolit MPF	2.41	2.42	2.40	2.11	2.21	2.21

TABLE 5.10 <u>MASS TRANSFER COEFFICIENTS FOR NEW IRA900 REGENERATED FROM BICARBONATE OR CHLORIDE FORM RESIN.</u>
<u>(Influent 83.3 μeq kg^{-1})</u>

	MASS TRANSFER COEFFICIENT (10^{-4} ms^{-1})			
Resin Form	Bicarbonate		Chloride	
Flow Rate (mh^{-1})	90	120	90	120
Influent Anion				
Chloride	2.18	2.57	2.05	2.42
Nitrate	2.16	2.50		
Sulphate	1.97	2.27	2.01	2.41
Mono hydrogen phosphate	1.59	1.88		

An additional complication in attempting to describe anion exchange
in a mixed bed is the cation exchange process occurring concurrently.
Thus the exchanging species may be either the sodium salt of the
anion or the acid. The product of anion exchange of an acid is water
but this also must be dispersed from the surface of the bead and may
interact with the rate controlling diffusion processes.

5.5.4 EFFECTS OF FLOW RATE

Various groups of workers have concluded that the mass transfer rate,
exchange zone height or mass transfer coefficient are proportional
to the square root of the linear superficial fluid velocity. This
has been shown for $\bar{H}$ - Na cation exchange (75) mixed bed exchange (161)
and the triple Cl- SO_4- PO_4 system (83). The relationship $M = KV_L^{\frac{1}{2}}$
has been tested for the new resin leakage data at 90 and 120 mh^{-1}
flow rates with good correlation (Table 5.08).

As the flow rate through a bed increases there is an increase in mass
transfer coefficient because the boundary layer thickness decreases.
At the same time there is a decrease in the residence time of the
water within the bed. Since the residence time ($\propto 1/V_L$) decreases
more rapidly than the mass transfer coefficient ($\propto \sqrt{V_L}$) increases
there is an increase in ionic leakage with flow rate.

5.5.5 INFLUENT CONCENTRATION

If liquid boundary layer diffusion is the rate controlling step
there should be no effect of influent concentration on the value of
M. Table 5.09 compares the calculated values of M at the three
influent concentrations used at the 120 mh^{-1} flow rate. Within the
bounds of experimental error there is no variation of M with
concentration indicating that boundary layer diffusion is the rate
controlling process.

5.5.6 EXCHANGE OF OTHER ANIONS

The new anion exchagers tested for chloride and sulphate leakage were
all regenerated from the chloride form. As the anion exchanger
exhibits a much higher selectivity for sulphate over chloride, there
was a small equilibrium dispacement of chloride during sulphate

injection. This varied between 0.4 μg kg^{-1} Cl at the lowest flow
rate and 1.1 μg kg^{-1} Cl at the higher flow rate with the larger
resins. To establish whether this leakage of chloride was influencing
the exchange processes a single test was run with new IRA900
conditioned to the bicarbonate form prior to standard regeneration.
This test was only operated at the 90 and 120 mh^{-1} flow rates and only
a single dosing concentration was used (83.3 μeq kg^{-1}). In addition
to sodium chloride or sodium sulphate equivalent concentrations of
sodium nitrate or disodium hydrogen phosphate (Na_2HPO_4) were injected.
This represented a larger monovalent ion and a divalent ion similar
in size to sulphate. As dosed the disodium hydrogen phosphate gave
a pH of 9.7 and the phosphate was mainly divalent but any leakage
would be at near neutral conditions which favours the presence of
monovalent dihydrogen phosphate.

Table 5.10 gives the mass transfer coefficients for the chloride,
sulphate, nitrate and phosphate exchange reactions. The two
monovalent anions, Cl and NO_3 have very similar values of M which
is to be expected as their ionic and molecular diffusion coefficients
are almost identical (Table 5.07). Leakage data for the regenerated
bicarbonate form resin are given in Table A5.15.

The divalent phosphate has a significantly lower mass transfer
coefficient than sulphate, which in turn is lower than chloride,
as previously observed. The ionic and molecular diffusion
coefficients of HPO_4^{2-} or $H_2PO_4^-$ are both lower than for sulphate
(Table 5.07) but, as with SO_4/Cl , the ratios of SO_4 : PO_4 diffusion
coefficients do not correspond with the ratio of the mass transfer
coefficients; M_{SO_4} : M_{PO_4} = 1.22 while $D_{Na_2SO_4}$: $D_{Na_2HPO_4}$ = 1.15.

In the exchange of divalent ions there would appear to be more
factors than boundary layer diffusion influencing the exchange rate.

Comparing the mass transfer coefficients for chloride and sulphate
on resin regenerated from the bicarbonate and chloride forms
(Table 5.10) there are slight differences that are outside the
likely errors in the method. Chloride exchange is a little faster
with bicarbonate form resin than with chloride form resin while
sulphate exchange is a little slower. Reasons for this are considered
in section 5.5.7. More recent work has confirmed the greater
difference between chloride and sulphate kinetics on regenerated
bicarbonate form resin (236a).

5.5.7 EXCHANGE MECHANISMS

5.5.7.1 Ion Hydration

In liquid boundary layer control of the rate of exchange an anion in
the bulk solution, and its associated cation(s), diffuse down a
concentration gradient towards the exchanger surface. At the bead
surface anions associated with the exchange groups are attempting to
move into the solution phase, to satisfy their hydration requirements
(21). This rapidly sets up the Donan double charge layer (20), positive
on the bead surface, negative in the adjacent liquid layer, which
prevents the anions from leaving the area adjacent to the bead surface.

As the incoming anion approaches the positively charged exchanger
surface the associated cation(s) will be prevented from too close an
approach by electrostatic repulsion, although they must remain
adjacent to maintain electroneutrality. The incoming anion, attracted
by a positive charge, will associate with an exchange site, perhaps,
as an activated complex of exchanger site, solution anion and
exchanger anion (71, 85). In order to associate closely with the
quaternary ammonium exchange group the solution anion must lose part
of its hydration sheath requiring an increase in free energy. If
either anion should leave the activated complex there will be a
decrease in free energy as that anion becomes fully hydrated in the
bulk solution. Chu et al (58) have proposed that a nett reduction
in free energy of exchanger and solution is the driving force behind
ion selectivity by the exchanger. Therefore the ion with the largest
free energy of hydration will prefer the solution phase to the resin
phase and will depart from the activated complex at the exchanger
surface. The OH^- ion has a higher hydration energy than most other
anions, therefore an anion exchanger is selective for other anions
over hydroxide. Similarly, a cation exchanger is selective for other
cations rather than the H^+ ion.

Once the incoming anion is exchanged it will then migrate into the
matrix of the resin and a further hydroxide ion will migrate to the
surface. The driving force for this migration is similar to that for
exchange, ie the exchanger will have a lower free energy if hydroxyl
ions are at the bead surface where their greater hydration requirement

can be more nearly satisfied. Inside the exchanger matrix, the
irregularity of the crosslinking is likely to produce individual
sites of differing selectivity. A high cross linked zone with low
moisture content, therefore a low potential for hydration, will be
less selective for hydroxyl ions than a low cross linked zones.
Therefore, the exchanged anions are likely to migrate to areas of
high crosslinking. The mechanism of migration may well be similar
to the exchange process, moving between adjacent sites. The conclusion
from this argument is that in dilute solution with liquid boundary
layer diffusion control all exchange takes place at the bead surface.

5.5.7.2 Steric Factors

The exchange of monovalent, monatomic ions (eg Cl^-) for hydroxide
should present few problems as the incoming anion is capable of close
approach to the exchange site. Polyatomic ions generally carry the
charge on a satellite atom. For a symmetrical ion such as nitrate
the charge may reside on any of the oxygen atoms so that orientation
with the exchange group would present less of a problem than with a
more bulky less symmetrical anion, (eg $H_2PO_4^-$).

The exchange of divalent, polyatomic ions is more likely to give
problems of steric orientation. A sulphate ion has tetrahedral
symmetry with a fixed distance between the two charged oxygen atoms.
Therefore, for sulphate exchange to occur there must be two adjacent
and available exchange sites with approximately the right separation.
If the site spacing is not correct sulphate exchange may be slowed
while sites of the correct orientation are located. It has been
reported (237) that by altering the spacing of the N atoms of the
anion exchange groups the selectivity sequence for $NO_3 - SO_4$ can be
reversed. The less symmetrical, more bulky divalent HPO_4^{2-} ion would
be expected to have a greater steric problem than the SO_4^{2-} ion.

5.5.7.3 Selectivity

The observed differences in exchange rate for an exchanger regenerated
from the bicarbonate or chloride form can be explained by examination
of selectivity and steric considerations. On a regenerated
bicarbonate form resin both sulphate and chloride will exchange for

TABLE 5.11   <u>MASS TRANSFER COEFFICIENTS FOR NEW AND DELIBERATELY</u>

<u>FOULED ANION EXCHANGERS</u>

<u>FLOW RATE 120 mh^{-1}</u>

| Anion Exchanger | MASS TRANSFER COEFFICIENT (10^{-4} ms^{-1}) | | | |
| | Chloride Exchange | | Sulphate Exchange | |
	New	Fouled	New	Fouled
Amberlite IRA402	2.39	2.37	2.33	2.07
Amberlite IRA458	2.51	2.23	2.36	2.01
Amberlite IRA900	2.42	2.32	2.41	1.95
Duolite A101D	2.29	2.38	2.37	2.08
Duolite A161	2.12	2.23	2.23	1.95
Zerolit MPF	2.41	2.25	2.18	1.97

<u>FLOW RATE 90 mh^{-1}</u>

| Anion Exchanger | MASS TRANSFER COEFFICIENT (10^{-4} ms^{-1}) | | | |
| | Chloride Exchange | | Sulphate Exchange | |
	New	Fouled	New	Fouled
Amberlite IRA402	1.88	1.92	1.90	1.77
Amberlite IRA458	1.97	1.87	1.97	1.69
Amberlite IRA900	2.05	1.92	2.01	1.65
Duolite A101D	1.85	1.96	1.92	1.75
Duolite A161	1.76	1.78	1.75	1.59
Zerolit MPF	1.98	1.92	1.92	1.70
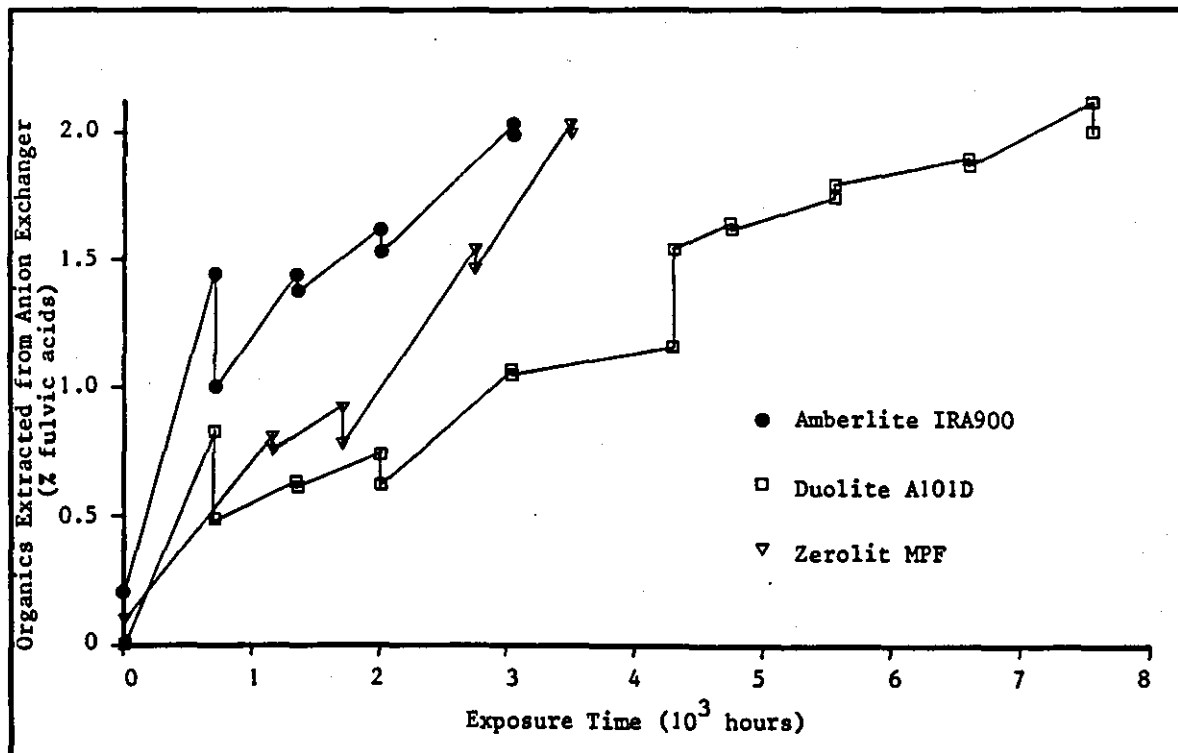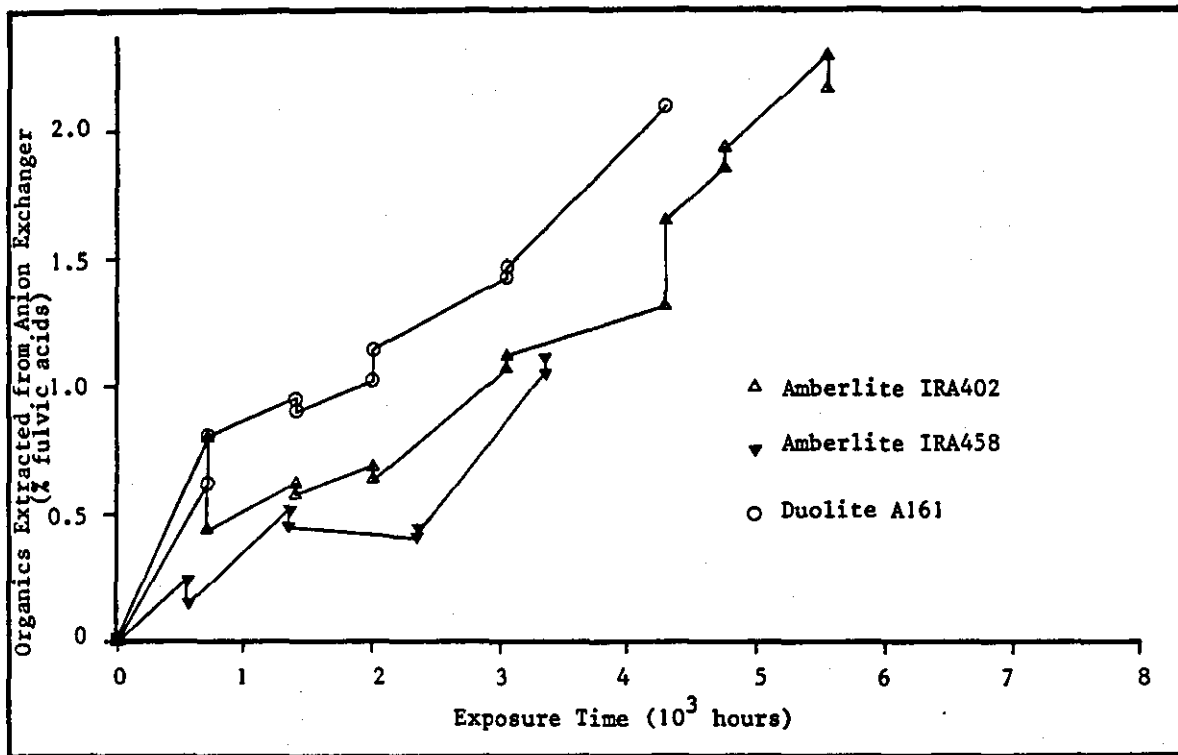
FIGURE
No. 5.07   INCREASE OF EXTRACTABLE ORGANICS WITH EXPOSURE
TIME TO FOULING ENVIRONMENT

bicarbonate whereas on the regenerated chloride form resin only sulphate will exchange for chloride. A trace chloride leakage during sulphate exchange was noted in the latter case. Therefore the rate of chloride exchange on the regenerated bicarbonate form resin may be slightly enhanced due to the additional exchange with bicarbonate that was not available on the regenerated chloride form resin. However, whilst $\overline{HCO_3^-} - \overline{SO_4^{2-}}$ exchange may also occur, there would be some difficulty in accommodating HCO_3^- and SO_4^- groups around a quaternary nitrogen atom. Such steric hindrance may marginally reduce the sulphate ion exchange rate on the bicarbonate resin.

5.6 ORGANICALLY FOULED ANION EXCHANGERS

5.6.1 DELIBERATELY FOULED RESINS

The deliberate organic fouling of the six types of new anion exchanger, described in section 5.3.8, was continued until each resin had accumulated 2% by weight of organic foulants expressed as fulvic acids (Table 5.11). The rate of accumulation varied for the different polymer matrix types. Figure 5.07 is a graphical illustration of the uptake of organics versus time. As the concentration of organics in the influent to the test resins varied with time the comparison is not fully quantified, but it is noticable that the three macroporous resins accumulated organic foulants more quickly than the gelular resins. The acrylic gel resin only accumulated 1.1% by weight of organic species in the time available for this resin to remain in the fouling rig.

Table 5.11 summarises and compares the average mass transfer coefficients for new and deliberately fouled resins at 90 mh^{-1} and 120 mh^{-1}. Full experimental results for the deliberately fouled resins are given in Tables A5.16 and A5.17 and the calculated mass transfer coefficients in Tables A5.18 and A5.19.

5.6.1.1 Polymer/Matrix Type

The differences between the effect of organic foulants on the various polymer/matrix types is small, and almost within the experimental error of the method. Certain minor trends can be discerned. The

three macroporous exchangers all have similar mass transfer coeff-
icients that are slightly smaller than the values for the styrene -
gel types. The acrylic - gel resin has shown a larger reduction in
mass transfer coefficients than the other resins, but as will be
discussed in section 5.7 all these variations are very small
compared with the variations found in used resins from operating
plant.

5.6.1.2 Flow Rate

The relationship $M = KV_L^{\frac{1}{2}}$ was tested for the deliberately fouled
resins at the 90 and 120 mh^{-1} flow rates. The correlation was poorer
than with new resins more particularly for sulphate ion exchange.
The comparisons are given in Table 5.08.

5.6.1.3 Relative Deterioration of Chloride and Sulphate Kinetics

An examination of the results given in Tables 5.06 and 5.11 reveals
one very important factor. In all cases the sulphate exchange
kinetics have shown a larger deterioration due to the organic
foulants compared with chloride exchange kinetics. This can be
seen more clearly in the sulphate:chloride leakage ratios (Table 5.06)
which average 2.5 for the fouled resins compared with 1.7 for the
new resins. A different expression of the same data shows that the
average chloride leakage from the deliberately fouled resins is 1.5
times greater than that from the new resins while the sulphate
leakage has increased by a factor of 2.6.

The relatively larger deterioration in sulphate exchange kinetics
helps to explain why sulphate leakage is the most commonly observed
feature of mixed beds containing aged and organically fouled resins.
However, the examination of anion exchangers from operating mixed
beds gives a much wider picture (5.6.2) and the influence of
foulants on the exchange mechanisms is discussed in section 5.6.3.

TABLE 5.12   MASS TRANSFER COEFFICIENTS FOR IN-SERVICE FOULED CPP ANION EXCHANGE RESINS

$(100mh^{-1}$ flow rate)

CPP Location	Anion Exchanger Type	Time in Service (Years)	Extractable Organics Foulants (% dry wt)	Extractable Iron (wt % Fe)	Mass Transfer Coefficient $(10^{-4} ms^{-1})$		Ratio $\dfrac{M_{SO_4}}{M_{Cl}}$
					Chloride Influent 500 µgkg^{-1} Cl	Sulphate Influent 676 µg kg^{-1} SO$_4$	
—	Typical New	—			2.40	2.20	0.92
Didcot[*]	IRA900	0.5	1.68		1.16	0.52	0.44
Fawley	A161	4	0.51	0.07	1.57	1.07	0.68
Hartlepool	IRA900	4	0.44	N.D.	1.77	1.26	0.71
Hinkley Point 'B'	A161/Z MPF (Mixture)	6	0.60	N.D	1.83	1.49	0.81
Pembroke	IRA900	2.5	0.83	0.09	1.55	0.95	0.61
Vandellos (Spain)	IRA900	6	0.94	0.28	1.36	0.78	0.57
Wylfa (i)	IRA900	1.1	1.07	0.19	1.77	1.42	0.80
Wylfa (ii)	IRA900	1.1	1.60	0.17	1.35	0.84	0.62
Test Resins	IRA900		2.0	N.D.	2.06	1.73	0.84
Deliberately	A161		2.1	N.D.	1.98	1.74	0.87
Fouled at	Z MPF		2.0	N.D.	2.00	1.75	0.87
Staythorpe							

[*]Combined make-up and CPP mixed beds   N.D. Not determined.

- 167 -

5.6.2 KINETIC DETERIORATION OF IN-SERVICE ANION EXCHANGERS

A number of samples of anion exchangers taken from condensate purification plants have been assessed by chloride and sulphate leakage tests. The anion exchangers were of various ages, from 6 months to 6 years in service and contained varying amounts of extractable organic and iron foulants.

The method used for resin assessment was a modification of that used for the new and deliberately fouled resins, as described in section 5.3.10. The mixed bed volume was reduced from 1200 to 900 ml in order to produce larger leakages that could be more accurately determined and the flow rate was limited to 100 mh^{-1}, typical of modern CPP. New resins were conditioned through the bicarbonate form and used resins were washed with dilute (0.05 M) sodium bicarbonate solution to exhaust them fully prior to regeneration.

Table 5.12 gives a list of used anion exchangers taken from a number of different operating CPP. The table also includes values for a typical new resin at 100 mh^{-1} and the deliberately fouled resins recalculated to 100 mh^{-1} using the $M = KV_L^{\frac{1}{2}}$ relationship. Table 5.13 gives the full mass transfer data for the in-service resins. (19)

Two important conclusions derived from Table 5.12 are :-
i) in the majority of cases there is a much greater deterioration in exchange kinetics with the in-service resins despite the resins having much smaller amounts of extractable organic foulants than the deliberately fouled resins, and
ii) the relative deterioration between chloride and sulphate is much greater for the in-service resins than the deliberately fouled resins and the ratio of sulphate to chloride mass transfer coefficient also varies quite widely.

The influent concentrations used for the in-service fouled resin tests are up to an order of magnitude lower than for new resins, otherwise the poorer kinetics would give rise to very large leakages that were outside the limits of determination by the ion chromatograph used in this work.

There is no apparent correlation between either the amount of
extractable organic foulants, expressed as fulvic acids, or the
amount of extractable iron and the degree of kinetic deterioration.
Neither is there any correlation between kinetic deterioration and
the length of time a resin has been in service. The resin with the
least deterioration (Hinkley Point, B) had been in service over six
years while the resin with the greatest deterioration (Didcot) had
been in service only six months. There can also be quite large
variations between resins taken from the same station but from
different polishing plant mixed beds as shown by the two resins from
Wylfa CPP.

Feedwater monitoring at several of the stations listed in Table 5.10
had shown that sulphate leakage from the CPP was a serious problem.
Anion exchanger kinetic assessment showed that serious deterioration
in sulphate exchange kinetics was the cause. The way in which the
test results can be used to predict mixed bed performance is
discussed in section 5.7.

5.6.3   THE INFLUENCE OF FOULANTS ON EXCHANGE MECHANISMS

The considerable differences in mass transfer coefficients between
deliberately and in-service fouled resins suggests that different
types of foulant, from different sources, may influence the exchange
processes. Identification of individual fouling species was beyond
the scope of this work, but a discussion on the possible effects of
foulants is presented below.

5.6.3.1 Nature of Foulants

The foulants likely to be found on CPP anion exchangers can be
divided into three groups.

The natural decay products of vegetation, humic and fulvic acids,
are found in many surface water supplies and were described in
section 2.8.1.

Secondly, the degradation products of cation exchangers, short chain
aromatic sulphonates, have been recorded as fouling the succeeding

anion exchanger (see section 2.8.1). The manufacturing residues from cation exchangers, noted earlier as a source of anion leakage, are also sulphonated polystyrene entities. These slowly eluted species are a source of potential organic fouling within a mixed bed and anion exchangers exhibit a very high selectivity towards aromatic sulphonates (176).

The third source of foulants for CPP anion exchangers is the boiler and turbine plant itself which can introduce particulate metallic oxides from the various heat exchanger surfaces and lubricating oils from pumps or the turbine into the condensate.

5.6.3.2 Kinetic Mechanisms on Fouled Resins

The large molecules of the organic foulants are unlikely to diffuse very far into the structure of the bead and are more likely to form a layer at the surface that inhibits the exchange process (17). This will even apply to resins with macroporous matrices as there appears to be a skin over the surface of the macroporous structure (A5.1.1)

The organic species may act as a physical barrier to be penetrated or circumvented by the exchanging ions, with larger ions, such as sulphate, finding this more difficult.

The foulants, being large multivalent and acidic, may occupy or hinder access to many exchange groups and a divalent ion, such as sulphate, could find it more difficult to orient itself onto two adjacent and available exchange sites, while monovalent chloride can exchange more easily.

As natural organic foulants are polyvalent acidic species those on the bead surface are likely to have some free acid groups pointing towards the bulk solution. These will, in effect, be carboxylic cation exchange groups which could set up a potential barrier with a negative charge at the bead surface. This would repel approaching anions, the double charged sulphate more than the single charged chloride. Such an effect has been deliberately used to prevent precipitation in cells used for the electrodialysis of sea water (238).

TABLE 5.13 VARIATION OF MASS TRANSFER COEFFICIENT WITH INFLUENT CONCENTRATION FOR IN-SERVICE FOULED RESINS. ($M = 10^{-4}ms^{-1}$)

CPP LOCATION	DIDCOT	FAWLEY	HARTLEPOOL	HINKLEY POINT 'B'	PEMBROKE	VANDELLOS (SPAIN)	WYLFA i	WYLFA ii
ANION EXCHANGER TYPE	AMBERLITE IRA900	DUOLITE A161	AMBERLITE IRA900	DUOLITE A161/MPF	AMBERLITE IRA900	AMBERLITE IRA900	AMBERLITE IRA900	AMBERLITE IRA900
CHLORIDE INFLUENT								
100 ($\mu gkg^{-1}Cl$)	0.82	-	-	-	1.25	0.98	-	1.03
250 " "	1.00	1.44	1.64	-	1.42	1.20	-	1.22
500 " "	1.16	1.57	1.77	1.83	1.55	1.36	1.77	1.35
1000 " "	-	1.69	1.89	1.89	-	-	1.92	-
2000 " "	-	-	-	1.95	-	-	2.02	-
5000 " "	-	-	-	-	-	-	2.12	-
SULPHATE INFLUENT								
135 ($\mu gkg^{-1}SO_4$)	0.26	-	-	-	0.63	0.43	-	0.50
338 " "	0.38	0.92	1.11	-	0.82	0.63	1.24	0.69
676 " "	0.52	1.07	1.26	1.49	0.95	0.78	1.42	0.84
1350 " "	-	1.20	1.42	1.57	-	-	1.53	-
2700 " "	-	-	-	1.65	-	-	-	-
6760 " "	-	-	-	-	-	-	-	-

Coating the anion exchange membrane with a negatively charged
poly-electrolyte produced a system that allowed the preferential
passage of monovalent anions but rejected divalent anions.
Sulphonic acid degradation products from cation exchangers could have
a similar effect if they were polyvalent oligomers or even fine
particulate species.

The pH of the bulk solution may also play a part. Sulphonic acids
are strong acids and would be fully ionised at all pH values likely
to occur in CPP mixed beds, ie pH 6.0 - pH 9.6 . The ionisation of
carboxylic acids will increase as the pH increases and these would
have a larger effect in alkaline conditions eg a mixed bed operating
in the ammonium form. Overall, sulphonic acid species would have a
more significant effect than carboxylic acid species.

The presence of oil on a bead surface is only likely to act as a
physical barrier. The finely divided iron or copper oxides may have
a small negative charge on them, by which they are attracted to the bead
surface. However, it is practice in those plants where oil or oxide
fouling are known to occur to include detergent washes and air scours
in the regeneration procedures to minimise the build up of these
foulants.

5.6.3.3 Influent Concentration Dependance

The calculated mass transfer coefficients, M_{obs}, for the used,
fouled anion exchangers show quite a marked dependance on the influent
concentration (Table 5.13). The value of M_{obs} declined with a
reduction in influent concentration and the rate of decline was
different for chloride and sulphate ions.

If liquid boundary layer diffusion is the rate controlling process
it is assumed that the ions are exchanged at the bead surface faster
than they are transported across the boundary layer. Therefore,
the concentration of exchanging solution phase ions at the bead
surface, C_b, tends to zero. Similarly the flux, J, of exchanging
ions across the boundary layer, defined by

$$J = M (C_o - C_b) \quad \text{tends to} \quad J = MC_o.$$

This is the prevailing situation for new, unfouled exchangers and the

value of M_{obs} equals M_L, the boundary layer mass transfer coefficient.

When a foulant is present on the bead surface it presents a resistance to the transport of ions to the bead surface and a concentration of ions will build up adjacent to the fouling layer. C_b no longer tends to zero and the ionic flux is now $J \propto C_o - C_b$, ie it is reduced. A lower ionic flux will result in an elongation of the exchange zone to a fixed length column and, consequently, a lower mass transfer coefficient than for an unfouled resin.

The mass transfer resistance at the bead surface due to foulants is a fixed quantity and it is likely that as C_o decreases the ratio C_b/C_o increases. Therefore the ionic flux will decline at a faster rate than C_o decreases with the nett result that the calculated mass transfer coefficient decreases with decreasing influent concentration. A single packed bed operation can be considered as a large number of shallow beds, each bed forwarding its leakage as the influent for the next stage. With new resins under boundary layer diffusion control the mass transfer coefficient will be constant at any point down the bed. However, with fouled resins the value of M will be decreasing at each successive stage. The calculated value of M represents an overall value for the particular column depth and influent concentration. Use of this value of M to predict leakages at lower influent concentrations or longer bed depths would lead to errors indicating a better bed performance than would be achieved in practice.

5.6.4 SODIUM ION LEAKAGE

Whilst not strictly influenced by organic fouling the exchange of sodium ions showed interesting trends, that were more apparent when operating with the deliberately fouled anion exchangers.

The sodium ion leakages were independent of flow rate indicating that kinetic leakage was not a significant factor. However, it was noted that sodium ion leakage increased with anion leakage and this was more apparent with the deliberately fouled resins, as the leakages were greater (Tables A5.17, A5.18) than for new resins (Tables A5.11, A5.12).

TABLE 5.14   TYPICAL CPP DESIGN, OPERATING AND RESIN DATA

Bed Diameter: 2.8 m

Resin Ratio: 2 : 1 Cation : Anion Exchanger

Resin Volumes: Anion Exchanger 1.85 m^3

                        Cation Exchanger 3.7 m^3

Bed Depth: 0.9 m

Flow Rate: 0.171 $m^3 s^{-1}$ ($\equiv$ 100 $m^3 m^{-2} h^{-1}$)

Influent Quality

Condensate containing 1000 $\mu g\ kg^{-1}$ NH_3 plus a sea water condenser
leak giving 325 $\mu g\ kg^{-1}$ Na, 500 $\mu g\ kg^{-1}$ Cl and 70 $\mu g\ kg^{-1}$ SO_4

Outlet Water Quality

Less than 2 $\mu g\ kg^{-1}$ each of Na, Cl, SO_4.

Anion Exchanger

Total anion exchange capacity   1000 eq m^{-3}

Regenerated capacity   500 eq m^{-3}

Packed bed voidage ε =   0.35

Cation Exchanger

Total operating capacity to sodium or ammonium break point equals
2500 equivalents. This would give an operating cycle time of
55.7 hours for combined ammonium plus sodium influent.

Cation exchange will also operate under liquid boundary layer
diffusion control, and probably at very similar rates to anion
exchange. However, the larger volume of cation exchanger in the
mixed bed would produce a shorter exchange zone for sodium ions so
that when anion leakage occurs the lower parts of the bed would be
slightly acidic. This would give rise to equilibrium leakage of
sodium left on the partially regenerated cation exchanger in the
lower bed. Larger anion leakages would cause greater acidity hence
a greater sodium ion leakage.

5.7 PLANT PERFORMANCE PREDICTIONS

Besides obtaining a greater understanding of the kinetic mechanisms
involved in mixed bed ion exchange another aim of the work was to be
able to offer constructive advice to plant operators on the ability
of their resins to perform satisfactorily.

Quality and capacity are the two features required from a CPP mixed
bed. The bed must produce water of the required purity and it must
do so for a sufficient period of time that allows an exhausted bed to
be regenerated and returned to service :- a minimum of 12 and
preferably 24 hours. Laboratory column generated mass transfer
coefficients can be used to predict plant performance, during
condenser leaks, albeit idealised, and can provide useful data on
the need for resin replacement. The application of mass transfer
data to plant performance predictions is illustrated by a series of
examples in which the depth of exchange zone required to achieve a
2 ug kg^{-1} leakage is calculated for three anion exchangers of
different diameters and in three stages of fouling. Anion exchangers
only are considered as the cation exchanger rarely gives trouble.

5.7.1 PLANT OPERATING DATA

Table 5.14 lists the design and operating data of the hypothetical
CPP for this example. The design dimensions are typical of a modern
CPP mixed bed operating directly on the condensate. The linear flow
rate is 100 mh^{-1}, the same as the laboratory columns. The influent
contains 1000 μg kg^{-1} NH_3 and there is a sea water condenser leak
giving 500 μg kg^{-1} Cl^- and 70 μg kg^{-1} SO_4^{2-} anion contamination as

TABLE 5.15   VARIATION OF EXCHANGE ZONE AND OPERATING CAPACITY WITH MEAN BEAD DIAMETER FOR NEW AND FOULED RESINS

INFLUENT	CHLORIDE $500 \mu g \ kg^{-1} Cl$			SULPHATE $70 \mu g \ kg^{-1} SO_4$		
MEAN BEAD DIAMETER (mm)	0.60	0.75	0.90	0.60	0.75	0.90
NEW RESIN	$M=2.30 \times 10^{-4} ms^{-1}$			$M=2.10 \times 10^{-4} ms^{-1}$		
Depth of exchange zone (m) to 2 $\mu g \ kg^{-1}$ leakage	0.31	0.39	0.46	0.22	0.27	0.33
Bed depth available as operating capacity (%total bed depth)	66	57	48	76	70	64
Available capacity (eq)	610	530	450	700	645	590
Hours run to 2 $\mu g \ kg^{-1}$ breakthrough	64	56	47	74	68	62
MODERATELY FOULED RESIN	$M=1.75 \times 10^{-4} ms^{-1}$			$M=1.25 \times 10^{-4} ms^{-1}$		
Depth of exchange zone (m) to 2 $\mu g \ kg^{-1}$ leakage	0.40	0.51	0.61	0.37	0.46	0.55
Bed depth available as op. cap. (%total bed depth)	55	44	33	59	49	39
Available capacity (eq)	510	405	300	550	455	365
Hours run to 2$\mu g \ kg^{-1}$ breakthrough	54	43	32	58	48	38
BADLY FOULED RESIN	$M=1.30 \times 10^{-4} ms^{-1}$			$M=0.65 \times 10^{-4} ms^{-1}$		
Depth of exchange zone (m) to 2 $\mu g \ kg^{-1}$ leakage	0.55	0.68	0.82	0.70	0.88	1.05
Bed depth available as op. cap. (%total bed depth)	39	24	9.2	22	2.7	0
Available capacity (eq)	365	225	85	205	25	0
Hours run to 2 $\mu g \ kg^{-1}$ breakthrough	38	24	9.0	21	2.6	0

FIGURE No. 5.08   EXCHANGE ZONE AND WORKING CAPACITY
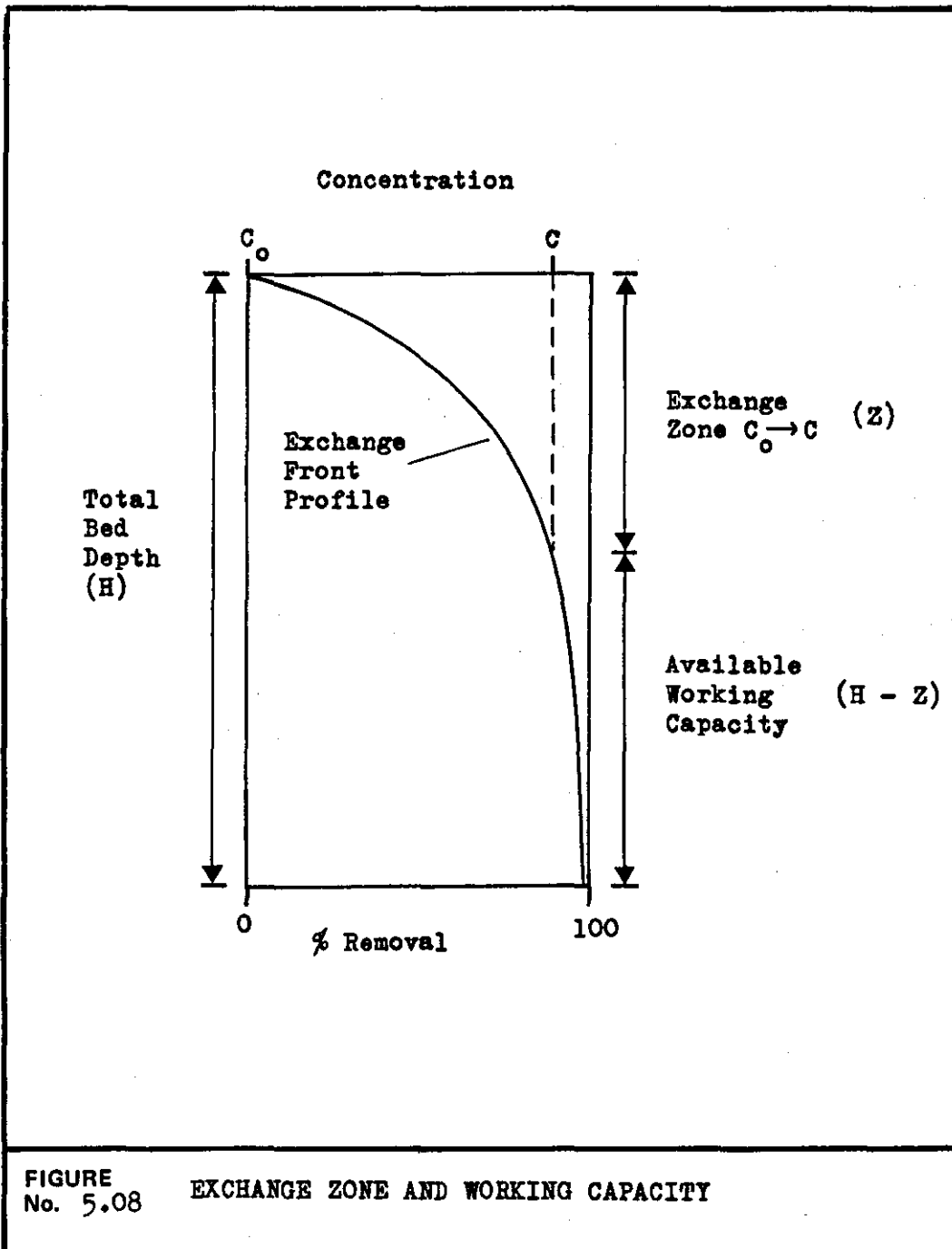
well as 325 μg kg^{-1} Na. It is assumed that the cation exchanger would exhaust after 55.7 hours under these operating conditions.

5.7.2 NEW RESINS

The baseline for any comparison is the performance of the new resins in the plant. Therefore it is necessary to know the actual volumes of resins loaded as well as their mean bead diameter. The latter factor is necessary as it is rarely possible to subsequently obtain a representative sample. As laboratory mass transfer coefficients are independent of bead size corrections for variations in mean bead diameter can easily be made through the mass transfer equation.

The example has been worked for three different mean bead diameters to demonstrate the effect of this parameter. Values of 0.60, 0.75 and 0.90 mm have been used as typical of the range from triple resin bed to 'C' grade resins.

The depths of exchange zone (Z) for a 500 $\longrightarrow$ 2 μg kg^{-1} Cl and a 70 $\longrightarrow$ 2 μg kg^{-1} SO_4 reduction have been calculated for each bead diameter assuming typical new resin mass transfer coefficients of 2.30 x 10^{-4} ms^{-1} for $\overline{OH}$ - Cl and 2.10 x 10^{-4} ms^{-1} for $\overline{OH}$ - SO_4. The results are given in Table 5.15.

The operating capacity and hours run to a 2 μg kg^{-1} breakthrough are calculated as follows. Figure 5.08 depicts the concentration profile down a bed as soon as the influent is admitted. The exchange zone occupies a depth Z of the total bed depth H. Assuming the profile remains stable it will progress through a bed depth (H - Z) before a 2 μg kg^{-1} leakage occurs at the outlet. Therefore the bed depth (H - Z) is the active resin. The volume of anion resin, hence the available capacity in depth (H - Z) can be easily calculated from the data in Table 5.14.

Operating capacity (equivalents) = Regenerated capacity (eq m^{-3}) x volume of anion exchanger in depth H - Z (m^3)

The time to 2 μg kg^{-1} breakthrough can then be calculated from :

Hours to breakthrough

= Op. Cap (eq) $\div$ Flow rate (m^3 h^{-1}) $\div$ Influent anion conc. (eq m^{-3})

Chloride Exchange $500 \rightarrow 2$ µg kg^{-1}Cl   Sulphate Exchange $70 \rightarrow 2$ µg kg^{-1}SO$_4$

$M(Cl) = 2.30 \times 10^{-4}$ms^{-1} NEW RESIN $M(SO_4) = 2.10 \times 10^{-4}$ms^{-1}

$M(Cl) = 1.75 \times 10^{-4}$ms^{-1} MODERATELY FOULED RESIN $M(SO_4) = 1.25 \times 10^{-4}$ms^{-1}

$M(Cl) = 1.30 \times 10^{-4}$ms^{-1} BADLY FOULED RESIN $M(SO_4) = 0.65 \times 10^{-4}$ms^{-1}

FIGURE No. 5.09   DEPTH OF EXCHANGE ZONE FOR CHLORIDE OR SULPHATE EXCHANGE $\rightarrow 2$ µg kg^{-1} NEW AND FOULED RESINS OF DIFFERENT BEAD DIAMETERS. SIMULATED CONDENSER LEAK 500 µg kg^{-1}Cl and 70 µg kg^{-1}SO$_4$.

As chloride and sulphate exchange are occurring simultaneously it
is necessary to use the total $(Cl + SO_4)$ anion concentration when
calculating the time to breakthrough for the individual anions.

From Table 5.15 it can be seen, for new resins, that chloride ion
breakthrough will occur before sulphate, despite the poorer kinetics
of sulphate exchange. This is because the lower sulphate influent
concentration gives a shorter exchange zone. The operating capacity
decreases with increasing bead size but this is only important for
the 0.90 mm resin where anion breakthrough (47 hours) will occur
before cation breakthrough (56 hours). Figure 5.09 depicts the
exchange zones (hatched) and resin available for operational
capacity (clear) for the various conditions and bead diameters.

5.7.3 FOULED RESINS

Two examples of fouled anion exchangers have also been examined. The
moderately fouled case has mass transfer coefficients
$\overline{OH} - Cl = 1.75 \times 10^{-4}$ ms^{-1} and $\overline{OH} - SO_4 = 1.25 \times 10^{-4}$ ms^{-1}. The
chloride exchange zone still exceeds that for sulphate but by a
much smaller margin than for new resins. The operational capacities
have been reduced due to longer exchange zones and anion break-
through occurs first in all instances. The differences between the
large and small diameter resins are becoming more significant.
Whereas with the new exchanger the larger resin had an operating
capacity 26% less than the smaller resin, the difference had increased
to 40% for the moderately fouled resin   (Figure 5.09).

The badly fouled example had mass transfer coefficients
$\overline{OH} - Cl = 1.30 \times 10^{-4}$ ms^{-1} and $\overline{OH} - SO_4 = 0.65 \times 10^{-4}$ ms^{-1}.
Sulphate exchange has now become the controlling factor and there
is no operational capacity with the largest, 0.90 mm diameter, resin
as there is an immediate breakthrough of more than 2 μg kg^{-1} SO$_4$.
The 0.75 mm diameter resin has no effective operating capacity,
lasting only 2.6 hours to exhaustion. The smaller, 0.60 mm, resin
however has an operational capacity lasting for 22 hours which is
very near to the acceptable limit. Note that there is still
significant capacity for chloride ion for the two smaller resins
at sulphate breakthrough (Figure 5.09).

It is clear that while mean bead diameter does not have a very
great influence on new resin performance it becomes more significant
as the exchange kinetics deteriorate. The overall performance of
the smaller resin deteriorates less quickly than that of the larger
resin, demonstrating the advantages of the trend towards smaller
mean size anion exchangers in CPP mixed beds.

5.7.4 FLOW RATE

Laboratory column tests are normally run at a single flow rate,
100 mh^{-1}. If the full scale plant operates at a different flow
rate the mass transfer coefficient is first recalculated for the new
flow rate using the $M = KV_L^{\frac{1}{2}}$ relationship. The process described in
section 5.7.2 for calculating exchange zone and operational
capacities is then repeated with the new mass transfer coefficient.

5.7.5 BED DEPTH

The calculations in sections 5.7.2 and 5.7.3 were based on a 0.9 m
bed depth, the shallowest normally used. An increase in bed depth
obviously increases the operational capacity but the improvements
can be quite substantial where the exchange kinetics show signif-
icant deterioration. For example under the conditions used in 5.7.3
the operational capacity for the 0.75 mm diameter badly fouled resin
in a 0.9 m bed depth is just 2.6 hours but if the bed depth were
increased by 50% to 1.35 m the operational capacity would increase
by an order of magnitude to about 50 hours. Therefore, the deepest
bed commensurate with an acceptable pressure drop is a desirable
design feature.

5.7.6 NON IDEAL FACTORS

The calculations described above assume ideal operation of the mixed
bed; correct resin volumes, thorough mixing, plug flow. In practice
there are preferential flow paths, poor mixing and incorrect resin
volumes. These unknowns cannot be taken into account in a
laboratory simulation test and the calculated values are an indication
of the potential performance of the resin. However, failure to
achieve the performance predicted by laboratory tests may be

indicative of design/operating problems on the plant. It must be remembered however, as noted in section 5.6.3.3 that the reducing mass transfer coefficient with reducing influent concentration on fouled resins may cause the practical bed to exhibit higher leakages and lower operational capacities than those calculated as described in sections 5.7.2 and 5.7.3. Work on the relationship between mass transfer coefficient and influent concentration is continuing.

6   CONCLUSIONS

The work described in the foregoing sections was to investigate various aspects of ion exchange mixed bed design and performance that could influence the purity of water produced. Particular emphasis was placed on water purification for use in high pressure steam raising boilers although the work has relevance to any application of mixed beds for water purification. Advances were made in all three aspects that were studied, resin separation by backwashing, resin mixing by air agitation and anion exchange kinetics. The greater understanding of the mechanisms and processes involved in mixed bed operation has led to new resin bead size specifications, revised design and operating parameters and improvements in fault condition diagnosis and the ability to predict the reduction in water purity as the resins age and deteriorate kinetically.

6.1   RESIN SEPARATION BY BACKWASHING

Complete separation of the anion and cation exchangers in a mixed bed, by backwashing, prior to regeneration is a necessary pre-requisite for the efficient and effective production of ultrapure water. Otherwise, cross contamination by the wrong regenerant may lead to an extended post regeneration rinse and subsequent trace leakage of ionic impurities.

An assessment of existing models for the prediction of the separability of particles of differing size and density were not sufficiently accurate for application to anion and cation exchange resins, which have similar bead size distributions and only slightly different bead densities. A graphical method was developed for predicting resin separability from bead diameter, bead density and a calculated separability parameter. This showed that the fluidised bed bulk density approach from the backwashing of multimedia filters and the single bead terminal velocity approach of the resin manufacturers were not suitable.

A new separability parameter, fluidised bed porosity, was developed on the assumption that there was a progressive increase in fluidised

bed porosity (FBP) up through a fluidised bed of separating resins and that there would be a stepwise increase in FBP across the interface between the separated cation (lower layer) and anion (upper layer) exchangers. The bulk density model was incompatible with the FBP model as it predicted a reduction in fluidised bed porosity across the interface.

The terminal velocity (TV) model and FBP model based on a perfectly classified component resins gave very similar resin separability predictions and both models indicated resin separation to be poorer than was actually achieved either in full scale beds or in laboratory pilot columns. Only the FBP model was able to accomodate variations in backwash flow rate, water temperature and column diameter. Assessment of these variables indicated that under normal operating conditions neither temperature nor flow rate had a significant effect on resin separability. However, resin separation is enhanced in a 25 mm diameter column compared with a 100 mm, but there is no difference between a 100 mm and a 2 m diameter column.

The practically measured separation data also showed that the range of bead diameters found at any point in a backwashed resin bed was greater than expected for perfect classification. This led to the concept of overlapping bulk circulation cells of resins, each cell being characterised by its Sauter mean bead diameter. Practical data indicated each cell to have a maximum to minimum bead diameter ratio of 1.4. Each bulk circulation cell had an average FBP equivalent to its mean bead diameter. Thus two resins would separate when the uppermost cell of cation exchange resins had an FBP just greater than the lowest cell of anion exchange resins. This approach led to separability predictions closer to the practically observed cases and the FBP - bulk circulation model was considered to be a close representation of the mechanisms of resin separation.

To apply any separation model to practical situations it was necessary to know how resin bead density varied with the ionic form of the exchangers. Cation exchangers increase in density with counter cations in the following order $H^+ \sim NH_4^+ < Na^+ < Mg^{2+} < Ca^{2+} < K^+$. Anion exchangers increase in density with counter anion in the order $OH^- < Cl^- < CO_3^{2-} < HSiO_3^- < HCO_3^- < SO_4^{2-}$ although differences in polymer/

matrix type led to some small variations in the centre of the order. Assessment of the various modes of exhaustion of the mixed beds showed that in all cases separation must be assured between the lowest density cation exchanger (H^+ or NH_4^+ form) and the highest density anion exchanger (SO_4^{2-} form) as these are likely to be present in all mixed beds.

Utilising the FBP – bulk circulation model it was predicted that for most likely combinations of polymer/matrix types used in mixed beds the following bead size ranges were necessary to ensure complete separation.

Anion exchanger   0.3 – 1.0 mm

Cation exchanger   0.6 – 1.2 mm

compared with 0.3 – 1.2 mm used previously. Where a high crosslinked, high density anion exchanger was used a smaller anion exchanger (0.3 – 0.8 mm) would be necessary. These bead size specifications are generally satisfied by the triple resin bed exchangers introduced in recent years by most resin manufacturers and, from this work, it is now a standard recommendation to use triple bed grade exchange resins without the intermediate inert resin, in all mixed beds.

A comparison of the separability of various manufacturers triple resin systems indicated that not all were likely to achieve complete three layer separation although in most cases the two exchangers should separate satisfactorily.

The model of resin separability based on the fluidised bed porosity of bulk circulation cells could have applications in other areas of particle separation by fluidisation eg backwashing of multi media filters.

6.2   RESIN MIXING

A second feature of a mixed bed, that ensures its success in producing ultra pure water, is the use of an intimate mixture of anion and cation exchangers. The investigations into resin mixing identified the basic mechanisms of mixing when low pressure compressed air is introduced to the bottom of a resin/water mixture. Resin beads are transported upwards by a bubble transport mechanism

through a resin/water slurry fluidised by the mixing air. Super-
imposed on this is a bulk circulation of resins upwards through the
centre of the bed and downward at the vessel walls. These two
mechanisms combine to progressively intermix the two exchangers.
A minimum time and a minimum air flow necessary to ensure thorough
mixing were identified in previously reported work. The studies
described in this thesis investigated the other main variable in
mixing, the depth of free water above the settled resins prior to
mixing.

Too little water resulted in the lower layers of resin drying out
and mixing becoming very sluggish at the bottom while apparently
mixing well at the top. The nett result was unmixed cation exchanger
at the bottom of the bed. Too much free water gave very fluid and
thorough mixing of the resins but, on cessation of mixing the resins
started to re-separate on settling. Down the bed this gave an
upper layer of anion exchanger progressing into a zone rich in anion
exchanger below this a zone rich in cation exchanger and correctly
mixed resins at the bottom of the bed. The degree of re-separation
increased with the depth of free water prior to mixing. An optimum
condition for free and fluid mixing without significant re-separation
was identified as 50 mm of free water per metre depth of settled
resins.

The knowledge obtained from investigations into the mechanisms of
resin mixing has enabled mixing fault conditions to be identified
from the analysis of vertical resin cores taken from full scale
mixed beds. Remedial action can then be recommended to the plant
operators. Additionally information has been obtained to improve
the design of future mixed bed installations by ensuring the correct
level of free water prior to mixing.

6.3 ANION EXCHANGE KINETICS

The factors influencing anion exchange kinetics in mixed beds, and
their subsequent deterioration in service, is an area that is still
receiving considerable attention particularly from the electric
power utilities. The work described in this thesis was the first
of a new generation of studies on factors affecting mixed bed
performance and anion exchanger fouling.

A mass transfer equation has been developed for use with a laboratory pilot column or full scale mixed bed. A mass transfer coefficient is calculated from the physical dimensions of the bed and its operating parameters, resin bead mean diameter, mixed resin ratio and the   anion leakage from a known influent concentration. The mass transfer coefficient was independent of bead size and was used as a measure of anion exchange kinetics and their variation with flow rate, exchanging counter anion and in service deterioration.

The assessment of six different strong base anion exchangers with different polymer/matrix types, gel and macroporous, styrene and acrylic, indicated that there was no significant difference in kinetics between polymer/matrix types. This is in agreement with the basic assumption of liquid boundary layer diffusion being the major rate controlling step in dilute solutions.

There were small but significant differences between the mass transfer coefficients for chloride exchange and those for sulphate exchange, the latter having the slower exchange rate. The differences in mass transfer coefficients between sulphate and chloride exchange could not be correlated with differences in aqueous diffusion coefficients derived from conductivity data.

Steric hindrance is a factor in the exchange of divalent anions such as sulphate. It is necessary for the divalent anion to orient onto two adjacent and correctly spaced exchange groups. Different divalent anions eg sulphate or hydrogen phosphate would require different spacings and would therefore exhibit differing degrees of steric hindrance. The nature of the counter anion associated with the exchange group may also influence the rate of exchange. Sulphate exchange on a resin regenerated from the bicarbonate form, ie a bulky anion, was marginally slower than on a resin regenerated from the chloride form.

The general relationship that the mass transfer coefficient is proportional to the square root of the superficial linear velocity through the bed was confirmed in this work.

Anion exchangers that had been deliberately fouled by naturally occurring organic matter showed a reduction in anion exchange kinetics. The relative reduction in mass transfer coefficient was greater for sulphate exchange compared with chloride. All six polymer/matrix types tested showed similar trends in kinetic deterioration.

The degree of kinetic deterioration found in the deliberately fouled resins was small compared with the degree of deterioration observed with in-service fouled anion exchangers. The general trend of greater deterioration in sulphate exchange compared with chloride exchange was always apparent but the actual and relative degree of deterioration of either ion varied from one plant to another. There was no apparent correlation between extractable organic foulants or extractable iron foulants and the degree of kinetic deterioration.

Three possible mechanisms to account for the impaired kinetics on fouled resins were proposed. A layer on the bead surface preventing physical access to exchange sites would affect all ions but the smaller monovalent chloride would find it easier to penetrate such a barrier than divalent sulphate. The occupation of individual surface exchange sites by foulants with a very high selectivity would prevent the use of those sites in subsequent exchange. This would affect sulphate exchange more than chloride exchange as it would reduce the availability of pairs of adjacent exchange sites. Thirdly, multivalent anionic foulants, eg fulvic acids or sulphonated polystyrene oligomers, could present negatively charged anionic groups to the solution phase which would induce electrostatic repulsion of the exchanging anions from the bulk solution.

The laboratory derived mass transfer data have been successfully applied to the prediction of full scale plant performance in terms of leakage concentrations or operational capacity by combining the laboratory derived mass transfer coefficient with the plant operating parameters in the mass transfer equation. This has become an established technique within the CEGB.

To obtain the best performance from a mixed bed in terms of minimising anion leakage, particularly as the anion exchange kinetics deteriorate, it is desirable to use an anion exchange resin with as small a mean bead diameter as is compatible with other plant operating constraints, particularly pressure drop.

7 REFERENCES

1 BWETPA Proc Symp The Need for High Purity Water. British Water and Effluent Treatment Plant Association, London 1980.

2 Garnsey R, Combustion, 1980, 52, (2), 36.

2a Proc Symp Water Treatment for Modern Power Plant Boilers, Instn Mech Eng, London, 1985.

3 Firman E C, CEGB Research, 1974, Number 1.

4 Styrikovich M A, Khaibullin I K and Tskhvirashvili D G, Doklady Akademi Nauk SSSR, 1955, 100, (6), 1123.

5 James D W, Nuclear Technology 1981, 55, Number 1, 55.

6 Bignold G J, Garbett K, Garnsey R and Woolsey I S, Proc 2nd Int Conf on Water Chem of Nucl Reactor Systems, British Nuclear Energy Soc, London, 1980.

7 Crow I G, Greene J C, Tyldesley J D and Walker M A, Proc Inst Mech Engrs, 1979, 193, 359.

8 Garnsey R, Proc Conf on Water Chemistry and Corrosion in Steam-Water Loops of Nucl Power Stations, ADERP/EDF, Paris, 1980.

9 Tittle K, Proc 45th Int Water Conf, Engrs Soc W Penn, Pittsburgh,1984.

10 Garnsey R, Nuclear Energy, 1979, 18, 117.

11 Auerswald D C, 4th EPRI Condensate Polishing Workshop, Los Angeles, Dec 1983. Electric Power Research Inst, Pao Alto, California, 1983.

12 EPRI Report NP-2704-SR, Electric Power Research Institute, Pao Alto, California.

13 Tomlinson K, UK/USSR Symposium on the Automatic Chem Control of Water Systems at Fossil Fired and Nucl Power Stations, October 1976, Central Electricity Generating Board, London.

14 Sadler M A and Bates J C, Proc Int Conf on Water Chem of Nucl Reactor Systems, British Nuclear Energy Soc, London 1977.

15 Bates J C and Sadler M A, The Theory and Practice of Ion Exchange, Society Chem Industry, London 1976.

16 Emmett J R, Proc Int Conf on Water Chem of Nucl Reactor Systems, Brit Nucl Energy Soc, London 1977.

17 Tittle K, Proc Amer Power Conf, 1981, 43, 1126.

18 Harries R R and Ray N J, Effluent and Water Treatment J, 1978, 18, 487.

19 Harries R R and Ray N J, Effluent and Water Treatment J, 1984, 24, 131.

20 Helfferich F, Ion Exchange, McGraw Hill, London, 1962.

21 Marinsky J A (Ed), Ion Exchange, Vol 1, Edward Arnold, London, 1966.

22 Paterson R, An Introduction to Ion Exchange, Heyden, London, 1970.

23 Kunin R, Ion Exchange Resins (2nd Edn), Kreiger, New York, 1972.

24 Applebaum S B, Demineralization by Ion Exchange, Academic Press,
    London, 1968.

25 Arden T V, Water Purification by Ion Exchange, Butterworths,
    London, 1968.

26 Thompson H S, J Roy Agr Soc, 1850, 11, 68.

27 Way J, J Roy Agr Soc, 1850, 11, 313.

28 Adams B A and Holmes E L, J Soc Ind Chem, 1935, 54, 1 T

29 D'Alelio G F, US Patent 2,366,007, 1944.

30 McBurney G H, US Patent 2,591,573, 1952.

31 Brit Patent 683,400, 1952.

32 Bauman E C and McKellar R, US Patent 2,614,099, 1952.

33 Gustafson R L and Lirio J A, I and E C Prod Res Dev, 1968, 7, 116.

34 Kunin R, Amber-hi-lites Number 175, Rohm & Haas Co, Philadelphia,1984

35 Kressman T R E, Effluent and Water Treatment J, 1966, 6, 119.

36 Kressman T R E, Ion Exchange in the Process Industries,
    Soc Chem Ind, London, 1969.

37 Roubinek L and Smith D G, The Theory and Practice of Ion Exchange,
    Soc Chem Ind, London 1976.

38 Kunin R, Meitzner E and Bartnick N, J Amer Chem Soc, 1962, 84, 305.

39 Kunin R, Ion Exchange in the Process Industries, Soc Chem Ind,
    London, 1976.

40 .Kun K and Kunin R, J Polymer Sci, Part C, 1967, 1457.

41 Kun K and Kunin R, Polymer Letters 1964, 2, 587.

42 Kun K and Kunin R, J Polymer Sci, Part A1, 1968, 6, 2689.

43 Kunin R and Barrett J, Proc 40th Int Water Conf, Engrs Soc
    W Penn, Pittsburgh, 1979.

44 Segar G A, Effluent and Water Treatment J, 1969, 9, 433.

45 McGarvey F X and Gottlieb M C, Proc 40th Int Water Conf,
    Engrs Soc W Penn, Pittsburgh, 1979.

46 Kunin R, Amber-hi-lite Number 145, Rohm & Haas Co, Philadelphia 1975.

47 Bennett B A, Cloete F L D and Streat M, Ion Exchange in the
    Process Industries, Soc Chem Ind, London 1969.

48 Slater M J, Ion Exchange in the Process Industries, Soc Chem Ind,
    London 1969.

49 Martinola F B, Proc 39th Int Water Conf, Engrs Soc W Penn,
    Pittsburgh, 1978.

50 Martinola F B and Siegers G, Proc 42nd Int Water Conf, Engrs Soc
    W Penn, Pittsburgh, 1981.

51 Emmett J R and Grainger P M, Proc 40th Int Water Conf, Engrs Soc
    W Penn, Pittsburgh 1979.

52 Boyd G E, Schubert J and Adamson A W, J Amer Chem Soc 1947, 69, 2818.

53 Glueckauf E and Kitt G P, Proc Roy Soc, 1955, A228, 322.

54 Gregor H P and Bregman J I, J Colloid Sci, 1951, 6, 323.

55 Glueckauf E, Proc Roy Soc, 1952, A214, 207.

56 Reichenberg D, Ion Exchange (Ed Marinsky) Vol 1, Chapter 7,
    Edward Arnold, London 1966.

57 Diamond R M and Whitney D C, Ion Exchange (Ed Marinsky) Vol 1,
    Chapter 8, Edward Arnold, London 1966.

58 Chu B, Whitney D C and Diamond R M, J Inorg Nucl Chem, 1962, 24, 1405.

59 Christophides C G, J Inst Water Engrs and Sci 1978, 32, 545.

60 Ehrlich F H, Water Services, 1977, 81, 463.

61 Jackson E W and Smith J H, Effluent and Water Treatment J,
    1978, 18, 21.

62 Jackson E W and Smith J H, Effluent and Water Treat J, 1978, 18, 131.

63 Brost H R and Martinola F, VGB Kraftwerkstechnik, 1980, 60, 53.

64 Moore W H, Physical Chemistry (4th Edn) Longmans, London, 1963.

65 Robinson R A and Stokes R H, Electrolyte Solutions, Butterworths,
    London, 1968.

66 Gilliland E R and Baddour R F, Ind Eng Chem, 1953, 45, 330.

67 Glueckauf E, Ion Exchange and its Applications, Soc Chem Ind,
    London, 1955.

68 Slater M J, Hydrometallurgy, 1979, 4, 299.

69 Boyd G E and Soldano B A, J Amer Chem Soc, 1954, 75, 6091.

70 Eliasek J and Talasek V, Collect Czech Chem Commun, 1968, 33, 3866.

71 Liberti L, Boari G and Passino R, Desalination 1978, 26, 181.

72 Kressman T R E and Kitchener J A, Disc Farad Soc, 1949, Number 7, 90.

73 Soldano B A and Boyd G E, J Amer Chem Soc, 1954, 75, 6099.

74 Boyd G E, Adamson A W and Myers L S, J Amer Chem Soc, 1947, 69, 2836.

75 Michaels A S, Ind Eng Chem, 1952, 44, 1922.

76 Moison R L and O'Hearn H A, Chem Eng Prog Symp Ser 1959, 55,(24),71.

77 Lapidus L and Rosen J B, Chem Eng Prog Symp Ser 1954, 50, (14),97.

78 Carberry J J, A I Chem E J, 1960, 6, 460.

79 Cooney D O and Lightfoot E N, Ind Eng Chem Fundamentals 1965,4,233.

80 Bunzl K, Israel J Chem, 1973, 11, 1.

81 Van Brocklin L P and David M M, A I Chem E Symp Ser 1975,71,(152),191.

82   Bradley W C and Sweed N H, A I Chem E Symp Ser, 1975,71,(152),59.

83   Gregory J, The Theory and Practice of Ion Exchange, Soc Chem Ind, London 1976.

84   Schmuckler G, Nativ M and Goldstein S, The Theory and Practice of Ion Exchange, Soc Chem Ind, London 1976.

85   Liberti L and Passino R, J Chromatography 1974, 102, 155.

86   Beyer W A and James D B, Ind Eng Chem Fundamentals 1966, 5, 433.

87   Scott R A F, Effluent and Water Treatment J, 1981, 21, 113 & 175.

88   Pemberton R T, Walter A J R and Holmes E L, Brit Pat 553,233, 1943.

89   Martin D, The Industrial Chemist 1952, 28, 448.

90   Kunin R and McGarvey F X, US Pat 2,578,937, 1951.

91   Kunin R and McGarvey F X, US Pat 2,692,244, 1954.

92   Thompson J and Reents A C, Proc Amer Power Conf, 1959, 21, 699.

93   Calise V J, Combustion, 1958, 29, (9), 40.

94   Frankenburg T T, Lloyd A G and Morris E B, Proc Amer Power Conf, 1959, 21,

95   Klein H A, Kurpen J J and Schuetzenduebel W G, Proc Amer Power Conf, 1965, 27, 756.

96   Brown J, Ray N J, Harries R R and Reeve E, Proc 8th Int Conf on Properties of Water and Steam, Giens (Fr) Sept 1974. Pub Ed Eur Therm et Ind, Paris, 1974.

97   Frazer H W, Proc 22nd Int Water Conf, Engrs Soc W Penn,Pittsburgh 1961

98   Frazer H W and Young J M, Proc Amer Power Conf, 1963, 25, 647.

99   Flynn G and Salem E, US Patent 4,065,388.

100 Crits G J, Combustion 1974, 45, (12), 33.

101 White J V and Crits G J, Proc Amer Power Conf, 1970, 32, 771.

102 Blight F C and Jackson E W, Filtration and Separation 1971,8,767.

103 Pocock F J and Stewart J F, Proc Amer Power Conf, 1964, 26, 735.

104 Harries R R and Ray N J, UK/USSR Symposium on the Automatic Chem Control of Water Systems in Fossil Fired and Nucl Power Stations, October 1976, Central Electricity Generating Board, 1976.

105 Effertz P H and Resch G, Proc 39th Int Water Conf, Engrs Soc W Penn, Pittsburgh 1978.

106 Bohnsack G, Combustion 1976, 48, (5), 34.

107 Brush E G and Pearl W L, Proc Amer Power Conf, 1970, 32, 751.

108 Asay R H, Report NEDO 21327 General Electric Co, 1976.

109   Wirth L F, Combustion, 1973, 44, (7), 31.

110 Wirth L F, Combustion 1981, 52, (7), 33.

111 Salem E, Proc Amer Power Conf, 1969, 31, 669.

112 Abrams I M, Proc 37th Int Water Conf, Engrs Soc W Penn,Pittsburgh,197

113 Kennedy C M, Meyers P S and Crits G J, Proc 28th Int Water Conf,
Engrs Soc W Penn, Pittsburgh, 1967.

114 Bates J C and Johnson T D, Ion Exchange Technology (Ed Naden and
Streat), Ellis Horwood, Chichester, 1984.

115 Ball M, Jenkins M A and Burrows R J, Ion Exchange Technology
(Ed Naden and Streat), Ellis Horwood, Chichester, 1984.

116 Decareaux C, Power, 1976, 120, (5), 52.

117 Dwyer R E, Zoppoli I E, Crits C J and Tamaki D T, Proc Amer
Power Conf, 1976, 38, 940.

118 Venderbosch H W, Overman L J and Snel A, Proc Conf Chemie und
Kraftwerk, VGB, Essen, 1977.

119 Solt G S and Spillan D M, A I Chem E - Inst Chem E, Symp Ser
Number 9, Inst Chem Engrs, London, 1965.

120 Down P and Salem E, Theory and Practice of Ion Exchange,
Soc Chem Ind, London, 1976.

121 Vincent R, Ion Exchange in the Process Industries, Soc Chem Ind,
London, 1970.

122 Ryan L F, Proc Amer Power Conf, 1973, 35, 864.

123 Rootham M W and Philippe R, Proc Int Conf on Water Chem of Nucl
Reactor Systems, Brit Nucl Energy Soc, London, 1977.

124 Seto I, EPRI Condensate Polishing Workshop, Phoenix, Arizona, 1978.
Electric Power Research Institute, Pao Alto, California.

125 Prokhorow F G, Energiya, Chapter 2, 12-33, Moscow 1975.

126 Hall G R, Klaschka J T, Nellestyn A and Streat M, Ion Exchange
in the Process Industries, Soc Chem Ind, London, 1970.

127 Gruel G, Flunkert F, Schiffers A and Schluck K, Energie, 1977,
29, 286.

128 Grunschlager E and Burgmann F, VGB Kraftwerkstechnik 1978,58,232.

129 Lannin T E, Power Engineering, 1975, 79, 52.

130 Sadler M A, O'Sullivan D J, Bates J C and Costello M E,
Proc Amer Power Conf, 1983, 45,

131 Coburn A E, US Pat 3,527,718, 1970.

132 Wieland G, German Offen 2,631,414, 1978.

133 Crits G J and Zahn W H, US Pat 3,385,787, 1968.

134 Calmon C, US Patent 3,501,401, 1970.

135 McMullen J F, US Patent 2,666,741, 1954

136 Sadler M A, Bates J C, Gardner D J and Thomas A D, Nucl Energy,
1979, 18, 389.

137 Wolff J J and Abrams I M, Proc 40th Int Water Conf, Engrs Soc
     W Penn, Pittsburgh, 1979.

138 Rootham M W and Philippe R, Conf on Water Chem and Corr in Steam
     Water Loops of Nucl Power Stations ADERP - Electricité de France,
     Paris, 1980.

139 Smith J H and Peploe T A, Proc Int Conf on Water Chem of Nucl
     Reactor Systems, Brit Nucl Energy Soc, London, 1980.

140 Harries R R and Ray N J, VGB Kraftwerkstechnik, 1980, 60, 718.

141 Midgley D and Torrance K, Potentiometric Water Analysis, Wiley,
     London 1978.

142 Tomlinson K and Torrance K, Brit Pat 1,497,669.

143 Dimmock N A, Garbett K and Goodfellow G J, Power Industry
     Research, 1981, 1, 307.

144 Small H, Stevens T S and Bauman W C, Anal Chem 1975, 47, 1801.

145 Auerswald D C, Cutler F M, Simmons S S and Houts J J, EPRI Research
     Project 1408 - 3 Final Report, Electric Power Res Inst, Pao Alto,
     California, 1984.

146 Thompson J, McGarvey F X, Wantz J F, Alling S F, Gilwood M E and
     Babbs R E, Chem Eng Prog, 1953, 44, 437.

148 Tittle K, Tyldesley J D, Tasker P W and Butcher C J, Proc 2nd
     Int Conf on Water Chem of Nucl Reactor Systems, British Nucl
     Energy Soc, London, 1980.

149 Sawochka S G and Pearl W L, Proc 44th Int Water Conf, Engrs Soc
     W Penn, Pittsburgh, 1983.

150 Sadler M A and Bates J C, Proc EPRI Condensate Polishing Workshop
     Miami Florida, Dec 1981, Electric Power Res Inst, Pao Alto,
     California, 1981.

151 Cadell J R and Moison R L, Chem Eng Prog Symp Ser, 1954, 50, (14),1.

152 Dick I B and Silliman P L, Proc 19th Int Water Conf, Engrs Soc
     W Penn, Pittsburgh, 1958.

153 Dickinson B N, Abrams I M and Benezra L, Ind Eng Chem,
     1959, 51, 1051.

154 Kunin R, Amberhi-lites Number 149, Rohm & Haas Co, Philadelphia 1975.

155 Wirth L F, Combustion 1975, 47, (5), 8.

156 Baumann E W, J Chem Eng Data, 1960, 5, 376.

157 McGarvey F X, Effluent and Water Treat J, 1966, 6, 421.

158 Ray N J, Ball M and Coates A, Proc 42nd Int Water Conf, Engrs Soc
     W Penn, Pittsburgh 1981.

159 Emmett J R and Hebbs A, Proc 44th Int Water Conf, Engrs Soc W Penn, Pittsburgh, 1983.

160 McNulty J T, Ion Exchange Technology, (Ed Naden and Streat), Ellis Horwood, Chichester, 1984.

161 Frisch N W and Kunin R, A I Chem E J, 1960, 6, 640.

162 McGarvey F X and Reents A C, Power, 1954, 98, (7), 76.

163 Frisch N, McGarvey F X, Kunin R and Moffet J, Proc 16th Int Water Conf, Engrs Soc W Penn, Pittsburgh, 1955.

164 Overman L J and Venderbosch H W, VGB Kraftwerkstechnik, 1981, 61, 62

165 Davies V R, Combustion, 1979, 51, (2), 24.

166 Tilsley G, Chemistry and Industry 1979, Number 5, 142.

167 Seidl J, Ion Exchange in the Process Industries, Soc Chem Ind, London, 1970.

168 Black A P and Christman R F, J Amer Waterworks Assoc, 1963, 55, 897.

169 Croll B T, Water Treatment Exam, 1972, 21, 213.

170 Parsons J W, Kibblewhite M G, Sithole B B and Voice E H, Proc 2nd Int Conf on Water Chem of Nucl Reactor Systems, British Nucl Energy Soc, London, 1980.

171 Black A P and Christman R F, J Amer Waterworks Assoc, 1963, 55, 753.

172 Packham R F, Water Treatment Exam, 1964, 13, 316.

173 Melhuish K R and Wallace D M, Proc 2nd Int Conf on Water Chem of Nucl Reactor Systems, British Nucl Energy Soc, London, 1980.

174 Wirth L F, Feldt C A and Odland K, Ind Eng Chem, 1961, 53, 638.

175 Reents A C, Heidhorn R F and Thompson J, Abstracts of Papers of 136th Mtg of Amer Chem Soc, 1959.

176 Semmen M J, A I Chem E Symp Ser 1975, 71, Number 152.

177 Duolite Ion Exchange Manual - Diamond Shamrock Chemical Co, 1969.

178 Gregory J and Semmens M J, J Chem Soc, 1972, 68, 1045.

178a Semmens M and Gregory J, Environ Sci and Technol 1974, 8, 834.

179 Gustafson R L, Albright R L, Heisler J, Lirio J A and Reid O T, Ind Eng Chem, Prod Res Dev, 1968, 7, (2), 107.

180 Baker B, Davies V R and Yarnell P A, Proc 38th Int Water Conf, Engrs Soc W Penn, Pittsburgh, 1977.

181 Herz G P, Tech Ubervachung, 1962, 3, 77.

182 Martinola F B, VGB Kraftwerkstechnik, 1975, 55, 40.

183 Frisch N W and Kunin R, J Amer Waterworks Assoc, 1960, 52, 875.

184 Ungar J, Effluent and Water Treat J, 1962, 2, 331.

185 Wall K H and Wakelin L P, J Appl Chem and Biotechnol, 1971, 21, (1), 1

186 Arden T V, A I Chem E - I Chem E, Symp Ser 1965, Number 9, 18.

187 Wolff J J, Proc 30th Int Water Conf, Engrs Soc W Penn, Pittsburgh, 1969.

188 Dowex Tech Bulletin 177-1372-84R (Monosphere TG) Dow Chemical Co, Midland, Michigan, 1984.

189 Abrams I M, de Dardel F, Grantham J G and Médète A, Duolite Triobed Bulletin PWT 8202 A - Duolite International SA, London 1982

190 Wolff J J, Paper presented at Duolite Symposium on Ion Exchange, Nottingham 1980. Duolite International, London.

191 Allen H S, Phil Mag, 1900, $\underline{1}$, 323.

193 Richardson J F and Zaki W N, Trans Instn Chem Engrs, 1954, $\underline{32}$, 35.

194 Carlos C R and Richardson J F, Chem Eng Sci, 1968, $\underline{23}$, 813 and 825.

195 Latif B A J and Richardson J F, Chem Eng Sci, 1972, $\underline{27}$, 1933.

196 Happel J and Brenner H, A I Chem E J, 1957, $\underline{3}$, 506.

197 Kennedy S C and Bretton R H, A I Chem E J, 1966, $\underline{12}$, 24.

198 Wen C Y and Yu Y H, Chem Eng Prog Symp Ser, 1966, $\underline{62}$, Number 62, 100

199 Hoffman R, Lapidus L and Elgin J C, A I Chem E J, 1960, $\underline{6}$, 321.

200 Finklestein E, Letan R and Elgin J C, A I Chem E J, 1971, $\underline{17}$, 867.

201 Al-Dibouni M R and Garside J, Trans I Chem E, 1978, $\underline{57}$, 94.

202 Scarlett B, Blogg M J and Freshwater D C, Rheologica Acta, 1965, $\underline{4}$, 197.

203 Scarlett B and Blogg M J, (Ed A Drinkenberg) Proc Int Symp on Fluidisation, Eindhoven, June 1967.

204 Camp T R, Graber D and Conklin G F, Proc Amer Soc Civil Engr, J Sanit Eng Div, 1971, $\underline{97}$, 903.

205 Cleasby J L and Woods C F, J Amer Waterworks Assoc, 1975, $\underline{67}$, 197.

206 Le Clair B P, M App Sc Thesis, Univ Brit Columbia, 1964.

207 Pruden B and Epstein N, Chem Eng Sci, 1964, $\underline{14}$, 696.

208 Pruden B, M App Sc Thesis, Univ Brit Columbia, 1964.

209 Perry's Chemical Engineers Handbook (6th Edn), McGraw-Hill, New York, 1984.

210 Heywood H, J Imperial Coll Chem Eng Soc, 1948, $\underline{4}$, 17.

211 Harries R R, Ball M and Ray N J, CEGB Internal Report SSD/MID/M35/78 Central Electricity Generating Board, 1978.

212 Eherts R F, Proc 41st Int Water Conf, Engrs Soc W Penn, Pittsburgh, 1980.

213 Sears F, EPRI Condensate Polishing Workshop, Miami Dec 1981, Electric Power Research Institute, Pao Alto, California, 1981

214 Fischer S and Otten G, Proc 44th Int Water Conf, Engrs Soc W Penn, Pittsburgh, 1983.

215   Pepper K W, Reichenberg D and Hale D K, J Chem Soc, 1952, 3129.

216   Kraus K A and Moore G E, J Amer Chem Soc, 1953, 75, 1457.

217   Attridge C J and Millar J R, J Chem Soc, 1964, 6053.

218   U S Patent, 4,444,961, 1984.

219   Mishenin Y E, Teploenergetika, 1971, 18, 20.

220   Smith T N, Trans Inst Chem Engrs, 1966, 44, T153.

221   Richardson J F and Meikle R A, Trans Inst Chem Engrs,1961,39,348.

222   Rowe P N and Partridge B A, The Interaction between Fluids and
      Particles, 3rd Congress of European Fed of Chem Eng (1962)
      Inst Chem Engrs, London, 1963. (pp 135 - 142).

223   Murray J P, Chem Eng Prog Symp Ser, 1966, 62,(Number 62), 71.

224   Reuter H, Chem Eng Prog Symp Ser, 1966, 62, (Number 62), 92.

225   Ostergaard K, A I Chem E Symp Ser, 1973, 69, (Number 128), 28.

226   Handley D, Doraisamy A, Butcher K L and Franklin N L, Trans Inst
      Chem Engrs, 1966, 44, T260.

227   Kunin R, Amber-hi-lites Number 154,Rohm & Haas Co, Philadelphia
      1977.

228   McNulty J T and Bevan C A, Proc 43rd Int Water Conf, Engrs Soc
      W Penn, Pittsburgh, 1982.

229   Wilson A L, CEGB Internal Report RD/L/R 794. Central
      Electricity Generating Board, 1958.

230   UK Patent 932,243, 1958

231   Ball M, Harries R R and Ray N J, CEGB Internal Report
      SSD/MID/R23/79, Central Electricity Generating Board, 1979.

232   Duolite Technical Bulletin 7800 3A, Duolite International,
      Vitry, France, 1978.

233   Dowex Technical Bulletin 177-1369-83, Dow Chemical Co, Midland,
      Michigan, 1983.

234   Leva M, Fluidization (Chap 3), McGraw-Hill, New York, 1959.

235   Lange's Hand Book of Chemistry, 12th Edn (Ed Dean), McGraw-Hill
      1979.

236   Snowdon C B and Turner J C R, Int Symp on Fluidisation (Paper 7.2)
      Eindhoven, 1968.

236a Harries R R, Paper 3.01 5th EPRI Condensate Polishing Workshop,
      Richmond Va (1985), Electric Power Research Inst, Pao Alto,
      California, 1985.

237   Clifford D and Weber M, Reactive Polymers, 1983, 1, 77.

238   Seko M, Miyauchi H and Imure I, Ion Exchange Membranes (Ed Flett)
      Ellis Horwood, Chichester.

239 Goodfellow G I, Midgley D and Webber H M, CEGB Internal Report
    RD/L/N108/76. Central Electricity Generating Board, 1976

240 Wilson A L, J Appl Chem, 1959, $\underline{9}$, 501.

241 Harries R R and Ray N J, CEGB Internal Report MID/SSD/81/0032/N,
    Central Electricity Generating Board, 1981.

242 Sadler M A, EPRI Condensate Polishing Workshop, Phoenix, Arizona,
    December 1978. Electric Power Research Institute, Pao Alto,
    California 1979.

APPENDIX – ABBREVIATIONS AND SYMBOLS

ABBREVIATIONS – Used throughout text

ABS	Acrylonitrilebutadienestyrene copolymer
AGR	Advanced Gas Cooled Reactor
BD	Bulk Density
BSP	British Standard Pipe
BWR	Boiling Water Reactor
CEGB	Central Electricity Generating Board
CPP	Condensate Purification Plant
DVB	Divinyl Benzene
FBP	Fluidised Bed Porosity
HPIC	High Pressure Ion Chromatography
KIM	Kent Industrial Measurements Ltd
M	Molarity of electrolyte solution
MB	Methylene Bridge (cross linking)
MW	Megawatt
PA	Polyacrylic, Polyacrylamide
PS	Polystyrene
TOC	Total Organic Carbon
TV	Terminal Velocity
UV	Ultra Violet

SYMBOLS – Chapter 2

$[A]$	Concentration of A etc in aqueous phase
$[\bar{A}]$	Concentration of A etc in exchanger phase
$C_{A,B}$	Concentration of A,B in solution
$D_{A,B}$	Aqueous diffusion coefficient (diffusivity) of A,B etc
F	Faraday constant
$J_{A,B}$	Ionic flux of species A,B etc
K_A^B	Equilibrium selectivity coefficient for B relative to A
R	Universal gas constant
T	Temperature
$Z_{A,B}$	Ionic charge of species A,B etc
$\lambda_{A,B}$	Equivalent ionic conductance of ion A,B etc
τ	Liquid boundary layer film thickness

SYMBOLS - Chapter 3

B	Fluidised bed bulk density (BD)
B_{A-max}	BD of maximum diameter anion exchange resin
B_{C-min}	BD of minimum diameter cation exchange resin
C_D	Drag coefficient
d	Resin bead diameter
d_{A-max}	Bead diameter of largest anion exchange resin
d_{A-mean}	Mean bead diameter of anion exchange resin
d_{C-mean}	Mean bead diameter of cation exchange resin
d_{C-min}	Bead diameter of smallest cation exchange resin
D_V	Fluidisation or backwash vessel/column diameter
$E_{A,C}$	Fluidised bed porosity for anion, cation exchange resin
g	Gravitational acceleration
M_v	Moisture content of resin - volume fraction
M_w	Moisture content of resin - weight fraction
n	Exponent in Richardson & Zaki equation
$P_{A,C}$	Separability parameter for anion, cation exchange resin
P_{A-max}	Separability parameter for largest diameter anion exchange resin
P_{C-min}	Separability parameter for smallest diameter cation exchange resin
Re	Reynolds number
Re_o	Reynolds number at resin bead terminal velocity
T	Temperature
V_f	Superficial backwash/fluidisation flow rate
V_i	Fluidisation velocity at infinite dilution of particles
V_{int}	Interstitial fluid velocity
V_o	Terminal velocity
$V_{o-A-max}$	Terminal velocity of largest diameter anion exchange resin
$V_{o\ C-min}$	Terminal velocity of smallest diameter cation exchange resin
$\delta_{A,C}$	Resin bead density of anion, cation exchanger
η	Backwash/fluidisation water viscosity
ρ	Backwash/fluidisation water density
ψ	Skeletal density of resin bead

SYMBOLS - Chapter 4

E_D	Voidage factor for resin bead/water dispersion
E_S	Voidage factor for settled resin
$f(E)$	Particle concentration factor
$V_{o(A),(C)}$	Terminal velocity of anion, cation exchange resin beads

$V_{sed(A),(C)}$	Sedimentation velocity of anion, cation exchange resin
$\delta_{A,C}$	Resin bead density for anion, cation exchanger
ρ	Density of water
ρ_D	Density of resin/water dispersion

SYMBOLS - Chapter 5

A	Cross sectional area of mixed bed column/vessel
C	Ionic concentration in aqueous phase after ion exchange
C_b	Ionic concentration at bead surface
C_o	Ionic concentration in bulk feed to mixed bed
d	Bead diameter
d_i	Mean bead diameter of size fraction
d_s	Harmonic (or Sauter) mean diameter
D	Diffusion coefficient (diffusivity)
D_i	Ionic diffusion coefficient
D_m	Molecular diffusion coefficient
H	Total bed depth of service mixed bed
J	Ionic flux across boundary layer
k	First order reaction rate constant
K	Corelation factor between linear flow rate and mass transfer
L	Bulk settled volume of mixed bed resin
M	Mass transfer coefficient
M_L	Mass transfer coefficient across liquid boundary layer
M_{obs}	Observed, measured mass transfer coefficient
q	Constant in general rate equation
R	Volume fraction of one resin in mixed bed
Re	Reynolds number
S	Resin bead surface area per unit settled volume of resin
S'	Resin bead surface area per unit mass mixed resin
S_c	Schmidt Number
T	Temperature
V	Volumetric flow rate
V'	Fluid mass flow rate
V_L	Superficial linear flow rate
x_i	Volume fraction of beads of mean diameter d_i
Z	Depth of exchange zone
β'	Bulk density of moist mixed bed resin
ϵ	Settled bed porosity (voidage) factor

η — Fluid viscosity

λ^o — Equivalent ionic conductance at infinite dilution

ρ — Fluid density

τ — Liquid boundary layer thickness

Ω — Resistance, ohms

A P P E N D I C E S   T O   C H A P T E R   3

A3.1   BEAD SIZE GRADING BY WET SIEVING

A3.2   RESIN MIXTURE ANALYSIS

A3.3   PILOT COLUMN TRIALS - RESIN SEPARATION BY BACKWASHING

        A3.3.1   TEST COLUMN CONSTRUCTION
        A3.3.2   TEST RIG ARRANGEMENT
        A3.3.3   TEST PROCEDURE
        A3.3.4   RESIN MIXTURES: TESTS 1 - 3

A3.4   MEASUREMENT OF BEAD DENSITY, SKELETAL DENSITY AND MOISTURE
        CONTENT

        A3.4.1   RESIN CONDITIONING
        A3.4.2   BEAD VOLUME, BEAD WEIGHT, BEAD MOISTURE
        A3.4.3   SPECIFIC GRAVITY MEASUREMENTS

A3.5   BEAD SIZE GRADING - PARTICLE SIZE ANALYSER

DATA TABLES

A3.01   REYNOLDS NUMBER AT BEAD TERMINAL VELOCITY
A3.02   RESIN BEAD TERMINAL VELOCITIES
A3.03   FLUIDISED BED POROSITIES (8 m h^{-1}, 20 ^{o}C)
A3.04   FLUIDISED BED POROSITIES (12 m h^{-1}, 20 ^{o}C)
A3.05   FLUIDISED BED POROSITIES (5, 20, 40 ^{o}C)
A3.06   BEAD SIZE DISTRIBUTIONS OF SEPARATION TRIAL RESINS
A3.07   BEAD SIZE ANALYSIS - WALSALL MIXED BED SAMPLE CORE
A3.08   BEAD SIZE ANALYSIS - LABORATORY COLUMN TEST 1
A3.09   BEAD SIZE ANALYSIS - LABORATORY COLUMN TEST 2
A3.10   BEAD SIZE ANALYSIS - LABORATORY COLUMN TEST 3
A3.11   BEAD DENSITY ETC. STANDARD DEVIATION

A 3.1   BEAD SIZE GRADING BY WET SIEVING

The grading of ion exchange resins by wet sieving requires a series
of stainless steel bodied sieves, 100 mm diameter with stainless
steel meshes to British Standard 410. The mesh apertures of the
sieves were 1.4, 1.19, 1.0, 0.85, 0.71, 0.60, 0.50, 0.425, 0.30 and
0.125 mm. The sieves were arranged in a stack with the largest
aperture sieve at the top and progressively diminishing mesh size.
The base of each sieve fitted inside the body of the one below.

About 20 millilitres (ml) of resin were placed on the upper sieve
and deionised water from a wash bottle was used to wash the resin
through the mesh. Any resin retained on the sieve or in the meshes
was collected by removing the sieve from the stack and inverting it
over a fine mesh (125 µm) sieve. With the aid of coarse bristled
brush the resin was removed from the mesh and washed onto the fine
mesh sieve. The test sieve was returned to the stack and the collected
resin was led through for a second time to ensure all beads that
should pass through did so. It is possible to get two small beads
lodged in a large aperture. The retained resin was collected again
and stored in a 10 ml or 25 ml graduated glass measuring cylinder.
The process of double sieving and collecting the retained resins was
carried out for each successive sieve down the stack. In certain
instances a large percentage of the sample would be collected between
two mesh sizes. In this case the retained sample was divided into
smaller lots, each sieved separately.

At the end of sieving a number of measuring cylinders contained resin
beads of different size fractions. Each cylinder was gently tapped
and the volume of settled resin, including interstices, read off
against the graduations. This is known as tapped and settled volume.
Each bead size fraction was expressed as eg + 0.85 - 1.0 mm, the
volume of resin that passed through the 1.0 mm mesh sieve but was
held on the 0.85 mm mesh sieve. The volumes of each fraction were
totalled and the settled volume percentage of each fraction calculated.
It is the latter value that has been recorded.

The Sauter, or surface area, mean bead diameter (d_s) could be

calculated from the expression

$$d_s = 1 \bigg/ \sum \frac{x_i}{d_i}$$

where x_i is the volume fraction of beads with mean diameter d_i. The value of d_i was taken as the arithmetic mean of the upper and lower limits of each bead size fraction.

A 3.2 RESIN MIXTURE ANALYSIS

To estimate the effectiveness of mixing and degree of reseparation it was necessary to separate each of the sieve fractions into anion and cation exchangers and inert resin and then measure the settled volume of each resin. For small volumes of resin as in the sample cores the simplest method was to add the resins to a solution of saturated sodium chloride (brine). At room temperature (20 $^{\circ}$C) a 26% solution of sodium chloride has a density of 1200 kg m^{-3} whereas the anion exchanger (Cl$^-$ form) is about 1070 - 1110 kg m^{-3} and the cation exchanger (Na form) has a density of 1250 - 1300 kg m^{-3}. Therefore the anion exchanger floats on the surface of the brine while the cation exchanger sinks. In practice some brine solution enters the resin matrices and increases their density so that it is necessary to use saturated brine ($\sim$35% NaCl solution density 1198 kg m^{-3} at 20 $^{\circ}$C) to achieve separation.

The samples of resin from the sieve fractions were placed in a 100 ml measuring cylinder, water added to 100 ml and sodium chloride added until residual solute remained after shaking. The anion exchanger rose to form a layer at the surface while the cation exchanger remained mixed with the excess salt at the base of the cylinder. Gentle swirling ensured all the anion exchanger was released.

The anion exchanger was decanted into a 100 mm diameter stainless steel sieve, mesh size 125 μm, and washed with deionised water to remove excess salt. (It is a common feature of ion exchange resins that they shrink slightly in concentrated electrolyte solutions).
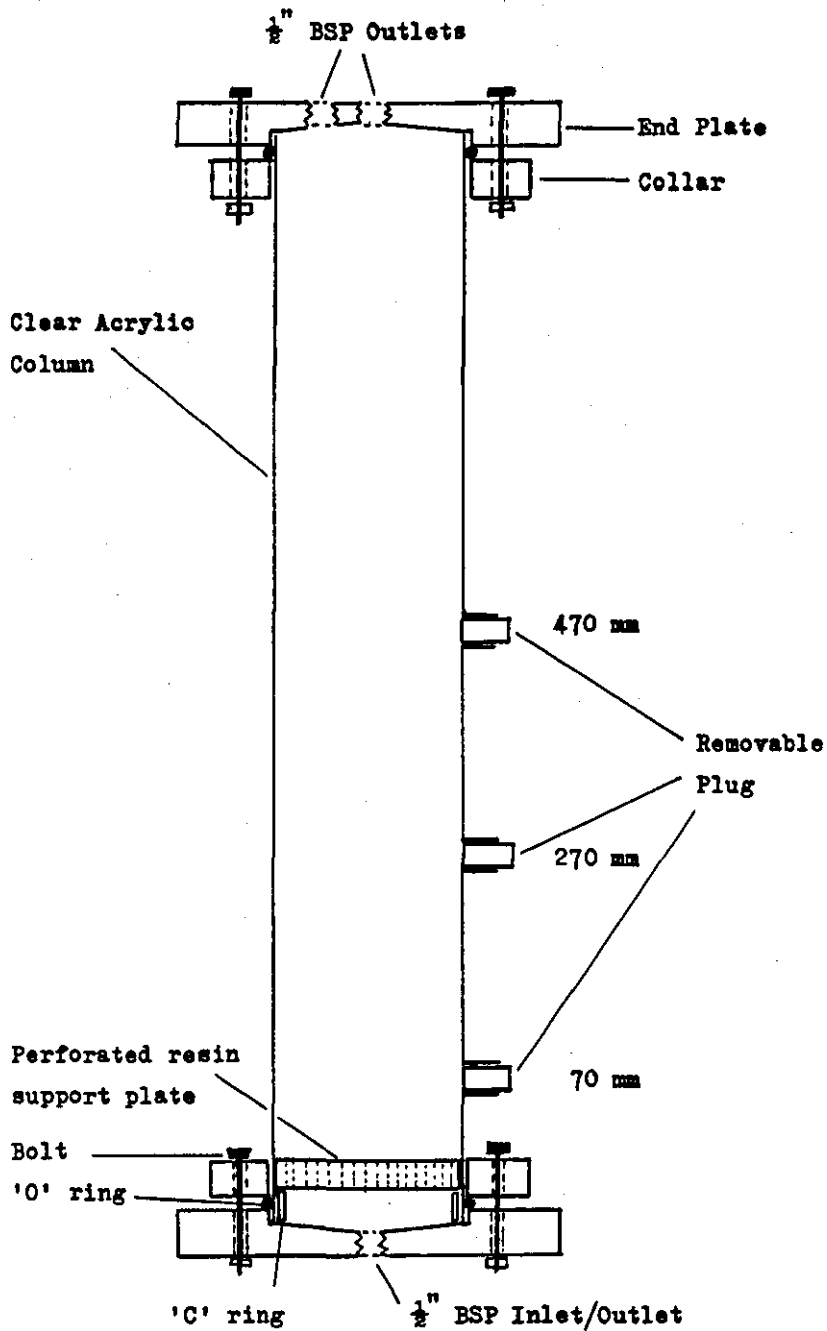
The rinsed resin was then washed into a smaller graduated measuring cylinder, 10 ml capacity for small volumes of resin or 25 ml capacity for larger volumes, the cylinder was tapped to settle resin and the volume of settled resin noted.

The cation exchanger plus excess salt was also poured onto a 125 µm mesh sieve, the residual salt washed away and the resin rinsed. The settled volume of cation exchanger was similarly measured and noted. The total volume of resin in the sample core and, hence, the percentage of anion and cation exchanger were calculated.

A 3.3 PILOT COLUMN TRIALS - RESIN SEPARATION BY BACKWASHING

A 3.3.1 TEST COLUMN CONSTRUCTION

Pilot scale mixed bed separations were carried out in a 95 mm internal diameter, 3 mm wall thickness, clear acrylic column. Figure A 3.01 depicts the column construction (not to scale). The column was 1300 mm long and was capped at either end by an end plate and retaining collar. The end plate was made from a 150 mm square, 25 mm thick block of clear acrylic plastic. A circular recess 101 mm diameter was machined to a depth of 6 mm in the centre of the block. A 5 mm wide flat shoulder was left and then the recess dished to a depth of 12 mm at the centre. A hole, tapped to half inch BSP, was made at the centre point to act as an inlet or outlet. The clear acrylic tube would just fit into the recess and stand on the shoulder in the end plate.

A circular collar 35 mm wide was machined from 25 mm thick acrylic block and was a sliding fit over the outside of the test column. Six holes 10 mm diameter were drilled at regular intervals through the collar together with six matching holes in the end plate. A neoprene 'O' ring was placed between the collar and the end plate and the two parts pulled together with $2\frac{1}{2}$ x 5/16 inch Whitworth bolts. The 'O' ring was compressed against the tube wall and made an effective watertight seal that could be easily dismantled. The bottom end plate has only one threaded penetration the top end plate contained two.

Waste

Drain

Air

A

D

E

f

g

e

b

c

d

a
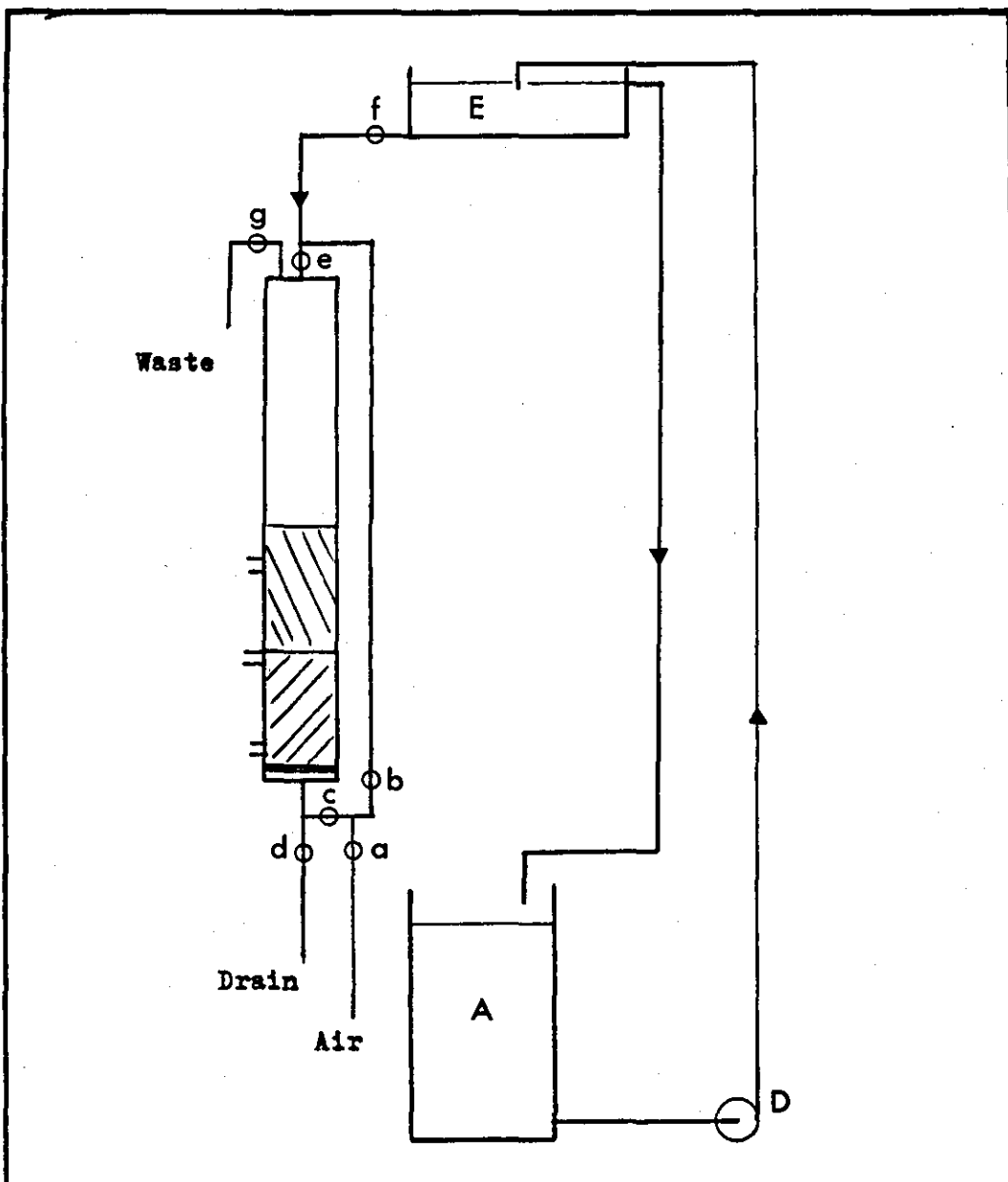
| FIGURE | TEST COLUMN ARRANGEMENT – BACKWASHING |
| No. A3.02 | AND SEPARATION |

The resin support plate consisted of a clear acrylic disc 12.5 mm
thick that was a tight sliding fit inside the 95 mm diameter test
column. It was perforated with 80 holes of 3 mm diameter arranged
in a regular pattern to give maximum collection efficiency. The top
face of the resin support plate was covered in a stainless steel mesh
of 75 µm aperture to prevent resin beads passing through. The mesh
was attached to the edge of the acrylic support plate using an acrylic
cement of the two pack, monomer plus activator, type. The resin
support plate was positioned so that a 30 mm gap was maintained
between its lower face and the threaded column inlet/outlet, to
ensure a more even distribution of the backwash water. The resin
support plate was itself supported on a acrylic 'C' ring which was
cut from the end of the test column with a segment removed. The
'C' ring was sprung into place.

At three separate heights above the resin support plate a sample port
was provided for taking horizontal resin core samples. These were
located at 70 mm, 270 mm and 470 mm above the resin support plate.
A 25 mm diameter hole was cut at each sample port and a 50 mm length
of 25 mm internal diameter acrylic tube was glued horizontally onto
the outside of the test column. The inner end of the sample port
was profiled to the curvature of the test column. Each sample port
was closed by a plug machined from acrylic rod. The plug was a
cylinder 75 mm long and 24 mm diameter. A shallow circumferential
groove was cut near one end and a neoprene 'O' ring stretched onto
the plug and into the groove. The 'O' ring made a watertight seal
when the plug was pushed into the sample port. The end of the plug
was left flush with the inside of the test column.

A 3.3.2 TEST RIG ARRANGEMENT

The arrangement of the test column, water supplies and valves is
outlined in Figure A 3.02. Tank A was a 200 litre polypropylene
storage tank for deionised water. Water was pumped continuously by
pump D to the 60 litre header tank E also polypropylene, and over-
flowed back to A maintaining a constant head in tank E. Water from
tank E could be fed via valves f and e to the top of the test column
or via valves f, b and c to the bottom of the column to act as

backwash water. An overflow line at the top of the column went to
waste via valve g. The column could be drained to waste via valve
d, valve g being also opened to admit air into the column. The resins
could be remixed by admitting nitrogen via valves a and c from a
compressed nitrogen cylinder with a flow regulator (see A 4.1.1).
All the pipework was ½ inch BSP ABS pipework with either solvent
cemented or screw threaded joints. The down comer from tank E to
tank A was a ¾ inch BSP ABS pipe. The valves were ABS bodied ball
valves, which were found to give better flow control and more positive
action than a Saunders type diaphragm valve. The pump was a brass
bodied, 200 watt centrifugal type.

The header tank E was mounted on a steel frame with a water level
4 m above ground level. The test column was mounted on the same
frame with the resin support plate 1 m above ground level.

A 3.3.3   TEST PROCEDURE

Approximately 4.0 - 4.2 litres of resin were used in each test. This
normally consisted of a 1:1 volume mixture of cation and anion
exchangers. Exact resin volumes are given below with details of each
test. Resins were added to the column via a funnel placed in the open
end of the column after removal of the upper end plate. Resins were
always added into water in the column to ensure no air became trapped
in the bed. Mixed resins, sampled from a full scale bed were added
in the mixed state. Otherwise, cation exchanger was first added
until the settled level after backwashing was in line with the centre
sampling port. An equal volume of anion exchanger was then added.
If inert resin was also included in the separation the resin volumes
were adjusted so that initially the inert resin was at the level of
the centre sampling port. Samples of the bulk resins added to the
column were taken for subsequent bead size and bead density measure-
ments.

The column end plate was replaced, all connections for water supplies
etc remade and the water level in the test column drained until
about 50 mm above the surface of the resins. The resins were then
air mixed for 20 minutes under the conditions and procedures given in
A 4.12.

After mixing was completed the bed was backwashed to effect separation. Valves f,b,c and g were opened to admit backwash water to the column and to allow it to go to waste. The backwash flow rate was controlled by valve c and the flow rate monitored by measuring the time required to fill a previously calibrated 1 litre measuring cylinder at the waste outlet. Backwash flow rates were typically in the range 0.95 - 1.3 litres per minute flow rate which was equivalent to 8 -11 m h^{-1} superficial flow rate. Backwash water temperature was ambient, normally about 20 $^\circ$C.

Backwashing was continued for about 20 minutes at which time the bed had established its steady equilibrium separation conditions. The backwash flow was then slowly reduced and the bed settled. The bed was then drained via valve d and the sample port plugs removed. The resin bed remained as a solid mass and did not slump out of the ports. A horizontal core was extracted from each port using a thin walled brass tube 22 mm diameter. The tube was pushed into the resin bed until the far wall was reached. The tube was then turned a complete revolution and withdrawn containing the sample core. The sample core was washed into a screwed cap glass jar and retained for subsequent analysis.

Resin analysis consisted of wet sieving each sample as outlined in A 3.1 and then separating the anion and cation exchangers by differential flotation in saturated sodium chloride solution (see A 3.2). In general because the interfacial samples contained large anion exchanger and small cation exchanger beads the initial wet sieving effected some separation of anion and cation exchangers. The same applied to separation of exchangers and inert resins. Where anion exchanger and inert resins occurred in the same separated sample, the relative proportions of each were estimated visually.

A 3.3.4   RESIN MIXTURES: TESTS 1 - 3

Test 1a was a two resin separation of resins taken from Walsall mixed bed containing Amberlite IR120 cation exchanger and Amberlite IRA402 anion exchanger. The sample was taken during air mixing of the bed, via an open manhole cover, to ensure a representative sample was

obtained. Four litres of mixed resin, nominally a 1:1 mixture, were placed in the test column and were backwashed, as described in A 3.1.3.3, for twenty minutes at a flow rate of 1.05 litres per minute equivalent to the 8.8 m h^{-1} backwash flow rate on the full scale mixed bed. After settling and draining the bed a sample core was taken at the centre port to assess the degree of intermixing in the interfacial zone. Table A 3.08 gives the resin analysis details of the sample core.

In test 1b 0.8 l of Ambersep 359 inert resin was added to the resins in test 1a. The size distribution of the inert resin is given in Table A 3.06. The three resins were thoroughly mixed by air injection and the bed backwashed again at 1.05 litres per minute. A second sample core was taken from the centre port. It contained mostly cation and inert resins (Table A 3.08) and the required displacement, upwards, of the anion exchanger had been achieved.

Test 2 was also a three resin bed consisting of regenerated Zerolit525 cation exchanger plus Ambersep359 inert resin plus partly exhausted IRA402 anion exchanger from Walsall. The IRA402 had been regenerated and partly exhausted since test 1. The initial mixed bed contained only 1.7 l of Zerolit 525 plus 0.3 l inert resin and 2.0 l of IRA 402, so that the centre port was opposite the nominal anion exchanger/inert resin interface. In test 2a the mixed resins were backwashed at 1.05 litres per minute and a sample core taken from the centre sample port of a drained bed. In test 2b 0.3 l of Zerolit 525 were added to the bed so that the centre port was now opposite the nominal cation exchanger/inert resin interface. A repeat separation was followed by sample coring the centre port. Finally, in test 2c, a further 0.3 l of Zerolit 525 was added to raise the bed further and see if inert resin penetrated significantly into the cation exchanger. Following a further backwash and drain down the centre port was again core sampled. The resin mixture and size analyses for test 2 are given in Table A 3.09.

Tests 3a, b and c were separations of a two resin system, Duolite C26 cation exchanger and Zerolit FF(ip) anion exchanger with the resins in various ionic forms. Size gradings of the two exchangers are given in Table A 3.06, and these were   . . . .

measured in the 'as received' sodium form cation exchanger and chloride form anion exchanger. Each exchanger was conditioned by two successive regeneration - rinse - exhaustion with 0.5M $(NH_4)_2SO_4$ - rinse cycles and were then regenerated with 64 g H_2SO_4 per litre cation exchanger introduced as a 0.5M solution and 64 g NaOH per litre anion exchanger as a 1M solution. Each resin was rinsed with deionised water until the conductivity of the rinse effluent was less than 10 μS cm^{-1}.

1.9 l of regenerated C26 and 2.1 l of regenerated FF(ip) were loaded into the column, air mixed and backwashed at 1.3 litres per minute. Test 3a with a single sample core from the centre port is recorded in Table A 3.10. After remixing, ammonia was dosed to the column to produce NH_4^+ form cation exchanger. Following this a second backwash and separation (test 3b) was carried out. Samples were taken from the centre and bottom ports after the bed had been drained. Bead density measurements were made on samples of separated anion and cation exchanger. Finally the bed was fully exhausted with ammonium sulphate solution to give NH_4^+ cation and SO_4^{2-} anion exchangers, rinsed and a third separation by backwashing carried out (test 3c). Sample cores were taken at all three ports and new bead density determinations made. The bead size distributions of the resins in the sample cores from tests 3b and 3c are also given in Table A 3.10.

A 3.4 MEASUREMENT OF BEAD DENSITY, SKELETAL DENSITY AND MOISTURE CONTENT

The bead density measurements required for separation predictions were initially gathered as part of a suite of physico-chemical measurements on anion and cation exchangers, designed to establish variations between exchangers based on different polymer/matrix types (241). The additional parameters were skeletal density and moisture content. Whereas bead density represented the mass of exchanger plus internal moisture per unit displaced swollen volume of resin bead, the skeletal density represented only the mass of exchanger (ie polymer, exchange groups and counter ions) per unit swollen volume of resin. Skeletal density gave an indication of between batch as well as between type variations.
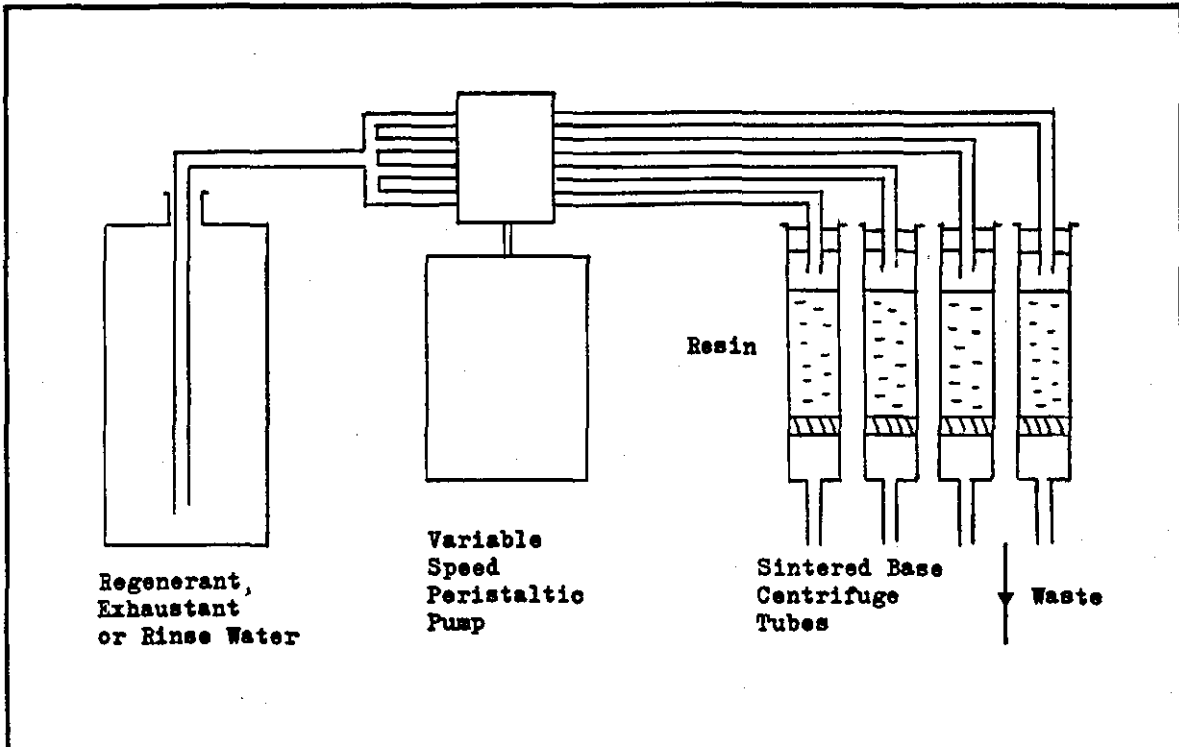
RESIN CONDITIONING APPARATUS FOR BEAD DENSITY MEASUREMENTS
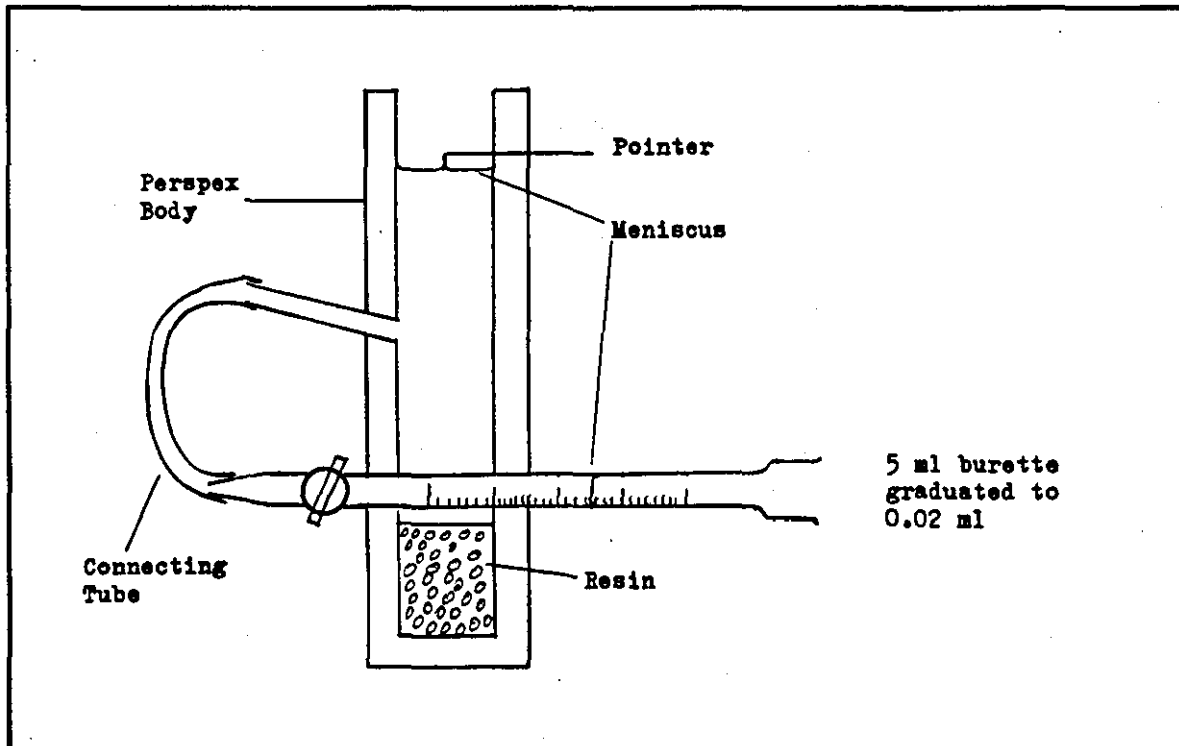
RESIN VOLUME MEASUREMENT APPARATUS

In order to make these measurements it was necessary to know both
the moist weight and dry weight of a given displaced volume of resin.
In any measurements on moist resin beads the resin phase moisture must
be maintained while extraneous surface water is excluded. In
addition, as exchangers lose moisture on exposure to air, the
handling of resins must be minimised. Two methods for producing
resins with minimal surface moisture have been recorded previously;
drying in moist air and blotting the resins with adsorbent paper (217)
or centrifuging the resins in a porous base centrifuge tube (215, 216).
The latter method was chosen as being more reproducible.

Two methods for measurement of displaced volume were also available.
A direct method involved the measurement of the volume of water
displaced by moist resin while an indirect method used a specific
gravity bottle to calculate the volume from the weight of water
displaced. Both methods have been used as described below. The
moisture content of a resin was measured by drying the resin at
105 $^\circ$C overnight (242), weighing before and after to establish the
weight of moisture lost.

A 3.4.1 RESIN CONDITIONING

Resins taken from separation trials had bead densities measured in
the 'as sampled' form, but in many cases it was necessary to convert
the resins to a specific ionic form. This was carried out in a
small rig (Figure A 3.03) in which the resins were retained in the
sintered base centrifuge tubes used for centrifuging the resin.
Each centrifuge tube was 12 mm diameter and 55 mm long with a
porosity 1 glass sintered base and contained about 2.5 ml displaced
volume of resin. Conditioning consisted of passing 250 ml regenerant
through each sample, either 1M NaOH for anion exchangers - or 1M HCl
for cation exchangers. This was followed by 250 ml deionised rinse
water then 250 ml exhaustant which was either the sodium salt of the
appropriate anion or the chloride salt of the appropriate cation,
both exhaustants were 0.5M concentration. A further 250 ml of rinse
water was then passed to remove residual exhaustant. All solutions
were pumped at 2 ml per minute per sample by a 4 channel peristaltic
pump.

A 3.4.2 BEAD VOLUME, BEAD WEIGHT, BEAD MOISTURE.

A minimum of two duplicate measurements were made for each resin.
The 2.5 ml of conditioned or sampled resin in the centrifuge tube
was centrifuged for 20 minutes at 2000 revolutions per minute. The
centrifuge tubes were removed, placed upright in a small beaker and
the top covered with a moist tissue to prevent the resin drying out.
The water level in the displaced volume apparatus (Figure A 3.04)
was adjusted to the pointer and the reading in the burette noted.
The centrifuged resin was transferred from the centrifuge tube to
the displaced volume apparatus and when it had settled water was
allowed to enter the burette until the meniscus was at the pointer
again. The resin volume was the difference between the two burette
readings.

The resin was recovered from the displaced volume apparatus onto a
fine mesh sieve, and returned to the centrifuge tube for a further
20 minutes centrifuging at 2000 rpm,(33.3 Hz). Resin recovery was
99.5% or better. The centrifuged resin was transferred to a small
tared aluminium tin with lid and weighed on a balance reading to
0.1 mg. The tin had been dried at 105 $^{\circ}$C and cooled in a dessicator.
The tin plus moist resin was dried overnight at 105 $^{\circ}$C, cooled in a
dessicator and reweighed.

The following calculations could be made

Bead density (δ) $=$ $\dfrac{\text{Weight of moist resin}}{\text{Displaced volume of resin}}$

Skeletal density (ψ) $=$ $\dfrac{\text{Weight of dry resin}}{\text{Displaced volume of resin}}$

Moisture content (M_w)
(weight fraction) $=$ $\dfrac{\text{Weight moist resin} - \text{Weight dry resin}}{\text{Weight moist resin}}$

Moisture content (M_v)
(volume fraction) $=$ $\dfrac{\text{Weight moist resin} - \text{Weight dry resin}}{\text{Volume moist resin} \times 0.998}$

The correction factor of 0.998 in calculating M_v is for the density
of water at 20 $^{\circ}$C.

To estimate the residual moisture left around the resins after

centrifuging, samples of glass beads 0.85 - 1.0 mm diameter were washed, centrifuged, weighed, dried and reweighed. The residual moisture was equivalent to 0.01 g per ml of resin and would introduce a very small negative bias of around 2 kg m^{-3} of bead density.

The major error lay in the displaced volume measurement with an accuracy of $\pm$0.01 ml in about 2.0 - 2.5 ml. However, replicate analyses on several different batches of resins showed remarkably small standard deviations of between 6.2 and 9.6 kg m^{-3} on bead densities between 1063 and 1286 kg m^{-3} (Table A 3.11) representing a standard deviation of 0.5 - 0.8%.

A 3.4.3 SPECIFIC GRAVITY MEASUREMENTS

The use of a specific gravity (SG) bottle to determine resin volume by weighing was tried initially but certain types of resin adhered to the glass walls of the SG bottle and could not be recovered. However, once the relationships

$$\delta = \psi + 1000M_v \quad \text{and} \quad M_v = M_w \times \frac{\delta}{1000}$$

had been established it was only necessary to determine δ and M_v to be able to calculate M_w and ψ . The values of δ and M_v could be determined on different aliquots of the same sample of resin. Standard practice was to centrifuge four samples of conditioned resins and retain them under a moist tissue as before. Two samples were transferred to tared tins for weighing, drying overnight at 105 ^{o}C and reweighing and determination of M_w. The other two samples were for duplicate bead density determinations using an SG bottle.

The dry SG bottle was weighed (W_1) filled with water and reweighed (W_2) The volume of the SG bottle = $(W_1 - W_2) \div 0.998$. The SG bottle was dried again, moist centrifuged resin added and reweighed (W_3).

Water was added to fill the SG bottle, care being taken to release
all air trapped between the resin beads. The SG bottle plus resin
plus water was reweighed (W_4). The volume of resin (V_R) is given by

$$V_R = \frac{(W_1 - W_2) - (W_4 - W_3)}{0.998}$$

Resin bead density is then given by $(W_3 - W_1) \div V_R$.

The precision of the SG method for measuring bead densities was, as
might be expected, better than the displaced volume method, with a
standard deviation of $\pm$ 1.04 kg m^{-3} on a bead density of 1232 kg m^{-3}
(Table A 3.11).

A 3.5 BEAD SIZE GRADING – PARTICLE SIZE ANALYSER

A HIAC PA 720 particle size analyser (Southern Pacific Instrument Co;
California) was used for some bead size analysis particularly the
sizing of triple bed resins and resins taken from operating condensate
purification mixed beds (5.3.10).

The analyser worked on the principle of light obscuration. A
parallel light source was passed through optically flat windows in
the measuring cell onto a photo electric sensor. Resin beads in
suspension in a stream of water are passed through the cell and cast
a shadow onto the photoelectric sensor. The change in output from
the sensor is proportional to the area of the shadow. Sample
presentation is important as only a single bead must be in front of
the sensor at any one time, otherwise two beads may be counted as
one larger one. This was achieved by feeding the cell from a 2 litre
separating funnel that contained a continuously stirred dilute
suspension of resin particles. The water in the separating funnel
was continuously replenished and fresh resin was added to this feed.
Samples of 5000 particle counts were sufficient to give reproducible
results.

The microprocessor incorporated into the instrument sorted the photo
sensor signals into 23 channels, each representing a bead diameter
range, and counted the particles in each range. A print out was

SUMMARY	MEAN,um	d(11),um	d(50),um	d(12),um	d(50/11)	d(12/50)
POP	562.1	466.1	561.1	582.3	1.20	1.04
VOL	604.6	497.4	598.7	621.4	1.20	1.04
FLAG						

FIGURE No. A3.05   HIAC PARTICLE SIZE DISTRIBUTION AND SUMMARY TABLE, RESIN VOLUME BASED
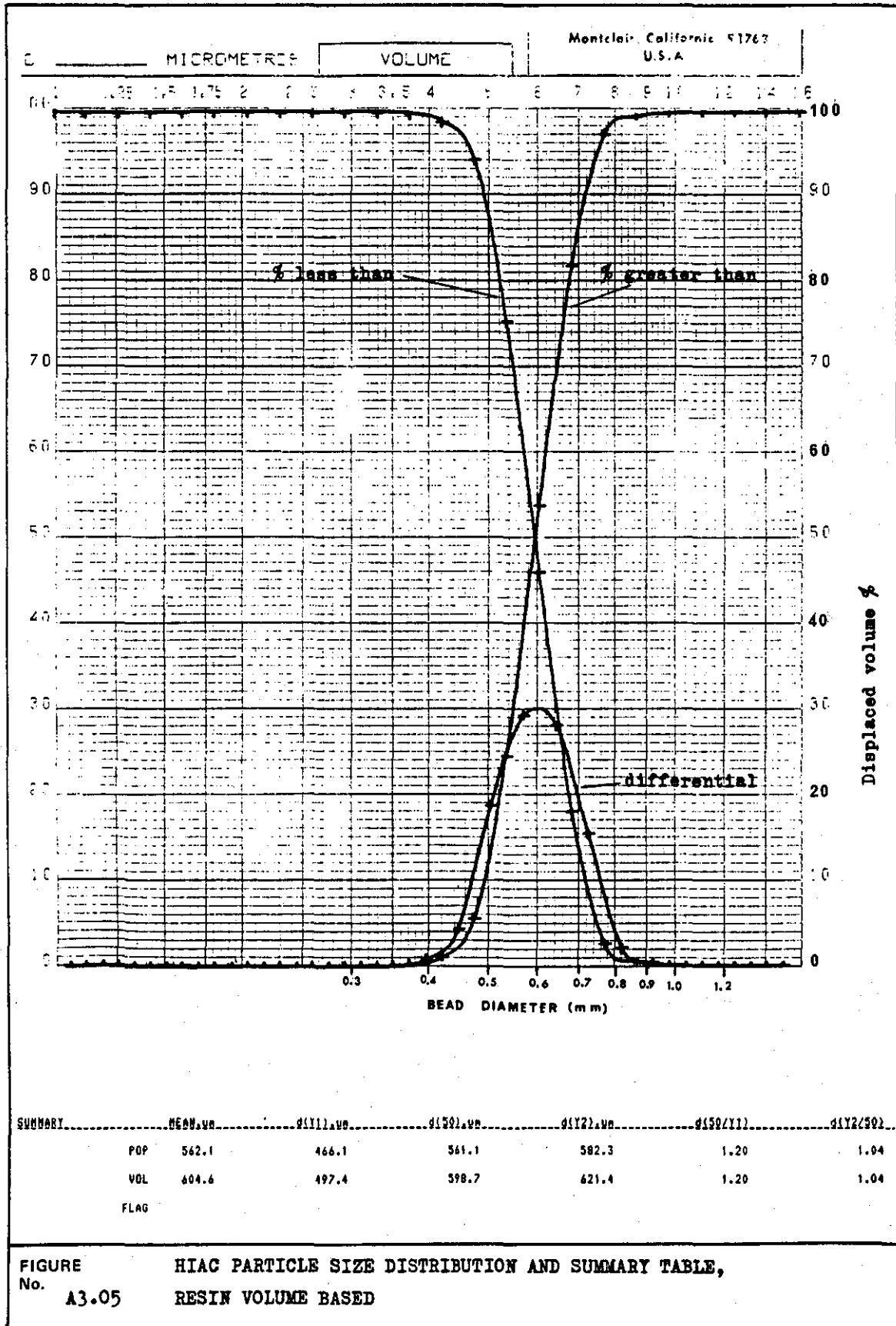
obtained giving details of the number of particles in each channel
and the percentages based on a particle count and bead volume basis.
A summary table included the volume based mean bead diameter. This
was equivalent to the Sauter mean. In addition the microprocessor
was linked to a plotter which gave a graphical record of the distribution.
Figure A 3.05 is an example of the plot and summary table for
Ambersep 359 inert resin.

The instrument was calibrated against wet sieved resins when first
delivered and the calibration is checked periodically.

TABLE A 3.01   REYNOLDS NUMBER AT BEAD TERMINAL VELOCITY - VARIATION WITH BEAD DIAMETER, BEAD DENSITY AND TEMPERATURE (T).

Bead Density (kg m^{-3})	T (°C)	Bead Diameter (mm)					
		0.3	0.5	0.7	1.0	1.2	1.4
1025	5	0.155	0.68	1.67	4.15	6.35	9.0
	20	0.38	1.51	3.6	8.3	12.8	18.0
	40	0.99	3.75	8.2	18.5	27.5	38.5
1050	5	0.31	1.27	3.05	7.2	11.0	15.4
	20	0.70	2.7	6.1	13.7	20.6	29.3
	40	1.62	5.8	12.4	28	42	56.5
1075	5	0.46	1.80	4.25	9.7	14.9	20.8
	20	1.00	3.8	8.2	18.5	27.7	38.5
	40	2.22	7.6	16.5	36.5	53	73
1100	5	0.59	2.33	5.4	12.1	18.1	25.7
	20	1.27	4.7	10.2	22.8	34	47
	40	2.80	9.4	20.2	44	64	87
1125	5	0.73	2.80	6.4	14.5	21.6	30.5
	20	1.55	5.6	12.0	26.8	40	54.5
	40	3.32	11.0	23.5	51	73.5	100
1150	5	0.86	3.26	7.3	16.4	24.9	34.5
	20	1.80	6.4	13.8	30.5	45.5	62
	40	3.85	12.4	26.8	57	82.5	112
1175	5	0.99	3.72	8.2	18.4	27.4	38.5
	20	2.07	7.1	15.4	34	50	69
	40	4.3	14.0	29.5	62.5	91	122
1200	5	1.12	4.15	9.1	20.3	30.4	42.5
	20	2.32	8.0	17.1	37.5	55	75.5
	40	4.75	15.6	32.7	68.5	99	133
1225	5	1.25	4.55	10.0	22.2	33.1	46
	20	2.55	8.7	18.6	40.5	59.5	81
	40	5.2	16.8	35.5	74.5	106	143
1250	5	1.35	4.95	10.9	24.1	36.0	49.5
	20	2.80	9.4	20.2	44	64	87
	40	5.7	18.1	38	80	113	154
1275	5	1.47	5.4	11.7	25.9	38.5	53
	20	3.05	10.2	21.5	47	68	94
	40	6.1	19.3	40.5	84	121	163
1300	5	1.6	5.8	12.6	27.7	40.5	56
	20	3.25	10.7	23	49	72.5	98
	40	6.45	20.7	43	90	128	172
1350	5	1.80	6.4	13.9	30.7	45.5	63
	20	3.7	12.1	26	55	80	108
	40	7.3	23.2	48	99	140	188

TABLE A 3.02   RESIN BEAD TERMINAL VELOCITIES (10^{-3} m s^{-1}) - VARIATION WITH BEAD DIAMETER, BEAD DENSITY AND TEMPERATURE (T).

Bead Density (kg m^{-3})	T ($^{\circ}$C)	Bead Diameter (mm)					
		0.3	0.5	0.7	1.0	1.2	1.4
1025	5	0.782	2.06	3.62	6.28	8.01	9.73
	20	1.25	3.03	5.15	8.32	10.7	12.8
	40	2.18	4.94	7.72	12.2	15.1	18.1
1050	5	1.54	3.85	6.60	10.9	13.9	16.7
	20	2.34	5.41	8.73	13.7	17.2	21.0
	40	3.56	7.65	11.7	18.5	23.1	26.6
1075	5	2.30	5.45	9.19	14.7	18.8	22.5
	20	3.34	7.52	11.7	18.5	23.1	27.6
	40	4.88	10.0	15.5	24.1	29.1	34.4
1100	5	2.98	7.06	11.7	18.3	22.8	27.8
	20	4.24	9.42	14.6	22.8	28.4	33.6
	40	6.15	12.4	19.0	29.0	35.2	41.0
1125	5	3.68	8.48	13.8	22.0	27.3	33.0
	20	5.18	11.2	17.2	26.9	33.4	39.0
	40	7.30	14.5	22.1	33.6	40.4	47.1
1150	5	4.34	9.87	15.8	24.8	31.4	37.3
	20	6.01	12.8	19.8	30.6	38.0	44.4
	40	8.46	16.4	25.2	37.6	45.3	52.7
1175	5	5.00	11.3	17.7	27.9	34.6	41.6
	20	6.91	14.2	22.0	34.1	41.8	49.4
	40	9.45	18.5	27.8	41.2	50.0	57.5
1200	5	5.65	12.6	19.7	30.7	38.4	46.0
	20	7.75	16.0	24.5	37.6	45.9	54.0
	40	10.4	20.6	30.8	45.2	54.4	62.6
1225	5	6.31	13.8	21.6	33.6	41.8	49.7
	20	8.52	17.4	26.6	40.6	49.7	58.0
	40	11.4	22.2	33.4	49.1	58.2	67.3
1250	5	6.81	15.0	23.6	36.5	45.4	53.5
	20	9.35	18.8	28.9	44.1	53.4	62.3
	40	12.5	23.9	35.8	52.7	62.1	72.5
1275	5	7.42	16.4	25.3	39.2	48.6	57.3
	20	10.2	20.4	30.8	47.1	56.8	67.2
	40	13.4	25.4	38.1	55.4	66.5	76.8
1300	5	8.07	17.6	27.3	41.9	51.1	60.6
	20	10.9	21.4	32.9	49.1	60.5	70.1
	40	14.2	27.3	40.5	59.3	70.3	81.0
1350	5	9.08	19.4	30.1	46.5	57.4	68.1
	20	12.4	24.2	37.2	55.1	66.8	77.3
	40	16.0	30.6	45.2	65.3	76.9	88.5

TABLE A 3.03 FLUIDISED BED POROSITY AT 8 m h^{-1} BACKWASH FLOW RATE
(20 $^{\circ}$C) VARIATION WITH COLUMN DIAMETER (D), BEAD
DIAMETER AND BEAD DENSITY.

BEAD DENSITY (kg m^{-3})	D (mm)	BEAD DIAMETER (mm)					
		0.3	0.5	0.7	1.0	1.2	1.4
1025	25	>1.0	0.944	0.835	0.744	0.699	0.669
	100	>1.0	0.933	0.813	0.705	0.650	0.609
	2000	>1.0	0.930	0.805	0.691	0.632	0.588
1050	25	0.995	0.822	0.727	0.645	0.608	0.578
	100	0.990	0.806	0.699	0.601	0.553	0.513
	2000	0.989	0.800	0.689	0.585	0.534	0.490
1075	25	0.921	0.755	0.669	0.588	0.554	0.529
	100	0.914	0.736	0.638	0.542	0.497	0.463
	2000	0.911	0.729	0.628	0.525	0.477	0.440
1100	25	0.872	0.710	0.626	0.550	0.518	0.495
	100	0.863	0.689	0.594	0.502	0.460	0.428
	2000	0.860	0.682	0.584	0.486	0.440	0.405
1125	25	0.831	0.675	0.596	0.521	0.490	0.470
	100	0.821	0.653	0.563	0.473	0.432	0.403
	2000	0.818	0.646	0.552	0.456	0.411	0.380
1150	25	0.801	0.649	0.570	0.499	0.468	0.449
	100	0.790	0.627	0.536	0.450	0.410	0.382
	2000	0.787	0.619	0.525	0.433	0.390	0.359
1175	25	0.773	0.630	0.550	0.480	0.453	0.432
	100	0.762	0.607	0.515	0.431	0.394	0.365
	2000	0.758	0.599	0.504	0.415	0.374	0.342
1200	25	0.750	0.607	0.531	0.464	0.437	0.418
	100	0.738	0.584	0.497	0.415	0.379	0.351
	2000	0.735	0.576	0.485	0.398	0.359	0.328
1225	25	0.731	0.591	0.516	0.451	0.425	0.407
	100	0.719	0.568	0.482	0.402	0.366	0.341
	2000	0.715	0.560	0.470	0.385	0.347	0.318
1250	25	0.713	0.577	0.502	0.438	0.413	0.396
	100	0.701	0.553	0.467	0.389	0.355	0.330
	2000	0.696	0.545	0.456	0.372	0.335	0.307
1275	25	0.696	0.562	0.491	0.427	0.404	0.385
	100	0.684	0.538	0.456	0.378	0.346	0.319
	2000	0.679	0.530	0.445	0.362	0.326	0.296
1300	25	0.684	0.554	0.480	0.421	0.394	0.378
	100	0.671	0.529	0.445	0.372	0.336	0.313
	2000	0.667	0.521	0.433	0.355	0.317	0.290
1350	25	0.659	0.532	0.459	0.403	0.379	0.364
	100	0.646	0.507	0.424	0.354	0.322	0.299
	2000	0.641	0.499	0.412	0.337	0.303	0.277

TABLE A 3.04   FLUIDISED BED POROSITY AT 12 m h^{-1} BACKWASH FLOW RATE
(20 ^{o}C) VARIATION WITH COLUMN DIAMETER (D), BEAD
DIAMETER AND BEAD DENSITY.

Bead Density (kg m^{-3})	D (mm)	Bead Diameter (mm)				
		0.3	0.5	0.7	1.0	1.2
1025	25	>1.0	>1.0	0.918	0.820	0.772
	100	>1.0	>1.0	0.900	0.786	0.728
	2000	>1.0	>1.0	0.894	0.774	0.711
1050	25	>1.0	0.903	0.803	0.715	0.675
	100	>1.0	0.890	0.778	0.674	0.623
	2000	>1.0	0.886	0.770	0.659	0.605
1075	25	>1.0	0.832	0.740	0.654	0.616
	100	>1.0	0.816	0.713	0.610	0.562
	2000	1.0	0.810	0.703	0.594	0.542
1100	25	0.954	0.784	0.695	0.613	0.577
	100	0.948	0.766	0.666	0.567	0.521
	2000	0.946	0.759	0.655	0.551	0.501
1125	25	0.911	0.747	0.662	0.582	0.547
	100	0.903	0.727	0.631	0.535	0.490
	2000	0.901	0.721	0.621	0.518	0.470
1150	25	0.879	0.720	0.635	0.558	0.524
	100	0.870	0.699	0.603	0.510	0.466
	2000	0.868	0.692	0.592	0.493	0.446
1175	25	0.849	0.698	0.613	0.538	0.507
	100	0.840	0.677	0.580	0.489	0.449
	2000	0.837	0.670	0.569	0.472	0.429
1200	25	0.825	0.674	0.593	0.520	0.490
	100	0.815	0.652	0.560	0.471	0.432
	2000	0.812	0.645	0.548	0.454	0.412
1225	25	0.805	0.657	0.577	0.506	0.477
	100	0.795	0.635	0.543	0.457	0.418
	2000	0.791	0.627	0.532	0.440	0.398
1250	25	0.786	0.642	0.561	0.492	0.464
	100	0.775	0.619	0.527	0.442	0.406
	2000	0.771	0.612	0.516	0.425	0.386
1275	25	0.768	0.626	0.550	0.480	0.454
	100	0.757	0.603	0.516	0.431	0.396
	2000	0.753	0.595	0.504	0.414	0.375
1300	25	0.755	0.617	0.537	0.473	0.443
	100	0.743	0.593	0.503	0.423	0.385
	2000	0.740	0.585	0.491	0.407	0.365

TABLE A 3.05 FLUIDISED BED POROSITY AT 8 m h^{-1} BACKWASH FLOW RATE.
VARIATION WITH TEMPERATURE (T) AND BEAD DIAMETER AT
SELECTED BEAD DENSITIES.

BEAD DENSITY (kg m^{-3})	T (°C)	BEAD DIAMETER (mm)					
		0.3	0.5	0.7	1.0	1.2	1.4
1075	5	0.995	0.811	0.699	0.600	0.550	0.514
	20	0.914	0.736	0.638	0.542	0.497	0.463
	40	0.827	0.665	0.569	0.478	0.440	0.409
1175	5	0.835	0.664	0.571	0.481	0.441	0.408
	20	0.790	0.627	0.536	0.450	0.410	0.382
	40	0.688	0.543	0.459	0.384	0.350	0.327
1250	5	0.773	0.609	0.518	0.435	0.396	0.368
	20	0.701	0.553	0.467	0.389	0.355	0.330
	40	0.631	0.495	0.415	0.345	0.317	0.293

TABLE A 3.06 <u>BEAD SIZE DISTRIBUTION OF INDIVIDUAL RESINS USED</u>
<u>IN SEPARATION TRIALS.</u>

AMBERSEP 359 Inert Resin

Bead Diameter Fraction (mm)	Settled Volume (%)	Cumulative (%)
−0.30	0	0
+0.30 − 0.425	6.6	6.6
+0.425 − 0.50	18.2	24.8
+0.50 − 0.60	50.5	75.3
+0.60 − 0.71	22.4	97.7
+0.71 − 0.85	1.6	99.3
+0.85 − 1.0	0.2	99.5
+1.0	0.5	100

Size Ratio (5 − 95%) 1.61

Mean Diameter 0.54 mm.

DUOLITE C26 AND ZEROLIT FF(ip)

Bead Diameter Fraction (mm)	C26		FF(ip)	
	Settled Volume (%)	Cumulative (%)	Settled Volume (%)	Cumulative (%)
−0.30	0		0.5	0.5
+0.30 − 0.425	2.0	2.0	2.4	2.9
+0.425 − 0.50	4.4	6.4	3.2	6.1
+0.50 − 0.60	12.7	19.1	7.9	14.0
+0.60 − 0.71	19.5	38.6	20.2	34.2
+0.71 − 0.85	20.5	59.1	25.3	59.5
+0.85 − 1.0	22.7	81.8	25.7	85.2
+1.0 − 1.2	17.3	99.1	11.8	97.0
+1.2 − 1.4	0.8	99.9	1.9	98.9
+1.4	0.2	100.1	1.0	99.9
Mean Diameter (mm)	0.77		0.76	

TABLE A 3.07   BEAD SIZE ANALYSIS OF SEPARATED RESIN CORE FROM WALSALL MIXED BED.

Depth 890 - 915 mm

Resin (volume %)	Anion (97)		Inert (-)		Cation (3)	
Bead Diameter Fraction (mm)	Settled Volume(%)	Cumulative (%)	Settled Volume(%)	Cumulative (%)	Settled Volume(%)	Cumulative (%)
-0.30	0.4	0.4				
+0.30 - 0.425	} 6.2	6.6				
+0.425 - 0.50	}					
+0.50 - 0.60	10.8	17.4				
+0.60 - 0.71	17.8	35.2				
+0.71 - 0.85	18.6	53.8				
+0.85 - 1.0	25.6	79.4				
+1.0 - 1.2	17.0	96.4				
+1.2 - 1.4	2.3	98.7				
+1.4	1.0	99.7				

Depth 675 - 700 mm

Resin (volume %)	Anion (96)		Inert Cation (4)			
Bead Diameter Fraction (mm)	Settled Volume(%)	Cumulative	Settled Volume(%)	Cumulative	Settled Volume(%)	Cumulative
-0.30	0		50	50		
+0.30 - 0.425	3.9	3.9	33	83		
+0.425 - 0.50	5.2	9.1	17	100		
+0.50 - 0.60	9.0	18.1				
+0.60 - 0.71	14.2	32.3				
+0.71 - 0.85	18.1	50.4				
+0.85 - 1.0	21.3	71.7				
+1.0 - 1.2	20.6	92.3				
+1.2 - 1.4	5.8	98.1				
+1.4	1.9	100				

Depth 590 - 620 mm

Resin (volume %)	Anion (50)		Inert (32)		Cation (18)	
Bead Diameter Fraction (mm)	Settled Volume(%)	Cumulative	Settled Volume(%)	Cumulative	Settled Volume(%)	Cumulative
-0.30			0	0	12.1	12.1
+0.30 - 0.425	0	0	10.3	10.3	69.7	81.8
+0.425 - 0.50	1.6	1.6	51.7	62.0	10.6	92.4
+0.50 - 0.60	2.7	4.3	34.5	96.5	7.6	100
+0.60 - 0.71	12.1	16.4	3.4	99.9		
+0.71 - 0.85	17.6	34.0	0			
+0.85 - 1.0	22.0	56.0				
+1.0 - 1.2	22.0	78.0				
+1.2 - 1.4	11.0	89.0				
+1.4	11.0	100				

TABLE A 3.07 (continued)

Bed Depth 450 - 480 mm

Resin(Volume%)	Anion(2)		Inert (33)		Cation (65)	
Bead Diameter Fraction (mm)	Settled Volume(%)		Settled Volume(%)	Cumulative (%)	Settled Volume(%)	Cumulative (%)
-0.30			0	0	0.9	0.9
+0.30 - 0.425			1.7	1.7	20.4	21.3
+0.425 - 0.50			12.0	13.7	25.5	46.8
+0.50 - 0.60			61.6	75.3	32.3	79.1
+0.60 - 0.71			23.9	99.2	16.2	95.3
+0.71 - 0.85			0.9	100.1	3.4	98.7
+0.85 - 1.0			0		1.3	100
+1.0 - 1.2					0	
+1.2 - 1.4						
+1.4						

Bed Depth 370 - 395 mm

Resin(Volume%)	Anion		Inert (4)		Cation (96)	
Bead Diameter Fraction (mm)			Settled Volume(%)	Cumulative (%)	Settled Volume(%)	Cumulative (%)
-0.30					0.7	0.7
+0.30 - 0.425					4.0	4.7
+0.425 - 0.50			Trace		10.7	15.4
+0.50 - 0.60			50	50	29.5	44.9
+0.60 - 0.71			50	100	30.2	75.1
+0.71 - 0.85			Trace		16.1	91.2
+0.85 - 1.0					7.4	98.6
+1.0 - 1.2					1.3	99.9
+1.2 - 1.4					0	
+1.4						

Bed Depth 190 - 215 mm

Resin(Volume%)	Anion		Inert (1)		Cation (99)	
Bead Diameter Fraction (mm)					Settled Volume(%)	Cumulative (%)
-0.30					0.3	
+0.30 - 0.425					2.8	3.1
+0.425 - 0.50					7.2	10.3
+0.50 - 0.60					19.4	29.7
+0.60 - 0.71					31.7	61.4
+0.71 - 0.85					23.3	84.7
+0.85 - 1.0					12.8	97.5
+1.0 - 1.2					1.7	99.2
+1.2 - 1.4					0.4	99.6
+1.4					0.4	100

TABLE A 3.08 BEAD SIZE ANALYSIS
LABORATORY COLUMN SEPARATION TEST 1.

Test 1a — Centre Port

Resin (volume %)	Anion (43)		Inert		Cation (57)	
Bead Diameter Fraction (mm)	Settled Volume (%)	Cumulative (%)			Settled Volume (%)	Cumulative (%)
−0.30						
+0.30 − 0.425					73.3	73.3
+0.425 − 0.50					22.3	95.6
+0.50 − 0.60					4.4	100.0
+0.60 − 0.71	} 2.9	2.9				
+0.71 − 0.85						
+0.85 − 1.0	14.7	17.6				
+1.0 − 1.2	29.4	48.0				
+1.2 − 1.4	52.9	99.9				
+1.4						

Test 1b — Centre Port

Resin (Volume %)	Anion (2)		Inert (64)		Cation (34)	
Bead Diameter Fraction (mm)			Settled Volume(%)	Cumulative (%)	Settled Volume(%)	Cumulative (%)
−0.30						
+0.30 − 0.425			1.9	1.9	48.3	48.3
+0.425 − 0.50			13.0	14.9	31.0	79.3
+0.50 − 0.60			44.4	59.3	13.8	93.1
+0.60 − 0.71			40.7	100	6.9	100
+0.71 − 0.85						
+0.85 − 1.0						
+1.0 − 1.2						
+1.2 − 1.4						
+1.4						

TABLE A 3.09   BEAD SIZE ANALYSIS
             LABORATORY COLUMN SEPARATION TEST 2.

Test 2a Centre Port

Resin(Volume%)	Anion (58)		Inert (17)		Cation (25)	
Bead Diameter Fraction (mm)	Settled Volume(%)	Cumulative (%)	Settled Volume(%)	Cumulative (%)	Settled Volume(%)	Cumulative (%)
-0.30						
+0.30 - 0.425			1.3	1.3	71.4	72.3
+0.425 - 0.50			71.0	72.3	20.3	92.6
+0.50 - 0.60	0.8	0.8	25.8	98.1	7.0	99.6
+0.60 - 0.71	2.3	3.1	1.9	100	0.4	100
+0.71 - 0.85	6.8	9.9				
+0.85 - 1.0	15.2	25.1				
+1.0 - 1.2	35.0	60.1				
+1.2 - 1.4	25.1	85.2				
+1.4	14.8	100				

Test 2b - Centre Port

Resin(Volume%)	Anion (7)		Inert (47)		Cation (46)	
Bead Diameter Fraction (mm)	Settled Volume(%)	Cumulative (%)	Settled Volume(%)	Cumulative (%)	Settled Volume(%)	Cumulative (%)
-0.30						
+0.30 - 0.425					31.4	31.4
+0.425 - 0.50			31.4	31.4	37.5	68.9
+0.50 - 0.60			58.8	90.2	28.2	97.1
+0.60 - 0.71	7.7	7.7	9.5	99.7	2.8	99.9
+0.71 - 0.85	3.8	11.5	0.3	100	0.3	100.2
+0.85 - 1.0	19.2	30.7				
+1.0 - 1.2	38.5	69.2				
+1.2 - 1.4	30.8	100				
+1.4						

Test 2c - Centre Port

Resin(Volume%)	Anion (3)		Inert (1)		Cation (96)	
Bead Diameter Fraction (mm)	Settled Volume(%)	Cumulative (%)	Settled Volume(%)	Cumulative (%)	Settled Volume(%)	Cumulative (%)
-0.30						
+0.30 - 0.425			20	20	1.3	1.3
+0.425 - 0.50			60	80	7.2	8.5
+0.50 - 0.60			20	100	40.9	49.4
+0.60 - 0.71	26.1	26.1			43.0	92.4
+0.71 - 0.85	43.5	69.6			6.1	98.5
+0.85 - 1.0	26.1	95.7			1.3	99.8
+1.0 - 1.2	4.3	100			0.1	99.9
+1.2 - 1.4						
+1.4						

TABLE A 3.10   BEAD SIZE ANALYSIS

LABORATORY COLUMN SEPARATION TEST 3

Test 3a - Centre Port

Resin (Volume %)	Anion (23)		Cation (77)	
Bead diameter Fraction (mm)	Settled Volume (%)	Cumulative (%)	Settled Volume (%)	Cumulative (%)
-0.30			0	
+0.30 - 0.425			0.7	0.7
+0.425 - 0.50	0		9.0	9.7
+0.50 - 0.60	2.3	2.3	70.7	80.4
+0.60 - 0.71	3.4	5.7	18.5	98.9
+0.71 - 0.85	6.8	12.5	0.7	99.6
+0.85 - 1.0	10.2	22.7	0.3	99.9
+1.0 - 1.2	22.7	45.4		
+1.2 - 1.4	20.5	65.9		
+1.4	34.1	100		

Test 3b - Centre Port

Resin (Volume%)	Anion (67)		Cation (33)	
Bead Diameter Fraction (mm)	Settled Volume (%)	Cumulative (%)	Settled Volume (%)	Cumulative (%)
-0.30			0	
+0.30 - 0.425			1.9	1.9
+0.425 - 0.50			22.7	24.6
+0.50 - 0.60	0.3	0.3	74.7	99.3
+0.60 - 0.71	1.6	1.9	0.6	99.9
+0.71 - 0.85	4.5	6.4		
+0.85 - 1.0	11.3	17.7		
+1.0 - 1.2	19.4	37.1		
+1.2 - 1.4	28.4	65.5		
+1.4	34.5	100		

Test 3b - Bottom Port

Resin (Volume %)	Anion		Cation (100)	
Bead Diameter Fraction (mm)			Settled Volume (%)	Cumulative (%)
-0.30				
+0.30 - 0.425				
+0.425 - 0.50				
+0.50 - 0.60			0	
+0.60 - 0.71			1.3	1.3
+0.71 - 0.85			16.0	17.3
+0.85 - 1.0			53.9	71.2
+1.0 - 1.2			23.4	94.6
+1.2 - 1.4			4.1	98.7
+1.4			1.3	100

TABLE A 3.10 (continued)

Test 3c - Top Port

Resin (Volume %)	Anion (96)		Cation (4)	
Bead Diameter Fraction (mm)	Settled Volume (%)	Cumulative (%)	Settled Volume (%)	Cumulative (%)
-0.30				
+0.30 - 0.425			84.6	84.6
+0.425 - 0.50	0.6	0.6	15.4	100
+0.50 - 0.60	5.7	6.3		
+0.60 - 0.71	50.0	56.3		
+0.71 - 0.85	37.1	93.4		
+0.85 - 1.0	6.6	100		
+1.0 - 1.2				
+1.2 - 1.4				
+1.4				

Test 3c - Centre Port

Resin (Volume %)	Anion (69)		Cation (31)	
Bead Diameter Fraction (mm)	Settled Volume (%)	Cumulative (%)	Settled Volume (%)	Cumulative (%)
-0.30			0	
+0.30 - 0.425			0.8	0.8
+0.425 - 0.50			19.1	19.9
+0.50 - 0.60			72.5	92.4
+0.60 - 0.71	0		7.6	100
+0.71 - 0.85	1.0	1.0		
+0.85 - 1.0	19.9	20.9		
+1.0 - 1.2	60.1	81.0		
+1.2 - 1.4	17.2	98.2		
+1.4	1.7	99.9		

Test 3c - Bottom Port

Resin (Volume %)	Anion		Cation (100)	
Bead Diameter Fraction (mm)			Settled Volume (%)	Cumulative (%)
-0.30				
+0.30 - 0.425				
+0.425 - 0.50				
+0.50 - 0.60				
+0.60 - 0.71			2.8	2.8
+0.71 - 0.85			19.7	22.5
+0.85 - 1.0			54.4	76.9
+1.0 - 1.2			17.9	94.8
+1.2 - 1.4			3.8	98.6
+1.4			1.3	99.9

TABLE A 3.11 STANDARD DEVIATIONS FOR DENSITY AND MOISTURE CONTENT DETERMINATIONS ON ION EXCHANGERS

EXCHANGER TYPE	IONIC FORM	NUMBER of RESULTS	Bead Density (δ) $(kg\ m^{-3})$		Moisture Content (M_v) (Volume Fraction)		Skeletal Density (ψ) $(kg\ m^{-3})$	
			Mean	Std. Dev.	Mean	Std. Dev.	Mean	Std. Dev.
Duolite C20 Gelular Cation Exchanger (DV)	Na^+	8	1286	6.8	.576	.005	710	3.6
Duolite C26 Macroporous Cation Exchanger (DV)	Na^+	6	1247	9.6	.619	.007	628	3.3
Amberlite IRA400 Gelular Anion Exchanger (DV)	SO_4^{2-}	8	1144	9.0	.562	.005	582	4.2
Duolite A101D Isoporous Anion Exchanger (DV)	Cl^-	8	1063	6.2	.537	.004	526	3.0
Dowex TG 650-C Gelular Cation Exchanger (SGB)	NH_4^+	8	1232	1.04				

DV Displaced Volume   SGB Specific Gravity Bottle

A P P E N D I C E S   T O   C H A P T E R   4

A4.1   RESIN MIXING COLUMN TESTS

    A4.1.1   COLUMN ARRANGEMENT

    A4.1.2   MIXING AND SAMPLING PROCEDURE

    A4.1.3   RESIN MIXTURE ANALYSIS

A4.2   SAMPLE CORES FROM PLANT MIXED BEDS

    A4.2.1   MAKE UP MIXED BEDS

    A4.2.2   CONDENSATE PURIFICATION MIXED BED

DATA TABLES

A4.01   VARIATION OF MIXED RESIN RATIO WITH FREE WATER

A4.02   RESIN MIXING PROFILE - MAKE UP MIXED BEDS

A4.03   RESIN MIXING PROFILE - CONDENSATE PURIFICATION MIXED BED

Deionised Water
from header tank

Vent

v○

e○

S60MG
Regulator

Free Water ─────

Sample
Ports

Compressed
Nitrogen
Cylinder

○b

Perforated
Support Plate

○c

d○   ○a

Drain
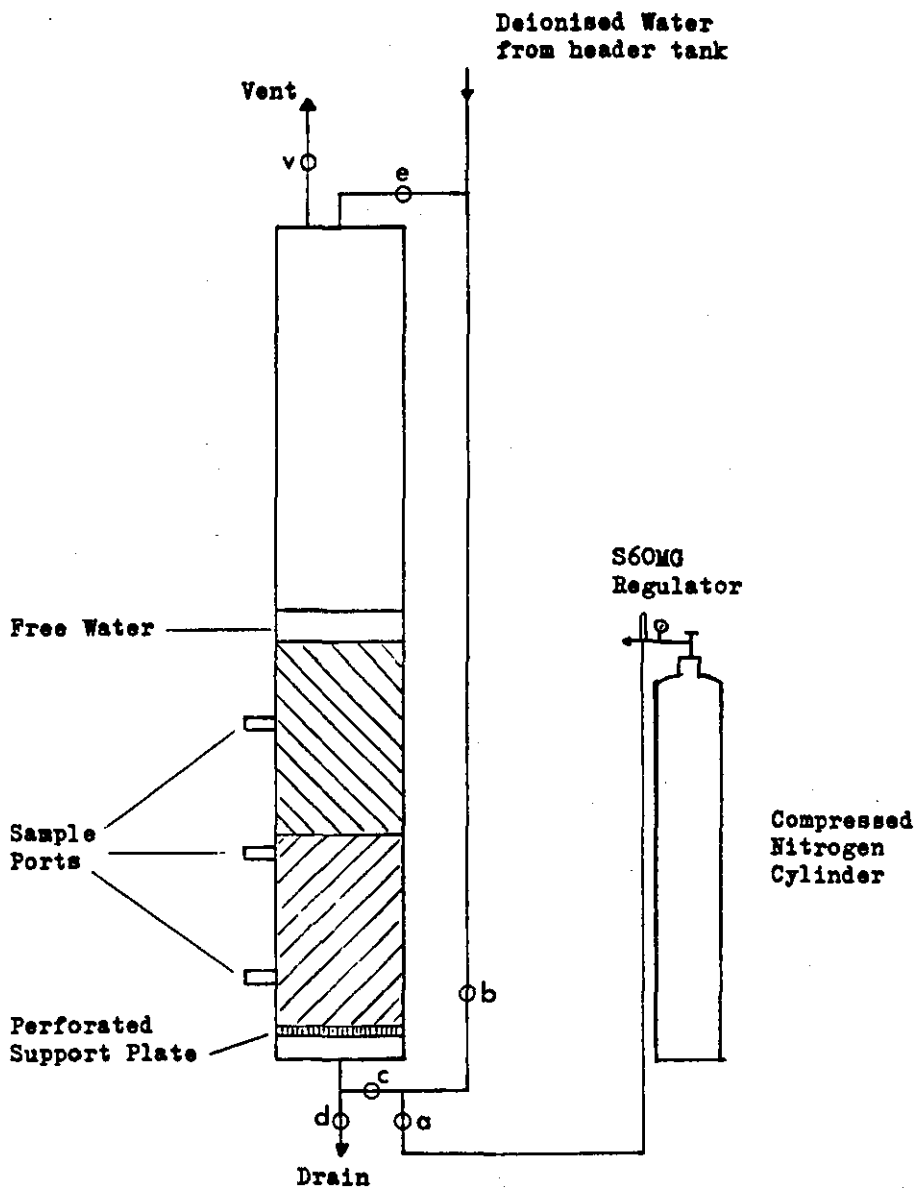
Column Data:
Height - 1300 mm;   Internal Diameter - 95 mm
Settled Bed Depth   600 - 610 mm
Anion Exchanger - 2.1 litres;   Cation Exchanger - 2.1 litres
Materials
Column - Clear Acrylic Tube   3 mm wall thickness
Fixed Pipework - ABS ½ inch BSP
Valves - ABS ball valves except (a) an ABS Saunders Valve

FIGURE
No.
A4.01   COLUMN ARRANGEMENT FOR RESIN MIXING TESTS

A 4.1 RESIN MIXING COLUMN TESTS

A 4.1.1 COLUMN ARRANGEMENT

The column was the same as that described in Appendix 3 except that provision was made for the admission of mixing gas into the pipework below the column base plate and bed support. The general arrangement of gas supply, control and admission to the column is shown in Figure A 4.01. The mixing gas was vented to the atmosphere at the top of the column.

Compressed nitrogen at 130 bar pressure in the cylinder was reduced in pressure and the flow controlled and monitored by a British Oxygen Co. type S 60 MG regulator. Nitrogen was used for mixing as the available compressed air cylinders were not suitable for use with the S 60 MG regulator in this application. The suspended ball flow meter on the S 60 MG was factory calibrated for 0 - 10 litre minute^{-1} oxygen flow and it was assumed that nitrogen would be similar. It was not considered necessary to have an accurate gas flow calibration as all tests would be operated at a gas flow well above the minimum for good mixing.

A 4.1.2 MIXING AND SAMPLING PROCEDURE

2.1 litres (settled volume) each of conditioned cation exchanger Zerolit 525 ($Na^+ \rightarrow H^+$ form) and conditioned anion exchanger Zerolit FF(ip) ($Cl^- \rightarrow OH^-$ form) were loaded into the column and the top collar and plate replaced. The vent valve (v) (Figure A4.01) was opened and the resins backwashed with water from the header tank via valves (b) and (c) to ensure maximum separation. The settled bed depth of separated resins was 610 mm. The water above the bed was drained via valve (d) to give the desired level of free water above the upper surface of the resin. Valve (d) was closed and valves (a) and (c) opened to admit the mixing nitrogen gas. The gas flow rate was adjusted to an indicated 10 litres per minute using the S 60 MG regulator. This was equivalent to 1.4 m^3 m^{-2} minute^{-1} gas flow rate, well above the minimum flow rates

of $0.85 \text{ m}^3 \text{ m}^{-2} \text{ minute}^{-1}$ (211) and $1.0 \text{ m}^3 \text{ m}^{-2} \text{ minute}^{-1}$ (140) noted
by earlier workers. Valve (e) remained closed at all times.

After 10 minutes mixing the gas flow was stopped, valves (a) and (c)
closed and the mixed resins were allowed to settle under gravity.
When settled, the level of free water was again measured, and was
generally slightly greater than at the start. Both before and after
depths of free water are given in Table A 4.01. The small increase
was due to two factors; the lower voidage of a mixed bed compared to
a backwashed bed, giving a smaller bed height for the former and
also a small volume of residual water below the bottom collector,
left after draining down, being pushed into the bed by the mixing gas.
The settled bed height after mixing was about 10 mm less than the bed
height with separated resins. If there was an upper layer of pure
anion exchanger its depth from the upper resin surface was estimated
(Table A4.01).

Once the bed had settled it was drained down completely via valve (d)
to remove the majority of the interstitial water. The plugs in the
sample ports were then removed and a 20 mm diameter thin walled brass
tube inserted into each port and pushed slowly, horizontally across
the bed. The core tube was rotated and slowly withdrawn bringing
with it a core containing about 25 ml of mixed resins. Each core
was washed into a glass screw topped jar for subsequent mixture
analysis.

The plugs were replaced into the sample ports and a volume of mixed
resins equal to that sampled was returned to the bed, and the bed
once again backwashed to separate the mixed resins. The free water
above the separated resins was drained to a different level and the
mixing, draining and core sampling procedures repeated. Eight mixing
tests were carried out with initial free water depths varying from
0 -190 mm.

A 4.1.3   RESIN MIXTURE ANALYSIS

The method of differential flotation in saturated sodium chloride
solution was used, as described in A 3.2.   From the settled volumes
of separated resin the total sample volume and the percentages of

cation and anion exchanger were calculated. The latter figures are recorded in Table A 4.01 for each of the three sample cores in the eight mixing tests.

A 4.2   SAMPLE CORES FROM PLANT MIXED BEDS

The samples taken from full scale mixed beds after normal mixing were not taken by the author and were not intended primarily as samples for estimating the mixed resin profiles down a bed.

A 4.2.1   MAKE UP MIXED BEDS

The samples depicted in Figure 4.03 were taken by the operating staff from two identical mixed beds operating in parallel. The samples were intended solely to examine resin from different bed depths and the sample depths supplied by the operators are only approximate. Nevertheless, when analysed the samples showed the pattern of cation exchanger rich lower layer, anion exchanger rich upper layer.

Because more sample was available a different technique of resin separation was used. About 100 ml of mixed resins was added to a 25 mm internal diameter clear perspex column, 600 mm long with a porous polyethylene support at the bottom. The top of the column was closed with a rubber bung that had a hole through it and a nylon hose connector inserted in the hole. A tube led from the hose connector to waste.

The resin was backwashed with tap water at a flow rate sufficient to fluidise and separate the resins but not high enough to wash the anion exchanger out of the column. When separated, the water flow was increased and the upper layer of anion exchanger was washed out of the column, collected on a fine mesh sieve and placed in a 100 ml measuring cylinder. Next the intermediate zone of mixed large anion and small cation exchangers were washed out of the column. The two resins were separated by sieving out the large anion exchangers on a 0.71 mm mesh sieve, the smaller cation exchanger beads passing through. The anion exchanger was added to the previous collected volume. The cation exchanger was similarly stored and to it was added the remaining separated cation exchanger from the columns. The separated

resin volumes and the percentage of each exchanger in the mixture are given in Table A 4.02.

This rather complicated method of separation was used because the separated samples were required for further analysis and contact with saturated brine would have altered the condition of the resins.

A.4.2.2 CONDENSATE PURIFICATION MIXED BED

In this example (Figure 4.04) the same charge of resins in the same operator vessel was sampled at the end of one operating cycle and again at the end of the next operating cycle after an external regeneration. The mixed bed was mixed 'blind' by an operator in a separate building 100 m away. The vertical sample cores were taken by colleagues using a 100 mm diameter post hole auger, which extracts a core about 150 mm deep. The technique was to use the auger to extract a vertical core in 150 mm segments and retain those at the appropriate bed depth as indicated by marks on the auger handle.

The mixed resin ratio for these samples was estimated by backwashing a 100 - 150 ml sample in the column described above (A 4.2.1) and then allowing the separated resins to settle. Because there was sufficient colour difference between the exchangers it was possible to measure the settled bed depth of each resin and estimate the mixed ratio in the small overlap zone. Therefore, the separated resin depths were proportional to the mixed resin ratio in the core samples. Both separated resin depths and percentages are given in Table A 4.03.

TABLE A 4.01   VARIATION OF MIXED RESIN RATIO WITH FREE WATER DEPTH.

SAMPLE CORES TAKEN AT 70, 270 and 470 mm ABOVE THE BOTTOM OF THE BED.

Depth of Free Water (mm)		RESIN MIXTURE IN SAMPLE CORES						Depth of 100% Anion Exchanger at top of bed (mm)	Notes
		TOP SAMPLE (470 mm)		CENTRE SAMPLE (270 mm)		BOTTOM SAMPLE (70 mm)			
Prior to mixing	After mixing	Anion Exch(%)	Cation Exch(%)	Anion Exch(%)	Cation Exch(%)	Anion Exch(%)	Cation Exch(%)		
0	10	49	51	48	52	49	51	3	Slow mix, pronounced slugging, voids left throughout bed.
7	15	49	51	48	52	48	52	5	Slugging in bottom half of bed leaving voids.
20	30	36	64	44	56	46	54	20	Fluid mixing
30	45	39	61	40	60	46	54	-	Fluid mixing
55	65	58	42	25	75	47	53	60	
100	110	95	5	19	81	40	60	150	Fluid mixing 115 secs to settle bed.
120	140	97	3	19	81	35	65	175	Very fluid mixing.
190	195	97	3	20	80	23	77	180-200	Very fluid mixing.

TABLE A 4.02   MIXED RESIN PROFILE DATA FOR MIXING IN
                IDENTICAL IN-SITU REGENERATED MIXED BEDS.

SAMPLE DEPTH BELOW TOP OF BED (m)	MIXED BED 2				MIXED BED 3			
	Separated Sample Resin Volume (ml)		Resin Mixture (%)		Separated Sample Resin Volume (ml)		Resin Mixture (%)	
	Anion Exch	Cation Exch	Anion Exch	Cation Exch	Anion Exch	Cation Exch	Anion Exch	Cation Exch
0.3	38.6	1.7	96	4	43.8	1.7	96	4
0.61	35.7	17.3	67	33	39.5	7.0	85	15
0.61 - 0.85	15.5	28.5	35	65	16.0	28.0	36	64
0.85 - 1.1	12.5	26.5	32	67	-	-	-	-

Mixed Bed: 1.82 m^3 each of anion and cation exchanger in a

2.13 m diameter vessel = bed depth 1.1 m

TABLE A 4.03   MIXED RESIN PROFILE DATA FOR REMOTELY
MIXED CONDENSATE PURIFICATION MIXED BED
ON TWO SEPARATE OCCASIONS.

Sample Depth Below Top of Bed (m)	MIXED BED SAMPLED 2.4.79				MIXED BED SAMPLED 25.4.79			
	Separated Sample Resin Height (mm)		Resin Mixture (%)		Separated Sample Resin Height (mm)		Resin Mixture (%)	
	Anion Exch	Cation Exch	Anion Exch	Cation Exch	Anion Exch	Cation Exch	Anion Exch	Cation Exch
TOP	305	3	99	1	320	10	97	3
0.30	310	7	98	2	280	30	90	10
0.61	145	165	45	55	145	155	48	52
0.91	70	245	22	78	125	200	38	62
1.22	110	23	32	68	135	190	41	59
1.52	130	210	38	62	175	220	44	56

Mixed Bed: 4.25 m^3 each of cation and anion exchanger
in 2.44 m diameter unit = bed depth 1.82 m.

APPENDICES TO CHAPTER 5

A5.1   SCANNING ELECTRON MICROGRAPHS OF NEW ANION EXCHANGE RESINS

    A5.1.1   MATRIX CONFIGURATIONS

A5.2   CONDITIONING, PREPARATION AND REGENERATION OF RESINS

    A5.2.1   APPARATUS
    A5.2.2   CONDITIONING NEW ANION EXCHANGE RESINS
    A5.2.3   SIEVING NEW ANION EXCHANGERS
    A5.2.4   ANION EXCHANGER REGENERATION
    A5.2.5   CONDITIONING RESINS FROM OPERATIONAL PLANTS
    A5.2.6   CONDITIONING AND REGENERATION OF CATION EXCHANGERS

A5.3   TEST RIG CONSTRUCTION AND OPERATION

    A5.3.1   MIXED BED TEST COLUMN
    A5.3.2   POLISHING MIXED BED COLUMNS
    A5.3.3   TEST COLUMN OPERATION

A5.4   INSTRUMENTATION AND ANALYSIS

    A5.4.1   CONDUCTIVITY
    A5.4.2   SODIUM ION ANALYSIS
    A5.4.3   ANION ANALYSIS
    A5.4.4   EXTRACTABLE ORGANIC FOULANTS
    A5.4.5   EXTRACTABLE IRON

DATA TABLES

A5.09   SIEVE ANALYSIS FOR NEW ANION EXCHANGE RESINS
A5.10   TEST COLUMN LEAKAGES - NEW RESINS CHLORIDE DOSING
A5.11   TEST COLUMN LEAKAGES - NEW RESINS SULPHATE DOSING
A5.12   MASS TRANSFER COEFFICIENTS - NEW RESINS CHLORIDE EXCHANGE
A5.13   MASS TRANSFER COEFFICIENTS - NEW RESINS SULPHATE EXCHANGE
A5.14   ANION LEAKAGES FROM NEW A161
A5.15   LEAKAGES FROM BICARBONATE FORM RESIN
A5.16   TEST COLUMN LEAKAGES - DELIBERATELY FOULED - CHLORIDE DOSING
A5.17   TEST COLUMN LEAKAGES - DELIBERATELY FOULED - SULPHATE DOSING
A5.18   MASS TRANSFER COEFFICIENTS - DELIBERATELY FOULED - CHLORIDE
       EXCHANGE
A5.19   MASS TRANSFER COEFFICIENTS - DELIBERATELY FOULED - SULPHATE
       EXCHANGE

FIGURE A5.01 ELECTRON MICROGRAPHS OF ANION EXCHANGE RESINS
MAGNIFICATION x 10^4
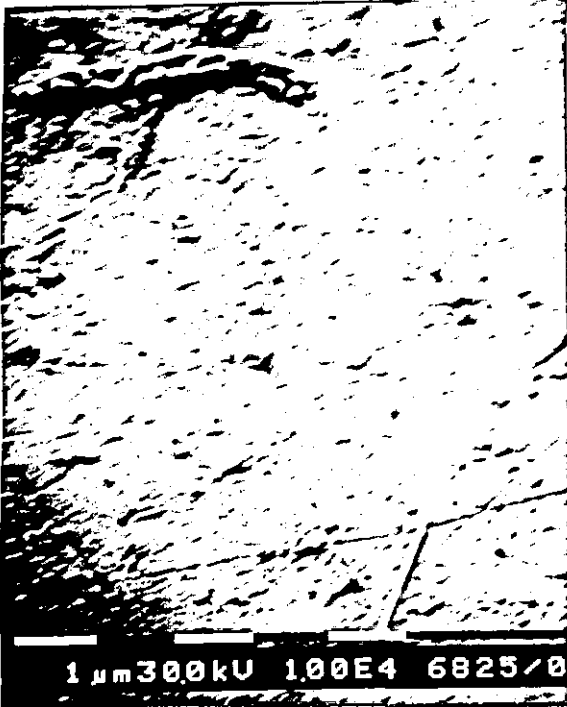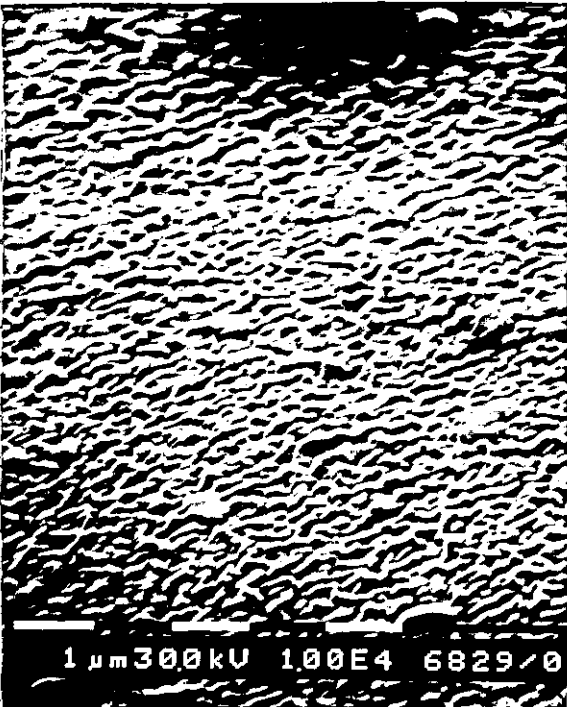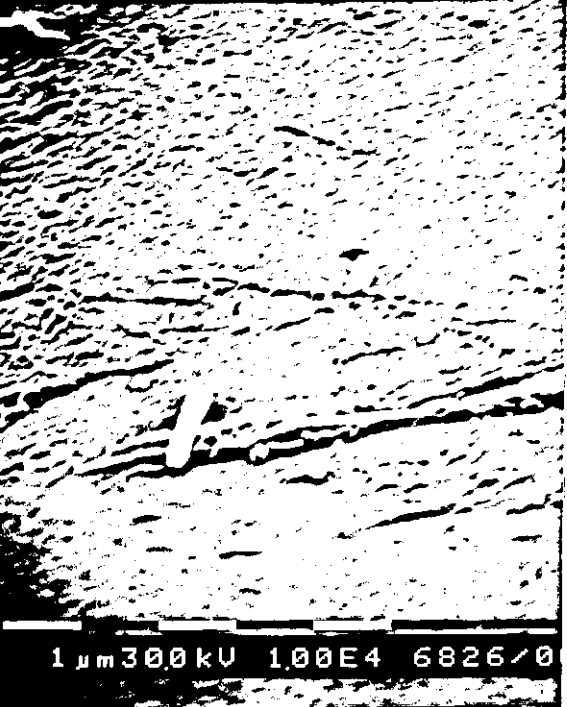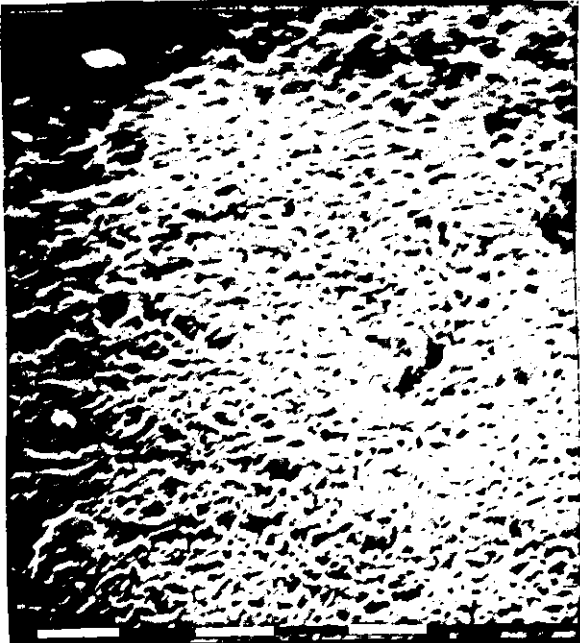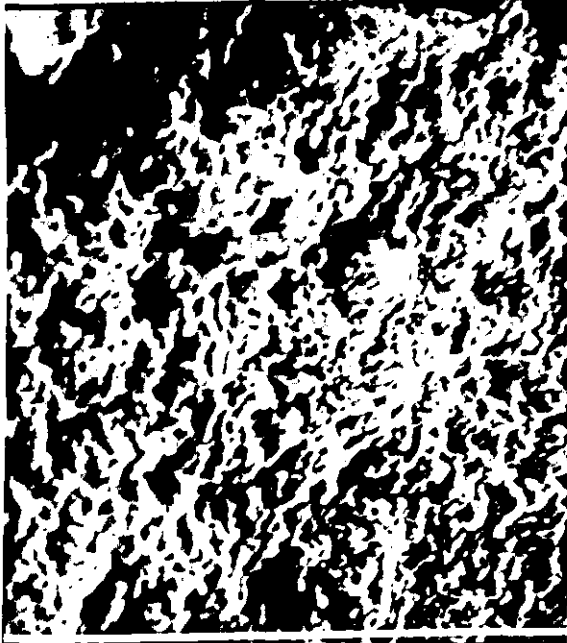
a.   IRA402 PS/DVB
     Gelular Surface

b.   A101D PS/MB
     Isoporous Internal

c.   IRA458 PA/DVB
     Gelular Surface

d.   A161 PS/DVB
     Macroporous Surface

FIGURE A5.01 (continued)

e.   IRA900 PS/DVB
      Macroporous Surface

f.   Z-MPF PS/DVB
      Macroporous Surface

g.   IRA900 PS/DVB
      Macroporous Internal

h.   Z-MPF PS/DVB
      Macroporous Internal

A5.1   SCANNING ELECTRON MICROGRAPHS OF NEW ANION EXCHANGER RESINS

The scanning electron micrographs were obtained on polaroid film
using a Philips Model 505 Scanning Electron Microscope.

The magnification is 10,000 times and micrographs of the external
and internal structure were obtained. The resin samples were
prepared by soaking in propan-2-ol to remove internal moisture and
then air drying. This process keeps the internal structure more
open than air drying the moist resin. Some of the dried resins were
cut open with a scapel. Whole beads and part beads were mounted on
aluminium stubs using a silver DAG adhesive. The mounted resins
were coated with a thin layer of platinum to provide a conducting
path between resin and stub.

A5.1.1   MATRIX CONFIGURATIONS

The two gelular styrene resins show no visible matrix structure, the
polymer being continuous. The large holes in the isoporous resin are
characteristic of this type of polymer but are not considered as
pores. (Figure A5.01a and b).

The gelular acrylic resin typically has the wrinkled surface shown
in Figure A5.01c. This wrinkling may be the product of resin drying.
The internal structure looks very similar.

The macroporous resins show a greater variation in both bead surface
and internal structure. A161 (Figure A5.01d).has an almost smooth
surface, while definite pore openings can be seen in the surface of
the IRA900 and Z-MPF resins. (Figures A5.01e and f). .Internally
the A161 and IRA900 matrices are similar (Figure A5.01g) and a
definite structure of agglomerated microspheres can be seen. The
internal structure of Z-MPF is quite different (Figure A5.01h)
consisting of much larger and more angular granules in the agglomerates.

Subsequent examination of other macroporous resins has shown that a
surface skin over a coaser internal structure is a common feature.

Backwash
Regeneration
Rinse
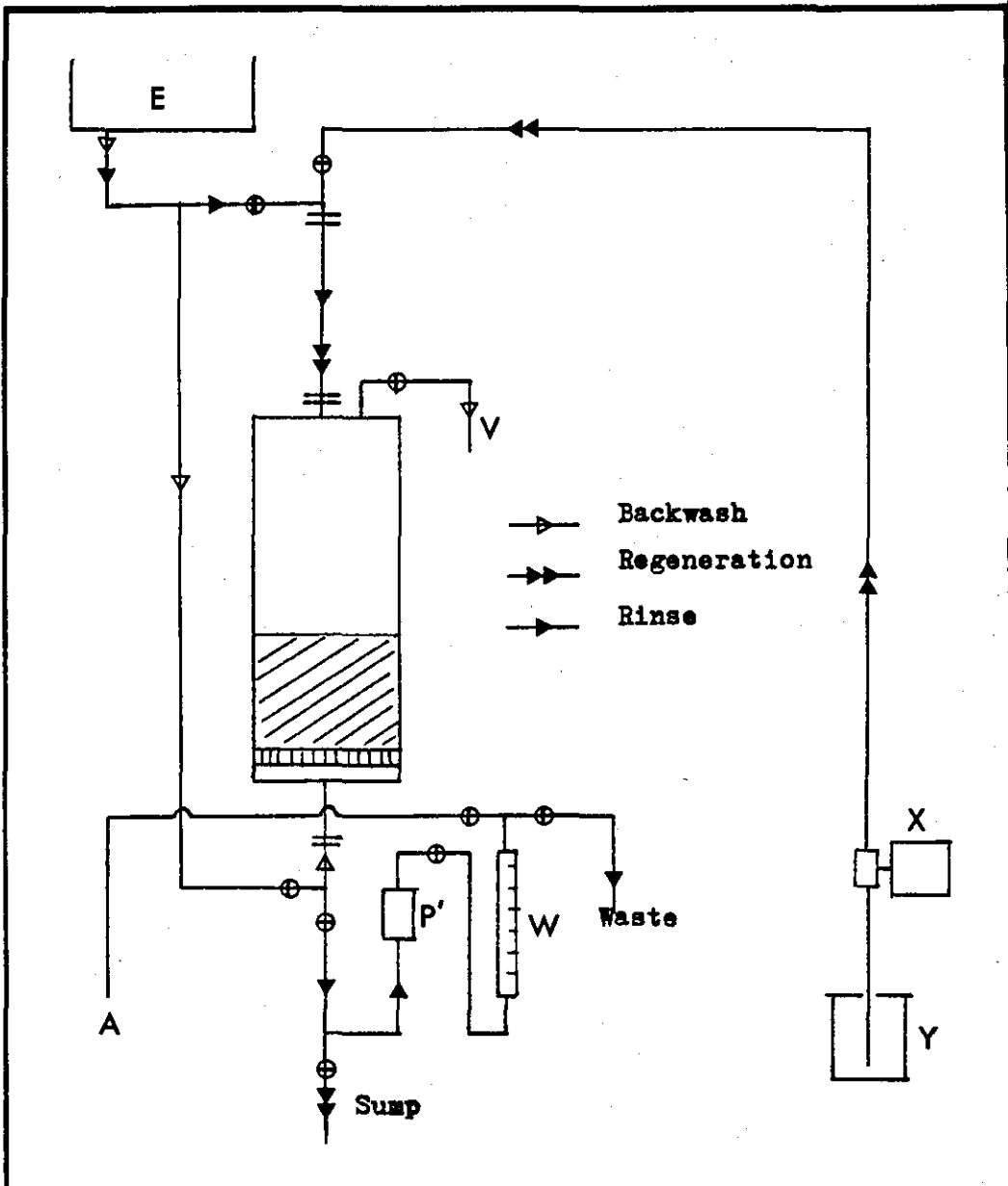
FIGURE
No. A5.02   CONDITIONING AND REGENERATION COLUMN

TABLE A5.01   <u>CONDITIONING CYCLE</u>

Regeneration:	10 litres of 1M NaOH injected at 5 litres per hour
Displacement rinse:	5 litres of deionised water injected via dosing pump at 5 litres per hour.
Fast rinse:	Deionised water at 30 litres per hour until the column outlet conductivity fell below $20\mu Scm^{-1}$.
Exhaustion:	10 litres of 1M NaCl injected at 5 litres per hour
Displacement rinse:	As above
Fast rinse:	As above

TABLE A5.02   <u>ANION EXCHANGER REGENERATION</u>

Regeneration level:	80 g NaOH per litre resin.
Regenerant injection:	3-4 litres per hour, minimum injection time of 20 minutes.
Displacement rinse:	2 Bed volumes of deionised water at the same flow rate as the regenerant injection.
Fast rinse:	Deionised water at 30 bed volumes per hour until the conductivity at the column outlet is $< 10 \mu S\ cm^{-1}$.

Note: 1 Bed volume = settled volume occupied by resin.

A5.2 CONDITIONING, PREPARATION AND REGENERATION OF RESINS

A5.2.1 APPARATUS

Resin conditioning was carried out in a 0.7 m long, 95 mm diameter column that was inserted in place of the polishing column in the kinetic test apparatus (Fig 5.02). This gave a ready supply of rinsing and backwashing water. The column construction was similar to that described in A3.3.1 except that there were no sampling ports. The column could accommodate up to four litres of resin. The general arrangement of the conditioning column is given in Figure A5.02.

Deionised water from the header tank E could be directed, by means of valves, either to the base of the column to flow upwards and out via the vent line V or down through the column and then via the conductivity cell P and flow meter W to waste. Regenerant or exhaustant solution was held in resevoir Y, a 20 litre polyethylene container, and was pumped via the dosing pump V (Nikkiso diaphragm displacement pump type BZ 10) to the top of the column through the resin and to the waste solution sump. Care was taken not to introduce regenerant/exhaustant into the conductivity cell P. When rinsing a resin with deionised water, via P and W, the valve leading to the sump was opened slightly to ensure any chemicals left in the dead leg were not eluted into the rinse water.

A5.2.2 CONDITIONING NEW ANION EXCHANGE RESINS

All the anion exchangers were received in the chloride form. Three litres of a resin were loaded into the column and backwashed to remove any debris. Conditioning, to elute manufacturing residues and ensure the resin was in a standard form, consisted of alternate regeneration with 1M sodium hydroxide solution and exhaustion with 1M sodium chloride solution, with intermediate rinsing, for three cycles. The solution volumes, injection rates and rinse conditions for one cycle are given in Table A5.01.

A5.2.3. SIEVING NEW ANION EXCHANGERS

The conditioned chloride form resins from the procedure in A5.2.2
contained the normal size range of resins from 0.3 - 1.2 mm,
although not all the different types would have the same distribution
or mean bead diameter. To minimise the extremes of the distributions
all conditioned samples were wet sieved to remove those beads above
1.0 mm and below 0.5 mm. Two sieves, each 0.6 m diameter, with
stainless steel mesh sizes 0.5 mm and 1.0 mm (BS 410   ) were
used and the resins washed through with deionised water.

A5.2.4 ANION EXCHANGER REGENERATION

All the anion exchange resins whether new, deliberately fouled or
taken from operational plants were all regenerated in an identical
manner. The regeneration level was 80 g NaOH per litre of resin
injected as a 1M solution, ie the volume of regenerant was adjusted
to the volume of resin being regenerated. The procedure is outlined
in Table A5.02.

The volume of resin regenerated varied with the test conditions.
For the new and deliberately fouled resins it was one litre, but
for the samples from operational plants it could be as little as
0.5 litre, although one litre was preferred.

A5.2.5 CONDITIONING RESINS FROM OPERATIONAL PLANTS

Resins that are sampled from operating plants may be exhausted or
partially regenerated. It is desirable to fully exhaust them before
regeneration to put them in a standard state. However, in order to
assess their performance potential it is necessary to retain any
foulants on the resin. Use of 1M NaCl as an exhaustant is likely
to elute organic foulants, therefore an excess of 0.05M $NaHCO_3$ was
used to exhaust the resin. The low selectivity of the resin for
$NaHCO_3$ is unlikely to displace significant quantities of organic
foulants at the concentrations employed.

TABLE A5.03 CATION EXCHANGER CONDITIONING

Delivered form: sodium

Pre-conditioning: soak in water for two weeks(minimum) and then
backwash to remove eluted sulphonated residues.
Four litres of resin loaded into regeneration
column.

A Sodium form cycle - 3 cycles

Regeneration:	10 litres 1M HCl injected at 5 litres per hour
Displacement rinse:	5 litres deionised water at 5 litres per hour
Fast rinse:	Deionised water at 30 BV hr^{-1} until column outlet conductivity below 20 μS cm^{-1}
Exhaustion:	10 litres 1M NaCl solution at 5 litres per hour
Displacement and Fast Rinse:	As above
Final Regeneration:	8 litres of 1M HCl at 5 litres per hour (73 g HCl per litre resin)
Displacement and Fast Rinse:	As above but to < 10 μS cm^{-1} outlet conductivity

B Ammonium form cycle

Conversion:	20 litres 0.5M $(NH_4)_2SO_4$ at 8 litres per hour to convert $Na^+ \rightarrow NH_4^+$ form
Regeneration:	10 litres 0.5M H_2SO_4 at 5 litres per hour
Displacement and Fast Rinse:	As above in A
Exhaustion:	10 litres 0.5M $(NH_4)_2SO_4$ at 5 litres per hour
Displacement and Fast Rinse:	As above
Final Regeneration:	16 litres of 0.5M H_2SO_4 at 8 litres per hour (200 g H_2SO_4 per litre resin)
Displacement and Fast Rinse	As above but to a conductivity of < 5 μS cm^{-1} at the column outlet.

FIGURE A5.03   KINETIC TEST RIG AND TEST COLUMN

A5.2.6 CONDITIONING AND REGENERATION OF CATION EXCHANGERS

A single production batch of Amberlite IR200 macroporous cation
exchanger has been used for all column tests. For the new and
deliberately fouled anion exchanger tests the cation exchanger was
conditioned to and regenerated from the sodium form, but for the
tests with operational plant samples the cation exchanger was
conditioned to and regenerated from the ammonium form, the most
likely ionic form of a CPP cation exchanger.

Table A5.03A gives the procedures for sodium form resin conditioning
and regeneration, Table A5.03B the procedures for ammonium form resin
conditioning and regeneration. The sodium form resin was regenerated
with hydrochloric acid to minimise residual sulphate elution from
the regenerated resin. The ammonium form resin was regenerated with
sulphuric acid, typical of full scale plant conditions. Three
conditioning cycles were run for each resin.

Prior to conditioning the new resins were left standing in water.
This eluted considerable amounts of dark coloured sulphonated
manufacturing residues, which were back-washed away when the resin
was first loaded into the column.

A5.3 TEST RIG CONSTRUCTION AND OPERATION

Outlines of the test column operation have been presented in section
5.3   together with diagramatic representations of the flow paths.
Figure A5.03 is photographs of the test column apparatus in its
final state as described in section 5.3.10. The mixed bed test
column is to the left and the regeneration column to the right.
The conductivity recorder is centre right and the sodium ion monitor
centre left. The heater/cooler units are at the far right hand side.
Table A5.04 is a list of the main materials of construction and types
of equipment.

A5.3.1 MIXED BED TEST COLUMN

The mixed bed test column was a clear acrylic tube 1250 mm long,
51 mm internal diameter and 3 mm wall thickness. The end terminations

TABLE A5.04   KINETIC TEST COLUMN RIG CONSTRUCTION

Framework: speedframe 25 mm square steel tube

(A)   Storage tanks - 2 x 200 litre (50 gallon) polypropylene

(B) (C)   Cooler/Heater - Grant types FC20 and FH15

(D)   Pump to Header Tank - Stuart Turner Centrifugal 100W

(E)   Header Tank- 60 litres capacity polypropylene

(F)   Booster Pump - Little Giant 4MD. Magnetically coupled centrifugal

　　　　　　　　　　pump

(G)   Test Column - Clear acrylic 51 mm internal diameter, 3 mm wall

　　　　　　　　　　thickness

(H)   Industrial pH cell - Kent Type 101A

(J)   Conductivity Cell (Inlet) - KIM type EFC.Cell constant 0.1

(L)   Influent Dosing Pump - Gilson Minipuls 2,4 channel pump

(N)   Flow Controller - Platon Type   FVA 0 - 10 litre min^{-1}

(P)   Conductivity Cell (Outlet) - KIM type EFD. Cell constant 0.01

(T)   Flow Meter - Platon Type   PGU 0 - 10 litre min^{-1}

Pipework and fittings : Half and three quarter inch BSP pipework in

　　　　　　　　　　　　acyrlonitrile butadiene styrene (ABS)

Valves : ABS bodied ball valves

Conductivity Recorder : KIM RC250L 3 point

Sodium Analyser : KIM Model 89 specific ion analyser using a sodium

　　　　　　　　　responsive glass electrode. Linked to KIM model

　　　　　　　　　7050 pH/pIon meter.

of the column were of a similar pattern to that described in A3.3.1 for the 95 mm diameter column, ie a recessed base plate and collar with an intervening 'O' ring seal. The base plate and collar were 113 mm overall diameter, machined from 25 mm thick acrylic block. Three bolts 60 mm long clamped the base plate and collar together. The base plate had a half inch BSP threaded inlet/outlet connection.

The resin support was of a similar pattern to that described in A3.3.1, ie a 12 mm thick perforated acrylic disc covered in fine mesh (70 μm) stainless steel gauze. There were 61 perforations, each 2 mm diameter. The perforated support plate was glued into the test column with the upper surface 30 mm above the base of the column. This was to ensure plug flow conditions were maintained right through the bed and the narrower outlet connection at the base of the column had little influence. The 40 ml volume chamber beneath the support plate was displaced every 1.3 seconds at the lowest flow rate.

A5.3.2   POLISHING MIXED BED COLUMNS

Two different arrangements of polishing mixed bed column were used (sections 5.3.5 and 5.3.10). In both cases 95 mm internal diameter columns were used with end plates and resin support plates as described in A3.3.1. In the earlier tests (Section 5.3.5) the polishing column was 700 mm long and contained 2.0 l of highly regenerated resins, in a 1:1 C:A mixture, while in the later arrangement (section 5.3.10) the column length was reduced to 500 mm with 1.5 l of mixed resins in a 2:3 ratio of cation:anion exchanger. The ratio of anion exchanger was increased as dissolved carbon dioxide was the major impurity in the column feed from the header tank.

A5.3.3   TEST COLUMN OPERATION

The deionised water in the lower storage tank was topped up from an Elga barrel 2000 deioniser. Circulation was set up between the lower storage and upper header tanks and the heater/cooler units switched on to adjust the bulk water temperature to 20 °C. While the water temperature reached equilibrium a mixed bed was prepared in the test column as described in section 5.3.6.

TABLE A5.05   <u>CONDUCTIVITY (20 $^{\circ}$C) OF DOSED INFLUENT</u>

Influent Concentration		Conductivity
(μg kg^{-1})	(μeq l^{-1})	(μS cm^{-1})
1480 μg kg^{-1}Cl^{-1} as NaCl	41.7	4.79
2960 μg kg^{-1}Cl^{-1} as NaCl	83.4	9.54
5920 μg kg^{-1}Cl^{-1} as NaCl	166.8	19.04
2000 μg kg^{-1}SO$_4^{2-}$ as Na$_2$SO$_4$	41.7	4.90
4000 μg kg^{-1}SO$_4^{2-}$ as Na$_2$SO$_4$	83.4	9.76
8000 μg kg^{-1}SO$_4^{2-}$ as Na$_2$SO$_4$	166.8	19.48
5165 μg kg^{-1}NO$_3^-$ as NaNO$_3$	83.4	9.19
4000 μg kg^{-1}HPO$_4^{2-}$ as Na$_2$HPO$_4$	83.4	8.04

DOSING SOLUTION/PUMP TUBE COMBINATIONS

Pump tubes were either a pair with 1.14 mm internal diameter or a pair with 1.85 mm internal diameter.

When the bulk water supply had reached 20 ^{o}C the polishing mixed bed
was brought into the circuit and operated at 2 litres min^{-1} flow
rate. Once the polishing mixed bed had rinsed down to give water
<0.1 µS cm^{-1} conductivity the test mixed bed was brought into the
circuit. The test column outlet conductivity was allowed to stabilise,
normally about 0.05 µS cm^{-1}, and the booster pump switched on. The
flow controller on the column outlet was then used to set the flow
rate. Flow was measured by timing the collection of one litre of
water. The measuring cylinder used for collection was calibrated
by weighing 1 kg of water into it. The 1.85, 3 and 4 litre per
minute flow rates represented the collection of 1 litre in 32.4,
20 and 15 seconds respectively. Timing was by means of a stopwatch
calibrated to 0.1 seconds.

The flow rate was initially set at 1.85 1 min^{-1} and , when the test
column outlet conductivity had stabilised, a sample of the outlet was
taken with no influent dosing. All samples were taken in 500 ml
screw capped polyethylene bottles. These bottles were conditioned by
filling and standing with deionised water several times over a two
week period and were always left full of deionised water. Each
bottle was marked with a particular flow rate/dosing concentration
and was used only for that combination.

As described in section 5.3.7 sodium chloride or sodium sulphate was
dosed into the test column influent at concentrations of 1480, 2960
and 5920 µg kg^{-1}Cl or the chemically equivalent 2000, 4000 and
8000 µg kg^{-1} SO$_4$. Dosing was controlled by the column inlet conduct-
ivity. Table A5.05 gives the conductivity values (20 ^{o}C) equivalent
to the various dosing concentrations. The speed of the infinitely
variable peristaltic pump used for dosing was adjusted to give the
required conductivity. Two different sized pump tubes were used to
obtain the necessary range of dosing rates to cover a four fold
increase in concentration and a two fold increase in flow rate.

Minor differences in procedure were used for the in service fouled
resins. The modified apparatus now contained the polishing mixed bed
in line before the dosing point (Figure 5.05). Therefore, once the
water temperature had stabilised at 20 ^{o}C, the flow was directed
through the polishing and test mixed beds. The test column flow

TABLE A5.06   DOSING CONDITIONS FOR IN SERVICE FOULED RESINS

(FLOW RATE 100 mh^{-1})

Influent Concentration	Influent Conductivity (μS cm^{-1}) (20 ^{o}C)	Dosing Solution Molarity
100 μg kg^{-1}Cl as NaCl	0.36	0.02
250 " " "	0.84	0.02
500 " " "	1.65	0.02
1000 " " "	3.25	0.2
2000 " " "	6.46	0.2
5000 " " "	16.09	0.2
135 μg kg^{-1}SO$_4$ as Na$_2$SO$_4$	0.37	0.01
338 " " "	0.86	0.01
676 " " "	1.68	0.01
1350 " " "	3.32	0.1
2700 " " "	6.60	0.1
6760 " " "	16.47	0.1

Pump tube 1.29 mm internal diameter.

was run under gravity from the header tank until the inlet and outlet
conductivities had stabilised. A single pump tube size was used on
the dosing pump and the dosing solution concentration varied to
achieve the necessary range of influent concentrations. Table A5.06
gives the influent conductivities and dosing solution concentration
details.

A5.4   INSTRUMENTATION AND ANALYSIS

A5.4.1   CONDUCTIVITY

Aqueous solution conductivity is the reciprocal of the resistance
of the solution. The resistance is measured as one arm of an a.c.
bridge circuit cell with electrodes of known dimensions. Commercial
conductivity cells have dimensions such that the cell constant is a
factor of ten times unity. In order to widen the measurement range
of a cell it is normal to include a replaceable range resistor.

The three conductivity cells used on the test rig were manufactured
by K.I.M and the bridge circuit was incorporated into a three channel
chart recorder (type RC250L) that read two decades of conductivity.
In order to fix the measurement range of a cell it is normal to
include a fixed resistor in the circuit Table A5.07 gives the
conductivity ranges for cells with cell constants 0.01 (test column
outlet) and 0.1 (test column inlet and regeneration side) for the
normal resistor values of 1K, 10K, and 100K ohm. To increase the
flexibility of conductivity measurement each conductivity measuring
circuit incorporated a switch that could vary the range resistor
between the three quoted values. This was particularly used for the
influent dosing and regenerant rinse down conductivity measurements.

Influent and effluent conductivity were monitored and recorded
throughout each test run.

TABLE A5.07 CONDUCTIVITY CELL RANGE RESISTORS

Range Resistor / Cell Constant	100 K Ω	10 K Ω	1K Ω
0.01	0.01-1.0μScm^{-1}	0.1-10μScm^{-1}	1.0-100μScm^{-1}
0.1	0.1-10μScm^{-1}	1.0-100μScm^{-1}	10-1000μScm^{-1}

A5.4.2 SODIUM ION ANALYSIS

The sodium ion responsive glass electrode was the only available
method for monitoring sodium ion concentrations in the 0 -20 μg kg^{-1}Na
region. A K.I.M model 89 specific ion monitor was used to house
the glass electrode and the saturated calomel reference electrode.
Integral peristaltic pumps fed in the sample, drawn from the test
column outlet sample point, and the ammonia vapour buffer. The
potential difference between the glass and reference electrodes was
fed to a K.I.M model 7050 pH/p ion meter which in turn fed a signal
to a chart recorder.

The sodium responsive glass electrode also exhibits a small response
to the ammonium ion introduced by the buffer. The theoretical limit
of detection for the glass elctrode with ammonia buffer is
0.3 μg kg^{-1} Na (239).

Because of the problems with maintaining μg kg^{-1} level sodium
standards free from contamination, calibration was carried out before
each run with standards containing 100, 500, 1000 and 2000 μg kg^{-1}Na.
The glass electrode response is a straight line log concentration vs
millivolts, ie Nernstian, correlation (239) and the calibration was
extrapolated back to 1 μg kg^{-1} Na, a standard procedure. Following
calibration the electrode assembly was fed with test column outlet
water to re-establish the undosed, base line conditions.

Each sodium chloride or sodium sulphate dosing condition lasted for
about five minutes. In this time period the response of the glass
electrode rose to about 95% of its equilibrium value. This was
considered acceptable.

Eluent Inlet

Anion
Concentrator
Column

Eluent Bypass
While Loading

Sample
Loading

Anion Separator
Guard Column

Anion Separator
Column

Anion Suppressor
Column
(H^+ form cation exchanger)

Conductivity Detector
(Output to recorder/integrator)
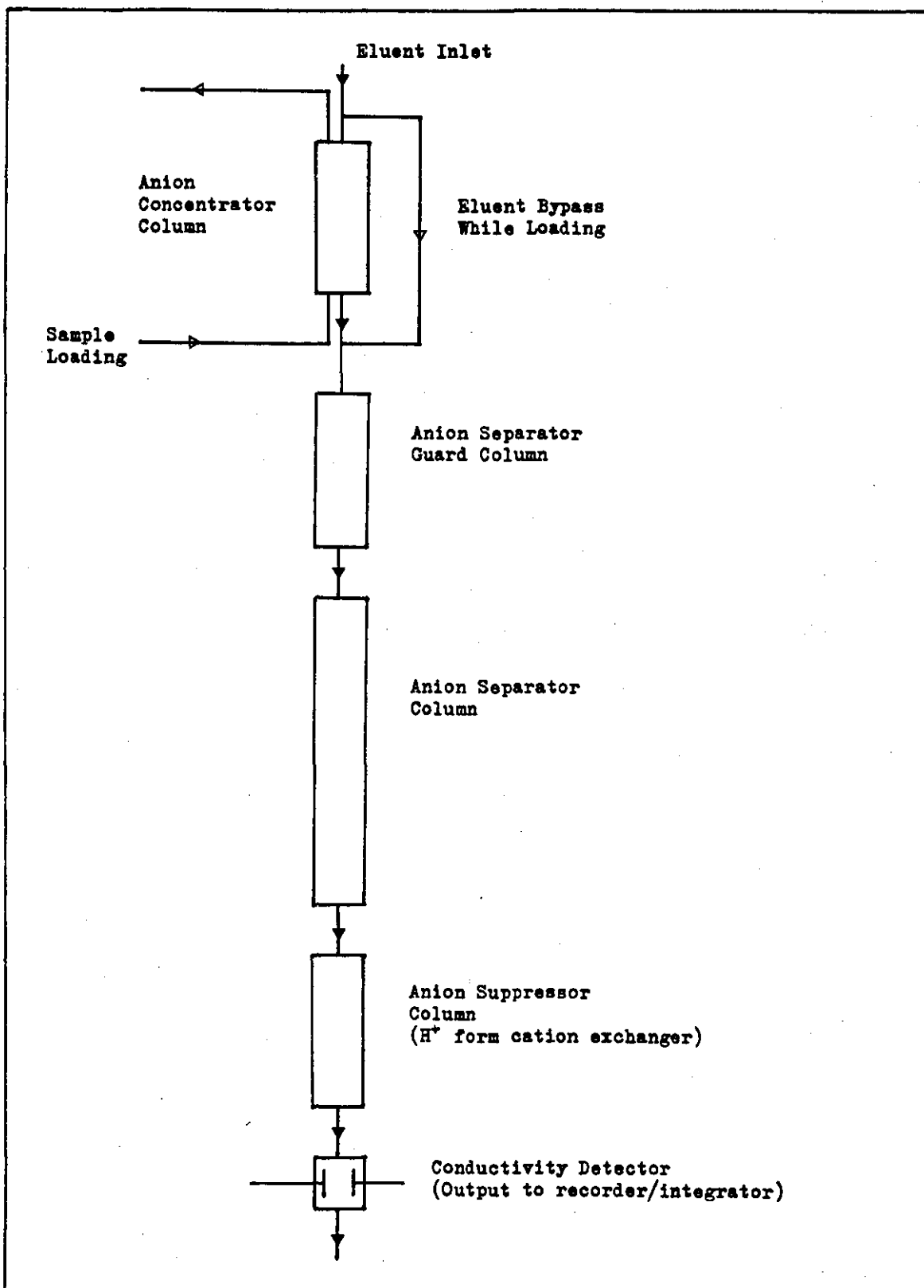
FIGURE
No. A5.04   HIGH PRESSURE ION CHROMATOGRAPHY

TABLE A5.08   <u>HPIC LATER CONDITIONS</u>

Concentrator column   AG2

Guard column   AG2

Separator column   AS2

Suppressor column   continuous fibre type

Eluent   0.001M NaOH +0.0035M Na_2CO_3

Eluent Flow Rate   3.5 ml min^{-1}

Chloride peak retention   270 secs

Sulphate peak retention   900 secs

Loading pump   Milton Roy Type 396-74

Integrator   Trivector - Trilab II
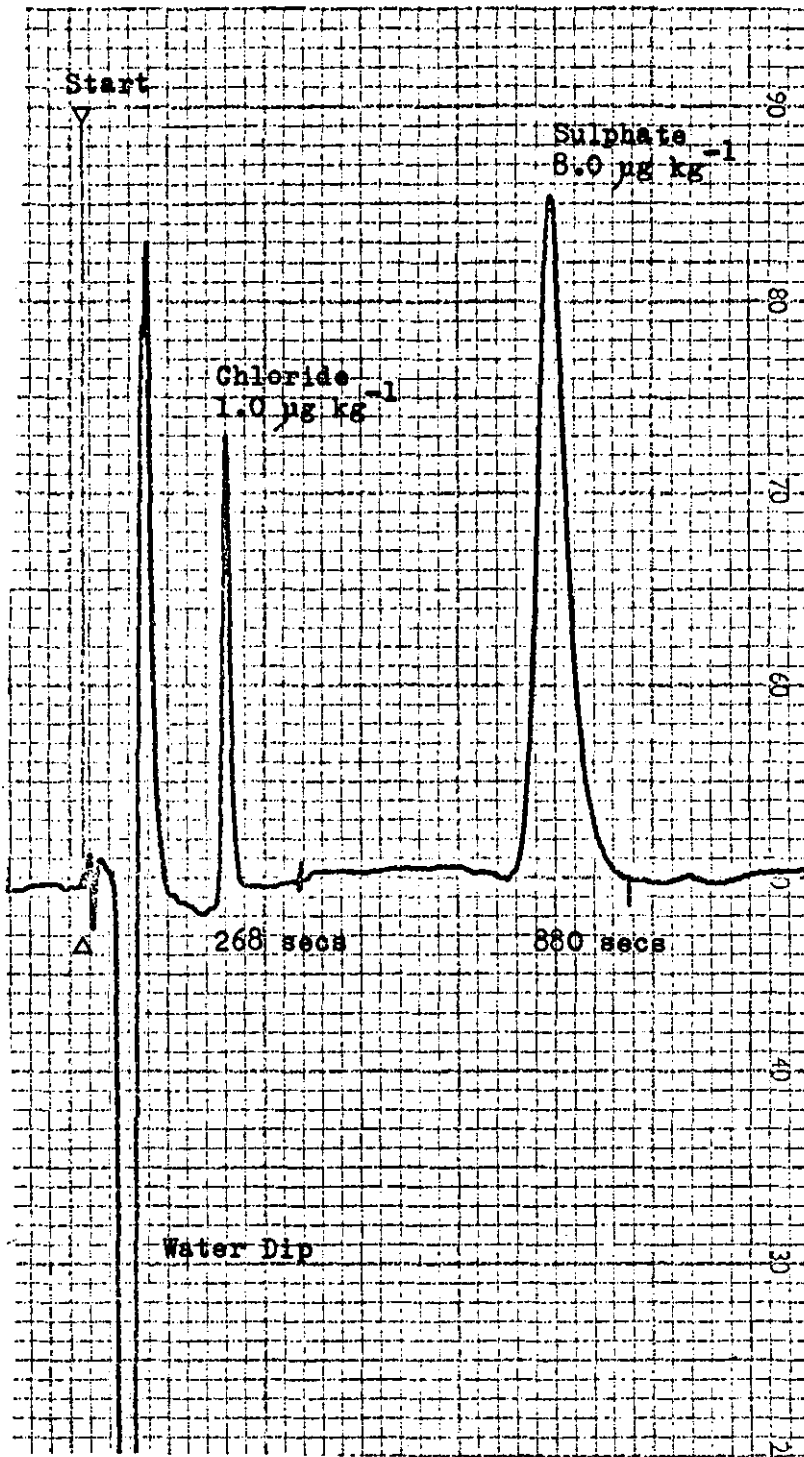
Chromatography Analysis 14.05
SAMPLE A056   (4.00R)

	RETN TIME	PEAK HT	PEAK AREA	%AREA	PEAK NO	PEAK START	PEAK END
Chloride	268.0	10.287	179.965	14.740	1	248.0B	316.0B
Sulphate	880.0	15.382	1040.955	85.260	2	804.0B	1072.0B

Eluent 0.001M NaOH, 0.0035M Na_2CO_3

Detector full scale 3 μScm^{-1}

FIGURE A5.05   ANION CHROMATOGRAPH

A5.4.3 ANION ANALYSIS

Anion analysis, Cl^-, NO_3^-, HPO_4^{2-}, SO_4^{2-}, was undertaken by high pressure ion chromatography (HPIC). The technique is a recent development (144, 145) and basically consists of a low capacity, high surface area packed column of anion exchange resin which, due to its differing selectivity for various anions, effects a separation. The anions are eluted by an alkaline (bicarbonate/carbonate) eluent and appear in a definite sequence. The anions are detected by conductivity changes and to enhance the conductivity peaks the solution of eluent plus anions is passed through a cation exchange column. This converts the anions to their more conducting acids but suppresses the background conductivity of the eluent as it is converted to weakly ionised carbonic acid. The conductivity trace is output to a chart recorder.

The technique is not sensitive enough to directly determine 0 - 50 μg kg^{-1} concentrations of anions and a water sample is first passed through a separate column of anion exchange resin to concentrate them before being eluted onto the separation column. (Figure A5.04).

The analysis was carried out using a Dionex model 10 HPIC (Dionex UK). This was one of the first commercial HPIC instruments available and the sample analysis for the new and deliberatly fouled resins was carried out with resins packed in glass columns and individually regenerated suppressor columns. Developments in HPIC, especially column technology, have advanced rapidly. The HPIC arrangement for analysis of samples from the in service fouled resins, incorporated a number of modifications, including separator columns that gave improved separation of Cl^- and SO_4^{2-}, a continuously regenerated suppressor column and a microprocessor link to the instrument that both integrated the peak areas and controlled the instrument operation. (Table A5.08). Included in this table is the column identification or dimensions and the eluent concentration and flow rate.

Figure A5.05 is an example of the later type conductivity traces for HPIC. Each peak, designated by peak height or peak area,

corresponds to a particular mass of that particular ion. To convert this to a sample concentration the volume of sample loaded onto the concentrator must be known accurately. In the early work the waste sample was collected in a measuring cylinder, a typical volume was around 70 ml. In the later work, with greater peak definition from improved separator columns and controlled sample loading, a 40 ml sample was used.

The instrument was calibrated at the beginning and end of each batch of analyses by loading a standard containing 25 μg kg^{-1} Cl$^-$ (as NaCl) and 25 μg kg^{-1} SO$_4^{2-}$ (as Na$_2$SO$_4$). The standard was prepared fresh each day from a stock solution containing 5 mg kg^{-1} each of Cl$^-$ and SO$_4^{2-}$ diluted into the best available deionised water, often from the test columns.

The limit of detection for chloride was $<$ 0.1 μg kg^{-1} Cl but for sulphate was 0.3 μg kg^{-1} SO$_4$. The latter was partly because of the flatter peak for sulphate but also because the instrument appeared to have a 'sulphate blank'. This is a feature of many Dionex systems and has been demonstrated to be due to the stainless steel bodied Milton-Roy sample loading pump. Replacement of this pump with a plastic bodied pump has subsequently reduced the sulphate background to $<$ 0.1 μg kg^{-1} SO$_4$.

A5.4.4 EXTRACTABLE ORGANIC FOULANTS

The method is based on that of Wilson (240).

About 10 gram. of anion exchange resin was spread on a petri dish and allowed to dry at room temperature overnight. About 1 g of air dried resin was weighed accurately in a tared tin and then placed in an oven at 105 ^{o}C overnight. The oven dry resin was reweighed and the moisture content of the air dried resin determined by loss of weight on drying.

A second 1 g aliquot of air dried resin was added to a 250 ml conical flask to which was added 100 ml of a solution containing 100 g NaCl and 50g NaOH per litre of 50% aqueous/absolute ethanol solution. The extractant was allowed to contact the resins overnight, (minimum

of 16 hours) after which the resins were filtered from the extractant
which was diluted to 250 ml with deionised water. 50 Ml of the
diluted extract were diluted to 150 ml and 6 ml of 5M HCl added.
The solution was heated to 75 $^\circ$C to dissolve any colloidal hydroxides
cooled and then made up to 200 ml. 0.5 Ml of 1 volume hydrogen
peroxide solution was added to oxidise any ferrous to ferric ion,
as ferrous ions interfere with the UV adsorbance. The UV adsorbance
of the diluted extract was measured at 300 nm using water as the
reference in 40 mm quartz cells. The UV adsorbance was related to an
equivalent concentration of fulvic acids using Wilson's correlation.
The extracted mass of fulvic acids could them be related to the
oven dry weight of the resin.

The method initially used a four hour extraction period. However,
in the course of this work it was found that gelular resins released
more organic foulants if left in contact with the extractant overnight.
Four hours was sufficient for the macroporous resins due to their
more open structure. Therefore, a standard extraction of a minimum
of sixteen hours was adopted.

A5.4.5 EXTRACTABLE IRON

A 1g aliquot of the air dried resin in A5.4.4 was weighed and added
to 100 ml of 10M HCl in a 250 ml conical flask. The resin and acid
were boiled for four hours and the resin filtered from the extractant.
The acidic extractant was diluted with deionised water and the iron
concentration determined by atomic absorption spectrophotometry. The
iron concentration was expressed as weight percent Fe on the dry resin.

TABLE A5.09   <u>SIEVE ANALYSES FOR NEW ANION EXCHANGE RESINS</u>

Sieve ∗ Size Fraction (mm)	% Settled Volume in Each Size Fraction					
	IRA 402	IRA 458	IRA 900	A 101D	A 161	Z MPF
-1.2 + 1.0	0.3	7.0	8.9	1.9	0.5	6.4
-1.0 + 0.85	13.0	32.2	41.4	17.5	7.7	36.4
-0.85 + 0.71	27.1	22.0	21.7	20.3	20.8	23.9
-0.71 + 0.60	37.5	20.7	21.2	34.4	38.6	24.5
-0.60 + 0.50	19.3	13.9	5.9	22.2	27.0	8.2
-0.50 + 0.425	2.9	4.1	1.0	3.8	5.3	0.6
Sauter Mean Diameter (mm)	0.66	0.74	0.79	0.67	0.63	0.77

∗ -1.2 +1.0 mm means the beads passing through a 1.2 mm mesh

sieve and held on a 1.0 mm mesh sieve.

TABLE A5.10   **MIXED BED TEST COLUMN LEAKAGE DATA.**

                NEW ANION EXCHANGERS (ex Chloride form)

                CHLORIDE DOSING   20 °C

Linear Flow Rate ($m^3m^{-2}h^{-1}$)		55			90			120		
Influent Dosing ($\mu g\ kg^{-1}$ Cl)		1480	2960	5920	1480	2960	5920	1480	2960	5920
Resin	Column Leakage									
Amberlite IRA402	Chloride $\mu g\ kg^{-1}$Cl	0.5	0.4	0.4	0.5	0.5	0.6	0.6	0.7	1.1
	Conductivity μScm^{-1}	0.045	0.045	0.045	0.044	0.045	0.046	0.045	0.046	0.048
	Sulphate $\mu g\ kg^{-1}SO_4$	0.6	0.6	0.5	0.5	0.5	0.5	0.5	0.5	0.4
	Sodium $\mu g\ kg^{-1}$Na	0.7	0.7	0.7	0.7	0.8	1.0	0.9	1.1	1.4
Amberlite IRA458	Chloride $\mu g\ kg^{-1}$Cl	0.6	0.4	0.5	0.7	0.9	1.3	0.7	1.4	2.4
	Conductivity μScm^{-1}	0.046	0.046	0.047	0.047	0.048	0.050	0.049	0.051	0.057
	Sulphate $\mu g\ kg^{-1}SO_4$	0.6	0.5	0.5	0.5	0.7	0.7	0.5	0.6	0.5
	Sodium $\mu g\ kg^{-1}$Na	0.7	0.7	0.7	0.7	0.7	0.9	0.7	0.9	1.3
Amberlite IRA900	Chloride $\mu g\ kg^{-1}$Cl	1.0	0.6	0.7	0.8	0.9	2.1	1.5	2.8	5.1
	Conductivity μScm^{-1}	0.047	0.046	0.049	0.048	0.049	0.055	0.052	0.056	0.067
	Sulphate $\mu g\ kg^{-1}SO_4$	0.7	0.5	0.9	0.7	0.5	0.6	0.6	0.6	0.6
	Sodium $\mu g\ kg^{-1}$Na	0.7	0.7	0.8	1.0	1.2	1.5	1.6	2.2	2.8
Duolite A101D	Chloride $\mu g\ kg^{-1}$Cl	0.5	0.6	0.4	0.5	0.5	1.3	0.7	1.1	2.6
	Conductivity μScm^{-1}	0.044	0.045	0.044	0.045	0.045	0.046	0.045	0.046	0.049
	Sulphate $\mu g\ kg^{-1}SO_4$	0.5	0.6	0.5	0.5	0.6	0.5	0.6	0.5	0.5
	Sodium $\mu g\ kg^{-1}$Na	0.7	0.7	0.7	0.8	0.8	0.8	0.9	1.0	1.1
Duolite A161	Chloride $\mu g\ kg^{-1}$Cl	0.6	0.6	0.7	0.4	0.7	0.9	0.8	1.3	1.8
	Conductivity μScm^{-1}	0.048	0.048	0.048	0.050	0.051	0.051	0.052	0.055	0.058
	Sulphate $\mu g\ kg^{-1}SO_4$	1.0	0.6	0.7	0.6	0.5	0.6	0.6	0.9	0.8
	Sodium $\mu g\ kg^{-1}$Na	0.7	0.8	0.8	1.2	1.5	2.0	1.7	2.4	3.0
Zerolit MPF	Chloride $\mu g\ kg^{-1}$Cl	0.5	0.5	0.8	0.8	0.9	2.6	1.2	2.3	4.9
	Conductivity μScm^{-1}	0.044	0.044	0.048	0.046	0.047	0.058	0.050	0.055	0.070
	Sulphate $\mu g\ kg^{-1}SO_4$	0.4	0.4	0.4	0.3	0.3	0.5	0.3	0.3	0.4
	Sodium $\mu g\ kg^{-1}$Na	-	-	-	1.1	1.3	1.8	1.4	1.9	3.0

TABLE A5.11 MIXED BED TEST COLUMN LEAKAGE DATA

NEW ANION EXCHANGERS (ex Chloride form)

SULPHATE DOSING   20 °C

Linear Flow Rate $m^3 m^{-2} h^{-1}$		55			90			120		
Influent Dosing ($\mu g\ kg^{-1} SO_4$)		2000	4000	8000	2000	4000	8000	2000	4000	8000
Resin	Column Leakage									
Amberlite IRA402	Sulphate $\mu g\ kg^{-1} SO_4$	0.7	1.0	0.6	0.5	0.6	1.0	0.7	1.6	1.9
	Conductivity $\mu S cm^{-1}$	0.045	0.045	0.045	0.045	0.045	0.047	0.046	0.047	0.051
	Chloride $\mu g\ kg^{-1} Cl$	0.5	0.5	0.3	0.5	0.5	0.5	0.6	0.6	0.7
	Sodium $\mu g\ kg^{-1} Na$	0.7	0.7	0.7	0.8	0.8	0.9	1.0	1.1	1.3
Amberlite IRA458	Sulphate $\mu g\ kg^{-1} SO_4$	0.5	1.0	0.9	1.0	1.1	1.8	1.3	2.9	6.3
	Conductivity $\mu S cm^{-1}$	0.046	0.046	0.048	0.048	0.049	0.054	0.052	0.058	0.070
	Chloride $\mu g\ kg^{-1} Cl$	0.4	0.4	0.5	0.5	0.3	0.3	0.3	0.4	0.5
	Sodium $\mu g\ kg^{-1} Na$	0.7	0.7	0.8	0.7	0.7	1.0	0.7	0.9	1.6
Amberlite IRA900	Sulphate $\mu g\ kg^{-1} SO_4$	1.2	0.8	1.8	0.9	1.0 (1.5)	2.2 (4.2)	1.5	3.8	10.3
	Conductivity $\mu S cm^{-1}$	0.047	0.046	0.050	0.048	0.050	0.064	0.053	0.062	0.095
	Chloride $\mu g\ kg^{-1} Cl$	1.0	0.6	0.4	0.9	0.9	0.6	0.8	0.7	1.0
	Sodium $\mu g\ kg^{-1} Na$	0.7	0.7	-	1.0	1.0	1.2	1.3	1.5	2.1
Duolite A101D	Sulphate $\mu g\ kg^{-1} SO_4$	0.5	0.6	0.5	0.5	0.5	1.3	0.7	1.1	2.7
	Conductivity $\mu S cm^{-1}$	0.044	0.045	0.044	0.045	0.045	0.048	0.046	0.048	0.054
	Chloride $\mu g\ kg^{-1} Cl$	0.7	0.7	0.4	0.6	0.5	0.5	0.5	0.5	0.7
	Sodium $\mu g\ kg^{-1} Na$	0.8	0.8	0.6	0.8	0.8	0.8	0.9	1.0	1.2
Duolite A161	Sulphate $\mu g\ kg^{-1} SO_4$	0.9	1.1	0.9	0.9	0.8	1.0	1.0	1.3	1.6
	Conductivity $\mu S cm^{-1}$	0.048	0.047	0.049	0.049	0.050	0.050	0.050	0.051	0.054
	Chloride $\mu g\ kg^{-1} Cl$	0.5	0.7	0.7	0.6	0.7	0.5	0.9	1.0	1.1
	Sodium $\mu g\ kg^{-1} Na$	0.7	0.8	0.8	1.1	1.2	1.2	1.5	1.7	2.3
Zerolit MPF	Sulphate $\mu g\ kg^{-1} SO_4$	0.3	0.5	1.3	0.9	1.9	5.2	3.9	5.8	11.6
	Conductivity $\mu S cm^{-1}$	0.044	0.045	0.051	0.047	0.050	0.067	0.055	0.067	0.100
	Chloride $\mu g\ kg^{-1} Cl$	0.5	0.6	0.5	0.3	0.4	0.7	0.6	0.7	1.1
	Sodium $\mu g\ kg^{-1} Na$	-	-	-	1.3	1.5	2.1	1.6	2.2	3.9

Values in brackets ( ) are calculated from conductivity and ionic concentrations.

TABLE A5.12   CALCULATED MASS TRANSFER COEFFICIENTS
              NEW ANION EXCHANGERS
              CHLORIDE EXCHANGE

RESIN	INFLUENT (μg kg^{-1}Cl)	Mass Transfer Coefficient (10^{-4} ms^{-1})		
		55 mh^{-1}	90 mh^{-1}	120 mh^{-1}
Amberlite IRA402	1480		1.74	2.27
	2960		1.89	2.42
	5920	1.28	2.00	2.49
Amberlite IRA458	1480		1.87	2.49
	2960		1.98	2.49
	5920	1.40	2.06	2.54
Amberlite IRA900	1480		1.96	2.39
	2960		2.11	2.42
	5920	1.44	2.07	2.45
Duolite A101D	1480		1.77	2.26
	2960		1.92	2.33
	5920	1.30	1.86	2.28
Duolite A161	1480		1.71	2.08
	2960		1.74	2.14
	5920	1.15	1.83	2.24
Zerolit MPF	1480		1.91	2.41
	2960		2.06	2.42
	5920	1.39	1.96	2.40

TABLE A5.13   <u>CALCULATED MASS TRANSFER COEFFICIENTS</u>
<u>NEW ANION EXCHANGERS</u>
<u>SULPHATE EXCHANGE</u>

RESIN	INFLUENT ($\mu g\ kg^{-1} SO_4$)	Mass Transfer Coefficient ($10^{-4} ms^{-1}$)		
		$55\ mh^{-1}$	$90\ mh^{-1}$	$120\ mh^{-1}$
Amberlite IRA402	2000		1.81	2.31
	4000		1.92	2.27
	8000	1.27	1.96	2.42
Amberlite IRA458	2000		1.86	2.39
	4000		2.00	2.35
	8000	1.36	2.05	2.33
Amberlite IRA900	2000		2.01	2.50
	4000		2.06	2.42
	8000	1.34	1.97	2.31
Duolite A101D	2000		1.83	2.34
	4000		1.99	2.41
	8000	1.35	1.93	2.36
Duolite A161	2000		1.60	2.10
	4000		1.77	2.23
	8000	1.15	1.87	2.36
Zerolit MPF	2000		1.96	2.11
	4000		1.95	2.21
	8000	1.36	1.87	2.21

TABLE A5.14 <u>CHLORIDE AND SULPHATE LEAKAGE FROM NEW DUOLITE A161</u>

<u>MACROPOROUS ANION EXCHANGE RESIN</u>

Flow Rate (mh^{-1})	Influent Anion Conc'n (As sodium salt)	Anion Leakage	Mass Transfer Coeff. $(10^{-4}ms^{-1})$
100	1000 μg $kg^{-1}Cl$	3.5 μg $kg^{-1}Cl$	2.38
100	2000 μg $kg^{-1}Cl$	5.2 μg $kg^{-1}Cl$	2.50
100	5000 μg $kg^{-1}Cl$	11.2 μg $kg^{-1}Cl$	2.56
100	676 μg $kg^{-1}SO_4$	6.3 μg $kg^{-1}SO_4$	1.96
100	1350 μg $kg^{-1}SO_4$	11.6 μg $kg^{-1}SO_4$	2.00
100	2700 μg $kg^{-1}SO_4$	21.2 μg $kg^{-1}SO_4$	2.04

Mean Diameter of A161 = 0.82 mm.

TABLE A5.15   <u>LEAKAGE AND OUTLET CONDUCTIVITY DATA FOR VARIOUS ANIONS</u>

<u>EXCHANGING ON AMBERLITE IRA900 REGENERATED FROM HCO_3^-</u>

<u>FORM RESIN</u>

Linear Flow Rate	$90m^3m^{-2}h^{-1}$		$120m^3m^{-2}h^{-1}$	
Influent Anion Concentration	Outlet Conductivity ($\mu S\ cm^{-1}$)	Anion Leakage (μgkg^{-1})	Outlet Conductivity ($\mu S\ cm^{-1}$)	Anion Leakage (μgkg^{-1})
Chloride 2960 $\mu gkg^{-1}Cl^-$	0.047	0.7	0.054	1.8
Sulphate 4000 $\mu gkg^{-1}SO_4^{2-}$	0.051	2.1	0.068	5.8
Nitrate 5165 $\mu gkg^{-1}NO_3^-$	0.048	1.3	0.057	3.8
Phosphate 4000 $\mu gkg^{-1}HPO_4^{2-}$	0.070	9.0	0.110	18.0
Carbonate 2500 $\mu gkg^{-1}CO_3^{2-}$	0.054	-	0.068	-
Bicarbonate 5085 $\mu gkg^{-1}HCO_3^-$	0.058	-	0.076	-

2 : 1, Cation : Anion mixed bed, 550 mm deep, 20 ^oC.

No dose outlet conductivity 0.0445 $\mu S\ cm^{-1}$.

TABLE A5.16 <u>MIXED BED TEST COLUMN LEAKAGE DATA.</u>

<u>DELIBERATELY FOULED ANION EXCHANGERS.</u>

<u>CHLORIDE DOSING</u>   20 °C

Linear Flow Rate $m^3m^{-2}h^{-1}$		55			90			120		
Influent Dosing ($\mu g\ kg^{-1}Cl$)		1480	2960	5920	1480	2960	5920	1480	2960	5920
Resin	Column Leakage									
Amberlite IRA402	Chloride $\mu gkg^{-1}Cl$	0.5	0.4	0.4	0.4	0.4	0.5	0.6	0.8	1.2
	Conductivity μScm^{-1}	0.045	0.045	0.046	0.045	0.046	0.047	0.047	0.048	0.051
	Sulphate $\mu gkg^{-1}SO_4$	-	-	0.5	0.6	0.3	0.6	0.5	0.5	0.5
	Sodium $\mu gkg^{-1}Na$	-	-	-	-	-	-	0.8	0.9	0.9
Amberlite IRA458	Chloride $\mu gkg^{-1}Cl$	0.5	0.6	0.6	1.0	1.3	2.2	1.5	3.1	6.2
	Conductivity μScm^{-1}	0.048	0.047	0.049	0.050	0.052	0.059	0.055	0.062	0.078
	Sulphate $\mu gkg^{-1}SO_4$	0.5	0.4	0.4	0.4	0.4	0.4	0.4	0.4	0.4
	Sodium $\mu gkg^{-1}Na$	-	-	1.3	1.8	2.2	2.5	2.3	3.5	4.8
Amberlite IRA900	Chloride $\mu gkg^{-1}Cl$	0.6	0.6	1.0	1.3	1.6	2.9	1.8	3.7	7.2
	Conductivity μScm^{-1}	0.048	0.048	0.051	0.053	0.057	0.069	0.065	0.080	0.110
	Sulphate $\mu gkg^{-1}SO_4$	0.7	0.6	0.6	0.6	0.5	0.6	-	0.6	0.9
	Sodium $\mu gkg^{-1}Na$	-	-	-	-	-	-	-	-	-
Duolite A101D	Chloride $\mu gkg^{-1}Cl$	0.5	0.4	0.4	0.3	0.4	0.6	0.6	0.9	1.5
	Conductivity μScm^{-1}	0.045	0.045	0.046	0.046	0.046	0.050	0.048	0.049	0.054
	Sulphate $\mu gkg^{-1}SO_4$	0.5	0.4	0.4	0.3	0.4	0.6	0.3	0.3	0.6
	Sodium $\mu gkg^{-1}Na$	steady trace at 1.0 $\mu gkg^{-1}Na$.								
Duolite A161	Chloride $\mu gkg^{-1}Cl$	<0.3	0.4	0.4	0.5	0.6	0.6	0.5	1.0	1.6
	Conductivity μScm^{-1}	0.046	0.046	0.046	0.046	0.047	0.048	0.048	0.050	0.054
	Sulphate $\mu gkg^{-1}SO_4$	0.5	0.5	0.5	0.5	0.6	0.4	0.4	0.4	0.5
	Sodium $\mu gkg^{-1}Na$	-	-	-	0.8	0.8	0.8	0.8	0.8	0.9
Zerolit MPF	Chloride $\mu gkg^{-1}Cl$	0.3	0.5	0.7	0.8	1.3	3.4	1.9	3.7	8.0
	Conductivity μScm^{-1}	0.046	0.046	0.051	0.050	0.053	0.072	0.059	0.071	0.109
	Sulphate $\mu gkg^{-1}SO_4$	0.5	0.4	0.4	0.4	0.4	0.4	0.3	0.3	0.5
	Sodium $\mu gkg^{-1}Na$	-	-	-	-	-	1.2	1.0	1.2	1.9

TABLE A5.17 MIXED BED TEST COLUMN LEAKAGE DATA
DELIBERATELY FOULED ANION EXCHANGERS
SULPHATE DOSING   20 °C

Linear Flow Rate $(m^3 m^{-2} h^{-1})$		55			90			120		
Influent Dosing µg kg^{-1} SO$_4$		2000	4000	8000	2000	4000	8000	2000	4000	8000
Resin	Column Leakage									
Amberlite IRA402	Sulphate µgkg^{-1}SO$_4$	0.5	0.5	0.6	0.7	1.2	2.0	2.0	3.7	4.4
	Conductivity µScm^{-1}	0.045	0.045	0.046	0.046	0.047	0.051	0.050	0.054	0.064
	Chloride µgkg^{-1}Cl	0.5	0.4	0.4	0.4	0.4	0.4	0.4	0.4	0.4
	Sodium µgkg^{-1}Na	-	-	-	-	-	-	0.8	0.9	1.1
Amberlite IRA458	Sulphate µgkg^{-1}SO$_4$	0.7	1.1	1.9	2.3	4.1	6.5	4.7	8.2	15.2
	Conductivity µScm^{-1}	0.047	0.047	0.051	0.051	0.058	0.075	0.064	0.083	0.129
	Chloride µgkg^{-1}Cl	0.4	0.5	0.4	0.4	0.4	0.3	0.3	0.3	0.3
	Sodium µgkg^{-1}Na	-	-	1.3	1.8	1.9	2.3	2.5	2.9	4.4
Amberlite IRA900	Sulphate µgkg^{-1}SO$_4$	1.7	2.9	3.5	4.3	7.0	12.3	7.5	15.1	28.0
	Conductivity µScm^{-1}	0.051	0.054	0.058	0.063	0.080	0.120	0.092	0.139	0.235
	Chloride µgkg^{-1}Cl	0.3	0.5	0.5	0.4	<0.3	0.5	<0.3	<0.3	0.6
	Sodium µgkg^{-1}Na	-	-	-	-	-	-	-	-	-
Duolite A101D	Sulphate µgkg^{-1}SO$_4$	0.8	0.8	0.8	0.8	1.4	2.8	2.1	3.2	6.3
	Conductivity µScm^{-1}	0.045	0.045	0.047	0.047	0.049	0.056	0.052	0.058	0.073
	Chloride µgkg^{-1}Cl	0.4	0.4	0.4	<0.3	<0.3	0.3	0.5	0.5	0.4
	Sodium µgkg^{-1}Na	-	Steady trace at 1.0 µgkg^{-1}Na								
Duolite A161	Sulphate µgkg^{-1}SO$_4$	0.6	0.8	0.9	1.2	2.0	2.7	2.0	3.4	6.2
	Conductivity µScm^{-1}	0.046	0.046	0.047	0.048	0.050	0.056	0.053	0.060	0.078
	Chloride µgkg^{-1}Cl	<0.3	<0.3	<0.3	<0.3	<0.3	<0.3	<0.3	<0.3	<0.3
	Sodium µgkg^{-1}Na	-	-	-	0.8	0.8	0.9	0.8	1.0	1.3
Zerolit MPF	Sulphate µgkg^{-1}SO$_4$	1.0	1.7	2.4	2.5	4.6	11.1	5.8	11.8	25.5
	Conductivity µScm^{-1}	0.048	0.049	0.058	0.056	0.066	0.112	0.076	0.112	0.210
	Chloride µgkg^{-1}Cl	<0.3	<0.3	<0.3	<0.3	0.3	0.3	0.3	0.3	0.3
	Sodium µgkg^{-1}Na	-	-	-	1.0	1.1	1.6	1.2	1.7	3.0

TABLE A5.18   CALCULATED MASS TRANSFER COEFFICIENTS

DELIBERATELY FOULED ANION EXCHANGERS

CHLORIDE EXCHANGE

RESIN	INFLUENT (μg kg^{-1}Cl)	Mass Transfer Coefficient (10^{-4}ms^{-1})		
		55mh^{-1}	90mh^{-1}	120mh^{-1}
Amberlite IRA402	1480		1.79	2.27
	2960		1.94	2.38
	5920	1.28	2.04	2.47
Amberlite IRA458	1480		1.78	2.24
	2960		1.89	2.23
	5920	1.37	1.93	2.23
Amberlite IRA900	1480		1.83	2.33
	2960		1.96	2.32
	5920	1.38	1.98	2.33
Duolite A101D	1480		1.88	2.30
	2960		1.97	2.39
	5920	1.30	2.03	2.44
Duolite A161	1480		1.66	2.21
	2960		1.77	2.21
	5920	1.22	1.91	2.28
Zerolit MPF	1480		1.91	2.25
	2960		1.96	2.26
	5920	1.41	1.90	2.24

TABLE A5.19 CALCULATED MASS TRANSFER COEFFICIENTS

DELIBERATELY FOULED ANION EXCHANGERS

SULPHATE EXCHANGE

RESIN	INFLUENT	MASS TRANSFER COEFFICIENTS ($10^{-4}ms^{-1}$)		
	($\mu g\ kg^{-1}SO_4$)	$55mh^{-1}$	$90mh^{-1}$	$120mh^{-1}$
Amberlite IRA402	2000	1.11	1.73	2.00
	4000	1.20	1.77	2.03
	8000	1.27	1.81	2.18
Amberlite IRA458	2000	1.19	1.65	1.97
	4000	1.23	1.68	2.01
	8000	1.25	1.74	2.04
Amberlite IRA900	2000	1.13	1.60	1.94
	4000	1.15	1.65	1.94
	8000	1.23	1.69	1.96
Duolite A101D	2000	1.06	1.73	2.02
	4000	1.15	1.76	2.10
	8000	1.25	1.76	2.11
Duolite A161	2000	1.03	1.54	1.91
	4000	1.08	1.58	1.96
	8000	1.16	1.66	1.98
Zerolit MPF	2000	1.18	1.70	1.98
	4000	1.21	1.72	1.97
	8000	1.26	1.67	1.95

ERRATA

p ii, l 1	interpreted
p 1, para 3, l 2	Siemens
p 24, para 2, l 2	Moisson
p 33, para 1, l 1	$K_{Na}^{NH}4$ is 1.33
p46, para 3, l 3	Semmens
p 65, para 2, 14	criterion
p 70, para 3, l 5	regenerated in-situ
p 87, para 3, l 3	absorbent
p 93, para 2, l 7	throughput
p 111, para 1, l 2	--- it is presumably constant.
p 132, para 1, 12	sieve
p 167, para 1, l 1	Donnan
p 196, ref 176	Semmens
p 196, ref 178	"JCS Farady" for "J.Chem.Soc."
p 216 para 2, l 6&8	desiccator